Applications of LC-MS metabolomic profiling in inflammatory bowel disease and the development of derivatisation methods to enhance selective detection of certain compound classes.

A thesis submitted for the degree of Doctor of Philosophy at the University of Strathclyde.

By
Ibrahim Alothaim

Strathclyde Institute of Pharmacy and Biomedical Sciences
University of Strathclyde
161 Cathedral Street
Glasgow G4 0RE

2018

Declaration

‘This thesis is the result of the author’s original research. It has been composed by the author and has not been previously submitted for examination which has led to the award of a degree.’

Acknowledgement

First of all, I thank almighty Allah for completing this task successfully. I am very grateful to my supervisor Dr David G Watson for his extensive support, guidance throughout my PhD and gave me opportunity to be trained in his lab with a lot of valuable advice.

Also I would to select this opportunity to thank Dr Daniel R Gaya from, Gastroenterology Clinic in Royal Infirmary Hospital, Glasgow, for providing control and UC samples that been used in the research.

My sincere thanks also go to all of Dave's research group, PhD student and co-workers in the laboratory for their cooperation, assistance and helpful discussions.

I want to express my gratitude to my mother , my wife, brothers, sisters and my two daughters (Toleen) and (Alen) , who have always taken great interest in and who have always been there with me and supporting me.

Finally special thanks to my sponsor Saudi Food and Drug Authority representative of the Saudi government for funding my studies at the University of Strathclyde, especially for the PhD project.

Table of Contents

List of Tables

List of Figures

List of Abbreviations

LC-ESI-MS	Liquid chromatography- Electrospray ionisation- Mass spectrometry.
LC-API-MS	Liquid chromatography- Atmospheric pressure ionization - Mass spectrometry.
GC/ MS	Gas chromatography / Mass spectrometry.
CE/MS	Capillary electrophoresis / Mass spectrometry.
Q-TOF	Quadruple-time of flight.
FT-ICR	Fourier transform-ion cyclotron resonance.
SIM	Selected ion monitoring.
SRM	Selected reaction monitoring.
NMR	Nuclear magnetic resonance
E_1	Estrone.
E_2	Estradiol.
TEA	Triethylamine
FMP	2-Fluoro -1-methylpyridine
FMPTS	2-Fluoro -1-methyl-pyridinium P-toluenesulfonate
FDMPTS	2-Fluoro -1,3-dimethyl-pyridinium P-toluenesulfonate
DPD	N,N-Dimethyl-p-phenylenediamine.
EDC	N-(-3-Dimethylaminopropyl)-N-ethyl carbodiimide. Hydrochloride.
I.S	Internal. Standard.
SCFA	Short chain fatty acids.
ACN	Acetonitrile.

THF	Tetrahydrofuran
HRMS	High Resolution Mass Spectrometry
TOF	Time-of-Flight
amu	Atomic Mass Unit
CD	Crohn's disease
ICD	Ileal Crohn's disease
UC	Ulcerative Colitis
CRC	Colorectal cancer
BMI	Body Mass Index
GIT	Gastro intestinal tract
GPC	Glycerophosphocholine
DMG	Dimethylglycine
PUFA	Fatty acids contain two or more double bonds
AA	Arachidonic acid
PG_S	prostaglandins
LT_S	Leukotrienes
TX_S	Thromboxanes
CLA	Conjugated linoleic acid
NAT	Arylamine *N*-acetyltransferase
DSS	Dextran sulfate sodium
ASA	Amino salicylic acid
LDL	Low density lipoprotein

BALF	Broncho alveolar lavage fluid
CS	Cholesterol sulfate
AID	Activation- induced cytidine deaminase
TNF-α	Tumour necrosis factor.
LCD	Low-calorie diet
GAPDH	Glyceraldehyde 3-phosphate dehydrogenase
IEC	Intestinal epithelial cell
LPMC	Lamina propria mononuclear
PET	Positron emission tomography
EG	N-Ethylglycine
ROS	reactive oxygen species
DHAP	Dihydroxyacetone phosphate
AUP	Area under the curve
FAP	Familial polyposis
C	Urine samples of healthy control cohorts
R	Urine samples of remission Ulcerative Colitis cohorts
A	Urine samples of active Ulcerative Colitis cohorts
HBT	Hydrogen breath test
SIBO	Small intestinal bacteria overgrowth
LAB	Lactic acid bactreria
SPF	Specific pathogen free
IL	Interleukin

EPS	Exopolysaccharide
MDA	Malondialdehyde
ROM	Reactive oxygen metabolites
BAL	Bronchoalveolar lavage
BALF	Bronchoalveolar lavage fluid

Abstract

Inflammatory bowel disease (IBD) is a chronic inflammation of all parts of the gastrointestinal tract and is represented by two major variations, ulcerative colitis (UC) and Crohn's disease (CD). It is diagnosed based on the pattern of inflammation. In order to understand the pathology of the disease better urine and saliva samples were collected from patients with IBD, patients in remission and a control group. The metabolomes of the urine and saliva samples were profiled by carrying out chromatography on a ZICpHILIC column in combination with high resolution mass spectrometry. It was possible to separate the different classes of urine samples on the basis of their metabolomic profiles by modelling with data using orthogonal partial least squares analysis (OPLSDA). A number of metabolites were found to vary between the three groups although the models for separation were weak. The OPLSDA models of the saliva data were much stronger and saliva analysis looks promising for diagnostic and prognostic purposes. Nine variables were able to discriminate the control and affected samples and these included four sphingosine bases. The analysis of short chain fatty acids (SCFAs) by LC-MS is a problem since they are too volatile to give good responses. SCFAs are potentially important makers for IBD. A quantitative LC-MS method for acetic, propionic, butyric and lactic acids was developed by carrying out derivatisation of the acids using a carbodimide to activate the acids and then reacting with dimethylaminophenylamine and separating the derivatives using HILIC chromatography. Quantification was carried out by using stable isotope dilution. The method was very sensitive but detection limits were set by the background contamination by the SCFAs rather than by absolute sensitivity. The method was applied to the urine samples and differences in acetate and butyrate were found between the affected and control samples. The microbiome plays a role in IBD and one marker for bacterial activity it the breakdown of dietary fibre in sugar monomers. Thus urine and saliva samples from controls and IBD samples were profiled using a reductive amination method previously developed. It was found that there were significant differences in the pattern of hexoses, pentoses and deoxy hexoses in the urine and saliva samples.

Chapter-1:

General Introduction

1.1 Metabolomics in general

Metabolomics is relatively new area of study being investigated as a useful tool for diagnosis and evaluation of the treatment of patients. It is applied to research into lipid metabolism, diabetes, oncology research, multiple sclerosis, diet modification and nutrition, drug use and pharmacological treatment as well as the study of metabolite responses to cardiovascular ischemia. Furthermore, metabolomics analysis can help to assess the levels low molecular weight metabolites that are affected in disease processes such as amino acids amines, fatty acids, organic acids, aromatic compounds, nucleotides and steroids. Metabolomics studies of human biofluids are useful to find out biomarker metabolites that diagnose disease or produce an early warning at the preclinical stage [1]. Several instruments can be used to carry out this analysis for instance NMR based metabolomics provides non-discriminatory and repeatable outcomes also it provides an effective diagnostics in conjunction with pattern recognition methods. However, due to the limited resolution between spectra of individual molecules and poor sensitivity it cannot always identify metabolites at low levels and a wider dynamic range can be achieved by using mass spectrometry (MS). Moreover, by coupling chromatography with MS metabolites can be differentiated by their retention times (Rt) as an additional dimension for identification. Liquid chromatography- mass spectrometry (LC-MS) and gas chromatography- mass spectrometry (GC-MS) and have been widely used for analysis of human urine in metabolite profiling studies and are suitable for the quantitative and qualitative measurement of individual metabolites for biomarker discovery. One study reported a method by using the GC/MS for profiling the human urine and mentioned that 150 putative metabolites were detected and 144 of them were given a name by using mass spectral matching scores with the NIST library and retention indices, but GC/MS is limited to analysing volatile and nonpolar compounds. Whereas in comparison LC-MS does not need any complex preparation steps prior to quantification and cannot cause the degradation of samples that are thermally unstable [2]. Therefore, an LC-MS is the instrument of choice for metabolomic profiling due to its advantages over the other instruments. For the preparation of sample there are often minimal requirements and chromatography offers diverse LC selectivities. To illustrate this reversed phase (RP) chromatography has been successfully used in humane urine metabolomic studies and has been commonly used to analyse human urine for disease diagnostics and biomarker discovery by hydrophobic interaction separation and retention of metabolites under these condition is predominantly determined by the hydrophobicity of the analytes. Nevertheless, a large number of highly polar metabolites exist in a human urine sample and those polar metabolites such as organic acids, glucuronide conjugates, amino acids and sulphates generally elute together close to the dead

time (t_0) from columns under RP LC conditions, therefore the retention time in this case will not make any contribution to their identification. Furthermore, at trace levels ion suppression is more likely occur for co-eluting polar metabolites. Aqueous normal phase (ANP) chromatography is another option and is an effective LC method. A study demonstrated that approximately 1000 features could be obtained by ANP-LC-MS system in human urine and similar to this number were obtained by RP-LCMS system. The hydrophilic partitioning of metabolites between an aqueous layer formed on the stationary phase and an organic solvent-rich mobile phase produces retention /separation and also ionisable compounds may undergo electrostatic interactions on charged or zwitterionic HILIC stationary phases producing improved selectivity[3]. Metabolomics studies of human urine can be carried out by using HILIC alone or together with RP columns. A study reported that measuring the metabolome of human urine allowed correct classification of diurnal variation, age and gender under both RP-LC-MS and HILIC-MS conditions according to their multivariate analysis results. However, evaluation of chromatographic performance in terms of repeatability and linearity for urine metabolites was not mentioned[4]. The most widespread HRMS instruments used in metabolomics are Time-of-Flight (TOF) mass spectrometers but the average mass error produced by TOF is around 5 ppm ,whereas Orbitrap instruments can provide a resolution (>100 000) and mass error <2 ppm. The Exactive is a benchtop Orbitrap MS system and has advantages over many other instruments with its high scan speed which is ideal for fast and comprehensive metabolite profiling of tissue extracts or biofluids due to its fast polarity switching when coupled with LC separation. Metabolomics profiling depends on high resolution mass spectrometry with regard to identification of elemental composition but isomer separation requires chromatography. Most urinary metabolites eluted very rapidly with little or no separation with a reversed phase column. In contrast the hydrophilic interaction (HILIC) and two zwitterionic HILIC columns displayed improved separation of isomers and the greatest coverage of polar metabolites in urine. The HILIC liquid chromatography platform with the Exactive Orbitrap mass spectrometer could be used for identifying approximately 970 metabolites signals with repeatable peak areas (relative standard deviation (RSD) ≤ 25%) with elemental composition assignment with < 3 ppm mass error in human urine. Moreover, the possibility of isomers discrimination and verification of non-molecular ions that arise from adduct formation could be achieved [5].

1.2 Instruments used in the metabolomics profiling and fingerprinting.

The chemical process of including metabolites is the scientific study is called metabolomics, whereas the metabolome indicates the group of metabolites in the tissue, biological cell, tissue, organ or organism and urine which are the end products of cellular processes .The physiology of the cell can be given in instantaneous way this snapshot called metabolic profiling. Detectors such as (MS) mass

spectrometers and tandem mass spectrometers (MS/MS) provide useful detection methods used with hyphenation with GC, CE, and HPLC due to their suitability in terms of specificity and sensitivity compared with RI, UV, and flame ionization detectors. In recent years numerous studies have focused on metabolic profiling and fingerprinting due to the emergence of the field of metabolomics. The ability to measure the absolute or relative amount of all metabolites (the metabolome) can be achieved by using hyphenated techniques; for instance LC-MS GC-MS and capillary electrophoresis/mass spectrometry (CE-MS).These instruments supply a chromatographic profile with details that rely on the specificity of the detection technique and the resolution of the chromatographic system. A mass spectrometer works as a highly specific chromatographic detector as well as a high resolution mass spectrometer. Advanced physico-chemical methods, such as LC-MS and GC-MS, can provide true specificity. Fingerprinting can also be fulfilled by using an NMR instrument or IR spectroscopy and that helps with complementary information obtained by using these rapid screening methods. The technique of electrospray ionization mass spectroscopy (ESI-MS) is a useful tool for the analysis of a wide range of different compounds in solution. The following properties should be available in the intended analyte for it to be suitable for analysis by LC-ESI-MS. Firstly, in gas-phase reaction its ionic form must be present in the solution phase or be chargeable through adduct formation. Secondarily, it should have some non-polar structural elements for it to be well separated from salts and avoid suppression effects by interfering compounds. Thirdly upon the collision and generation of a product ion it is desirable that the target analyte fragments with good efficiency for sensitive MS/MS detection [6].

As mentioned above the major instruments for metabolic profiling: are GC-MS and LC-MS. In contrast, direct MS techniques, such as such as quadruple-time of flight (Q-TOF), are used for metabolic fingerprinting. In addition direct spectroscopic techniques - for example, nuclear magnetic resonance (NMR)- Raman and Fourier transform infra-red(FT-IR) can be used for the same purposes. In general, metabolic fingerprinting includes several numbers of measurements greater than metabolic profiling [7, 8].

1.3 Type of analysis used to profile metabolomes.

There are two types of analysis for the metabolome. Targeted analyses: these analyses focus on a small number of analytes and can also be applied quantitatively with the availability of a specific stable isotope labelled internal standard. Such standards are available commercially and are costly. By ignoring the signals of all other compounds that do not need to be measured, only a tiny fraction of metabolome will be measured in targeted analyses. For this reason this type of analysis can be accomplished with high accuracy and precision. Conversely, the other type of analysis, called non-

targeted analyses, can be implemented by using GC-MS when all peaks are characterized by GC retention indices and their mass spectral patterns, above a certain intensity. Metabolomic profiling is also employed in combination with the availability of many software programs [9]. In addition, non-targeted analyses can be applied in LC-MS for metabolic profiling. The third technique used for metabolic profiling is called capillary electrophoresis mass spectrometry (CE/MS) and can be potentially exploited in this subject. However, certain drawbacks reduce the usefulness of this technique, as problems with sample loading and robustness still need to be overcome [10]. Fingerprinting techniques, especially with high mass resolution and the potential for the initial detection of putative biomarkers, allows determination molecular formulae and then attempts to elucidate their structures in combination with highly–specific chromatographic techniques [11].

1.4 Definition of Derivatisation Methods

Derivatisation methods are mainly used to change the chemical structure or increase the molecular weight of an intended analyte, which leads to alteration in the physiochemical properties of the particular molecule which forms a novel compound after being derivatised. Changing the chemical and physical characteristics of a certain sample plays an important role in the analytical field, especially in chemical and pharmaceutical analysis. In recent years bioanalysis has encountered many difficulties in the quantification and detection of an intended analyte. Derivatisation can be used to overcome some of these issues [6]. Derivatisation is a technique that converts a chemical compound into a component with a similar chemical structure that results in the modification of solubility, melting point, boiling point, and new chemical composition, which facilitates separation, detection, intensity, abundance, and quantification by using analytical tools [12, 13]. In mass spectrometry this can lead to enhancing the ionization efficiency and promoting particular product ions by collision induced dissociation (CID) [6]. Thus derivatisation can be the optimum solution for the analysis of substances that cannot be separated or detected with normal analysis, particularly in the area of bioanalysis [6]. Furthermore, chemical derivatisation can lead to a significant change in the ionization properties of the analyte molecules. For instance, esterification of organic acids may reduce the polarity of a molecule [14]. A number of published studies have used derivatisation methods to assist in the detection of their target substances, whether to increase the intensity or abundances that appear with low intensity or to enable analysis of those that cannot be quantified without derivatisation. Specific derivatisation and derivatisation strategies are used for the modification of simple groups such as phenols, thiols, ketones, alkyl halides to form ionic or solution ionisable derivatives. This allows the detection of ionisable derivatives in order to enhance sensitivity, selectivity, and detectability by using MS, LCMS, LCMS/MS, GCMS, and CEMS [14, 15].

1.5 The Gut Microbiome

The mammalian gut microbiota includes over the 55 bacterial divisions, Firmicutes, Bacteroidetes, Actinobacteria and Proteobacteria. Bacteroidetes and Firmicutes account for 90% of the bacterial population in the colon, while Enterobacteriaceae which involve Proteobacteria and Actinobacteria are regularly present but are rare (<1%-5%) a change in the ratio between these groups is suggested to affect intestinal inflammation [16, 17].The interaction between the gut microbiota and human host can trigger specific biological responses both systemically or locally called symbiosis. Therefore the gut microbiota have co-evolved with human host in the context of this symbiosis to fulfil a physiological homeostasis [16]. Different types of gut diseases lead to alteration in the gut microbiota [18]. In the gut, mouth, in saliva and oral mucosa, on the skin and everywhere in human body there are between 10 to 100 trillion bacteria[18].These symbiotic microbial communities and have several beneficial functions for maintaining human health by preventing disease causing bacteria from invading the body, to protect the body from the penetration of pathogenic microbes and also provide the human body with essential nutrition and vitamins by synthesizing them. Human gut microbiota include at least 1000 known different species of bacteria with more than three million genes outnumbering human genes by factor of 150-to 1. Therefore, the microbiome has extensive metabolic capabilities and these microbes provide the host with inaccessible metabolic capabilities. The human gut microbiota contain tens of trillions of microorganisms, with the total weight being up to 2Kg. Two thirds of this microorganisms are specific to each of individual person, whereas one third of gut microbiota is common to most people. Consequently microbiota in the intestine is an individual identity card for each person. Gut microbiota can assist in the digestion of certain foods when the stomach and small intestine are unable to digest this type of food, it also helps with production of some vitamins (B and K). Moreover, gut microbiota can assist in maintaining the integrity of the intestinal mucosa by combating aggression from other microorganisms as well as playing a substantial role in the immune system. When the gut microbiota is balanced and healthy this ensures proper digestive functioning [19]. Dysbacteriosis also called also dysbiosis refers to a microbial imbalance on or inside the body, it is more common as a condition in the digestive tract and has been reported to be connected with diseases such as inflammatory bowel disease, obesity, chronic fatigue syndrome, cancer and colitis. This is due to a microbial imbalance leading to decreasing levels of beneficial bacteria and increasing levels of harmful bacteria (microbial pathogens) this can then lead to the progression and development of many conditions such as inflammatory bowel disease (IBD). Projects on the microbiome have been initiated for recognizing and understanding the roles of these microbial cells and their impact on the human health. Collection of more data on DNA and metabolites will increase the understanding of the connection between metabolites and intestinal microbiota and also how the

specific levels of metabolites can be determined by microbiota and then the physiological state can be assessed by the metabolite profile. The microbiome is relatively plastic unlike the human genome and factors such as probiotics, drugs, diet and microbially produced metabolites can rapidly alter the microbiome. This alteration can affect health. Specific xenobiotics can be activated or deactivated by specific microbes which can alter the effect of various therapeutic agents, thereby intestinal microbiota can be viewed increasingly as an important target of pharmacological agents. The effect of the entire microbial community system on metabolite profiles are just starting to be understood [20]. For example a previous study [21] mentioned that alteration of gut microbiota have been located in patients with cirrhosis that can affect their cognition and systemic inflammatory profile. Therefore the manipulation of the gut microbiota is the basis of treatment for minimal hepatic encephalopathy (MHE). Although the effect of probiotic administration to the patient with MHE using standardized probiotic strains is not clear with regards to the systems biology. Inflammatory bowel disease (IBD) is one of the notable chronic relapsing inflammatory disorders of the bowel. This debilitating disease is widespread in the US with more than a million patients suffering from IBD. The risk of colorectal cancer in humans increases significantly in the presence of IBD. The etiology of IBD remains unclear and many factors such as environmental and genetic factors participate in the appearance and perpetuation of this disease and may play an important role. In addition, the disease progression in the lower bowel is mainly affected by the host immunity and intestinal microbiota, especially the commensal enteric bacteria are important factors that drive the progression of IBD. In the IBD patient alteration of the gut microflora is a common component of the pathophysiology [22]. Metabolite profiling analyses and metabolomics have been widely used to identify disease biomarkers and with the emergence of metabolomics has become a powerful tool for developing and characterizing biomarkers associated with human diseases involving IBD, which can provide valuable information for the detection and development of therapeutic targets [22]. For example, cholesterol, triglyceride and glucose levels in the blood can be quantified to determine the risk of heart disease. The two main instruments LC-MS and NMR are used to analyze metabolites in diverse biological samples such as biopsy samples (tissues), feces and urine [22]. Thousands of metabolites can be analysed simultaneously by these tools which in turn allows researchers to determine the effects of distribution or treatment occurring in the host`s metabolic profile. Moreover, quantitative analysis of global number of metabolites can be achieved by. After that the abundance metabolites demonstrating the biochemical information then can be ascribed to a biological read-out [23]. The effect determination can be achieved through the comparison between the pre-perturbation and post-perturbation metabolomics profiles using multivariate statistics then significantly affected metabolites can be identified and then placed into a larger context to demonstrate how the host was affected overall. LC-MS is the most attractive tool

because of its ability to detect molecules with diverse structures, high sensitivity, dynamic range and quantitative capability. Metabolomics profiling as non-targeted metabolomics using LC-MS analysed metabolite changes in Rag2-/- mice infected with *H. hepaticus* for different time periods (10 week postinfection and 20 week post-infection) and revealed that the majority of metabolites were down regulated in infected animals. There were remarkable effects of the gut microflora on the blood metabolites and several metabolite pathways involving glycerophospholipids, the methionine-homocysteine cycle, the citrate cycle, tryptophan metabolism, purine metabolism and fatty acid metabolism were changed dramatically. Thus by integrating LC-MS with the relevant animal model, metabolomics profiling provided mechanistic insights into IBD and may offer potential biomarkers that can assist for the diagnosis and in measuring the progression of this disease [22]. IBD has been associated with the disturbance of the normally stable intestinal microbiota but the reasons for such an association are not fully understood. Factors contributing to human microbial composition are beginning to emerge through dietary and environmental studies. Understanding the extent and influence of the host genetics on the gut microbiome composition and the mechanisms connecting the microbial function with these genetic traits and disease biology needs much work. Some factors play an important role in the shaping of the intestinal microbial communities such as BMI and age. Of the microbial communities naturally populating the GIT, Firmicutes and Bacteroidetes are the main two classes. Several reports have clarified the correlation between the ratio of Firmicutes to Bacteroidetes and obesity. Obesity leads to a reduction in Bacteroidetes by 50% and proportional increase in Firmicutes [24]. Moreover, the reduction in the protective commensal anaerobes such as *Feacalibacterium prausnitii* and an increase in *E. coli* have been associated with aging. There are significant differences in taxa between cohorts of healthy controls and colorectal cancer (CRC) patients in stool samples this was a consequence of disease status not of the differences in BMI or age [19]. SCFAs especially butyrate are widely studied metabolites and were reported to have anti- tumorigenic effects[19]. Several studies have observed that bacterial species which produce butyrate such as *Ruminoccus* spp and *Pseudobutyrivibrio ruminis* were lower in CRC stool samples compared to the healthy individual samples. Stool samples have many small molecules as result of co-metabolism or metabolic exchange between host cells and microbes. The metabolomic profiling demonstrated a relationship between the metabolites and bacterial populations to figure out biomarkers. The three major SCFAs were produced and detected as microbial metabolites, acetate, butyrate and propionate. The stool samples from CRC patients were significantly higher with acetic acid while the butyric acid was higher in the samples of healthy controls. There were no differences in the detected propionic acid between the two groups. The healthy colon can be maintained by acetate as well and acetate can be used to produce butyrate. Therefore the reduction of butyrate in CRC samples may reflect the

depletion of microbes that conduct this reaction inside the colon or as consequence of degradation of butyrate under low colonic pH associated acetate production. Butyrate is one of the important nutrients for mature non dividing epithelial cells forming colonic, normal (colonocytes) and has also has been shown to induce apoptosis and reduce proliferation in the carcinomas of human colon alone or combination with propionate[19]. Furthermore, the concentrations of the amino acids were increased in the stools of CRC samples except glutamine; this observation has been previously reported in stomach and colon tissue compared to healthy control. It was hypothesized that conversion of glutamine to glutamate was due to increased glutaminase activity [19]. Consistent with these findings, [19] it was found that in the large intestine an approximately 76% increase in glutamate without any increase in glutamine was observed in the samples of CRC patients. Proline, serine and threonine that were monitored in the samples of colon cancer patients result from the degradation of intestinal mucins and may indicate enrichment of mucin- degrading bacteria like *Akker-mansia muciniphila* , observed in CRC stool samples.

1.6 Alterations in the community of the Microbiome can affect the Metabolome.

The metabolic outcome in a host can be directly compared with the metabolism of gut microbiota by using the metabolomic analyses. A comparison of the plasma metabolome between germ-free and conventionally raised mice via untargeted analyses measured the effect of the gut microbiota on the host. It was found that more than 10 % of all metabolites between germ-free mice and mice with gut microbes detected in plasma differed by at least 50%. For example the serum level of tryptophan was decreased by 40% in the conventionally raised mice in comparison to the serum level of tryptophan in the mice without gut microbes. This was attributed to the absence of bacteria producing tryptophanases [25]. Short chain fatty acids such as propionate, butyrate and acetate can be obtained through the fermentation of carbohydrates by intestinal microbiota, several dietary components are not digested in the upper gastrointestinal tract and can provide most of the substrates for intestinal microbiota. Studies have shown that patients with IBDs, as group of inflammatory conditions of colon and small intestine such as Crohn's disease and Ulcerative colitis, have fewer butyrate producing bacteria in their intestine like (*Faecali-bacterium prausnitzii*) leading to lowering of the butyrate level. Treatment of IBD can be achieved by modulation of propionate- and-butyrate producing microbes. Nevertheless, the anti-inflammatory mechanism of butyrate and other SCFA is not fully understood [20]. Studies have explained that the microbial diversity decreases in the obese persons in comparison with lean persons and it was observed that the less diverse microbiota consist of higher proportions of inflammatory effects bacteria. Whereas, the more diverse microbiota consists of higher proportions of the anti-inflammatory microbes in comparison with obese people [18].

1.7 Inflammatory bowel disease (IBD)

IBD is a chronic inflammation of all parts of the gastrointestinal tract and is represented by two major variations, ulcerative colitis (UC) and Crohn's disease (CD). It is diagnosed based on the pattern of inflammation. The pathogenesis of IBD involves dysregulation or ongoing activation of the mucosal immune system driven by alteration of the intestinal microbiota. Although susceptibility genes in genetically predisposed patient also play a role. The exact pathophysiology and etiology are still to be fully clarified. The manner for development of both diseases and their pathogenesis is influenced by environmental factors, diet, smoking habits and microbial factors. Currently, there is an emerging consensus hypothesis proposing that the initiating or maintaining of the disease comes from variable factors such as microbial dysbiosis or changes in the microbial community. Therefore the compositional alteration may be reflected in altered metabolic activities of the gut microbiota which in turn lead to alteration in the metabolites produced [26]

1.8 The aim of this project

1. Qualitative metabolomics profiling for wide range of metabolites in urine and saliva samples from control subjects, patients with active UC, patients with UC in remission in order to try to find diagnostic and prognostic biomarkers.
2. To develop a derivatization method that will increase sensitivity of techniques such as Orbitrap mass spectrometry and tandem mass spectrometry for the quantitative analysis of metabolites containing carboxylic acid groups in particular for the detection of low levels of short chain fatty acids (SCFAs) such as acetic acid, propionic acid, lactic and butyric acid in the urine samples from control subjects, patients with active UC, patients with UC in remission in order to try to find diagnostic and prognostic biomarkers.
3. Application of a previously developed derivatization method for profiling of sugars in urine and saliva samples of control subjects, patients with active UC, patients with UC in remission in order to try to find diagnostic and prognostic biomarkers.

Chapter-2:

Qualitative Metabolomic Profiling of Urine and Saliva by LCMS in order to discriminate between patients with IBD and healthy individuals.

2.1 Introduction

IBD disease has a high incidence in areas such as North America and North Europe and is raised in traditionally low-incidence areas such as Asia and Southern Europe and also in developing countries. 2.2 million individuals from Europe and 1.4 million in the United States suffer from IBD with several factors playing an important role its incidence [27]. The recent therapeutic option for IBD consists of anti-inflammatory medications as well as immunosuppressive and novel biological agents and corticosteroids. Some individuals fail to respond to these remedies and these agents are associated with significant adverse effects. Therefore accurate diagnosis and regular surveillance of IBD is crucial. Presently diagnosis depend upon clinical histologic, serologic, endoscopic and radiologic techniques that are costly and time-consuming in addition to the incomplete expression of IBD or deficiency in histological response of intestinal mucosa. The commonly used erythrocyte sedimentation rate and C-reactive protein do not always correlate with the disease activity and are not specific to IBD inflammation. There are risks including a 1 in 1000 risk of bowel perforation by using technique like endoscopy. Metabolomic analysis refers to the comprehensive study of several small molecules as metabolites found in the biological matrix as well as metabolomic profiles can help for understanding of disease perturbation. Thus mass spectrometry based metabolomic profiling is a technique which can be used for the discovery of biomarkers which could be used for the non-invasive diagnosis and monitoring of disease by sampling bodily fluids and the great clinical value can be obtained from a single test that provides strong diagnostic ability and that could be used to provide disease surveillance and prognostic. Additionally non-invasive biomarkers could be used by gastroenterologist to triage referral for patients with symptoms such as diarrhea and abdominal pain. Several investigators have addressed this issue by performing non-targeted analysis of metabolites. In this study investigation will be applied to urinary metabolomic profiles of patients with active UC, quiescent (remission) UC and controls with IBD attending the GI clinic at Glasgow Royal Infirmary. In this study the biofluids were used will be urine and saliva [26].

2.2 Experimental

2.2.1 Materials, Chemical and reagents

LC-MS grade acetonitrile and ammonium carbonate were obtained from Sigma Aldrich Dorset UK. A range of 200 metabolite standards were available from previous studies and were obtained from Sigma Aldrich. LC-MS grade water was prepared in-house using a Milli Q purification system.

2.2.2 General Equipment

My Fluge mini centrifuge, Type : C100-B (Fisher Scientific, Leicestershire) Tube one®, 1.5 ml Natural Flat cap microcentrifuge tubes (STAR Lab, UK). Model: G-560E was obtained from Scientific Industries, USA (Fisher Scientific, Leicestershire). Gilson Pipetman Pipettes (Star Lab, UK). The columns used in these experiments were a ZIC-pHILIC column SeQuant®,ZIC®pHILIC,150mm x 4.6, 5 µm particle size and a ZIC®pHILIC, peek 20x2.1 mm, metal-free guard column (Hichrom Limited, Reading, UK).

2.2.3 LC-MS instrument and Conditions

LC-MS: Accela HPLC with Orbitrap Exactive supplied by Thermo Scientific, Bremen, Germany. The ESI interface was operated in a positive/negative polarity switching mode. The spray voltage was 4.5 kV for positive mode and 4.0 kV for negative mode. The temperature of the ion transfer capillary was 275°C and sheath and auxiliary gases was 50 and 17 arbitrary units respectively. The full scan range was 75 to 1200 m/z for both positive and negative modes with settings of Automatic Gain Control (AGC) target and resolution as Balanced and High (1E6 and 50,000) respectively. The data were recorded using Xcalibur 2.1.2 software package (Thermo Fisher Scientific). Mass calibration was performed for both ESI polarities before the analysis using the standard Thermo Calmix solution and the signals of 83.0604 m/z (2 x ACN+H) and 91.0037 m/z (2 x formate-H) were selected as lock masses for positive and negative mode respectively during each analytical run.

2.2.4 Methodology

Mobile phase A (aqueous phase) was prepared by dissolving 1.92g of ammonium carbonate in 1 litre of distilled water, and adjusting the pH to approximately 9.1. Mobile phase B was pure acetonitrile. Metabolite separation was achieved using a ZICpHILIC column on an Accela HPLC interfaced to an Orbitrap Exactive system equipped with an Electrospray Ionization Source (ESI) operated in both positive and negative modes. The separation was achieved by running samples in a random sequence to minimize bias after running a blank (extraction solution). Using two mobile phases, mobile phase A

(20mM ammonium carbonate) and mobile phase B (100 % Acetonitrile), in a gradient system for 46 minutes as shown in Table 2. 1.

Table 2. 1: Display mobile phase gradient programme in LC-MS analysis.

Time (min)	A%	B%	Flow rate(µl/min)
0	20	80	300
30	80	20	300
31	92	8	300
36	92	8	300
37	20	80	300
46	20	80	300

2.2.5 Collection of Clinical Samples

After obtaining written informed consent, urine samples were collected from 63 patients (Table 2.2) attending the GI clinic with a confirmed diagnosis of either active UC (12), quiescent UC (26) controls without IBD (25). Unfortunately in some cases the sample was missing or there was no bar code so only 51 samples could be used in the study. At the same time saliva samples were collected from 65 patients (Table 2.3). Ethical approval was obtained from both NHS and University of Strathclyde ethical committees.

2.2.6 Preparation of the urine samples

Urine samples were taken from the freezer to be thawed out and well mixed, after that 0.2 ml was transferred from each urine sample into an Eppendorf and each sample was mixed with 0.8 ml of acetonitrile (ACN) inside the Eppendorf. Then each Eppendorf was centrifuged until two layers formed a precipitate and supernatant. The supernatant was removed from each Eppendorf and transferred to a HPLC vial for analysis using the ZICpHilic metabolomics method.

Table 2. 2: Details of 56 urine samples provided from Gastroenterology Unit, Glasgow Royal Infirmary hospital , Divided into three groups .

Samples	Group type	Barcode	Samples	Group type	Barcode
Urine1	----------	(NOT AVAILABLE)	Urine34	C(healthy control)	0608706132
Urine2	R(remission UC)	2208816293	Urine35	R(remission UC)	0105535176
Urine3	R(remission UC)	0108486028	Urine36	C(healthy control)	1503546276
Urine4	R(remission UC)	0501456112	Urine37	C(healthy control)	2202526412
Urine5	C(healthy control)	1603860681	Urine38	R(remission UC)	1910436348
Urine6	----------	(NOT AVAILABLE)	Urine39	C(healthy control)	1412666260
Urine7	----------	(empty)	Urine40	R(remission UC)	2402395168
Urine8	R(remission UC)	1710800992	Urine41	R(remission UC)	0403356024
Urine9	A (UC active)	2309735299	Urine42	R(remission UC)	1906506205
Urine10	C(healthy control)	2403426008	Urine43	C(healthy control)	1208646680
Urine11	A (UC active)	1309446156	Urine44	----------	(NOT AVAILABLE)
Urine12	R(remission UC)	1202465293	Urine45	C(healthy control)	2012456243
Urine13	R(remission UC)	0607425172	Urine46	R(remission UC)	3105626964
Urine14	----------	(empty)	Urine47	A (UC active)	1903566134
Urine15	R(remission UC)	2801796247	Urine48	R(remission UC)	2001416121
Urine16	A (UC active)	1001913361	Urine49	R(remission UC)	2205576313
Urine17	R(remission UC)	0511550618	Urine50	A (UC active)	2603775057
Urine18	R(remission UC)	0503725927	Urine51	R(remission UC)	2707825972
Urine19	C(healthy control)	1606906003	Urine52	C(healthy control)	0507686047
Urine20	A (UC active)	1508905290	Urine53	R(remission UC)	1508915075
Urine21	A (UC active)	2906706221	Urine54	R(remission UC)	0409475041
Urine22	A (UC active)	1411676572	Urine55	A (UC active)	0505606585
Urine23	R(remission UC)	0701956291	Urine56	C(healthy control)	0906716020
Urine24	R(remission UC)	2808586426	Urine57	C(healthy control)	2106606524
Urine25	C(healthy control)	2208726367	Urine58	A (UC active)	1711895296

Urine26	**C(healthy control)**	**2310666408**	**Urine59**	**R(remission UC)**	**1306526000**
Urine27	**C(healthy control)**	**1302796186**	**Urine60**	**A (UC active)**	**2502575192**
Urine28	**C(healthy control)**	**2303566185**	**Urine61**	**A (UC active)**	**2809668000**
Urine29	**R(remission UC)**	**1312466510**	**Urine62**	**C(healthy control)**	**1501676024**
Urine30	**A (UC active)**	**2109646543**	**Urine63**	----------	**No barcode**
Urine31	**R(remission UC)**	**1901945138**	----------	----------	----------
Urine32	**A (UC active)**	**0806626216**	----------	----------	----------
Urine33	----------	**No barcode**	----------	----------	----------

2.2.7 Preparation of the Saliva samples

Saliva samples were taken from the freezer left to thaw out and then well mixed. After that 0.2 ml was transferred from each saliva sample into the Eppendorf and each sample was mixed with 0.6 ml of ACN inside the Eppendorf. Then each Eppendorf was centrifuged until two layers formed precipitate and supernatant. The supernatant was removed from each Eppendorf and transferred to a HPLC vial for analysis using the ZICpHilic metabolomics method.

Table 2. 3: Details of 65 saliva samples provided from the Gastroenterology Unit, Glasgow Royal Infirmary hospital , Divided into three groups .

Samples	Group type	Barcode	Samples	Group type	Barcode
Saliva1	**R(remission UC)**	2205576313	**Saliva34**	**C(healthy control)**	1606906003
Saliva2	**A (UC active)**	1309446156	**Saliva35**	**R(remission UC)**	0105535176
Saliva3	**R(remission UC)**	2001416121	**Saliva36**	**C(healthy control)**	0906716020
Saliva4	**A (UC active)**	1411676572	**Saliva37**	**C(healthy control)**	1412666260
Saliva5	**C(healthy control)**	0608706132	**Saliva38**	**R(remission UC)**	0701956291
Saliva6	**A (UC active)**	2603775057	**Saliva39**	**R(remission UC)**	1708985913
Saliva7	**A (UC active)**	0505606585	**Saliva40**	**R(remission UC)**	0403356024
Saliva8	**A (UC active)**	1508905290	**Saliva41**	**A (UC active)**	2906706221
Saliva9	**R(remission UC)**	1202465293	**Saliva42**	**C(healthy control)**	0102416060

Saliva10	**C(healthy control)**	0808423185	**Saliva43**	**C(healthy control)**	2208726367
Saliva11	**A (UC active)**	0806626216	**Saliva44**	**R(remission UC)**	0503725927
Saliva12	**R(remission UC)**	3105626964	**Saliva45**	**A (UC active)**	1711895296
Saliva13	**R(remission UC)**	0511550618	**Saliva46**	**R(remission UC)**	1901945138
Saliva14	**A (UC active)**	0505606585	**Saliva47**	**A (UC active)**	3010776489
Saliva15	**R(remission UC)**	2801796247	**Saliva48**	**R(remission UC)**	1910436348
Saliva16	**C(healthy control)**	1603860681	**Saliva49**	**C(healthy control)**	1302796186
Saliva17	**R(remission UC)**	1906506205	**Saliva50**	**C(healthy control)**	0507686047
Saliva18	**C(healthy control)**	1001726049	**Saliva51**	**R(remission UC)**	0409475041
Saliva19	**A (UC active)**	2809668000	**Saliva52**	**R(remission UC)**	2102733432
Saliva20	**C(healthy control)**	1312466510	**Saliva53**	**A (UC active)**	1903566134
Saliva21	**C(healthy control)**	2403426008	**Saliva54**	**A (UC active)**	2502575192
Saliva22	**C(healthy control)**	1409606007	**Saliva55**	**C(healthy control)**	2106606524
Saliva23	**C(healthy control)**	1503546276	**Saliva56**	**R(remission UC)**	0607425172
Saliva24	**R(remission UC)**	0501456112	**Saliva57**	**R(remission UC)**	2402395168
Saliva25	**R(remission UC)**	1710800992	**Saliva58**	**C(healthy control)**	2310666408
Saliva26	**A (UC active)**	2309735299	**Saliva59**	**A (UC active)**	2310796212
Saliva27	**A (UC active)**	2909856054	**Saliva60**	**C(healthy control)**	1501676024
Saliva28	**R(remission UC)**	2208816293	**Saliva61**	**C(healthy control)**	2202526412
Saliva29	**R(remission UC)**	1508915075	**Saliva62**	**C(healthy control)**	2303566185
Saliva30	**C(healthy control)**	1208646680	**Saliva63**	**R(remission UC)**	2808586426
Saliva31	**R(remission UC)**	0108486028	**Saliva64**	**C(healthy control)**	2101585170

Saliva32	**R(remission UC)**	2707825972	**Saliva65**	**A (UC active)**	1001913361
Saliva33	**C(healthy control)**	2012456243	----------	----------	----------

2.2.8 Data processing and analysis

After collection of Raw LC-MS data by using Xcalibur software, data processing can be achieved by several types of software e.g., mzMatch[28], XCMS[29]and IDEOM[30].Raw LC-MS data are processed with conversion of instrument-specific data format to XCMS for Untargeted peak- picking and mzMatch for annotation and peak matching, then the identification done by IDEOM, IDEOM using default parameters was applied for identification and noise filtering. Metabolite identification was fulfilled by matching accurate masses and where available the retention time of metabolite standards. LC-MS data were processed with mzMatch, the peaks fits with accurate retention time and accurate masses were then selected for interpretation . Extracted MS data were modelled by using Simca P 14.0 (Umetrics, Sweden). The aim of using Simca P is to reduce the dimensionality of datasets and provide better visualization and it reveals relationships between datasets[31, 32]. It can be simply used by uploading Excel spreadsheets derived from the output of mzMatch.

2.3 Results and discussion

2.3.1 Results from the Analysis of urine samples From Active, Quiescent and Control

Urinary metabolites are highly prone variation due to environmental factors, such as medications and diet, resulting in great inter-subject variability, for example treatment with antibiotics lead to changes in the composition of gut bacterial in mice which then may alter the urinary metabolites, therefore other biofluids may provide a more reliable approach for quantitative metabolite analysis. In this present study urine samples were analysed by using a LCMS based metabolomics approach to show a comparison of urinary metabolite profiles of healthy individuals with those of participants having UC (active and remission). The data was extracted from m/z Match and Principal Component Analysis (PCA), an unsupervised classification method was applied by using Simca P. PCA is useful for identifying unexpected variation and trends in the data. In this study PCA was used to discover whether or not there are large variations between the three groups but it was unable to distinguish between the three groups (Figure 2.1) in the first two components although there was some separation in the third component (Figure 2.2).

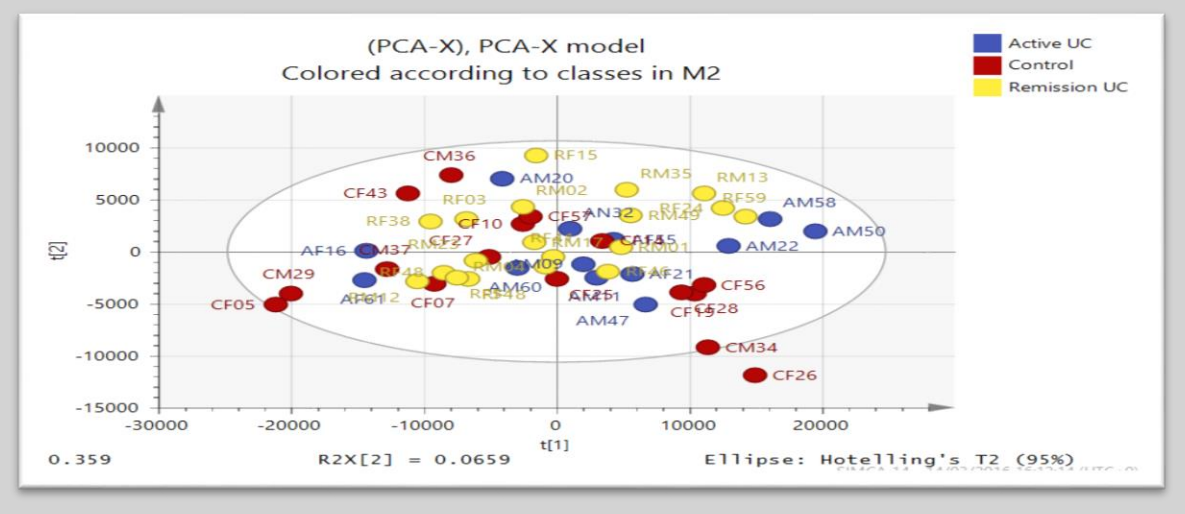

Figure 2. 1: Two dimensional PCA score scatter plot showing the relationship between three groups

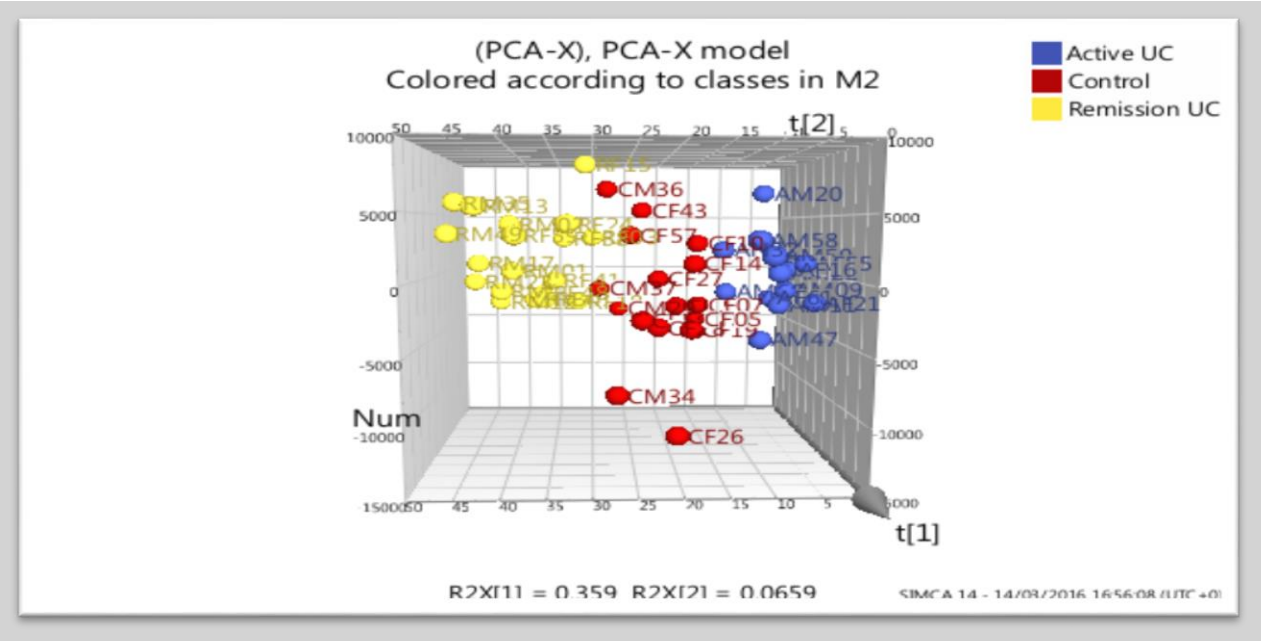

Figure 2. 2: Three dimensional PCA score scatter plot showing the relationship between three groups.

PCA: Is statistical method used to explain variance structure of set of variables through linear combination.

OPLSD: multi variate analysis method has prediction and modeling properites depend on regression analysis that based on principle component analysis.

Hierarchical clustering analysis (HCA) HCA classified the groups into two main groups as shown in Figure 2. 3 but there was no separation according to condition[32].

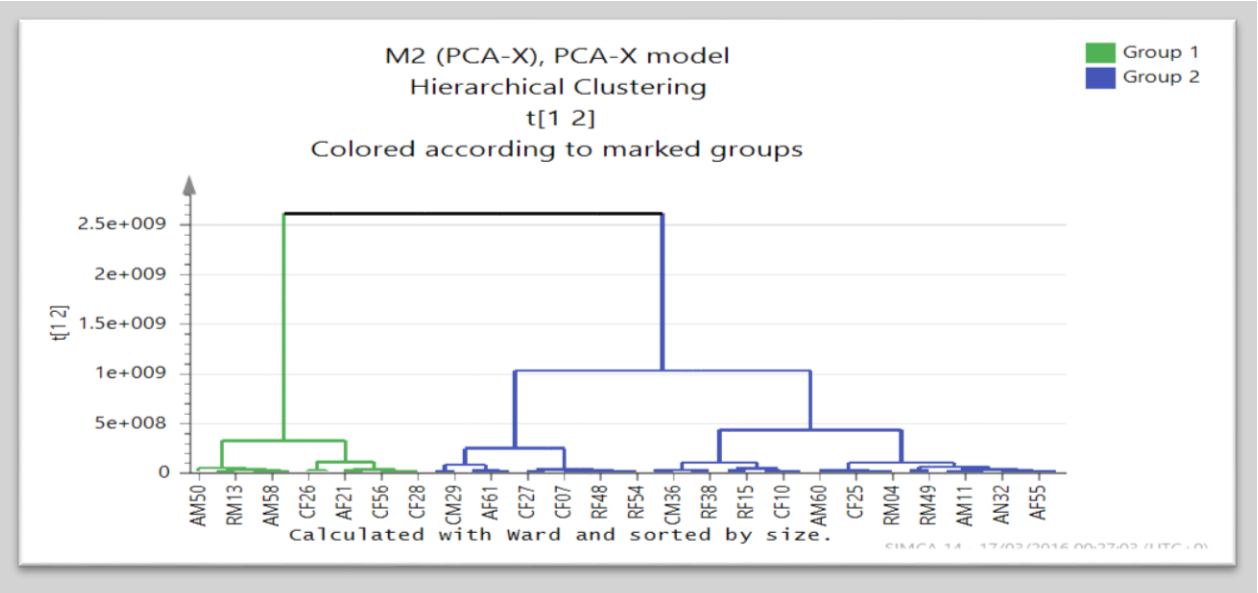

Figure 2. 3: Hierarchical Clustering Analysis (HCA)display the degree of similarity between groups as unsupervised model.

The dendrogram shows observations clustered into three groups. X-axis represents the samples and y-axis shows the variability index. The higher the variability index the larger between group variability and the lower the variability index, the smaller the between group variability. The plot divides samples into two groups; group 1 (green) and group 2 (blue). Characters on the x-axis are (AM) active UC male, (RM) remission UC male, (AF) active UC female, (RF) remission UC female, (CM) control male and (CF) control female, the last two characters represents the patient's number.

2.3.1.1 Log transformation of the data

In order to minimise the effect of skewing in the data log transformation of the data from m/z Match was carried out. There was still no separation of the classes by PCA (figure 2.4). In addition, HCA produced no separation of the classes (figure 2.5).

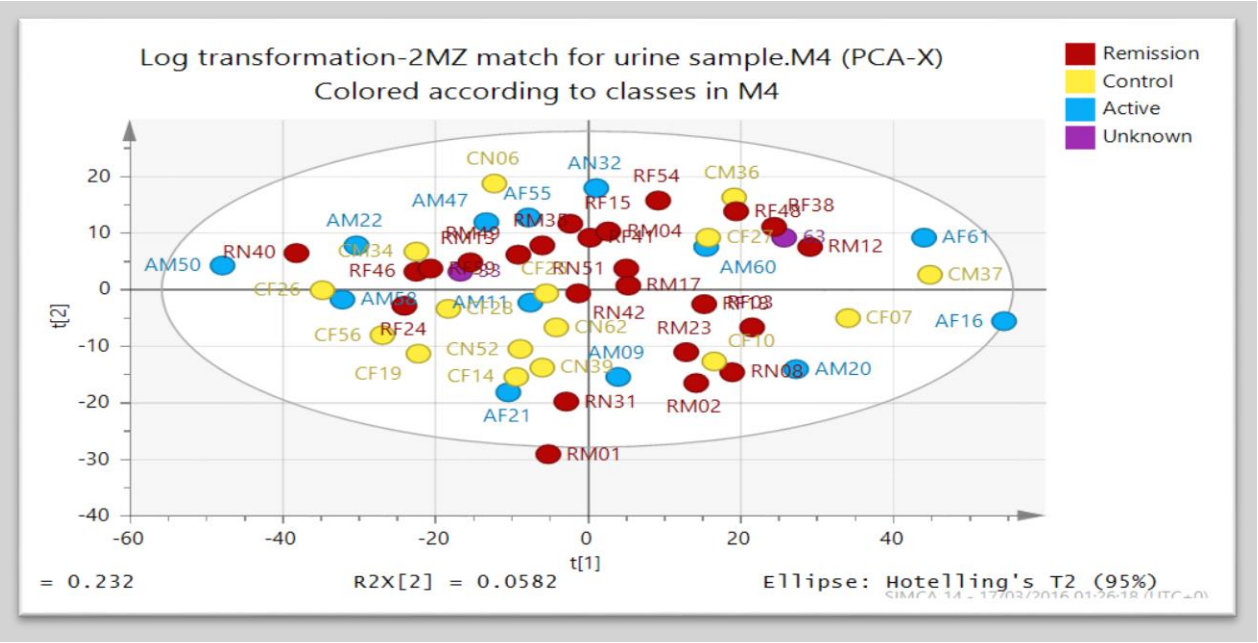

Figure 2. 4: 2D PCA score scatter plot display the relationship between three groups after log transformation output from the M/Z match.

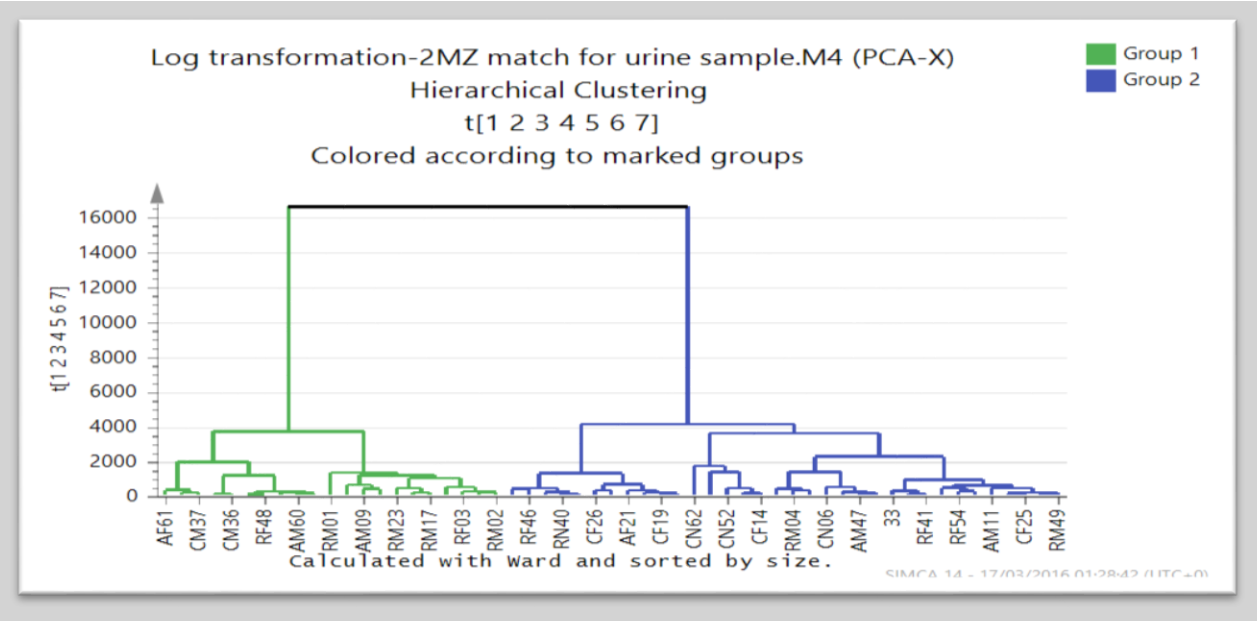

Figure 2. 5: HCA display the degree of similarity between groups as unsupervised model after log transformation output from the M/Z match.

An orthogonal partial least squares discriminant analysis (OPLSDA) model, where the groups are specified, produced separation between the three sample groups (figure 2.6). The separation between the groups is in the X-direction while the Y-direction shows a large amount of orthogonal within group variation that does not provide any classification.

.

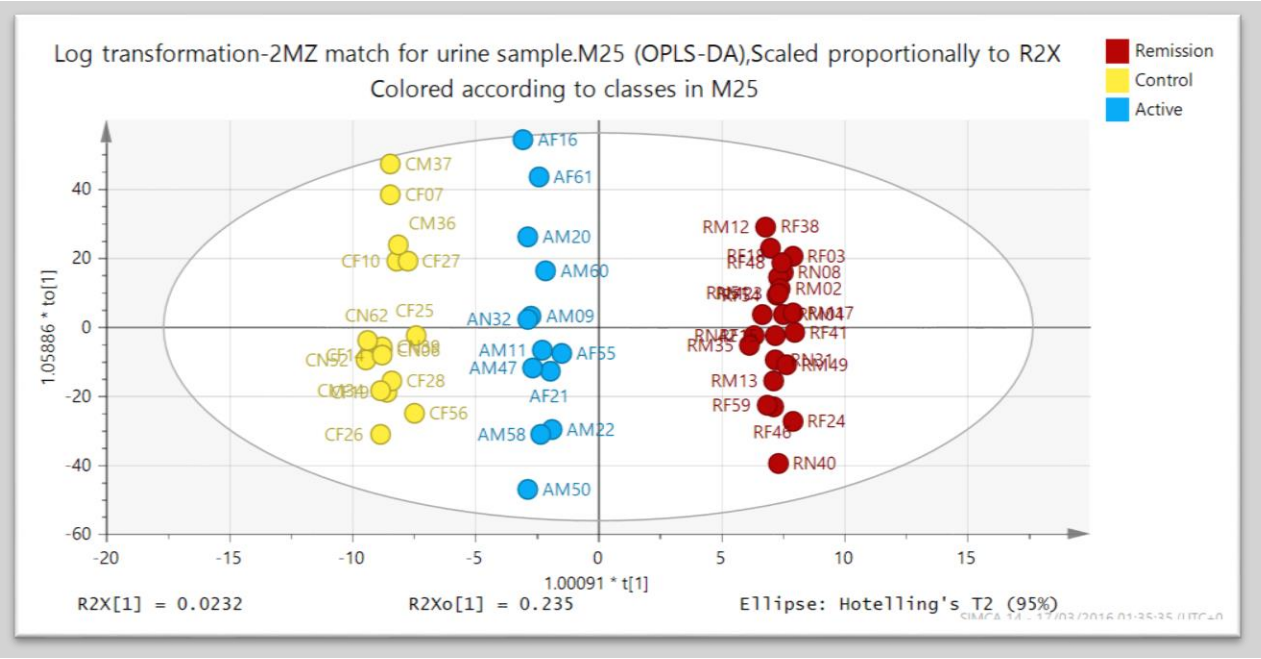

Figure 2. 6: Orthogonal partial least squares discriminant analysis model comparing patients with active UC male (AM), active UC female (AF), remission UC male(RM), remission UC female (RF),controls male(CM) and control female(CF) OPLS-DA as score plot showing the classification of the three groups as supervised model after log transformation output from the M/Z match.

Figure 2.7 shows the cross-validation test for the model which is not particularly strong since in particular some of the blue squares in the permutation test are above the blue square on the right hand side although the intercept is below 1 which lends some validity.

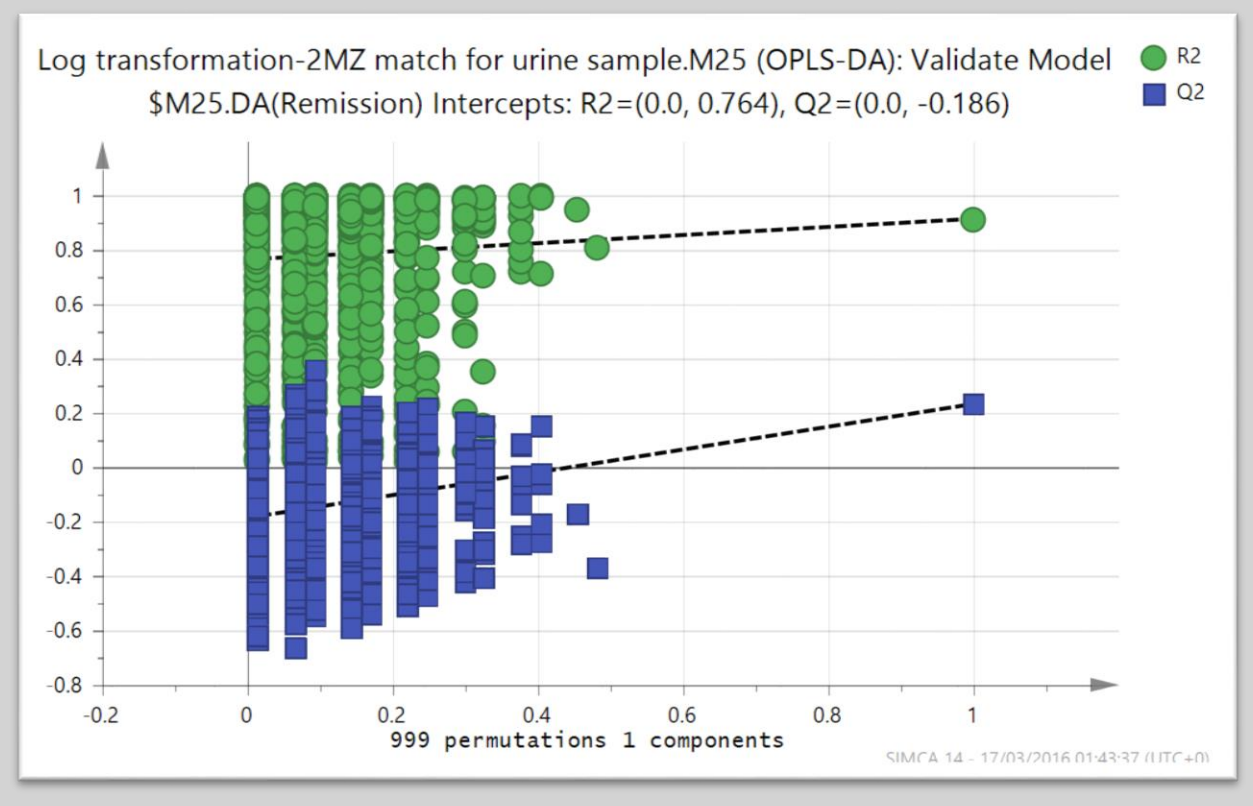

Figure 2. 7: permutation plot as validation of the model to compare the goodness of fit (R2 and Q2) of the original model with the goodness of fit of several models based on data where the order of the Y-observations has been randomly permuted, while the X-matrix has been kept intact after log transformation output from the M/Z match

Figure 2.8 Shows comparison of urine metabolite profiles from 13 patients with active IBD in comparison with 16 control samples. The comparisons were simplified by comparing just the IBD patients with controls (figure 2.8). The model had some validity as indicated in figures 2.9 and 2.10. The most important markers separating active and control samples are shown in table 2.4.

2.3.1.1.1Comparison of Control and active

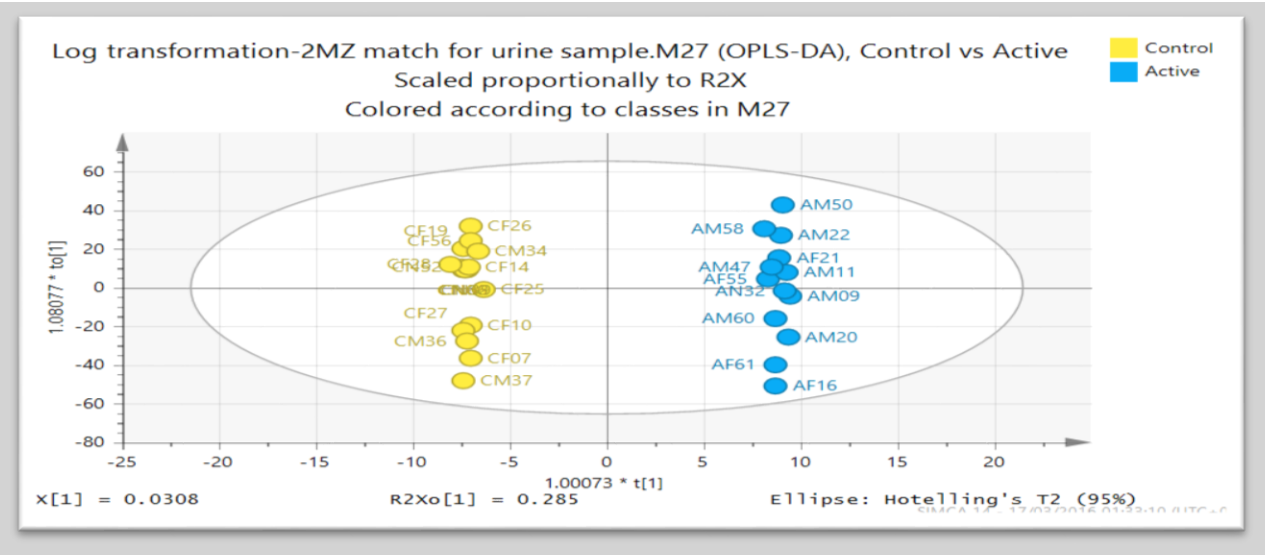

Figure 2. 8: Orthogonal partial least squares discriminant analysis (OPLSDA) model comparing patients with active UC male (AM), active UC female (AF), controls male (CM) and control female (CF). R2X (cum) 0.458, R2 Y (cum) 0.998, Q2 (cum) 0.282.

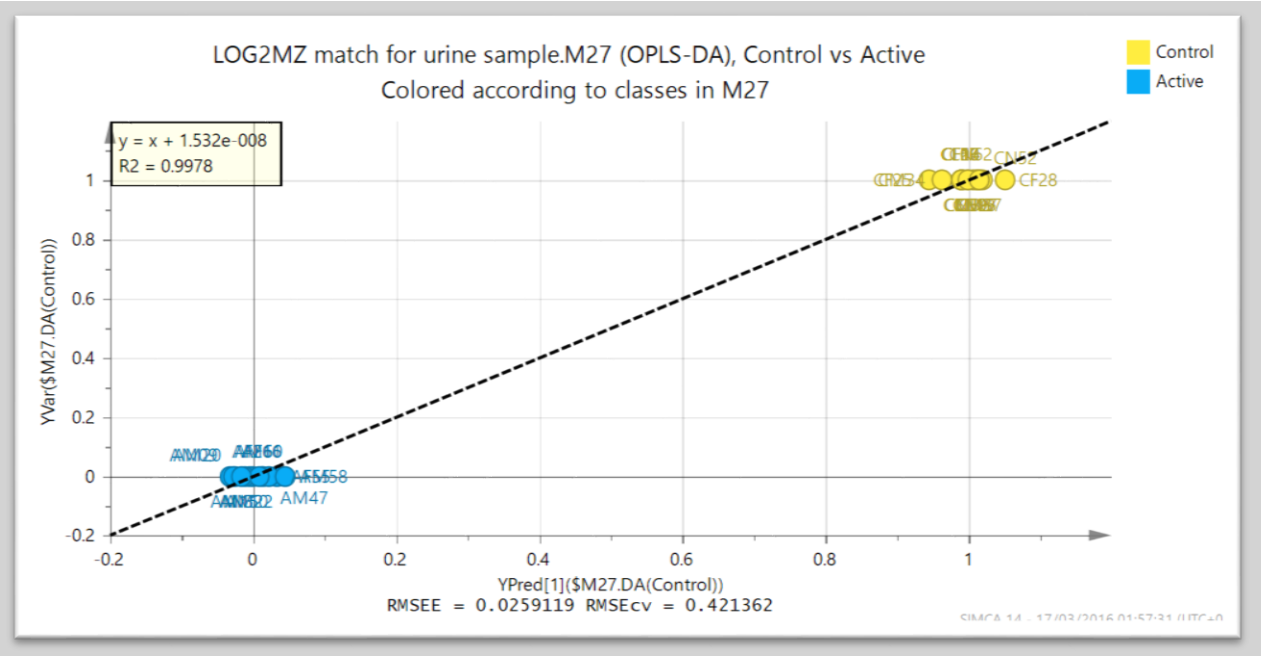

Figure 2. 9: This plot display the observed versus predicted value of the selected Y- variable and the regression line R2 close to one that indicate and excellent model and valid.

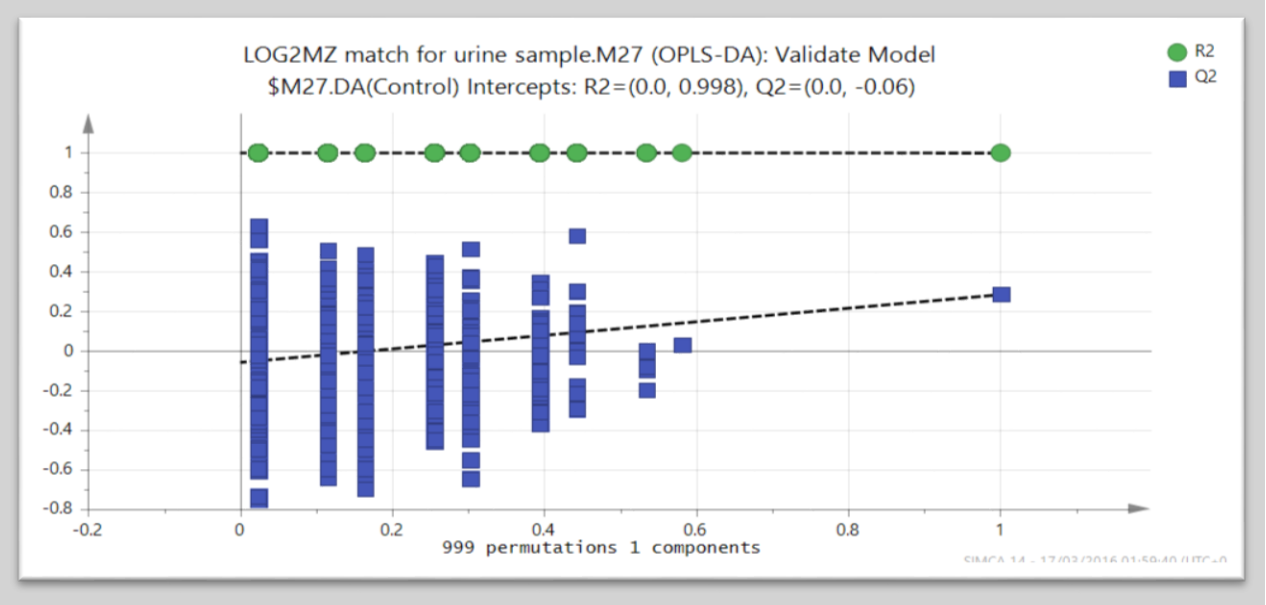

Figure 2. 10: permutation plot as validation of the model to compare the goodness of fit (R2 and Q2) of the original model with the goodness of fit of several models based on data where the order of the Y-observations has been randomly permuted, while the X-matrix has been kept intact after log transformation output from the M/Z match.

Table 2. 4: Biomarkers used in the model separating controls and active UC.

Metabolite	P value	Ratio control/active
N-Hydroxyarylamine	0.0163	0.0731
N-acetyl-isatin	0.0038	0.2157
3, 4-Dihydroxymandlate	0.0452	0.2976
N, N-Dimethylglycine	0.0439	0.8803
Hexadecanoic acid	0.0234	1.7420
Octadecanoic acid	0.0102	1.7717
N-Formyl-L-aspartate	0.0465	3.1109
3-Amino-3-(4-hydroxyphenyl) propanoate (Beta tyrosine)	0.0140	6.8440
D-Glucuronolactone	0.0203	6.7977

Several metabolites were found to be significantly different between the active UC and healthy controls and there were significant differences between the remission and healthy control cohorts. For example, 3,4-Dihydroxymandelic acid was increased in the urine samples of active UC compared with healthy control as well as the level of this metabolite was higher in the samples of remission cohorts than control and this result was correlated with a prior study where by using animal model and they demonstrated that the 3,4-Dihydroxymandelic acid was higher in non-polyp tissues of APC $^{min/+}$ mice with a mutated *APC* gene than in the normal tissues of the control mice[33]. N, N-Dimethylglycine is the other metabolite that was significantly different between the active UC and healthy control and significantly different between the remission group and healthy control group. A previous study demonstrated that N,N-Dimethylglycine (DMG) appears to be an effective immunomodulator and intermediate in the degradation of choline. Also it is a significant biosynthetic intermediate in formation of pangamic acid which is an immunomodulatory compound. DMG was reported in guinea pigs to assist in reversing immunosuppression after irradiation. In the human body and in rabbits DMG alone enhanced lymphocyte proliferation and antibody levels. *In vitro* when the DMG was administrated to hybridoma cells antibody output significantly increased. In addition to that because DMG has properties of cytoprotection of the gastric lining and its free radical scavenging

activity, DMG was shown to reduce ulcer size, number and index after the induction of gastric ulcer [34]. In this study, N, N-Dimethylglycine was up regulated in the active UC samples and quiescent UC samples in comparison to the control samples. Prior study by using a mouse model showed that N, N-Dimethylglycine was increased in the case of interleukin-10 gene-deficiency in a mouse model of IBD in comparison to control wild-type mice [35]. Moreover, by measuring metabolites in urine samples as metabolic markers of inflammatory bowel disease in of an interleukin-10 gene-deficient mice and metabolic profiles of wild type mice it was found that the urinary fingerprint of IL-10 gene-deficient and wild-type mice was similar at 4 weeks, before development of IBD in the IL-10 gene-deficient mouse model. A major change occurred after 8 weeks between metabolites of the IL-10 gene-deficient mouse model and wild-type mouse. N, N-Dimethylglycine appeared at week 20 in the IL-10 gene-deficient mouse model but in the wild-type mouse was not found at week 20 [36].

N-acetyl-isatin is metabolite found to be significantly different between the UC active and healthy participants as well as being observed to be up regulated in the urine of patients who had UC (active and remission) in comparison to those with non UC illness. During tryptophan metabolism first tryptophan is converted indole after that indole converted to indoxyl, following this indoxyl is converted to acetylindoxyl finally N-acetyl-isatin formed from acetylindoxyl via an oxidoreductase enzyme. Hence catabolism of tryptophan leads to the formation of N-acetyl-isatin. Therefore, when the level of tryptophan is increased as result there is up regulation of N-acetyl-isatin since tryptophan is the one of the sources for the formation of N-acetyl-isatin. In a previous study it was mentioned that the level of tryptophan was increased in the urine of UC patients compared to healthy individuals which is compatible with the finding in the current research[37]. Also it was found that there was up regulation of tryptophan in CD patients in comparison with healthy control in fecal extracts[38]. In contrast, another paper indicated the down regulation of tryptophan in the urine of individuals who had IBD in comparison with healthy individuals [39]. Moreover N-acetyl-isatin and its derivatives have been used as anticonvulsants for the treatment of epilepsy[40]. Isatin was found to be anti-inflammatory, antimicrobial and have anti-fungal activities. In addition, isatin has been identified in humans as endogenous compound that has a broad range of biological activities such as sedative activity[41]. Another metabolite N-Formyl-L-aspartate is significantly different between control vs active UC and control vs remission, this metabolite is one of the precursors of histidine metabolism and was found down regulated in the urine samples of active UC compared to the urine samples of healthy controls. In addition, the level of N-Formyl-L-aspartate was decreased in quiescent UC urine samples in comparison to control samples. Examining the pathway of histidine metabolism, L-histidine is converted to histamine and this reaction is carried out by decarboxylation via histidine decarboxylase. Histamine can be inactivated in mammals by two major routes 1- methylation of the

imidazole ring by histamine-N-methyltransferase 2- oxidative deamination of the primary amine group catalysed by diamine oxidase for the formation of imidazole acetaldehyde and imidazole acetic acid (Figure 2. 11). Histamine plays an important role in inflammatory conditions, gastric acid secretion and as a neurotransmitter. The inflammatory responses resulting from the liberation of histamine are mediated by the histamine H_1 receptor and antihistamines act at the H_1 receptor antagonist [42]. Histidine metabolism leads to the conversion of L-histidine to histamine and then histamine is deactivated to imidazole acetaldehyde then to imidazole acetate which in turn is converted to *N*-formimino- L-aspartate and finally to N-Formyl-L-aspartate. In the current study the level of N-Formyl-L-aspartate was decreased in UC patients appearing to be logical consequence of the inflammatory process, due to the formation and release of histamine which in turn led to less production of N-Formyl-L-aspartate. Whereas in the healthy control group the deactivation of histamine occurs leading greater production of N-Formyl-L-aspartate. Other studies compatible with the current research mentioned that histidine was down regulated in IBD patients compared to healthy people by analysing their urine samples, for example one study demonstrated histidine was reduced in patients with IBD in remission[43]. Furthermore, it was found that there was a reduction of histidine in the urine samples of patients with UC compared to healthy controls[39].

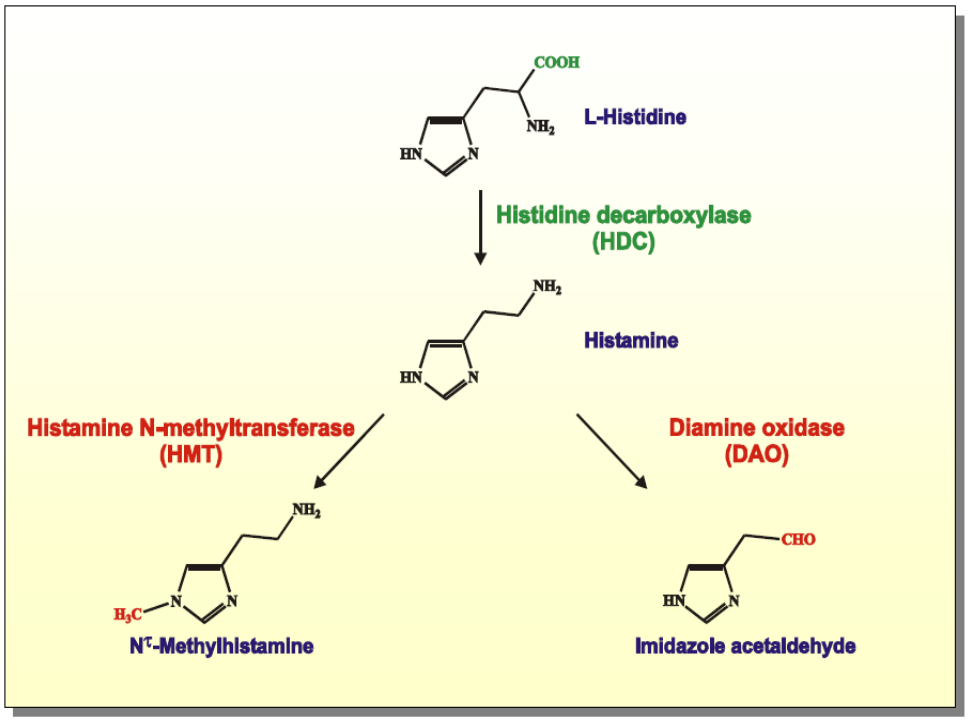

Figure 2. 11: The histidine metabolism pathway and the conversion of histidine to histamine as well as the two main routes for the deactivation of histamine [44].

Moreover, 3-Amino-3-(4-hydroxyphenyl) propanoate was found to be significantly different between UC patients and healthy controls. From the tyrosine metabolism pathway tyrosine is converted into 3-

Amino-3-(4-hydroxyphenyl) propanoate via the tyrosine 2, 3- aminomutase enzyme. This enzyme participates in tyrosine metabolism. From previous information tyrosine decrease lead to 3-Amino-3-(4-hydroxyphenyl) propanoate decrease as well. As a result was 3-amino-3-(4-hydroxyphenyl) propanoate was observed to be down regulated in the urine samples of patients with UC (active and remission) compared to samples of healthy controls which is correlated to of the findings of previously published study[44]. The current study demonstrated a decrease in tyrosine in the urine of individuals who had IBD compared to the healthy control, an explanation could be from the intestinal malabsorption caused by the disease which is a correlates with the finding of increased amino acids in the faeces [39, 44, 45]. D-Glucuronolactone is another metabolite was detected to be significantly different between the two cohorts control and active. This metabolite was reduced in the urine samples of active UC and quiescent UC compared with healthy individuals. Glucuronolactone is a precursor of ascorbate and aldarate metabolism. Previous studies found that *myo*- inositol was downregulated in urine samples of active UC versus control by using NMR [46], and decreased as well in active UC of the colon mucosal tissue extracts in comparison with controls[47]. Myo-inositol is also involved in the ascorbate and aldarate metabolism pathway as well and is converted to the D –glucoronate via the inositol oxygenase enzyme, after that D –Glucoronate is converted to to D-glucuronolactone through the glucuronolactonase. Therefore, by reduction of *myo*- inositol leads to the downregulation of D-glucuronolactone which is compatible with the result which was obtained from the current study.

Octadecanoic acid and hexadecanoic acid were significantly different between healthy control and active UC. A previous study analysed the colonic mucosa of patients with ulcerative colitis and controls and found that the ratios of oleic acid to stearic acid and to palmitic acid were lower in inflammatory bowel disease and the arachidonic acid was significantly higher in UC than in controls as well as the alteration of the fatty acids profile may be partly demonstrate the increased synthesis of eicosanoids in colonic mucosa in inflammatory bowel disease which is compatible with results were obtained in the current study [48]. Another study determined the fatty acid pattern in Crohn's disease, by measuring the serum fatty acids in 20 patients and 18 healthy controls ,the results obtained showed that the serum concentrations of stearic acid ($C_{18:0}$), eicosapentaenoic acid ($C_{20:5}$n3), dihomo- γ-linolenic ($C_{20:3}$n6), γ-linolenic acid ($C_{18:3}$n6) and total n3 PUFAs as polyunsaturated were significantly lower in patients with active CD in comparison to those with inactive CD which is correlates with the findings in the results of the current research[49]. Another study using an animal model demonstrated that conjugated linoleic acid (CLA) ameliorated colonic inflammation where it was triggered by enteric bacterial pathogen (Brachyspira hyodysenteriae), palmitic acid was slightly lower in the group with colonic inflammation in comparison to the other groups which is similar to that observed in the current

study [50]. In contrast, another reference mentioned that the level of palmitic acids ($C_{16:0}$) and palmitoleic acid ($C_{16:1}$n7) were higher in CD patients than in controls [49]. Furthermore, one of the prior studies carried out by using FT- ICR-MS, indicated that the masses corresponding to both unsaturated and saturated fatty acids, involving stearic acid , palmitic acid, 6Z-,9Z- , linoleic acid and arachidonic acid are relatively higher in patients with ICD than in a healthy group [38] which is not consistent with the current results. Another study reported that plasma fatty acids were significantly increased in remission IBD in comparison to controls, contrary to the decreased levels which were observed in the current study[51].

N-Hydroxyarylamine was significantly different between active IBD and control and was shown to be increased in active UC compared to control and remission, whereas the N-Hydroxyarylamine was more decreased in control samples than in quiescent samples. A previous study explained that the accumulation of multiple and specific genetic mutations with the endogenous carcinogenic compounds such as arylamines promotes neoplasia [52] therefore more importantly for intestinal exposure to carcinogens heterocyclic amines and their hydroxyl amine metabolites, which are substrate for NAT (arylamine *N*-acetyltransferase) in humans. NAT determines the vulnerability to colorectal cancer the activity of NAT detected and determined in the epithelial cells of the intestine. In addition, UC and CD are associated with epithelial dysplasia, the role of NAT is very important due to the formation of ultimate carcinogenic compounds which react with DNA. Moreover, NAT is more active with heterocyclic amines and NAT catalyses both activation (*O*-acetylation) and deactivation(*N*-acetylation) [53]. It was suggested that the rapid acetylator phenotype, via the enhanced colonocytic activation of N-hydroxyarylamine through *O*-acetylation, may be predisposed to colorectal cancer. Catalysis of the metabolic activation of N-hydroxyarylamine determines the capacity of human arylamine N-acetyltransferase suggesting a role for the acetylator genotype in the metabolic activation of N-hydroxyarylamine to form DNA adducts which can initiate cancer of the colon and rectum. Therefore, variation of intestinal activity of NAT probably to affects a range of carcinogens. From two previous studies NAT was determined in the epithelial cell of intestine and the epithelial cells in colorectal cancer became damaged also UC and CD are associated with epithelial dysplasia. Thus N-hydroxyarylamine could increase in patients with active UC due to activity of NAT being decreased compared to controls. This finding is compatible with results taken from the current study were the level of N-hydroxyarylamine is higher in active UC group than the control.

2.3.1.1.2 Comparison of Control and remission

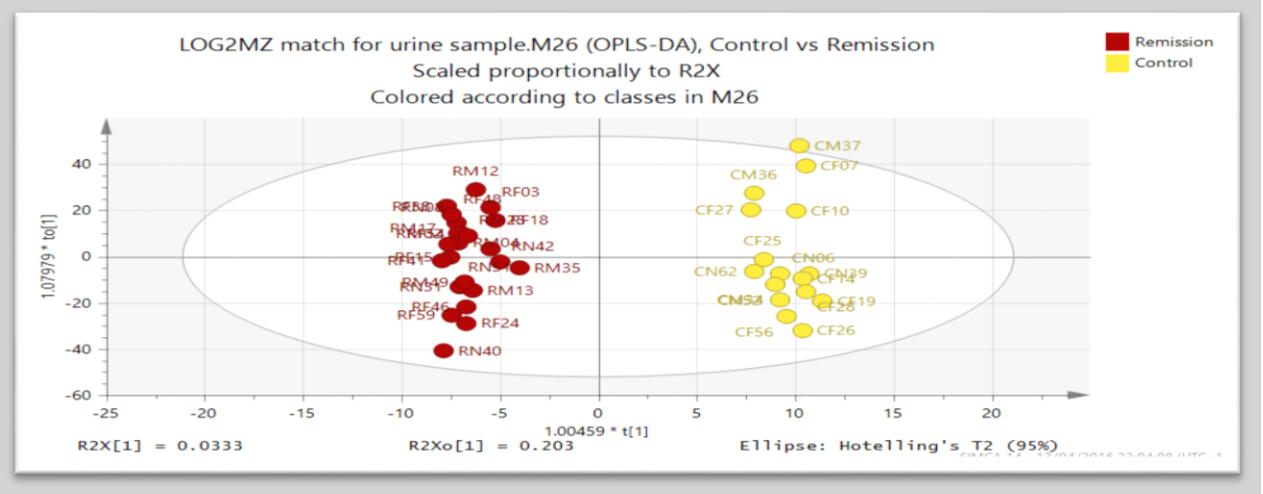

Figure 2. 12: Orthogonal partial least squares discriminant analysis (OPLSDA) model comparing patients with remission UC male(RM), remission UC female (RF),controls male(CM) and control female(CF). R2X (cum) 0.332, R2 Y (cum) 0.983, Q2 (cum) 0.282.

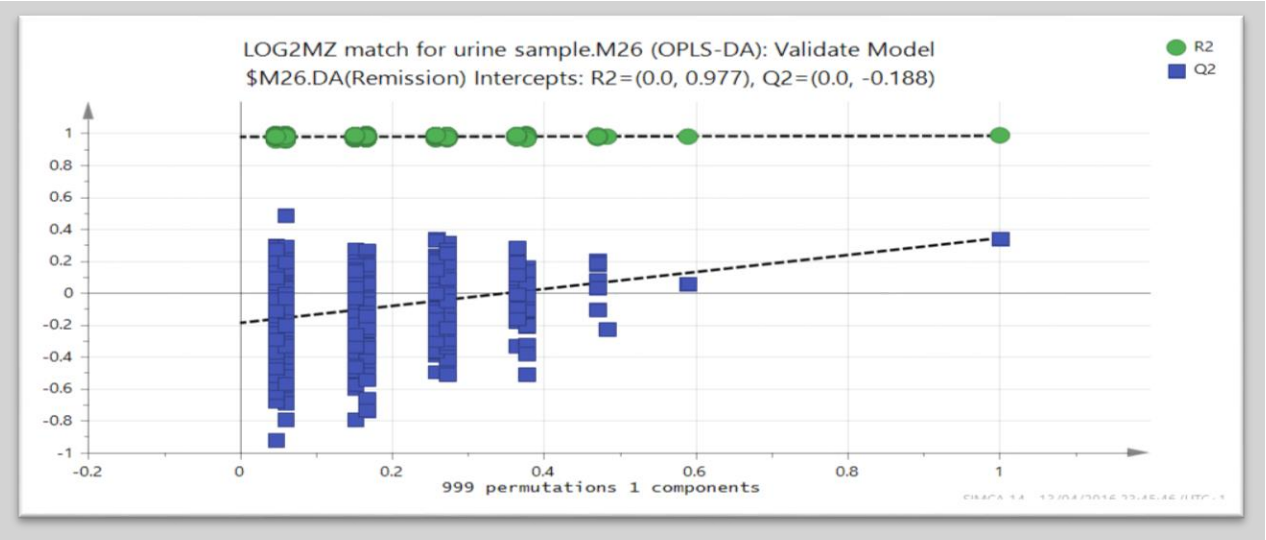

Figure 2. 13: permutation plot as validation of the model to compare the goodness of fit (R2 and Q2) of the original model with the goodness of fit of several models based on data where the order of the Y-observations has been randomly permuted, while the X-matrix has been kept intact after log transformation output from the M/Z match.

Validation by random permutation revealed Q2 cross the zero.

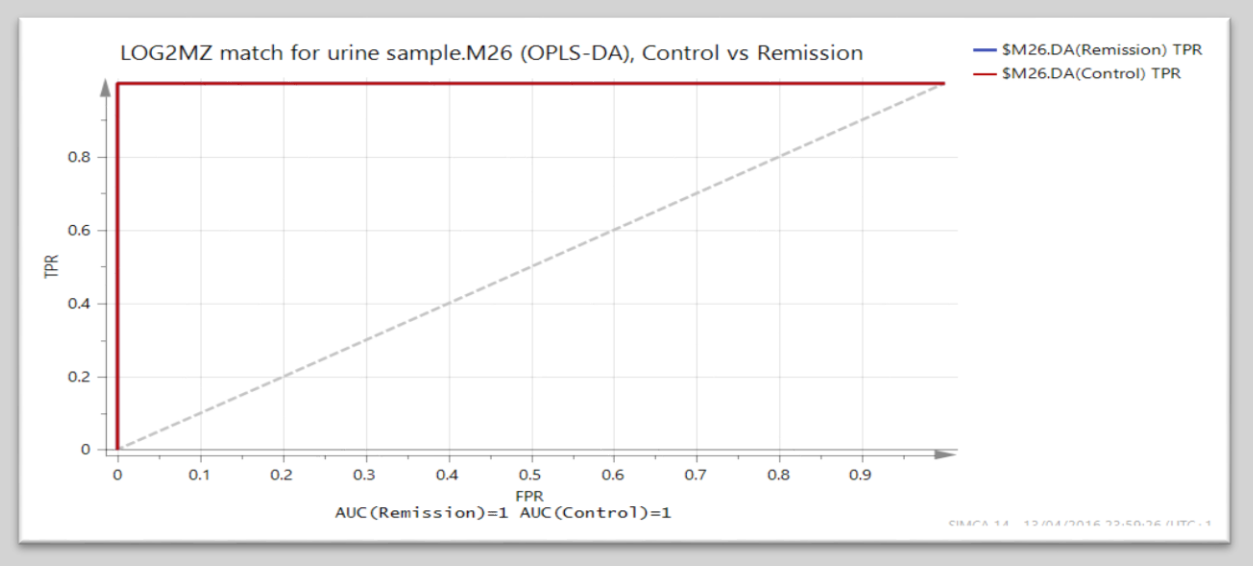

Figure 2. 14: ROC curve show the graphical summary of the performance of binary classifier.

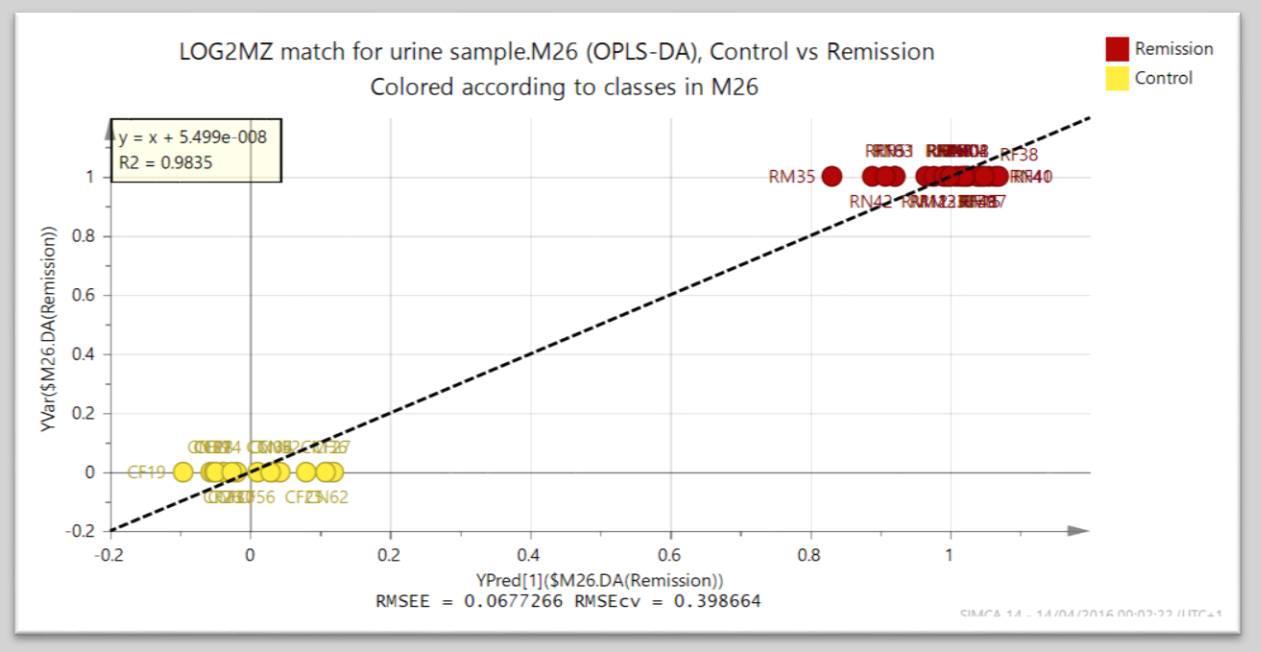

Figure 2. 15: This plot displays the observed versus predicted value of the selected Y- variable and the regression line R2 close to one that indicate and excellent model and valid.

Table 2. 5: Biomarkers used in the model separating controls and Remission UC.

Metabolite	P value	Ratio control/remission
Cytidine	0.0030	0.3971
5,6-Dihydrouracil	0.0188	0.5465
3, 4-Dihydroxymandlate	0.0065	0.6780
N, N-Dimethylglycine	0.0104	0.8141
Isoleucine	0.0426	1.3915
N-Formyl-L-aspartate	0.0491	1.6889
Uracil	0.0035	2.0160
Phenylalanine	0.0339	2.9102
N-Methylanthranilate	0.0011	2.9648
[FA (18:1)] 9Z-octadecenoic acid	0.0205	3.0492
Cholesterolsulfate	0.0346	4.2746

In patients with IBD there are only very few studies between active vs remission or remission vs control The earlier studies in animals mainly used an acute colitis model like dextran sulfate sodium induced colitis or interleukin-10 gene deficient mice and only demonstrated the comparison of the disease state vs healthy In this study we have carried out a comparison between remission and healthy control groups. Uracil is the one of the metabolites that is significantly different between the remission UC group and the control group, the level of uracil was down regulated in the remission cohort compared with control. A previous study used mice as an animal, the first group was control group administrated phosphate buffered saline for 14 days and the second group was the acute colitis induced with dextran sulfate sodium (DSS) for 7 days following the administration buffered phosphate with saline for seven days. DSS was used to induce colitis because exposure to DSS gives symptoms similar to those found in human UC. Their results indicated that uracil was decreased in the fecal extracts of the group that was exposed to the DSS compared to the control more than in control mice. This was attributed to a reduction in the fecal microflora population and their finding are compatible with the results observed

in the current research [54]. Another prior study carried out discrimination between the experimental groups analysed by OPLS-DA from the ^{1}H NMR spectral data sets of plasma and tissue extracts between the DSS-treated mice as a group and control as the other group. The key metabolites that contributed to the separation and were significantly different between cohorts were illustrated and uracil was observed to be decreased in the colons of DSS-treated mice compared with control which is consistent with the current study result [55]. On the other hand the in the urine samples of mice, with the data obtained from GCMS, uracil was increased in the interleukin-10-deficient ($Il10^{-/-}$) mice compared with control. Lack of IL-10 leads to colitis [53, 54]. 5,6-Dihydrouracil is a metabolite of uracil due to resulting from three consecutive steps in the catabolism pathway of uracil. The enzyme known as dihydropyrimidine dehydrogenase catalyses the reduction of thymine and uracil to 5,6-dihydrothymine and 5,6-dihydrouracil consecutively, and the product is converted by dihydropyrimidinase via hydrolysis of 5,6-Dihydrouracil to *N*- Carbamyl-β- alanine. Therefore patients with dihydropyrimidinase deficiency have elevated concentrations of 5,6-Dihydrouracil in urine [58]. In the current research the metabolite 5,6-Dihydrouracil was found to be significantly different between the two groups healthy individuals and quiescent UC and the level of this metabolite was increased in urine samples of quiescent UC in comparison to control samples and depending to the previous information elevation of dihydrouracil may be due to a deficiency of dihydropyrimidinase in the remission cohort compared with control.

Octadecenoic acid is an unsaturated fatty acid that is significantly different between the remission group and the control group and was observed to be decreased in the remission compared to control. This finding supports the hypothesis mentioned above that in IBD there is increased consumption of fatty acids and unsaturated fatty acids. On the other hand another demonstrated that oleic acid was elevated in patients with CD by using the fecal extracts samples which is not compatible with the current study [59].

Isoleucine is an essential amino acids and the body is unable to produce this amino acid along with leucine and valine, therefore it has to be obtained from the diet. Isoleucine can assist specifically in hemoglobin formation, energy regulation, blood clotting and maintaining blood sugar levels [60]. This amino acid was significantly different between the remission and controls and appeared to be decreased in the active and remission urine, this finding was consistent with an earlier study which showed that isoleucine was downregulated in the both types of IBD (UC and CD) which analysed mucosal colonic biopsies from IBD patients by using NMR[47]. However, the current result is contradicted other prior studies [61] which found that isoleucine was elevated in the fecal extracts of patients with active IBD. Furthermore, another study found that isoleucine was elevated in the serum

and plasma of patients with UC and CD versus control subjects [37, 62]. Phenylalanine in the urine of remission samples was lower than in control urine samples. Prior studies indicated that the phenylalanine was increased in the plasma of IL10-/-mice [63]. Also another study indicated that phenylalanine was increased in fecal extracts from patients with CD [43, 59]. In addition it was shown that phenylalanine was increased in the serum of an active IBD group in comparison and a remission group in comparison with healthy control. Also phenylalanine was increased in the serum of active UC in comparison to control [64]. All the previous studies were not consistent with this current study.

Cholesterol sulfate (CS) was found to be significantly different between remission and control. Unlike cholesterol, CS is water soluble and can travel freely in the blood stream rather than being packaged up inside LDL for delivery to the tissue. Thus CS has very special feature as opposed to cholesterol itself and can be easily cross the cell membranes and also can readily enter fat or muscle cells. With insufficient CS muscle and fat cells become damaged and as result become glucose intolerant. Hence low amounts of cholesterol sulfate results in muscle and fat cells being unable utilize glucose as fuel. CS plays an essential role as barrier to prevent penetration of pathogens into the skin and in a similar role this metabolite prevents bacteria from invading the endothelial barrier in the intestine. In addition, atheromatous plaques replenish the supply of cholesterol and sulfate to the microvasculature by utilizing the inflammatory agent superoxide to take sulfate from homocysteine and other sulfur sources. Thus it is hypothesized that the intestinal inflammation is due pathogens having easier access to the endothelial cells of intestine due to deficient cholesterol sulfate also other hypothesis showed that sulfur deficiency caused the liver to shift from producing cholesterol sulfate to producing arginine (and subsequent nitric oxide) which led to the intestine and muscle cells to become susceptible to oxidation damage [65].These finding are consistent with the findings in the current study where the CS was down regulated in the urine samples of quiescent UC in comparison to the level of this metabolite in the samples of healthy individuals. Moreover, another study noted that CS exhibited a mucosal protective activity in a mouse ulcer model and examined the inhibitory activity of CS towards neutrophil elastase, CS was a powerful protective agent in inflammation [66]. N-Methylanthranilate was significantly different between the remission and control urine samples. A previous study illustrated the identification of natural anthranilic acid derivatives such as methyl- *N*-Methylanthranilate and isopropyl- *N*-Methylanthranilate. These two *N*-methylanthranilic acid esters were found to possess a number of pharmacological properties including anti-inflammatory activity [67]. Cytidine is a nucleoside that is composed of the base cytosine linked to the five-carbon sugar D-ribose, cytidine deaminase is an enzyme responsible for the conversion of cytidine to uridine. It was significantly higher in remission compared to controls. A study reported that the endogenous activation- induced cytidine deaminase (AID) was detected in quiescent human colonic epithelial cells

[68, 69]and cytidine will be increased in remission UC patient due to low amount of AID as mentioned before and this finding compatible with the current study findings where the cytidine was elevated in quiescent UC samples in comparison to healthy control samples.

2.3.1.1.3 Comparison of Urines from Remission and Active Subjects

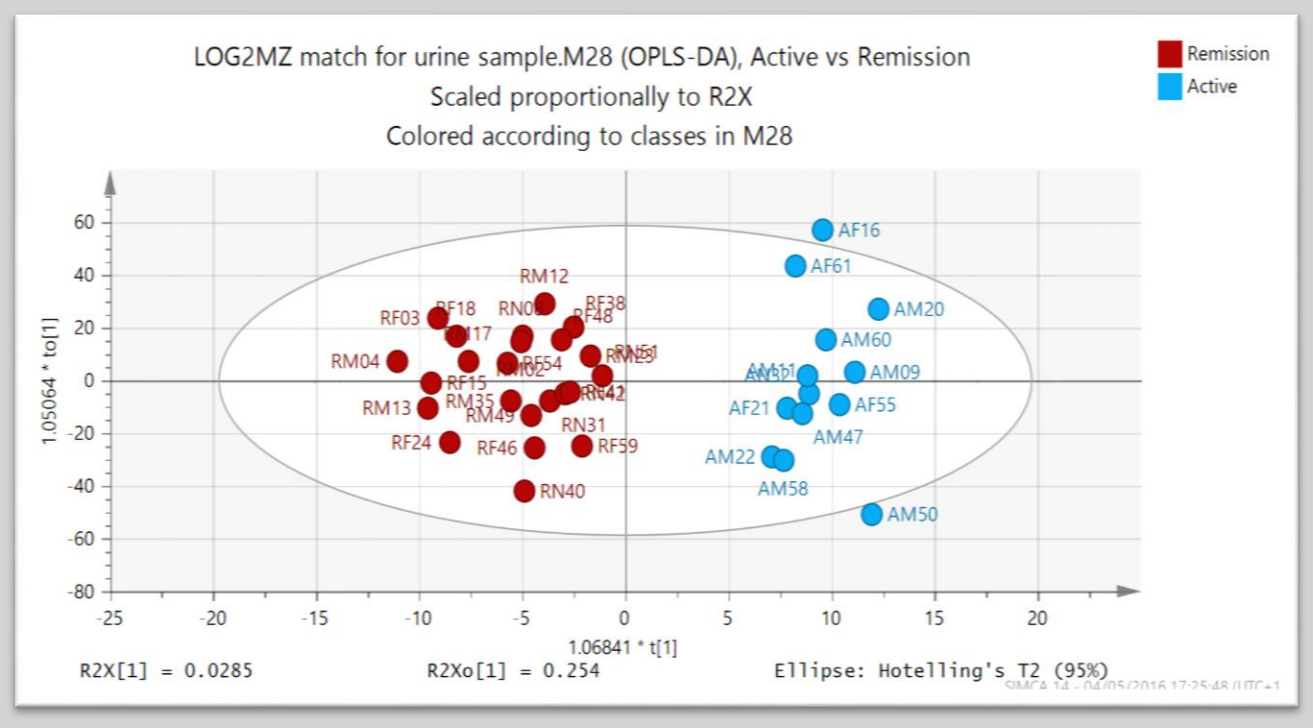

Figure 2. 16: Orthogonal partial least squares discriminant analysis (OPLSDA) model comparing patients with active UC male (AM), active UC female (AF), remission UC male (RM) and remission UC female (RF).

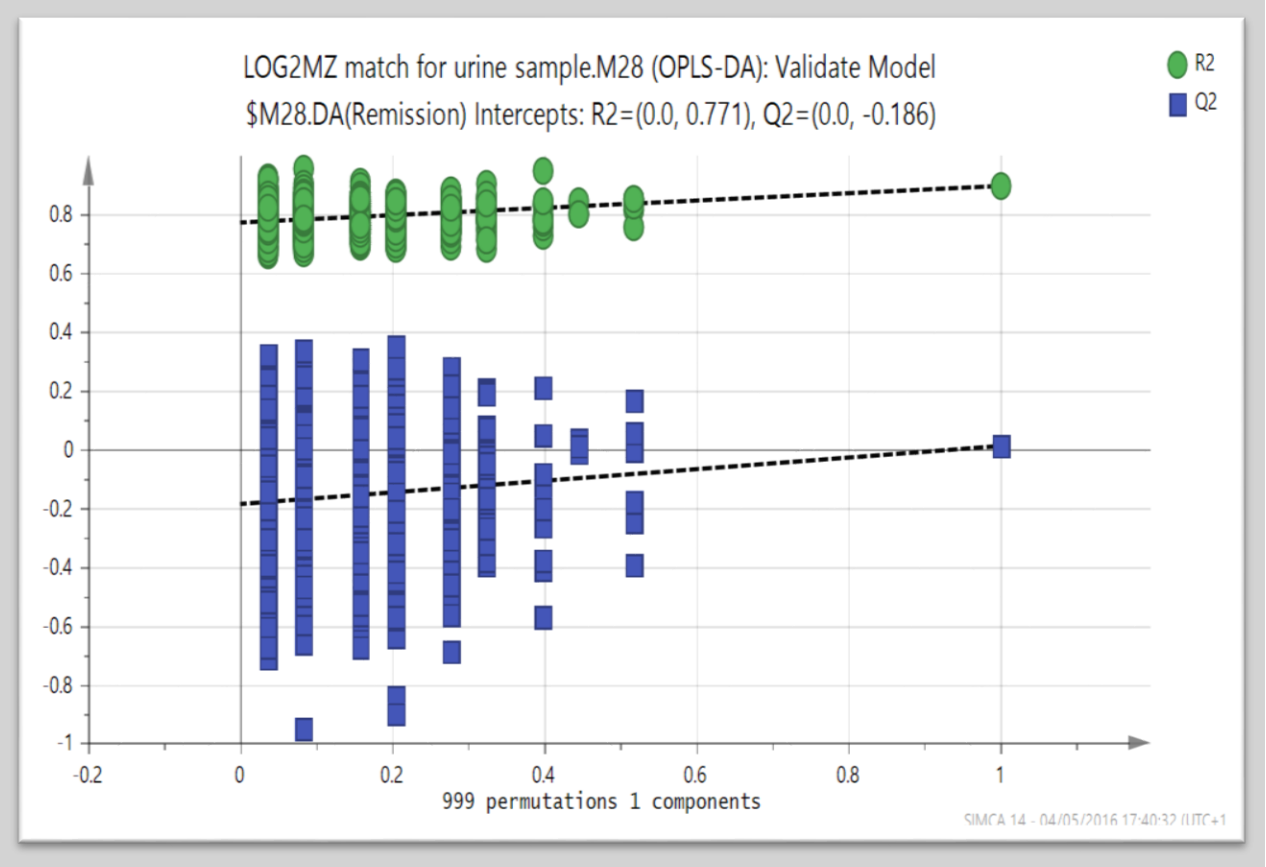

Figure 2. 17: Permutation plot as validation of the model to compare the goodness of fit (R2 and Q2) of the original model with the goodness of fit of several models based on data where the order of the Y-observations has been randomly permuted, while the X-matrix has been kept intact after log transformation output from the M/Z match.

Validation by random permutation revealed that Q2 crosses the zero.

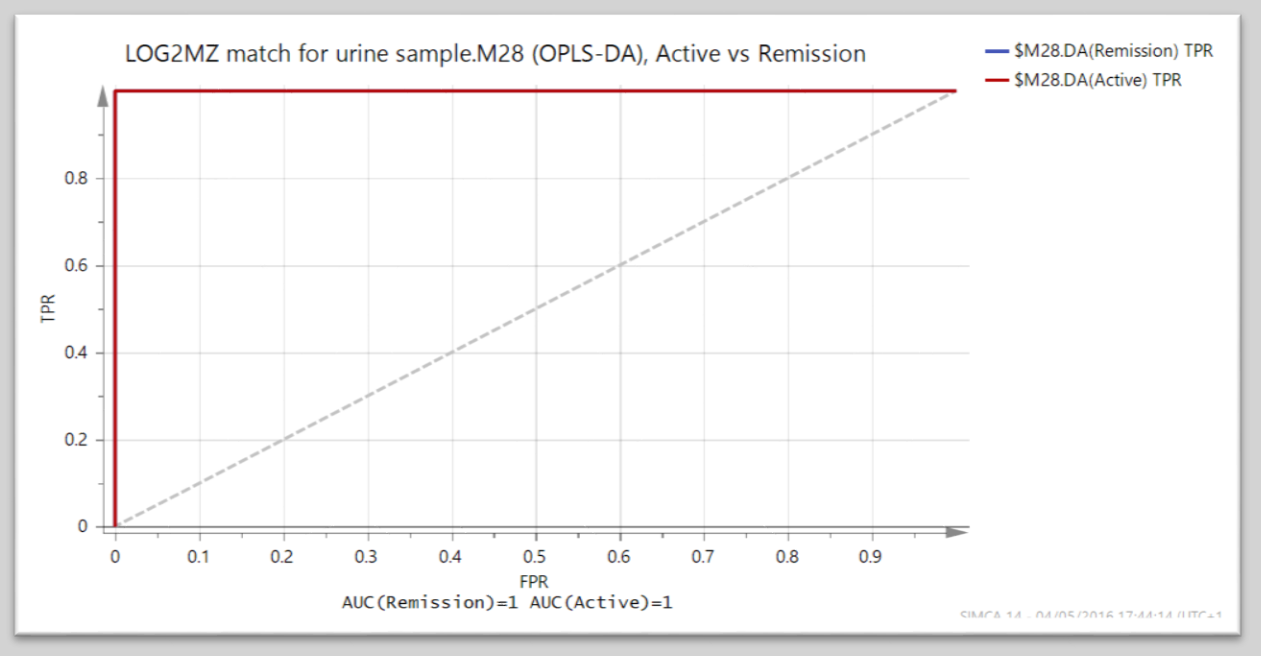

Figure 2. 18: ROC curve show the graphical summary of the performance of binary classifier.

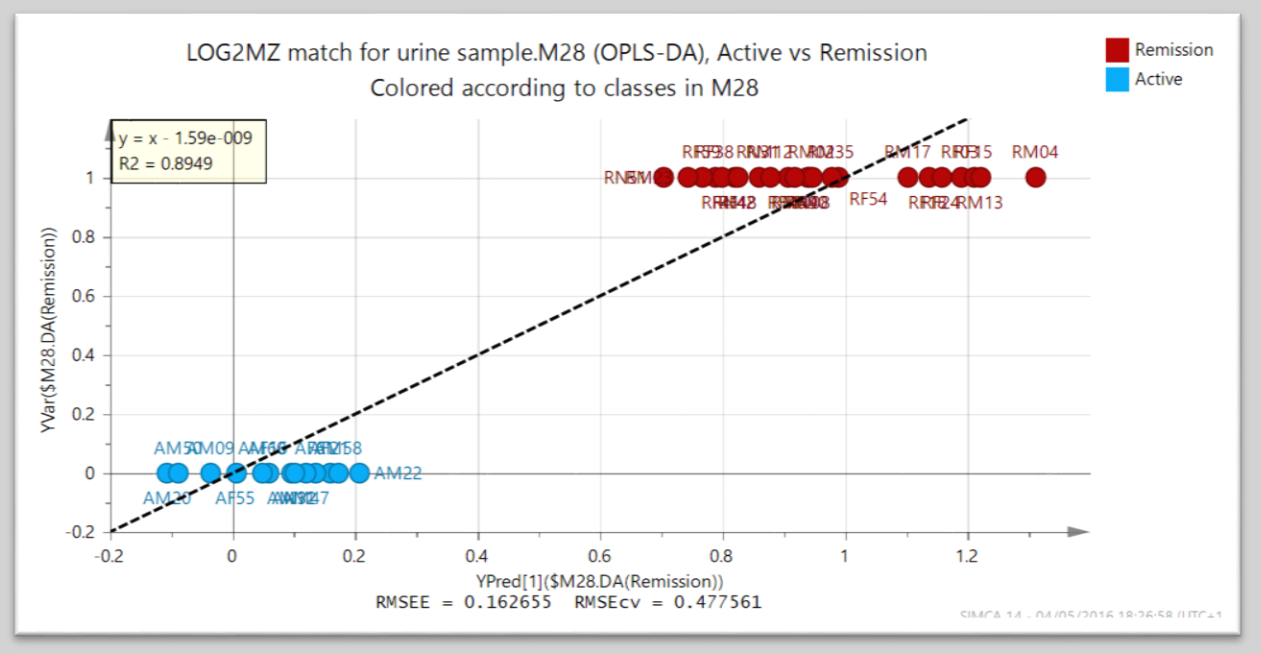

Figure 2. 19: This plot display the observed versus predicted value of the selected Y- variable and the regression line R2 close to one that indicate and very good model and valid.

Table 2. 6: Biomarkers used in the model separating active and Remission UC.

Metabolite	P value	Ratio Remission/active
Picolinamide	0.03116	0.15031
2,5-Dihydroxybenzoate	0.03147	0.25735
2-Amino-4-oxopentanoic acid	0.03724	0.55466
2-Oxoglutaramate	0.04951	0.59753
6-Aminohexanoate	0.04890	1.33576

2,5-Dihydroxybenzoate is the metabolite was significantly different between the two cohorts active vs remission and was increased in the urine samples of quiescent UC than active UC urine samples , 2,5-

dihydroxybenzoate can be found from the salicylic acid degradation as active metabolite also its by-product of tyrosine and benzoate metabolism .

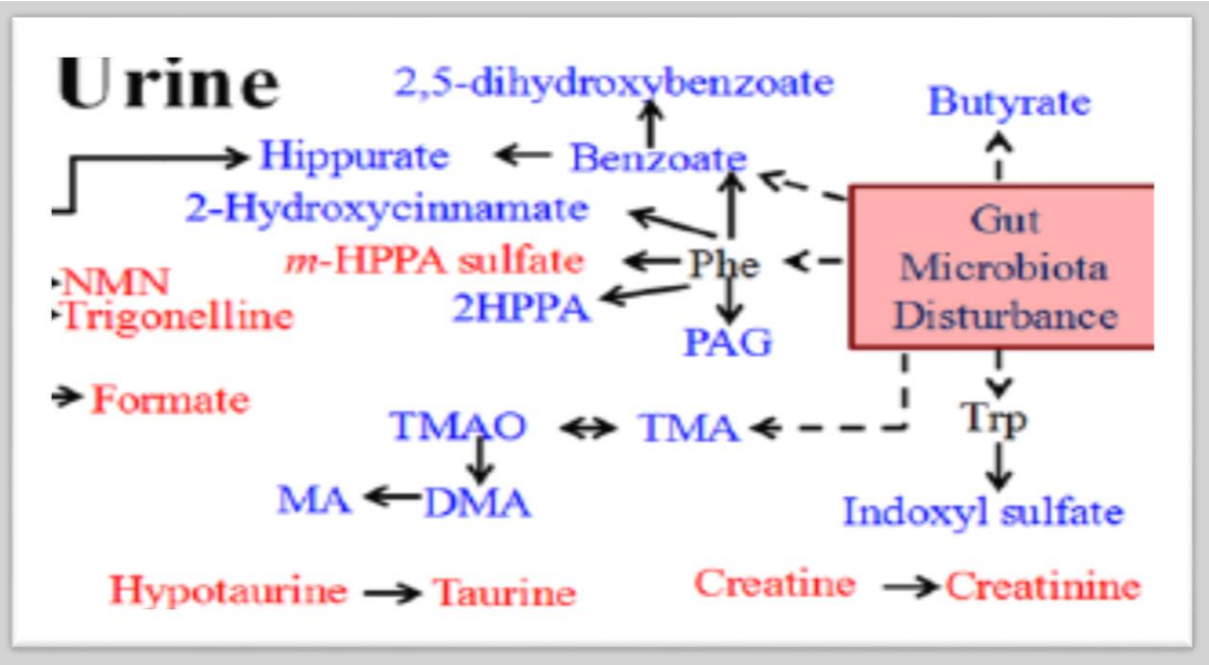

Figure 2. 20: The co-metabolism between the host and gut microbiota [70].

A previous study used cyadox as an antibiotic drug and compared control mice and mice dosed with a high level of cyadox. Thus ingestion of cyadox cause disturbance in gut microbial community and the co-metabolism between the host and the gut microbial community. 2,5- dihydroxybenzoate was one of the co-metabolites between host and gut microbiota that was reduced in urine of mice dosed with a high level of cyadox which indicates a disturbance of gut microbiota[70]. The prior study was consistent with the results obtained in this study where the level of 2,5- dihydroxybenzoate was reduced in the urine sample of the active UC group compared to the samples of quiescent UC and samples of healthy control , which indicate the disturbance of gut microbial community in active UC cohorts. Other studies reported that the reactive nitrogen and oxygen species are involved as mediators of mucosal injury in IBD and are produced by stimulated inflammatory cells such as neutrophils, lymphocytes and macrophages. Hydroxyl radical (˙OH) generation in the inflamed colon was investigated by measuring 2,5- dihydroxybenzoate as indicator for (˙OH) specific products of salicylate hydroxylation. Aromatic hydroxylation is a trapping method depending on the reaction of (˙OH) that gives rise to hydroxylated products which can then be measured by HPLC . Salycilic acid is used to trap (˙OH) as aromatic compound and then produces two major compounds2,5-dihydroxybenzoate and 2,3- dihydroxybenzoate. The experiment was carried out by using control mice and mice exposed DSS induced colitis to mimic UC in humans and the two group were injected with salicylic acid. The hydroxylated products of salicylic acid were analysed by HPLC. The level of 2,5-dihydroxybenzoate was significantly decreased in the mice exposed to DSS colitis compared to control

mice, the unexpected decrease in the level of 2,5- dihydroxybenzoate may be due to decomposition of hydroxylated products by oxidants present in inflammatory lesion and the decrease in the ratio of 2,5- dihydroxybenzoate in the mucosa of DSS induced colitis may result from an increase of ($^{\cdot}$OH) generation within inflamed mucosa [71-73]. Gentisic acid (2,5- dihydroxybenzoate) is the second line metabolite of aspirin and has anti-oxidant properties by trapping free radicals [74]. Those studies displayed results than are consistent with the current study where 2,5- dihydroxybenzoate is down regulated in the active UC samples more than in samples of remission and control groups.

2-Amino-4-oxopentanoic acid was significantly different between the active UC group and remission UC group. This metabolite arises from the D-Arginine and D-ornithine metabolism pathway and it was down regulated in the urine samples of the active UC group in comparison to the samples for quiescent UC cohort. A study reported that 2-Amino-4-oxopentanoic acid was significantly downregulated by (LCD) low-calorie diet group the significance was driven by the (GAPDH) Glyceraldehyde 3-phosphate dehydrogenase which is downregulated in the LCD group during caloric restriction the study was designed to assess whether change in subcutaneous adipose tissue (scAT) gene expression through LCD in order to differentiate and predict subjects who experience weight regain from subjects who experience successful short term weight maintenance[75]. Another study found an increased GAPDH in both intestinal EC and LMPC from CD compared to UC patients and controls [76] as an indication of reduction in the levels of 2-amino-4-oxopentanoic acid due to the downregulation of GAPDH gene [75] which reflects the results of the current study. GAPDH is known as housekeeping protein and is implicated in basic cell catabolic process. GAPDH functions in cytoplasm in the translational control of gene expression, in endocytosis and in nucleus like DNA replication, tRNA export and DNA repair [77].

2-Oxoglutaramate was significantly different was down regulated in the active UC urine samples compared to the remission UC urine samples. Through the metabolism pathway of glutamate, glutamate can be converted to glutamine via glutamate ammonia ligase and then L-glutamine can be converted to 2-oxoglutaramate by glutamine aminotransferase also the 2-oxoglutaramate can be translated to 2-oxoglutarate then 2-oxoglutarate can be converted to glutamate. Therefore depending on the metabolism pathway the down regulation in the level of 2-oxoglutaramate leads to a reduction in glutamate and then glutamine. Previous studies mentioned that the glutamine/glutamate amino acids have been reduced in the IBD patients with UC than control healthy individuals by using NMR as the analytical tool [47]. Moreover, another study using the animal model found the 2-oxoglutarate was reduced in the urine samples of diseased IL10-/- mice compared to control mice [36]. Another study showed that the glutamine metabolism increased in the distal colon of patients with quiescent

UC [78] .Their results are consistent with the current study where the level of 2-oxoglutaramate has been increased in the urine samples of remission UC. Picolinamide was found to be significantly different between the remission and active cohorts urine samples. It was down regulated in the urine samples of active UC compared to urine samples of quiescent UC and control UC. Studies reported that the Picolinamide had antitumor and potent anti-inflammatory properties [79]. Nicotinamide and its isomers like picolinamide and isonicotinamide have anti-inflammatory activity in addition to anti nociceptive activity [80]. It has been demonstrated that a ^{18}F-picolinamide-based PET probe can help with the early diagnosis of melanoma [81].

2.3.2 Results from the Analysis of Saliva samples From IBD Active and Remission Patients and Controls

Table 2. 7: A heat map showing the 50 most abundant metabolites in saliva apart from aminopentanoic acid. (red = highest value, yellow = 5%, blue = 1%)

row m/z	row retention time	Name	Mean A	Mean R	Mean C
100.0758	6.6	N-Methyl-2-pyrrolidinone			
114.0663	10.3	Creatinine			
144.102	11.3	Stachydrine			
132.0768	15.4	Creatine			
166.0864	11.0	L-Phenylalanine			
139.0503	11.0	Urocanate			
118.0863	11.9	L-Valine			
147.0765	15.9	L-Glutamine			
141.0659	10.7	Methylimidazoleacetic acid			
150.0584	12.3	L-Methionine			
162.1125	14.0	L-Carnitine			
76.07577	11.6	(R)-1-Aminopropan-2-ol			
175.1191	29.3	L-Arginine			
219.134	8.2	N2-(D-1-Carboxyethyl)-L-lysine			
176.1031	16.7	L-Citrulline			
146.1176	14.1	4-Trimethylammoniobutanoate			
139.0503	7.2	Urocanate			
265.1183	6.3	alpha-N-Phenylacetyl-L-glutamine			
204.1232	11.7	O-Acetylcarnitine			
148.0605	15.0	L-Glutamate			
163.123	5.9	Nicotine			
147.1129	27.4	L-Lysine			
760.5859	4.2	PC34:1			
310.1132	13.6	N-Acetylneuraminate			
120.0656	15.3	L-Threonine			
129.0658	15.6	5,6-Dihydrothymine			
136.0619	10.1	Adenine			
222.0973	12.4	N-Acetyl-D-glucosamine			
133.0971	26.0	L-Ornithine			
758.57	4.2	PC34:2			
253.0931	10.0	Deoxyinosine			
196.0605	6.0	Dopaquinone			
786.6016	4.1	PC36:2			

496.3398	4.9	LPC 16:0			
106.0499	16.6	L-Serine			
126.022	15.4	Taurine			
230.1864	18.3	N1,N8-diacetylspermidine			
146.0812	13.3	[FA oxo,amino(6:0)] 3-oxo-5S-amino-hexanoic acid			
138.055	12.4	Anthranilate			
228.0979	11.0	Deoxycytidine			
205.1184	9.7	N6-Acetyl-N6-hydroxy-L-lysine			
130.0863	11.8	L-Pipecolate			
134.0447	15.3	L-Aspartate			
244.0928	12.5	Cytidine			
269.088	11.5	Inosine			
204.0868	12.5	N2-Acetyl-L-aminoadipate			
746.6067	4.2	PC(16:0/P-18:0)			
152.0567	13.1	Guanine			
118.0611	16.6	Guanidinoacetate			
124.0393	7.4	Nicotinate			

Saliva samples were analysed by using the LCMS to give saliva metabolite profiles of healthy individuals in comparison with those of participants having UC (active and remission). Table 2.7 shows the relative abundance of the top 50 metabolites in the control, active and remission samples with the omission of one metabolite. The most abundant metabolite in saliva is an isomer of valine. It is probable that this compound is aminopentanoic acid; it was omitted from table 2.7 it was far more abundant than the other metabolites and thus dominated the heat map. This compound is a metabolite of cadaverine a diamine which is derived from animal tissue and aminopentanoic acid is believed to be produced from cadaverine by microbial activity [82]. The data was extracted with m/z mine and the list of metabolites was refine by removing all the metabolites with RSD > ±20 in the pooled sample leaving a list of 203 putatively identified markers The PCA model shows no separation between the active control and remission samples (figure 2.21). The pooled samples (purple) show good clustering although not in the centre of the plot which is the ideal.

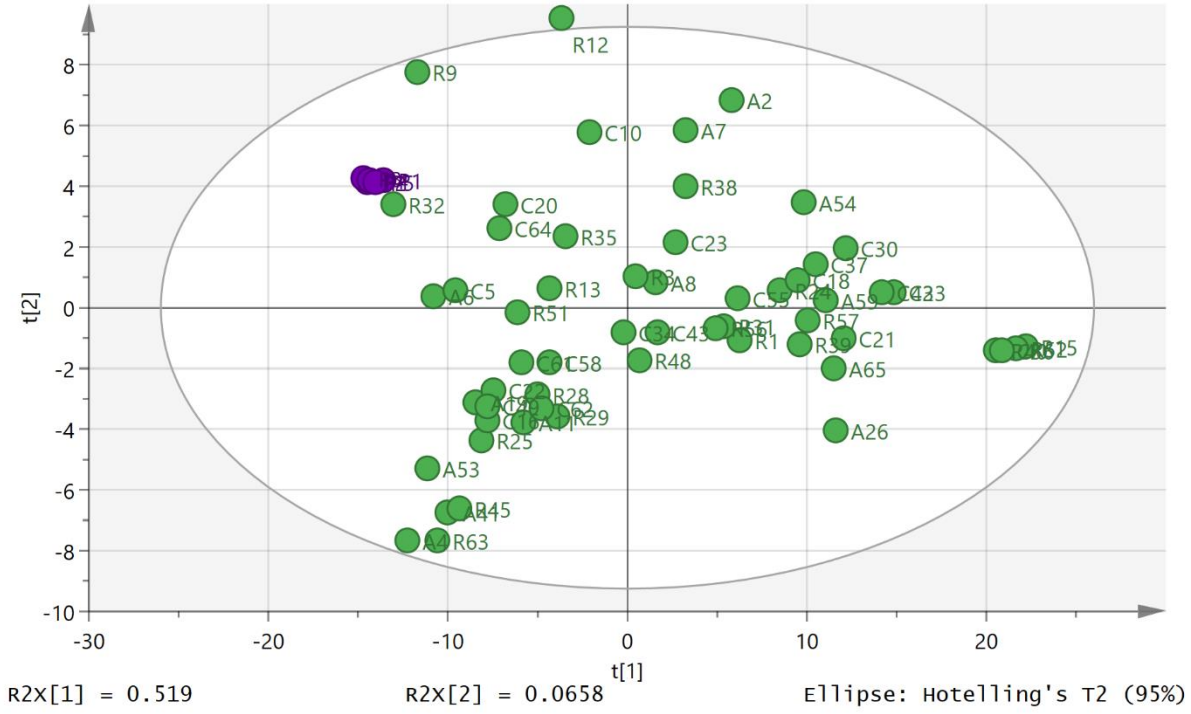

Figure 2. 21: 2D PCA score scatter plot display the relationship between three groups in saliva samples after log transformation output from the M/Z mine using positive ion data.

The different groups were modelled using OPLSDA. A strong model (CVANOVA 1.3 x 10^{-5}) could be built for separating control from active samples (figure 2.22). The cross validation of the model (figure 2.3) indicated that the model had a high level of validity. Nine marker compounds were involved in the model and are shown in table 2.8. Not all of the markers had significant P values but the modelling in Simca P does not assume data normality.

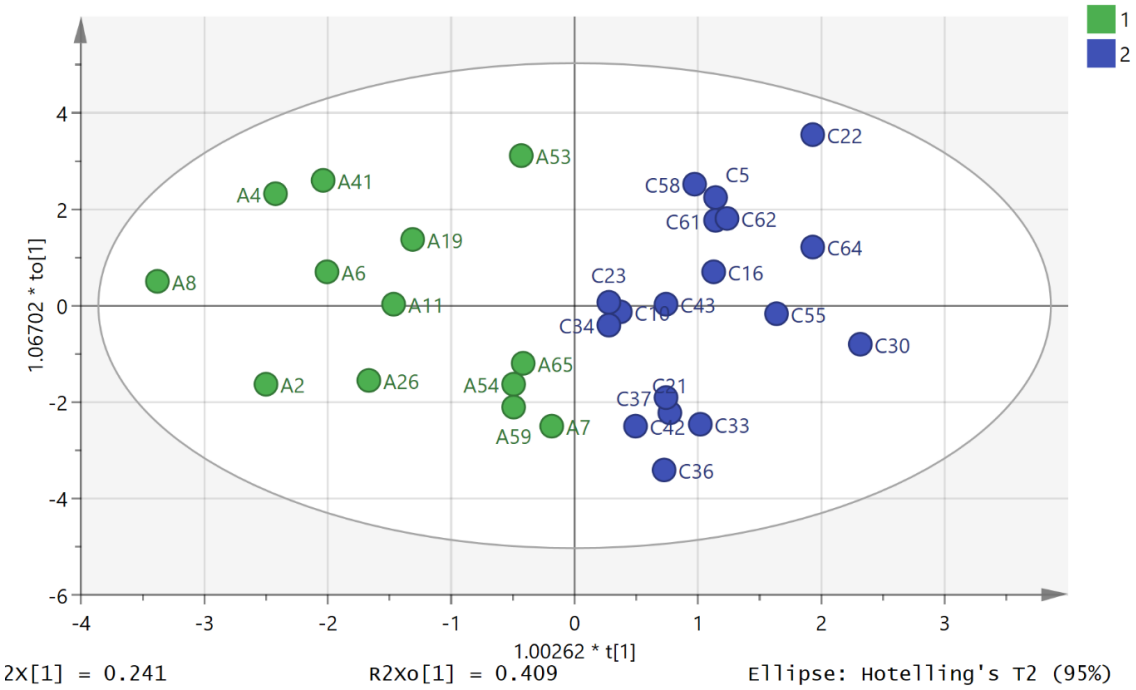

Figure 2. 22: Separation of active and control saliva samples based on nine putative biomarkers.

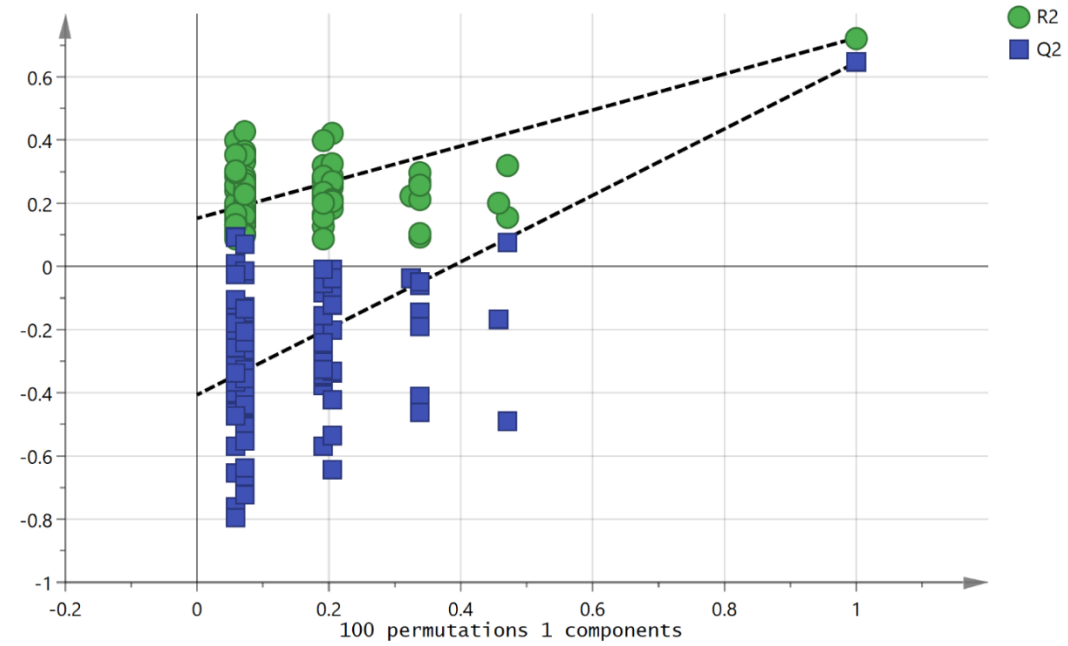

Figure 2. 23: Figure 2.23 Cross validation model for the OPLSA model shown in figure 2.22.

Table 2. 8: Nine marker compounds separating controls and active IBD samples

metabolite	P value	fold change A/C
formylkynurenine	0.012	47.20
C8H12N2O2	0.005	0.10

sphingadiene	0.003	7.20
octadecatetraenoic acid	0.007	5.60
hydroxysphinganine	0.077	3.60
pathothenate	0.312	2.30
Sphingosine	0.001	5.10
deoxytetrasphinganine	0.035	0.67
N-acetylornithine	0.328	1.03

It was also possible to separate the remission samples and the control samples based on and OPLSDA model using seven maker compounds although these were mainly not the same as those producing the separation between active and controls (figure 2.24). The model had high validity (CVANOVA 3.4 x 10^{-8}) and gave a strong cross validation model (figure 2.25).

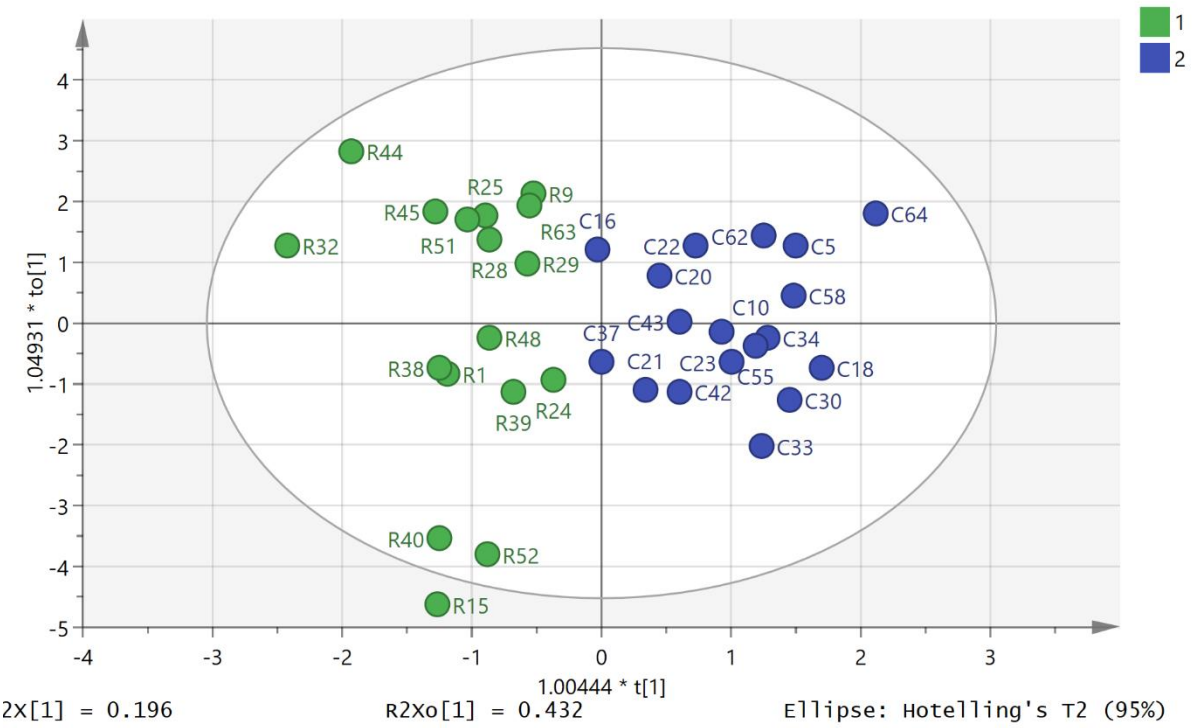

Figure 2. 24: Separation of remission and control saliva samples based on seven putative biomarkers.

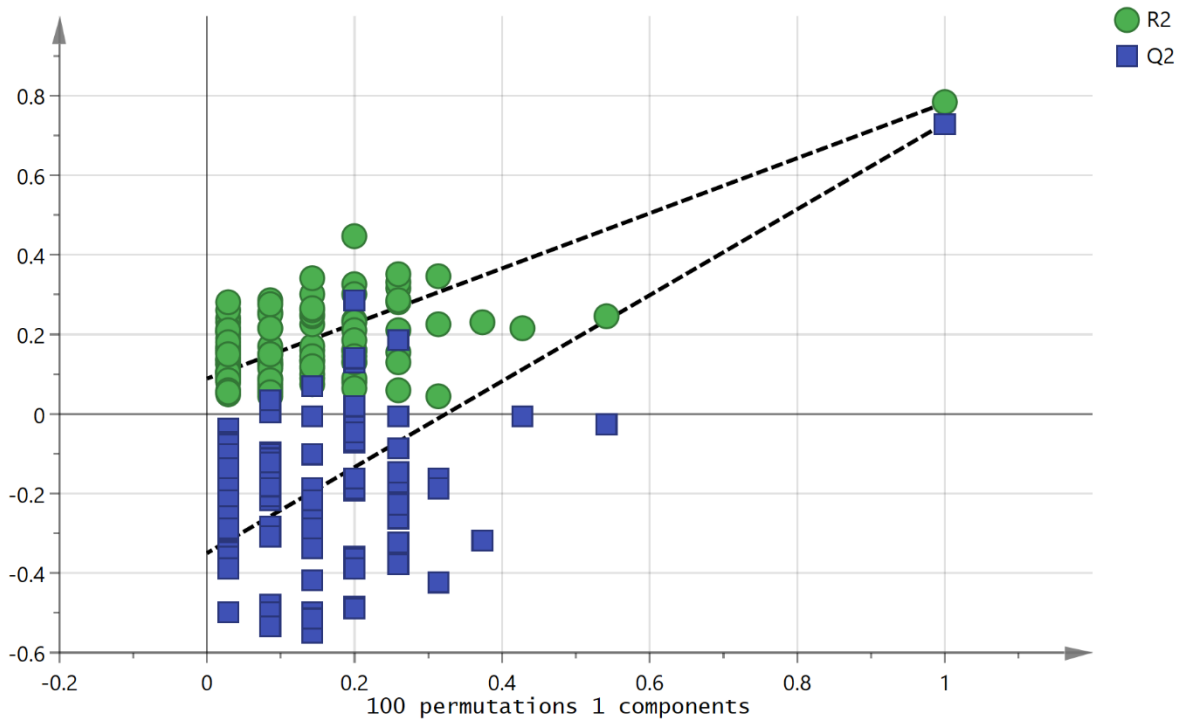

Figure 2. 25: Cross validation of the model shown in figure 2.24.

The seven variables used to construct the model are shown in table 2.9.

Table 2. 9: Seven variables used to separate control and remission samples.

metabolite	**P value**	**fold change R/C**
formylkynurenine	0.006	4.65
methyldioxyindole	0.006	0.03
GPC	0.070	1.21
N-acetylornithine isomer	0.015	4.82
guanine	0.057	3.38
ornithine	0.025	2.39
adenine	0.031	0.73

Finally, it was possible to separate the remission and active samples using an OPLSDA model with seven variables which were largely those separating the active and control samples (figure 2.26). The model had strong validity (CVANOVA 0.0014) and gave a strong cross validation model (Figure 2.27). The seven metabolites producing the separation are shown in table 2.10.

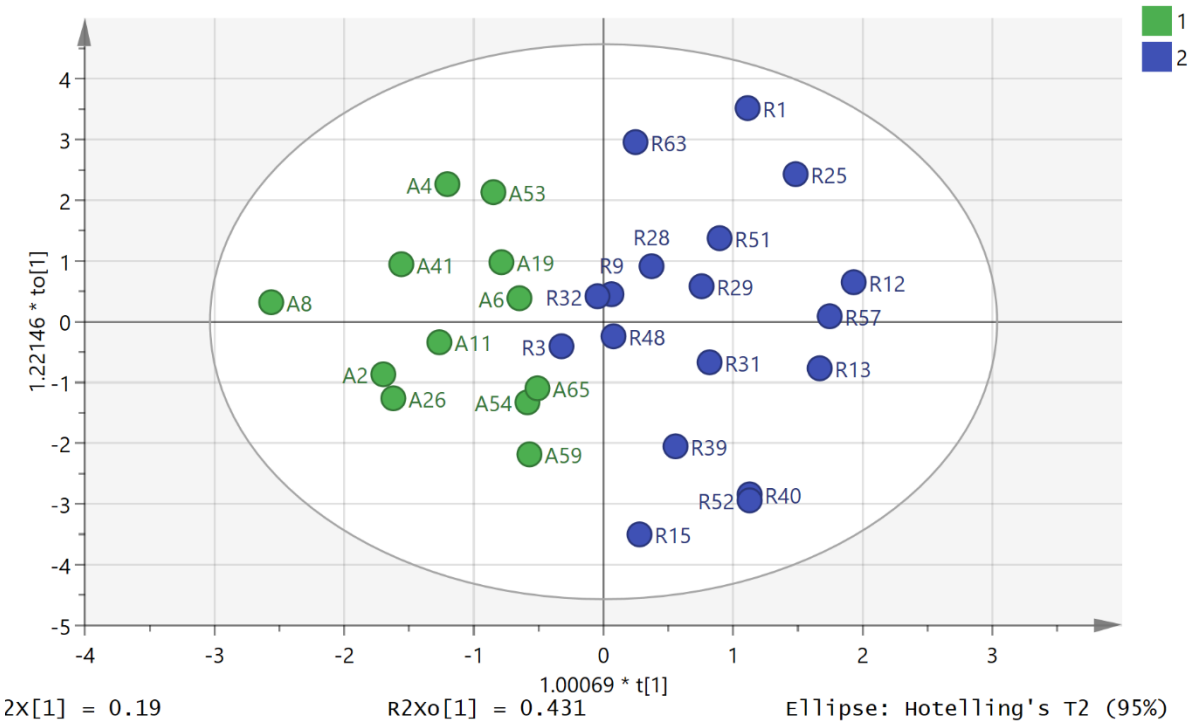

Figure 2. 26: Figure 2.26 OPLSDA model separating the active and remission samples based on seven variables.

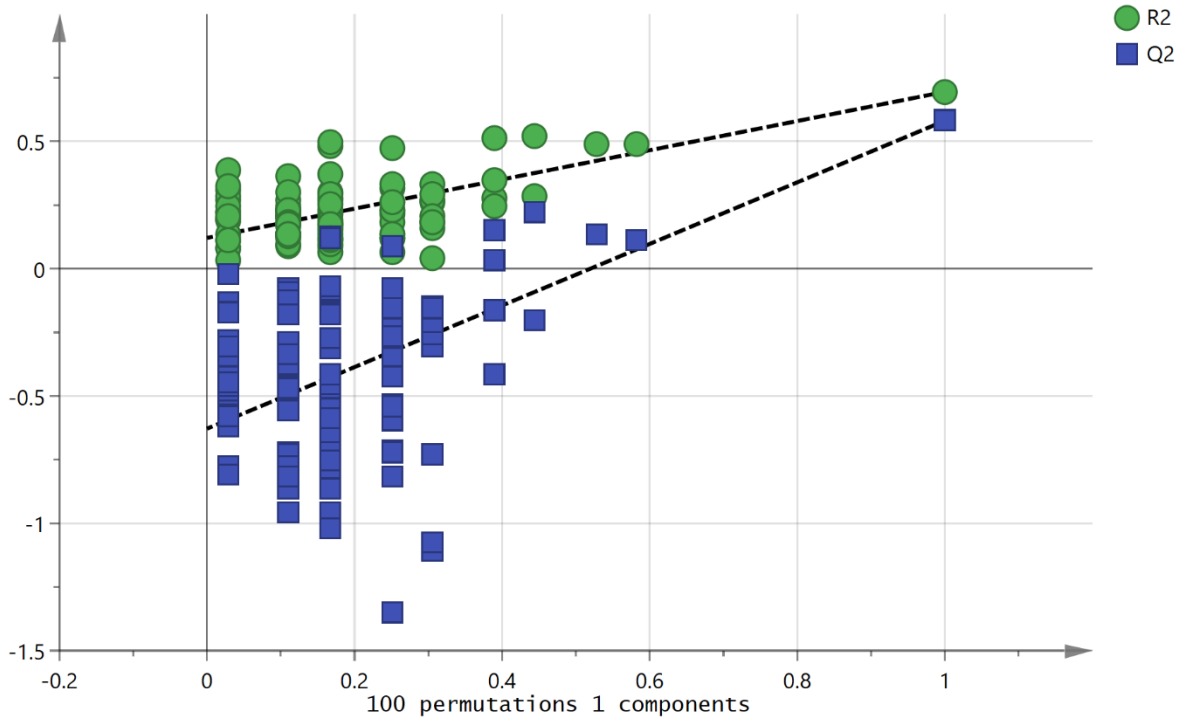

Figure 2. 27: Cross-validation of OPLSDA model shown in figure 2.26.

Table 2. 10: Seven variables used to separate active and remission samples.

	P value	fold change R/A
C8H12N2O	0.319	2.39
sphingadiene	0.034	0.36
octadecatetraenoic acid	0.003	0.18
hydroxysphinganine	0.135	0.37
pantothenate	0.419	0.59
Sphingosine	0.003	0.52
deoxytetrasphinganine	0.099	1.46

Saliva is the ideal biofluid for diagnosic/prognostic monitoring since its collection is minimally invasive. However, it has not been extensively monitored in previous research possibly since it is uncertain to what extent it can be standardised. It contains quite high levels of xenobiotic metabolites such as aminopentanoic acid which is derived from microbial metabolism. In the current samples it was also possible to observe high levels of nicotine and hydroxynicotine from cigarette smoking. However, despite background contamination there is a clear set of markers discriminating between active and remission and control samples. The metabolite with the largest fold difference between active and control samples was formylkynurenine which is a metabolite of tryptophan. Figure 2.28 shows extracted ion traces for formylkynurenine for active, control and remission samples. Formylkynurenine has been found to be produced in incubations of meat with fecal inocula indicating that the microbiome has the capability of producing this metabolite [83]. Tryptophan metabolism has an important role in the interaction between a host and pathogenic organisms since many pathogens require tryptophan [84, 85].

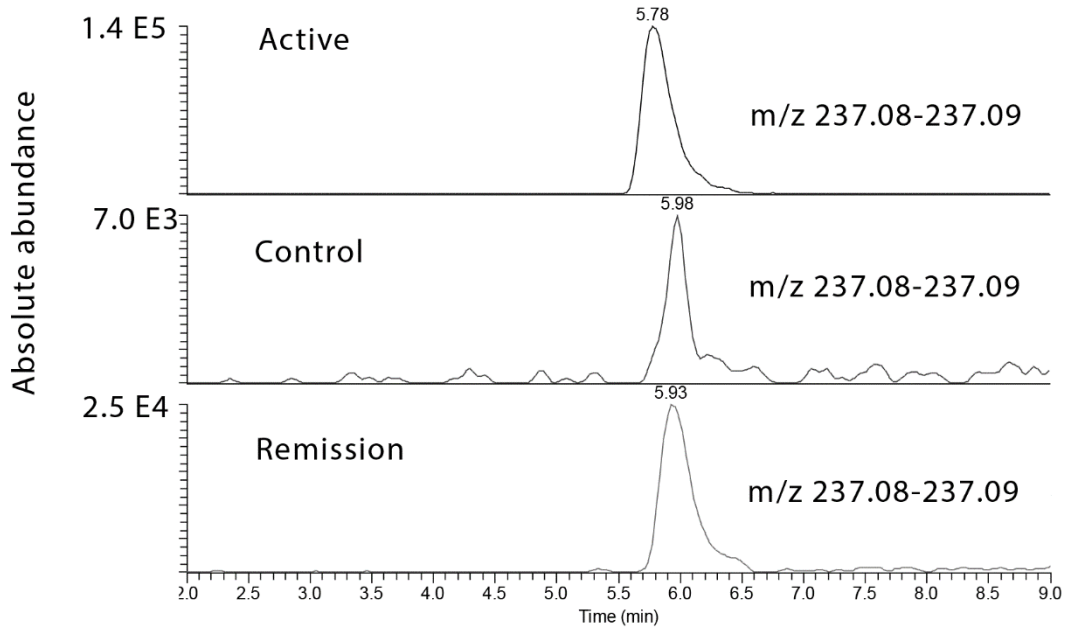

.

Figure 2. 28: Extracted ion traces for formylkynurenine in active, remission and control samples.

The active samples contain higher levels of formylkynurenine than both the control and remission samples thus possibly indicating some differences in the gut microbiome metabolism. There are several sphingosine metabolites in the active samples that are elevated. Sphingosine may be produced from mucosal lipids by the action of microbial enzymes. Figure 2.29 shows extracted ion traces for

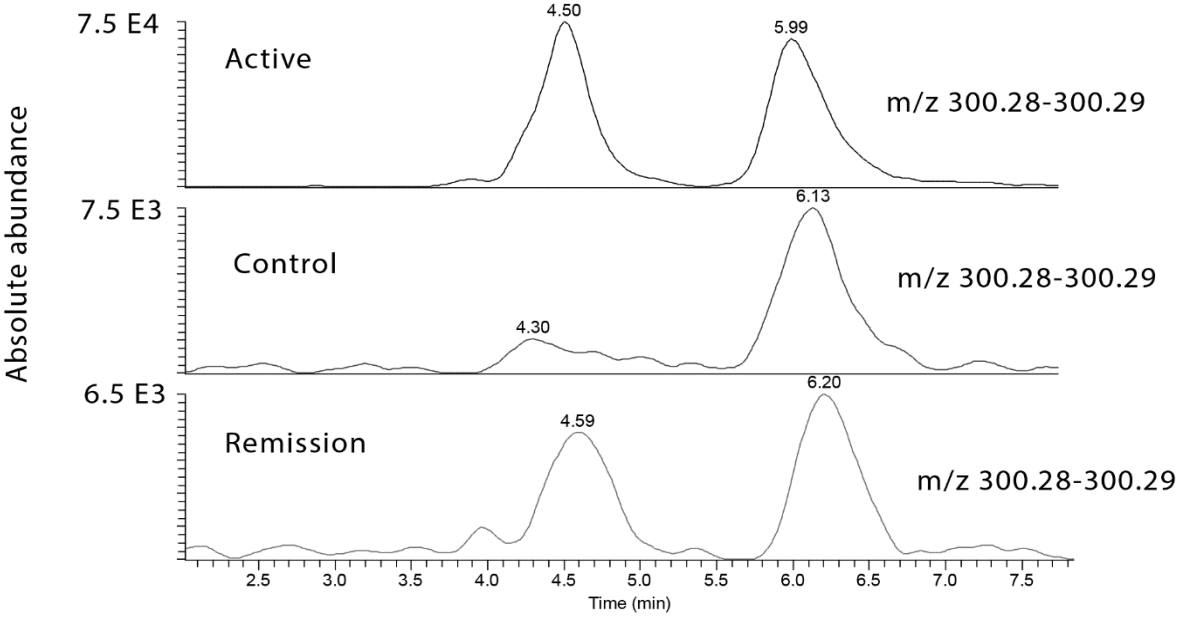

Figure 2. 29: Extracted ion traces for sphingosine in active, remission and control samples.

sphingosine in active, remission and control samples. Sphingosine may then be absorbed and converted to sphingosine phosphate which is pro-inflammatory. The level of sphingosine is lower in the remission samples suggesting that lowering its levels might be a marker of the success of treatment. Sphingosine diene and hydroxysphingosine may be produced from dietary lipids via the action of the microbiome and thus might also indicate alteration in the microbiome between active and control samples [84, 85]. Finally octatetraenoic acid may be a metabolite resulting of the action of peroxisomes on arachidonic acid. Figure 2.30 shows extracted ion traces for octadecatetraenoic acid in active, remission and control samples. Induction of peroxisome proliferation has been associated with protection against inflammatory bowel disease and the higher levels of the unusual unsaturated fatty acid octadectetraenoic acid might indicated upregulation of a potential protective mechanism in the active samples. Unlike mitochondrial beta-oxidation of fatty acids peroxisomal beta-oxidation of fatty acids does not necessarily go to completion and acids may only be shortened by 3-4 cycles of 2 carbon chain shortening [86]yielding a molecule of acetyl CoA/acetyl carnitine at each cycle. Oxidation cycle can stop at the point where a double bond is encountered in the fatty acid chain which in the case of the oxidation of arachidonic acid would result in the formation of octatetraenoic acid.

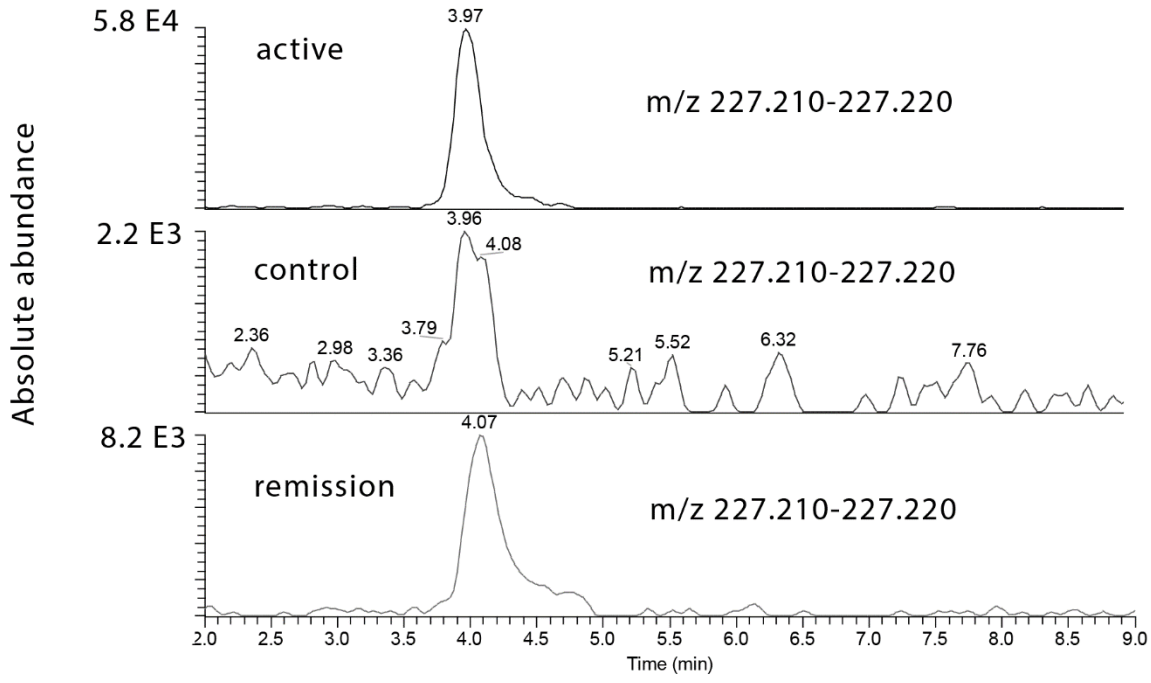

Figure 2. 30: Extracted ion traces for octadecatetrenoic acid in active, remission and control samples.

2.4 Conclusion:

Thus the profiling of saliva in diagnostic and prognostic purposes in IBD looks quite promising with clear separations being produced between the three groups in the current study based on a few markers that have some biochemical basis. Overall there are strong indicators of metabolic changes in the urine of patients with active UC, remission UC compared to the control urine samples and there are several metabolites were significantly different between three cohorts in urine samples and saliva samples between active UC and control, quiescent UC and control, also active UC and remission UC.

Chapter-3:

Derivatization of acids: Development of derivatization method for carboxylic acids.

3.1 Introduction:

Non-digestible carbohydrates are degraded by bacterial fermentation in the large intestine to yield short-chain fatty acids (SCFAs), such as acetate, propionate and butyrate, which are the principal SCFAs in the gut, constitute more than 95 % of all the SCFA content [87, 88]. Their concentrations in the gut are typically found in a ratio of 3:1:1 [89].SCFAs accumulate at different sites throughout the intestines: acetate and propionate are found in both small and large intestines, while butyrate is found mainly in the colon and cecum [90]. About 400–800 mmol SCFAs per day are produced with a high-fibre diet which is equivalent to the fermentation of 10 g of dietary fibre. SCFAs are known to induce beneficial physiological and metabolic effects in the gut and the host [87-92] and have been demonstrated to have anti-inflammatory effects with reductions, particularly in butyrate, being noted in several studies [87, 93-96]. Several approaches have been used for the determination of SCFAs but there remain discrepancies in the measurement of SCFA levels in blood. A European double-blind ring-test based on one human serum sample produced disagreements in the concentrations measured. Acetate concentrations ranged from 119 to 559 µM with concentrations of propionate and butyrate ranging from 1 to 20 µM [97]. Most methods for the determination of SCFAs use gas chromatography or gas chromatography mass spectrometry with different sample preparation procedures being used prior to analysis. One of the earliest approaches was to freeze the sample and distil off and trap the volatile organic fraction. While this requires specialist apparatus it has the advantage that it minimises sample handling and thus potential contamination [98-102]. Extraction of SCFAs followed either directly by GC-MS analysis or extraction and then derivatisation followed by GC-MS analysis has also been used [92, 97]. A membrane extraction method for SCFAs prior to GC-MS analysis has been used in order to concentrate the analytes and improve limits of detection [103]. A direct HPLC-UV method has been used to determine acetate, propionate and butyrate in plasma and urine [104] and also a method using a HPLC coupled to a mass spectrometer [105]. Acetate and butyrate have been directly measured in urine by using ^{1}H NMR [106]. Thus the literature on the determination of SCFAs is not large, many of the papers are old and there is only one report of an LC-MS method being used for this purpose. In order to fit into metabolomics work-flows based on LC-MS it would be desirable to have an LC-MS method for the determination of SCFAs. Aqueous phase derivatisation followed by LC-MS has been used to determine other small organic acids in urine [107]. Several chemical reactions have been used for the derivatization of carboxylic acids. Earlier studies showed the feasibility for the reaction of an aniline based derivatisation reagents with the aldehydes and carboxylic acids. Activation of the carboxylate and deprotonation of acid was achieved when the acid such as carboxylic acid was

react with carbodiimide such as EDC result in the formation of *O*- acylisourea as key intermediate . This intermediate (*O*- acylisourea) will react with amines to give the stable amide and urea (Figure 3.1). This reaction was successfully derivatised the mono-carboxylic acid and the short- chain-carboxylic acid due to the columbic repulsion rendering causing the derivatisation of the second and third carboxylic acid function to be more difficult. In this design the fatty acids and acids have been successfully derivatised and the derivatives was showed favourable detection by LC-ESI-MS in the positive ion mode. Therefore In this study two derivatisation reagent have were used first reagent 3-(Ethyliminomethyleneamino)-N,N-dimethylpropan-1-amine hydrochloride (EDC) was used as co-reagent and the second reagent N,N-dimethyl-P-Phenylenediamine (DPD, figure 3.2) was coupled as an amine for conferring positive charge [107].

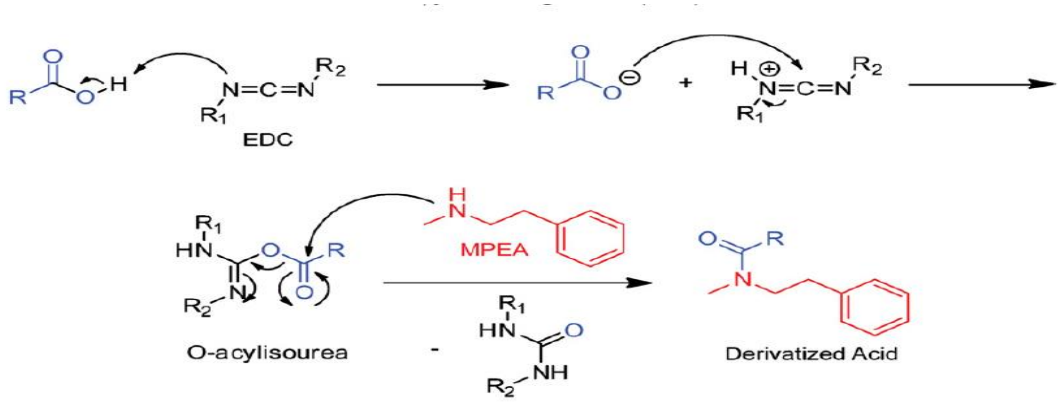

Figure 3. 1 : Show reaction mechanism for the coupling of amine to carboxylic acid (blue), induced by EDC (carbodiimide) via an O- acylisourea intermediate[113].

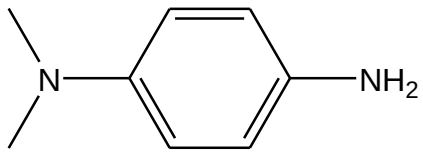

Figure 3. 2 : N,N-dimethyl-p-Phenylenediamine (DPD).

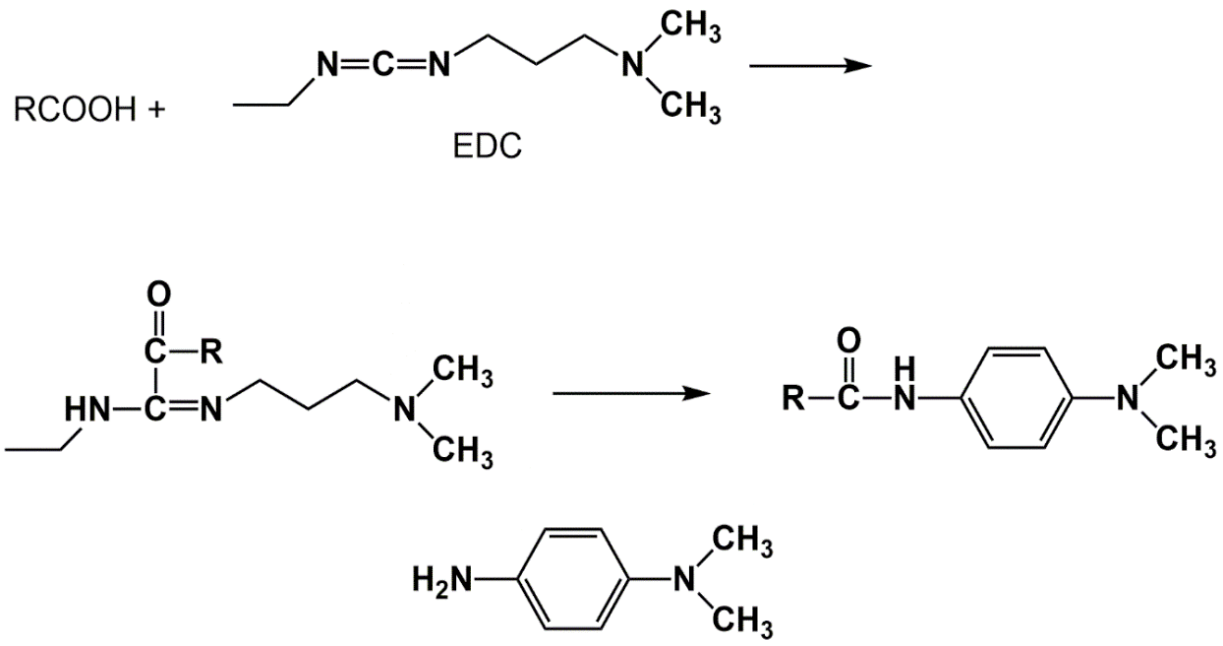

Figure 3. 3: The coupling reaction used to derivatise SCFAs.

The carboxylic acid group in the acid first reacts with the carbodiimide as a co-reagent (EDC) reagent leading to deprotonation of acid and activation of the carboxylate function. This results in the formation of an O-acylisourea (figure 3.2). This intermediate is then attacked by an amine (N,N-dimethyl--phenylenediamine) (DPD) to form a stable amide and urea.

It was of interest to see it would be possible to produce a sensitive derivatisation method for the analysis of SCFAs in biological fluids by LC-MS since in their underivatised form these acids are too low MW and too volatile for direct LC-MS determination. Having developed a method, the aim was then to apply it to determination of SCFAs in urine samples collected from patients with IBD, patients in remission and a control group. The applicability of the method to analysis of SCFAs in plasma samples was also tested.

3.2 Experimental (Derivatisation of acids):

3.2.1 Materials, Chemical and reagents.

L-(+)-Lactic acid solution 30%, Propionic acid, Sodium acetate- $^{13}C_2$ 99% , Propionic acid-2,2-d_2, Sodium L-lactate -$^{13}C_3$. Butyric acid were obtained from Sigma Aldrich, Dorset UK. Sodium butyrate (3,3,4,4,4-D_5,98%) was obtained from CK gases, Leicestershire UK. N-(-3-Dimethylaminopropyl)-N-ethylcarbodiimide,N,N-Dimethyl-p-phenylenediamine(momohydrochloride). Acetonitrile CHROMASOLV® gradient grade, tetrahydrofuran (THF) HPLC grade and formic acid and aluminium oxide activated were obtained from Sigma-Aldrich, Dorset UK. LC-MS grade water was prepared in house using a Milli Q purification system.

3.2.2 Equipment.

SeQuant™ ZIC®-HILIC - 150x4.6 mm, 5µm, 200A.PEEK HPLC Column – serial No. 129362.

Sorbent lot No. L011001477 (HiChrom, Reading UK).

Heating block Stuart®, SB162 (VWR, Leicestershire UK). The rest of the equipment is described in section 2.2.2.

3.2.2.1 LC-MS instrumentation

The conditions were as described in section 2.2.3.

3.2.3 Solutions.

3.2.3.1 Preparation of acetic acid solution (stock solution)

The stock solution was prepared at 0.1g/ml by weighing 200mg of acetic acid and adding 1800µl of ACN. Then the stock solution was diluted to 1mg/ml then diluted to 0.1mg/ml, then diluted to 0. 01 mg/ml, then diluted to 0.001mg/ml.

3.2.3.2 Preparation of propionic acid solution (stock solution)

The stock solution was prepared at 0.1g/ml by weighing 200mg of propionic acid and adding 1800µl of ACN. Then the stock solution was diluted to 1mg/ml then diluted to 0.1mg/ml, then diluted to 0. 01 mg/ml, then diluted to 0.001mg/ml.

3.2.3.3 Preparation of lactic acid solution (stock solution)

The stock solution was prepared at 0.1g/ml by weighing 100mg of lactic acid bottle and adding 200µl of ACN (due to L-(+)-Lactic acid solution being 30% w/v). Then the stock solution was diluted to 1mg/ml then diluted to 0.1mg/ml, then diluted to 0. 01 mg/ml, then diluted to 0.001mg/ml.

3.2.3.4 Preparation of butyric acid solution (stock solution)

The stock solution was prepared at 0.1g/ml by weighing 200mg of butryic acid and adding 1800µl of ACN. Then the stock solution was diluted to 1mg/ml then diluted to 0.1mg/ml, then diluted to 0. 01 mg/ml, then diluted to 0.001mg/ml.

3.2.3.5 Preparation of sodium $^{13}C_2$ acetate solution (stock solution)

Sodium $^{13}C_2$ acetate was used as internal standard for the acetic acid. 10mg from the bottle as powder was dissolved in 500µl of H_2O and 500µl THF (1:1) instead of ACN .Due to the salt can't be totally dissolve in ACN only or THF only. The stock solution was 10mg/ml. Then it was diluted to 1mg/ml then diluted to 0.1mg/ml then to 0.01mg/ml.

3.2.3.6 Preparation of sodium Lactate -$^{13}C_3$ solution (stock solution)

Sodium$^{13}C_3$ lactate was used as internal standard for the lactic acid. Stock solution was prepared by taking 10 µl from the bottle due to sodium Lactate -$^{13}C_3$ is in liquid form. Then 10 µl was dissolved to 5ml Water/THF (1:1) to give the final concentration 1mg/ml.

3.2.3.7 Preparation of propionic acid-2, 2-d2solution (stock solution).

The stock solution was 1g/ml by adding 5ml of THF to the 5gm propionic acid-2, 2-d2 in the volumetric flask instead of ACN. Then the stock solution was diluted to 0.1gm/ml then diluted to 1mg/ml then diluted to 0.1mg/ml then to 0. 01 mg/ml.

3.2.3.8 Preparation of sodium butyrate (3,3,4,4,4-D5, 98%) (stock solution).

Sodium butyrate was used as internal standard for butyric acid. 10mg of powder was dissolved in 500µl of H_2O and 500µl THF (1:1) due to the salt can't be totally dissolve in THF only. The stock solution was 10mg/ml. Then this was diluted to 1mg/ml then diluted to 0.1mg/ml then to 0.01mg/ml.

3.2.3.9 Preparation of 1 M EDC in 10% H2O, 90% ACN (v/v)

M.W = 191.70 g/mole So 191.70 mg in 1ml. 38.34 mg was dissolved in 20µl H_2O and 180 µl ACN.

3.2.3.10 Preparation of 1 M EDC in 75% H_2O, 25% THF (v/v)

M.W = 191.70 g/mole, So 191.70 mg in 1ml. 76.68 mg was dissolved in 300µl H_2O and 100 µl THF.

3.2.3.11 Preparation of 10mM DPD (monohydrochloride) in ACN.

M.W = 136.19 g/mole , 10mM equal to 0.01M then 0.01X 136.19 gm equal to 1.3619 gm, So 1.3619 mg was dissolved in 1ml ACN .

3.2.3.12 Preparation of 10mM DPD (monohydrochloride) in 50% H2O, 50% THF (v/v).

M.W = 172.66 g/mole , 10mM equal to 0.01M then 0.01X 172.66 gm equal to 1.7266 gm ,So 1.7266 mg was dissolved in 500µl H_2o and 500 µl THF .

3.2.3.13 Preparation of 100mM DPD (monohydrochloride) in 50% H2O, 50% THF (v/v).

M.W = 172.66 g/mole, 100mM equal to 0. 1M then 0. 1X 172.66 gm equal to 17.266 gm ,So 17.266 mg was dissolved in 500µl H_2o and 500 µl THF.

3.2.3.14 Purification of ACN.

This purification has been carried out by packing the column with base activated alumina and two frits one in the top and the other in the bottom of the column then pour the ACN into the column finally the liquid was passed through the column and collected in a conical flask.

3.2.3.15 Purification of THF.

This purification has been carried out by packing the column with base activated alumina and two frits one in the top and the other in the bottom of the column then pour the THF into the column finally the liquid passed through the column and collected in a conical flask.

3.2.3.16 Preparation of plasma for derivatisation.

Plasma was prepared first by adding 400 µl of plasma and 1200 µl of THF into an Eppendorf tube then followed by centrifugation for 15 min at 5000 rpm then the supernatant was removed for derivatisation.

3.2.3.17 Preparation of urine for derivatisation.

Urine was prepared first by adding 100 µl of urine and 300 µl of THF into an Eppendorf tube followed by centrifugation for 15 min at 5000 rpm then the supernatant was removed for derivatisation.

3.2.4 Method procedures and protocols.

3.2.4.1 Mobile phase

Mobile phase was prepared by putting water in one bottle containing 0.1 % v/v formic acid (inlet A) as aqueous phase and other bottle with acetonitrile containing 0.1 % v/v formic acid as organic phase (inlet B). The gradient programme was as shown in table 3.1.

Table 3. 1: Display mobile phase gradient programme in LC-MS analysis.

Time (min)	A%	B%	Flow rate(µl/min)
0	20	80	300
20	50	50	300
21	20	80	300
25	20	80	300

3.2.4.2 Derivatisation of acetic, propionic, lactic and butyric acids.

Stock solutions of 0.1mg/ml were prepared and then 100µl aliquots were taken from the acetic, propionic, lactic and butyric acids solutions. Thus 10µg/ml was added for every acid then 25µl of 1M EDC in 10%H_2O 90% ACN and 50µl of 10mM DPD in ACN was transferred to each vial then those vials were placed in a heating block at 60°C for 45 min. The resulting mixture was diluted with water to 1.0 ml and then was transferred to HPLC vial prior to LC–MS analysis.

3.2.4.3 Derivatisation of (urine or plasma) sample by using EDC and DPD and ACN solvent (before optimisation).

To 100µl of urine or plasma sample (supernatant) was added to 25µl of the 1M EDC in 10%H_2O 90% ACN and 50µl of 10mM DPD in ACN in one vial. After that the vial was placed in a heating block at 60 ◦C for 45 min. The resulting mixture was diluted with water to 1.0 mL (1000µl) and then was transferred to HPLC vial before to be subjected to LC–MS analysis.

3.2.4.4 Derivatisation of (urine or plasma) sample by using EDC and DPD and purified THF solvent (After optimisation).

To 100µl of urine or plasma sample (supernatant) was added to 50 µl of the 1M EDC in 75% H_2O, 25% THF (v/v) and 40µl of 100mM grade DPD in 50% H_2O, 50% THF (v/v) in one vial then 300µl of purified THF was added and 20µl of internal standard solutions A, B, C, D. After that the vial was placed in a

heating block at 60°C for 60 min. The resulting mixture was diluted with water/THF (1:1) to 1.0 mL (1000µl) and then was transferred to HPLC vial before to being subjected to LC–MS analysis.

3.2.4.5 Calibration curve for acetic acid with $^{13}C_2$ sodium acetate as (Internal standard) as well as for propionic acid with propionic acid-2, 2-d2 as (Internal standard) and purified THF as solvent.

A calibration curve was constructed for acetic acid with amounts of: 0µg, 0.02µg, 0.04µg, 0.08µg, 0.16µg, 0.32µg and 0.64µg with the (I.S) $^{13}C_2$ sodium acetate at constant amount of 1µg .Furthermore calibration points were constructed for the propionic acid as well with amounts of 0µg, 0.02µg, 0.04µg, 0.08µg, 0.16µg, 0.32µg and 0.64µg. The internal standard was added to each amount propionic acid-2, 2-d2 (I.S) in a constant amount 1µg. Thus seven vials were prepared and each vial containing one concentration from the calibration points of acetic and propionic in addition to 20ml from the mixture of internal standards with 25µlof the 1M EDC in 10%H2o 90% THF, 50µl of 10mM DPD in THF then the resulting mixture was vortexed for ten second and was placed in a heating block at 60°C for 45 min. After that diluted with water for ion chromatography to 1.0 mL (1000µl) and then was transferred to HPLC vial prior to LC–MS analysis.

3.2.4.6 Calibration curve for acetic, propionic, lactic and butyric acid with their (Internal standards) and purified THF as solvent by carrying out the (optimised method).

Finally the optimised method was applied to carry calibration for acetic, propionic, lactic and butyric acid (0µg, 0.05µg, 0.1µg, 0.2µg, 0.4µg, 0.8µg, 1.6 and 3.2µg) with their internal standard (I.S) $^{13}C_2$ sodium acetate, propionic acid-2, 2-d2, sodium lactate and sodium butyrate respectively at a constant concentration 1µg for every calibration point. 50µl of 1M EDC (3:1) (H_2O/THF) and 40µl of 100mM of DPD (1:1) (H_2O/THF) were added then the resulting mixture was vortexed for ten seconds and was placed in a heating block at 60°C for 60 min. After that the sample was diluted with water for ion chromatography to 1.0 mL (1000µl) and then was transferred to HPLC vial prior to LC–MS analysis.

3.3 Results and Discussion

Derivatisation of (Short Chain Fatty Acid (SCFA) standards

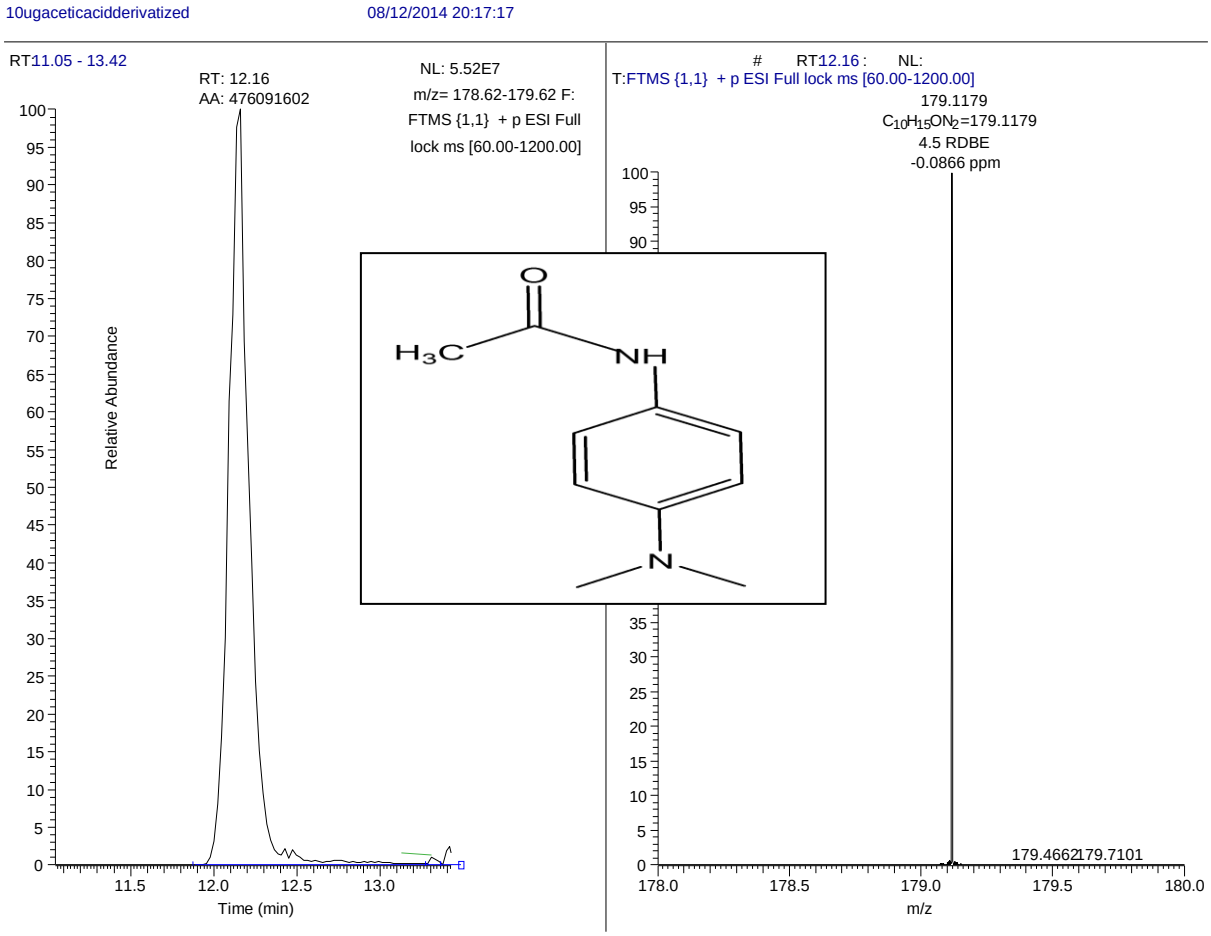

Figure 3. 4: Show the positive ESI-mass spectra for derivatised acetic acid at 10µg [M+H]⁺. HILIC chromatographic conditions as in 3.2.4.1.

Figures 3.4-3.8 show the chromatographic peaks and mass spectra obtained for the DPD derivatives of acetic, propionic, lactic butyric and pyruvic acids respectively. The chromatographic peak shapes were all good and the sensitivity was excellent. The retention times followed a logical pattern for HILIC with the derivatives of the longer chain acids running earlier.

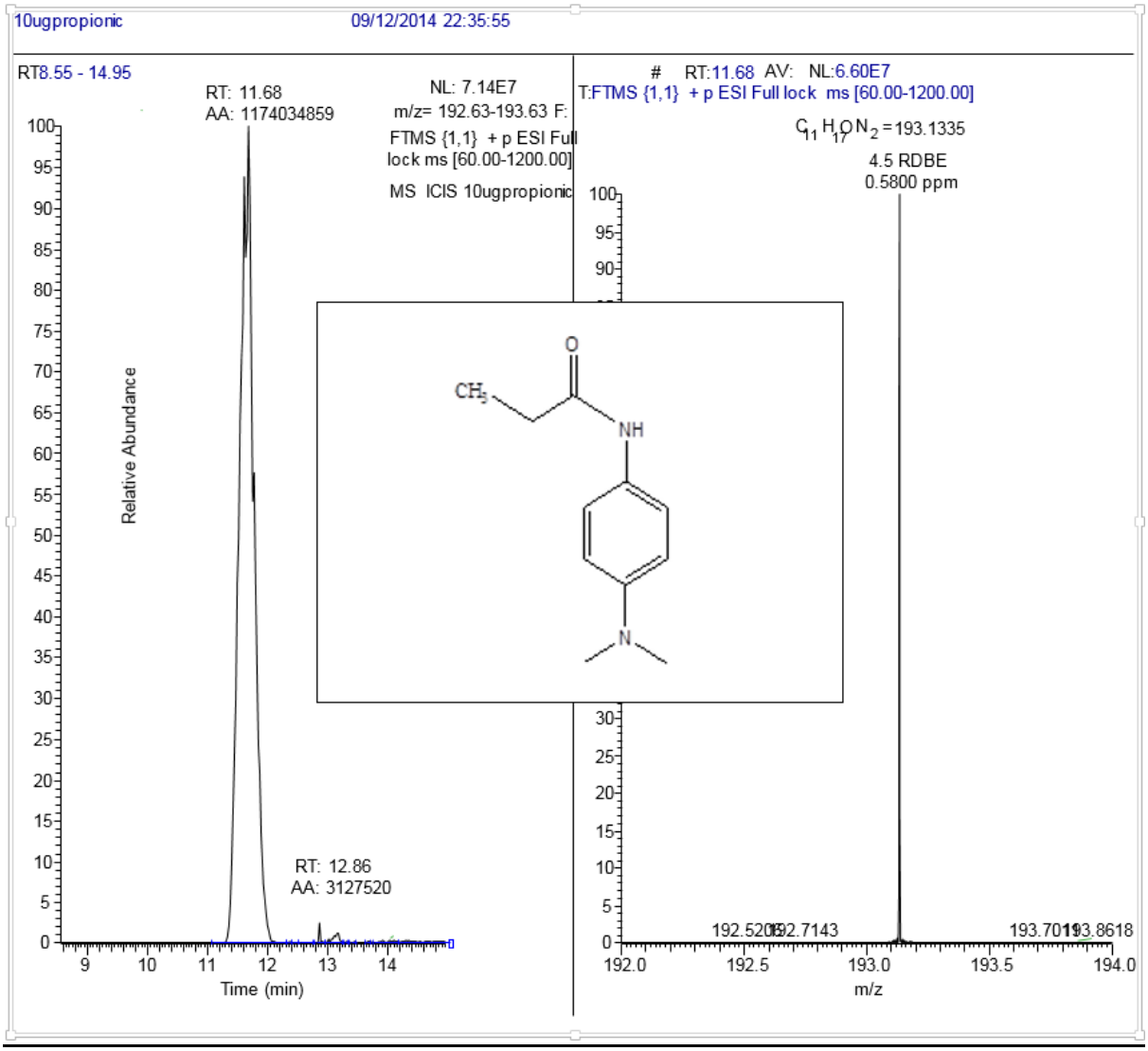

Figure 3. 5: Show the positive ESI-mass spectra for derivatised propionic acid at 10µg [M+H]⁺. HILIC chromatographic conditions as in 3.2.4.1.

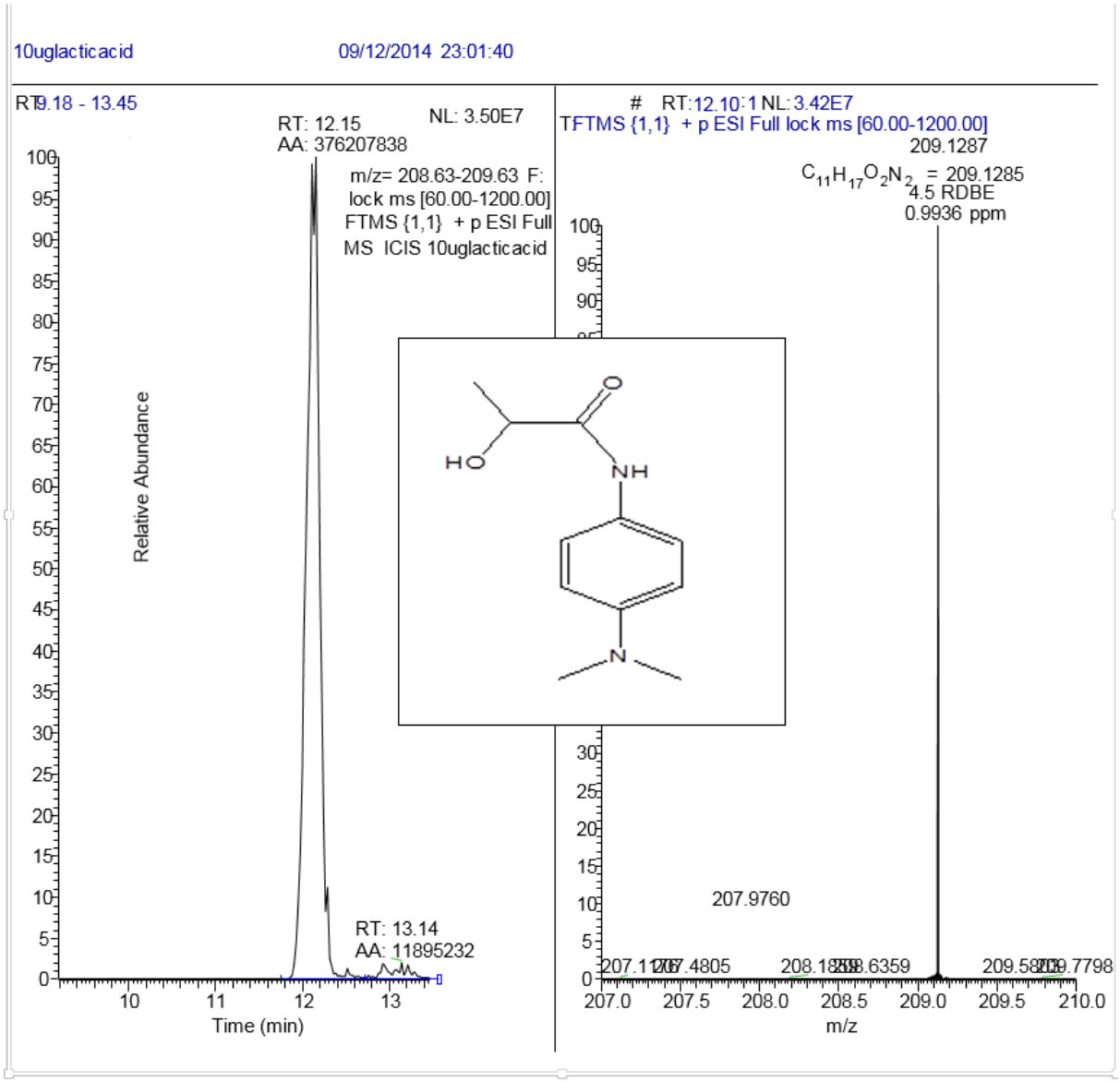

Figure 3. 6: Show the positive ESI-mass spectra for derivatised lactic acid at 10µg [$M+H]^+$. HILIC chromatographic conditions as in 3.2.4.1.

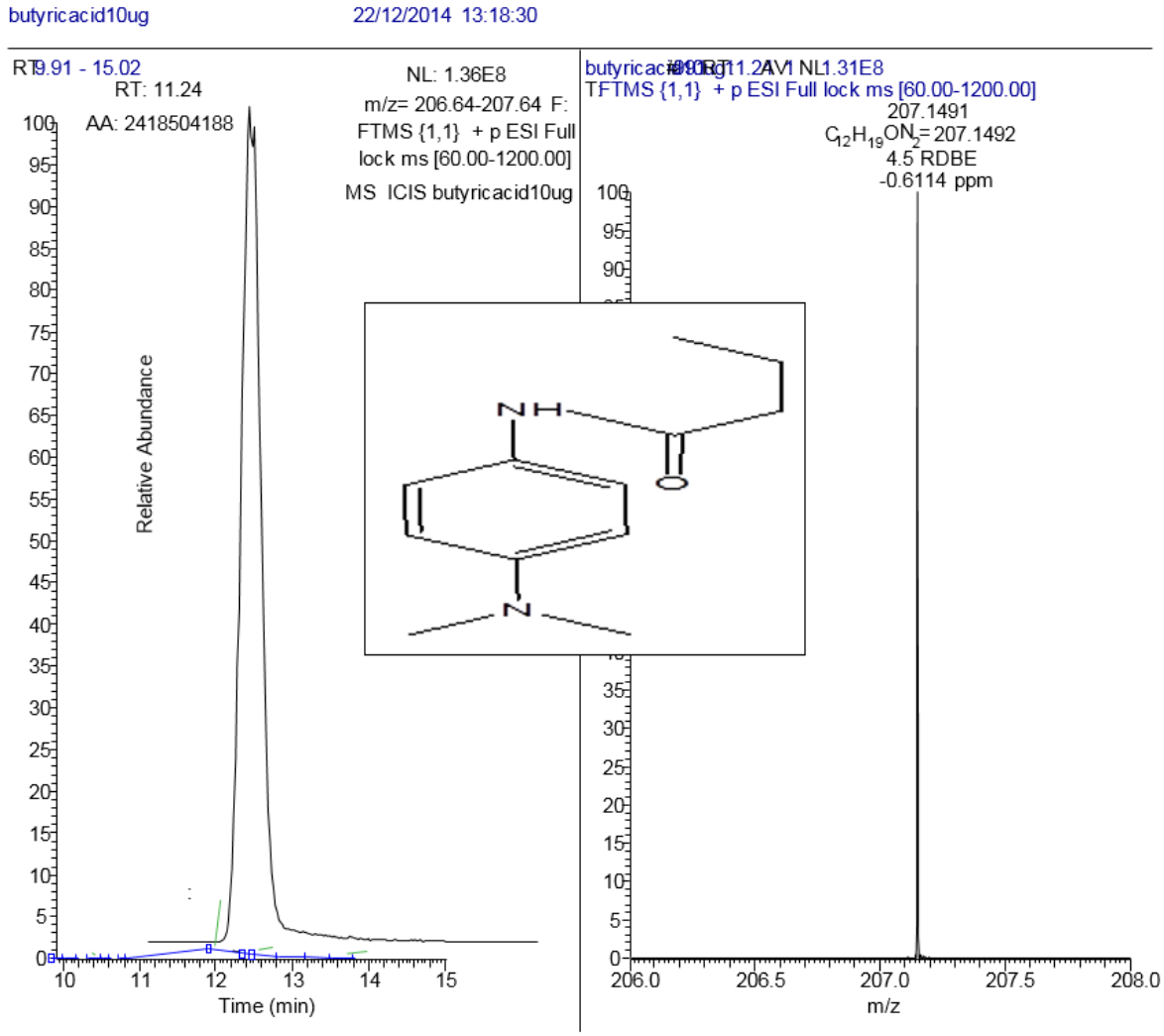

Figure 3. 7: Show the positive ESI-mass spectra for derivatised butyric acid at 10µg [M+H]⁺. HILIC chromatographic conditions as in 3.2.4.1.

3.3.2 Derivatisation of acids in urine samples

In urine sample the main SCFAs were derivatised by using this derivatisation reagent. Figure 3.8 shows extracted ion traces for SCFAs in a urine sample

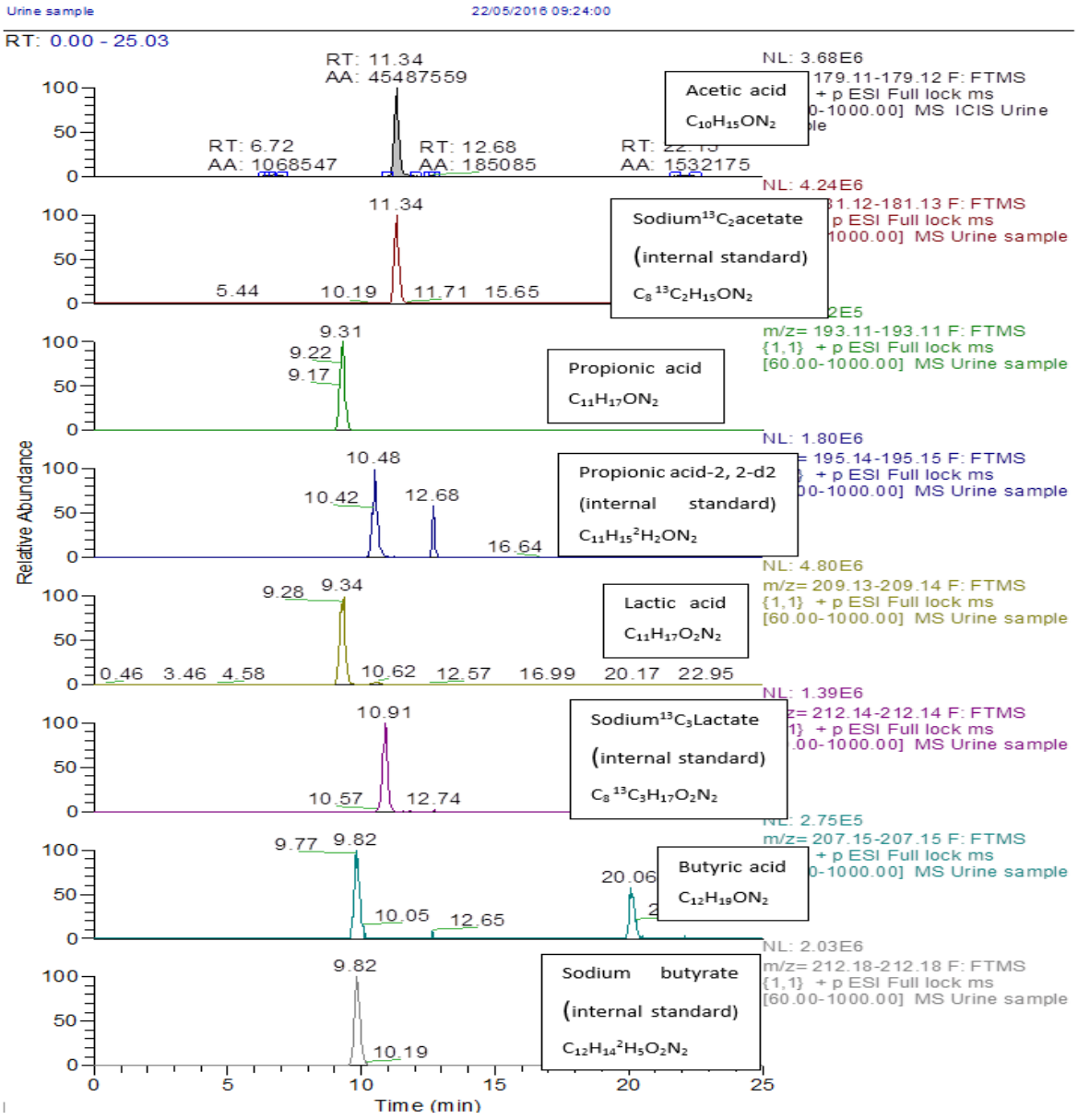

Figure 3. 8: Extracted ion traces for derivatised SCFAs (acetic, propionic, lactic, and butyric) in a urine sample.

3.3.3 Preparation of calibration curves of SCFAs

Different solvents and different samples of DPD were used in order to optimise the derivatisation, eventually calibration curves were prepared for propionic and acetic acids with varying amounts of acetic and propionic acids and fixed amounts of $^{13}C_2$-acetate and D2-propionate as internal standards.

Eventually the solvent used was THF and the DPD monohydrochloride was used as the derivatisation agent. The calibration curves in the range of 0 -640 ng (figure 3.9, 3.10) were reasonably linear but there was considerable background contamination for acetic acid below the 50 ng level. The chromatographic traces for the calibration points are shown in Appendix 1.

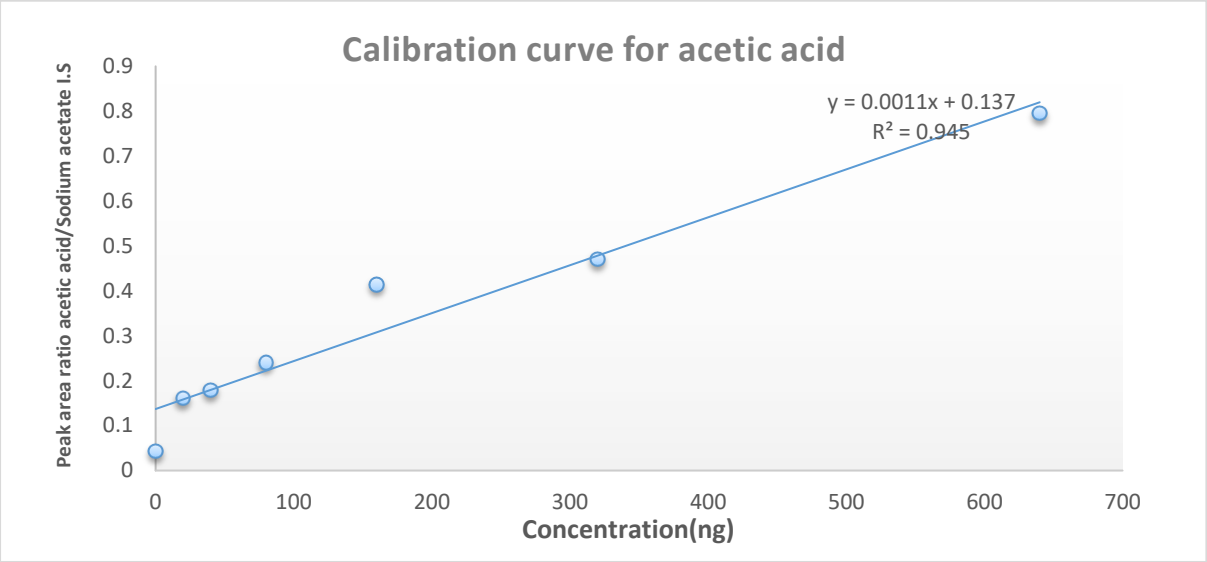

Figure 3. 9 : Calibration curve were constructed by plotting the peak area ratio of acetic acid and $^{13}C_2$ acetate as internal Standard (a/Sa $_{(internal\ standard)}$) versus the concentration by using DPD monohydrochloride & EDC.

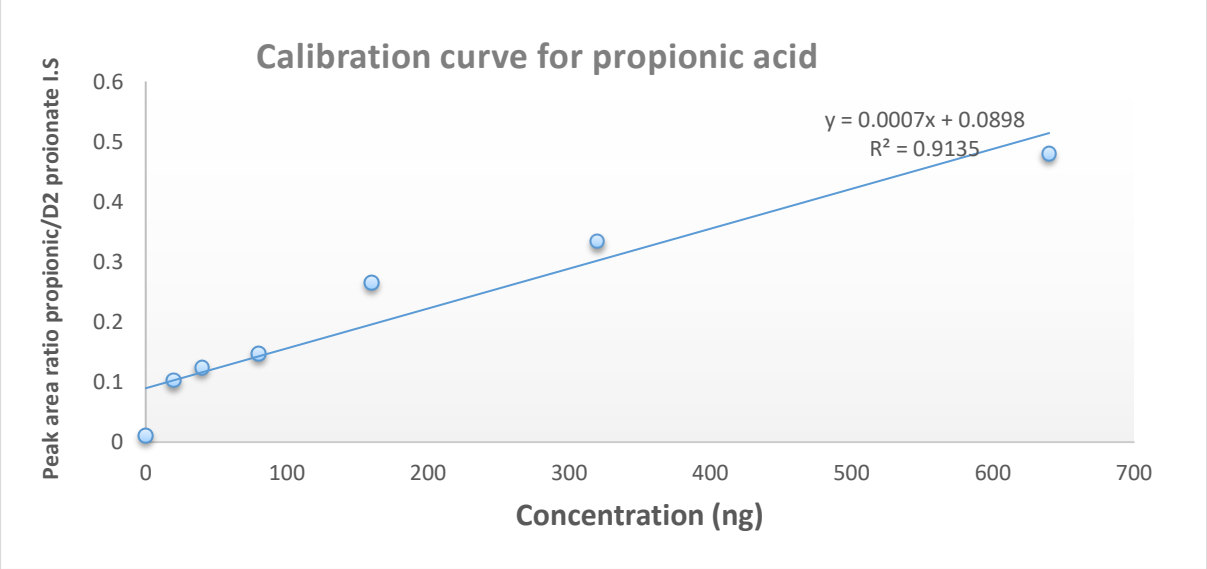

Figure 3. 10 : Calibration curve were constructed by plotting the peak area ratio of propionic acid and D2-propionate as internal standard (P/PD $_{(internal\ standard)}$) versus the concentration by using DPD monohydrochloride & EDC.

EDC was used for the three blank sample with usual regent DPD monohydrochloride then the results showed better background for the blank sample as well the RSD= ±1.24 %for acetic acid and ±1.07% for propionic acid (table 3.2, 3.3). Our results area ratios of acetic and $^{13}C_2$ acetate as internal Standard

in the blanks are shown in table 3.2 and those for propionic acid with D2 propionic acid as IS shown in table 3.3.

Table 3. 2: The areas obtained for acetic acid and 1µg of $^{13}C_2$ acetate with a fixed volume 20 µl of blank (water for ion chromatography) with same solvent (water for ion chromatography) and EDC in the method .

Blank Sample	(Peak area) acetic acid(a) Derivatised	(Peak area) (I.S) Sodium acetate (Sa) derivatised	a/Sa(internal standard)
1 – Blank1	33192052	171784821	0.193219
2 – Blank2	33113253	182534273	0.181408
3 – Blank3	34202642	175242444	0.195171

Table 3. 3: The areas obtained for propionic acid and 1µg of D2 propionic acid with a fixed volume 20 µl of blank (water for ion chromatography) with same solvent (water for ion chromatography) and EDC in the method.

Blank Sample	(Peak area) Propionic acid(P) derivatised	(Peak area) (I.S) propionic aid-2,2-d2 (PD) derivatised	P/PD(internal standard)
1 - Blank1	9061169	176454202	0.051351
2 – Blank2	9243221	178332312	0.051831
3 – Blank3	9130523	177233453	0.051516

However, there was still the contamination remaining at about 5- 10% of the intensity of the internal standard. The limiting reagent is the DPD which is only added 50µl of 10mM. Therefore, the strategy of the usual method was changed by changing two main things. The modification to the normal method and changed by addition more of the DPD reagent this was conducted by adding 400 µl water/THF (1:1) 50µl of the 1M EDC in water/THF (1:1) and 200µl of 10mM DPD in water/THF 1:1. Normal reaction was conducted and finally the mixture was diluted with 0.4 ml of water for ion chromatography at the end. The results indicated that it was very difficult to get rid of acetate background even by modifying the normal method (tables 3.4 and 3.5).

Table 3. 4: The areas obtained for acetic acid and 1µg of $^{13}C_2$ acetate with a fixed volume 20 µl of blank (water for ion chromatography) and more DPD reagent and EDC in the method.

Blank Sample	(Peak area) acetic acid(a) Derivatised	(Peak area) (I.S) Sodium acetate (Sa) derivatised	a/Sa(internal standard)
1 – Blank1 with 200µl of 10Mm DPD reagent	1937345	48028896	**0.040337**
2 – Blank2 with 200µl of 10Mm DPD reagent	1548751	46736910	**0.033138**
3 – Blank3 with 200µl of 10Mm DPD reagent	1724598	55997255	**0.030798**

Table 3. 5: The areas obtained for propionic acid and 1µg of D2 propionic acid with a fixed volume 20 µl of blank (water for ion chromatography) and more DPD reagent and EDC in the method.

Blank Sample	(Peak area) Propionic acid(P) derivatised	(Peak area) (I.S) propionic aid-2,2-d2 (PD) derivatised	P/PD(internal standard)
1 - Blank1 with 200µl of 10Mm DPD reagent	6952496	24511074	**0.283647**
2 – Blank2 with 200µl of 10Mm DPD reagent	6472937	23035960	**0.280993**
3 – Blank3 with 200µl of 10Mm DPD reagent	6091560	25512277	**0.23877**

However, using a larger volume of DPD reagent seemed to have worked without much increase in the background in the blank. Therefore, the modified version with more DPD reagent was carried out with urine sample 400 µl urine/THF (1:1) instead 400 µl water/THF (1:1). The urine was prepared first by mixing 500 µl urine + 500 µl of THF in an Eppendorf and centrifuging then by taking 400 µl of the supernatant to use in the method. Then 50 µl of the 1M EDC in water/THF (1:1) and 200µl of 10mM DPD in water/THF (1:1) was added and finally the mixture was diluted with 0.4 ml of water for ion chromatography. The RSD for peak area ratio of acetic in urine was ±9.78 %. The RSD for propionic in the urine was ±7.42 % (tables 3.6 and 3.7).

Table 3. 6: The areas obtained for acetic acid and 1µg of $^{13}C_2$ acetate with a fixed volume 400 µl of urine sample and more DPD reagent and EDC in the method.

urine Sample	(Peak area) acetic acid(a) Derivatised	(Peak area) (I.S) Sodium acetate (Sa) derivatised	a/Sa(internal standard)
1 –urine1 with 200µl of 10Mm DPD reagent	36439479	3435911	**10.60548**
2 – urine2 with 200µl of 10Mm DPD reagent	35343781	2804895	**12.60075**
3 – urine 3 with 200µl of 10Mm DPD reagent	37109262	3445507	**10.77033**

Table 3. 7: The areas obtained for propionic acid and 1µg of D2 propionic acid with a fixed volume 400 µl of urine sample and more DPD reagent and EDC in the method.

Urine Sample	(Peak area) Propionic acid(P) derivatised	(Peak area) (I.S) propionic aid-2,2-d2 (PD) derivatised	P/PD(internal standard)
1 –urine1 with 200µl of 10Mm DPD reagent	1294744	4362589	**0.296783**
2 – urine 2 with 200µl of 10Mm DPD reagent	1253134	3724869	**0.336424**
3 – urine 3 with 200µl of 10Mm DPD reagent	1319293	3876243	**0.340354**

3.3.3.1 Experimental design

In order to further optimise the method further an experimental design was developed by using Umetrics MODDE to see if the acetate derivatisation method could be improved by using 1 µg of $^2C_{13}$ acetate and applying the design proposed by MODDE shown in table 3.8 (1 ---7 experiments). In this case two factors were varied the amount of 1M EDC added and the ratio of THF to water. The DPD could not be changed since it was not in large excess unlike the EDC. After heating the volume was completed to 1 ml with water/THF (1:1) for each vial. By using the model of produced by MODDE (Figure 3.11) it could be seen that 10ul of 1 M EDC solution was enough and that it was better to use a high ratio of THF to water in the sample. The experiment was carried out 3 times for the blank

containing internal standard only. In addition the experiment was repeated three times with a sample of urine. It can be seen in tables 3.10 and 3.11 that although the background of acetate in the blank is at about 10% of the internal standard peak the levels in urine are much higher. The precision of the assay is also good.

Table 3. 8 : Experimental design with two varying factors the amount of EDC added and the ratio of THF to water.

Experiment	Run order	THF µl	Water µl	EDC µl	DPD µl
1	1	40	360	10	50
2	2	360	40	10	50
3	3	40	360	100	50
4	4	360	40	100	50
5	5	200	200	55	50
6	6	200	200	55	50
7	7	200	200	55	50

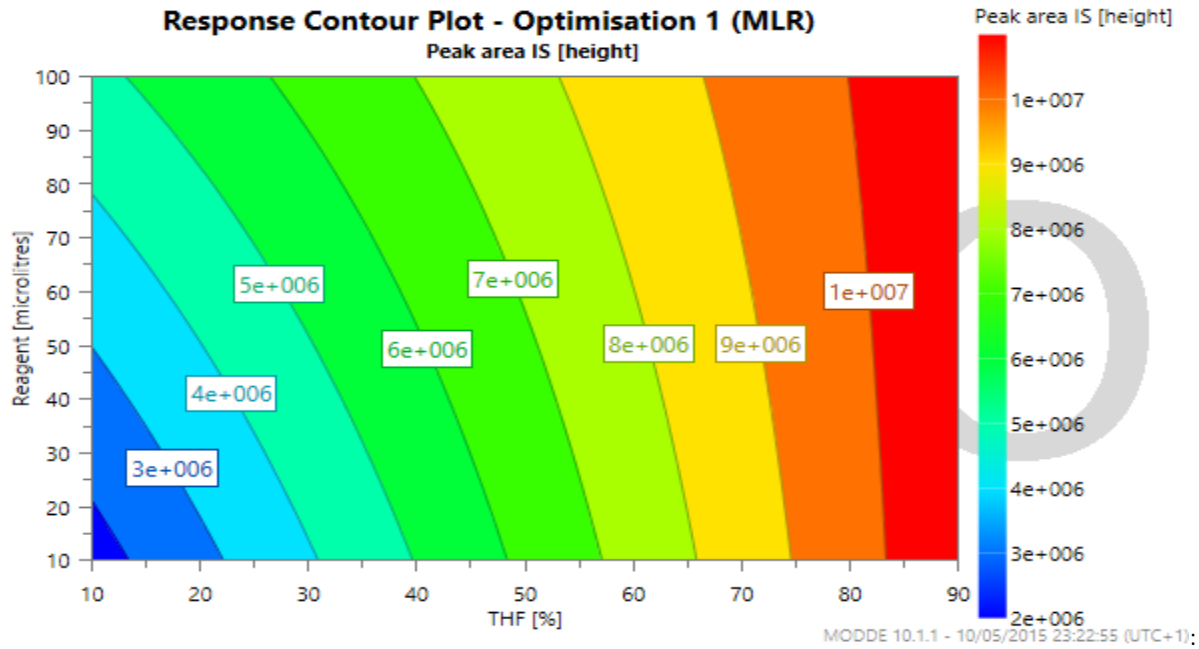

Figure 3. 11: The model of the IS response

Table 3. 9: The areas obtained for acetic acid and 1µg of $^{13}C_2$ acetate with a fixed volume 400 µl THF:water(300:100) of blank ,50 µl 10MmDPD(THE/water(1:1)and 20µl 1MEDC(THE/water(1:3) in the method.

Blank Sample	(Peak area) acetic acid(a) Derivatised	(Peak area) (I.S) Sodium acetate (Sa) derivatised	a/Sa(internal standard)
1 –Blank1 with 20µl of EDC and 50µl 10Mm DPD	43771405	409503914	**0.106889**
2 – Blank2 with 20µl of EDC and 50µl 10Mm DPD	2577625	26758787	**0.096328**
3 – Blank3 with 20µl of EDC and 50µl 10Mm DPD	2355423	24673321	**0.095464**

Table 3. 10: The areas obtained for acetic acid and 1µg of $^{13}C_2$ acetate with a fixed volume 400 µl THF:urine(300:100) of urine sample,50µl 10MmDPD(THE/water(1:1) reagent and 20µl 1MEDC (THE/water(1:3) in the method.

Urine Sample	(Peak area) acetic acid(a) Derivatised	(Peak area) (I.S) Sodium acetate (Sa) derivatised	a/Sa(internal standard)
1 – Urine1 with 20µl of EDC and 50µl 10Mm DPD	22457499	9206704	**2.439255**
2 – Urine2 with 20µl of EDC and 50µl 10Mm DPD	25328359	11026954	**2.29695**
3 – Urine3 with 20µl of EDC and 50µl 10Mm DPD	25044624	10631925	**2.355606**

At this stage another experimental design was developed in order to optimise the heating time used in the derivatisation. The protocol was carried out as indicated in table 3.11 table and it was found that a heating time of 45 minutes gave the best result along with the addition of 50 µl of 1M EDC.

Table 3. 11: Experimental design with two varying factors the amount of 1M EDC added and the heating time.

Experiment	Run order	THF µl	Urine µl	EDC µl	DPD µl	Heat min
1	1	300	100	20	50	15
2	2	360	40	50	50	15
3	3	40	360	20	50	60
4	4	360	40	50	50	60
5	5	200	200	35	50	37.5
6	6	200	200	35	50	37.5
7	7	200	200	35	50	37.5

The derivatisation of the blank and urine samples was repeated adding internal standards for propionic acid and acetic acid. The results are shown in tables 3.12-3.14. There was no background contamination for propionic acid. Both the acetic acid and propionic acid could be measured with good precision in the urine The RSD for acetic in the blank is ±9.88% , whilst the RSD in urine sample is ±4.19% There was no propionic in the blank and it gave an RSD of ±18.68 % in urine.

Table 3. 12: The areas obtained for acetic acid and 1µg of $^{13}C_2$ acetate with a fixed volume 400 µl THF:water(300:100) of blank ,50 µl 10MmDPD(THE/water(1:1), 50µl 1MEDC(THE/water(1:3) and heating 60 min at 60°C in the method.

Blank Sample	**(Peak area) acetic acid(a)** **Derivatised**	**(Peak area) (I.S) Sodium acetate (Sa) derivatised**	**a/Sa(internal standard)**
1 –Blank1 with 50µl of EDC and 50µl 10Mm DPD	18957845	136098610	**0.139295**
2 – Blank2 with 50µl of EDC and 50µl 10Mm DPD	24397951	145015985	**0.168243**
3 – Blank3 with 50µl of EDC and 50µl 10Mm DPD	21502523	146127892	**0.147149**

Table 3. 13:The areas obtained for acetic acid and 1µg of $^{13}C_2$ acetate with a fixed volume 400 µl THF:urine(300:100)of urine sample ,50 µl 10MmDPD(THE/water(1:1), 50µl 1MEDC(THE/water(1:3) and heating 60 min at 60°C in the method.

Urine Sample	(Peak area) acetic acid(a) Derivatised	(Peak area) (I.S) Sodium acetate (Sa) derivatised	a/Sa(internal standard)
1 – Urine1 with 50µl of EDC and 50µl 10Mm DPD	31847362	9402947	**3.386955**
2 – Urine2 with 50µl of EDC and 50µl 10Mm DPD	31056429	8544147	**3.634819**
3 – Urine3 with 50µl of EDC and 50µl 10Mm DPD	30866671	8445965	**3.654606**

Table 3. 14: The areas obtained for propionic acid and 1µg of D2 propionic acid with a fixed volume 400 µl THF:urine(300:100)of urine sample ,50 µl 10MmDPD(THE/water(1:1), 50µl 1MEDC(THE/water(1:3) and heating 60 min at 60°C in the method.

Urine Sample	(Peak area) Propionic acid(P) derivatised	(Peak area) (I.S) propionic aid-2,2-d2 (PD) derivatised	P/PD(internal standard)
1 –urine1 with 50µl of EDC and 50µl 10Mm DPD	1294744	4362589	**0.296783**
2 –urine2with 50µl of EDC and 50µl 10Mm DPD	1253134	3724869	**0.336424**
3 –urine3 with 50µl of EDC and 50µl 10Mm DPD	1319293	3876243	**0.340354**

However, it was observed that the area of the internal standard peaks fell in the urine relative to the blank and this might be due to the small volume of 10mM of DPD has been added since there are many other acids present in the urine that could react with DPD. Therefore, 100 µl of 10mM DPD was added rather than 50 µl of 10mM DPD. The derivatisation of urine was better with more 10 mM DPD (tables 3.15-3.17).

Table 3. 15: The areas obtained for acetic acid and 1µg of $^{13}C_2$ acetate with a fixed volume 400 µl THF:water(300:100) of blank ,100 µl 10MmDPD(THE/water(1:1), 50µl 1MEDC(THE/water(1:3) and heating 60 min at 60°C in the method.

Blank Sample	(Peak area) acetic acid(a) Derivatised	(Peak area) (I.S) Sodium acetate (Sa) derivatised	a/Sa(internal standard)
1 –Blank1 with 50µl of EDC and 100µl 10Mm DPD	37763829	242501929	**0.155726**
2 – Blank2 with 50µl of EDC and 100µl 10Mm DPD	48037241	325711691	**0.147484**
3 – Blank3 with 50µl of EDC and 100µl 10Mm DPD	28526048	191054731	**0.149308**

Table 3. 16: The areas obtained for acetic acid and 1µg of $^{13}C_2$ acetate with a fixed volume 400 µl THF:urine(300:100)of urine sample ,100 µl 10MmDPD(THE/water(1:1), 50µl 1MEDC(THE/water(1:3) and heating 60 min at 60°C in the method.

Urine Sample	(Peak area) acetic acid(a) Derivatised	(Peak area) (I.S) Sodium acetate (Sa) derivatised	a/Sa(internal standard)
1 –Urine1with 50µl of EDC and 100µl 10Mm DPD	36089725	10303887	**3.502535**
2 –Urine2 with 50µl of EDC and 100µl 10Mm DPD	37583524	9834716	**3.821516**
3 –Urine3 with 50µl of EDC and 100µl 10Mm DPD	40337180	10475155	**3.850748**

Table 3. 17: The areas obtained for propionic acid and 1µg of D2 propionic acid with a fixed volume 400 µl THF:urine(300:100)of urine sample ,100 µl 10MmDPD(THE/water(1:1), 50µl 1MEDC(THE/water(1:3) and heating 60 min at 60°C in the method.

Urine Sample	(Peak area) Propionic acid(P) derivatised	(Peak area) (I.S) propionic aid-2,2-d2 (PD) derivatised	P/PD(internal standard)
1 –urine1with 50µl of EDC and 100µl 10Mm DPD	4118549	3382305	**1.217675**
2 –urine2with50µl of EDC and 100µl 10Mm DPD	4306332	3580323	**1.202778**
3 –urine3 with50µl of EDC and 100µl 10Mm DPD	4224227	4993095	**0.846014**

The method was carried out with the plasma supernatant after mixing 1:1 with THF followed by centrifugation. The RSD obtained for acetic acid in the plasma was ±3.09% were good (table 3.19). While for the propionic in plasma the RSD was ±10.56% but the peak intensity was very low for the propionic acid in plasma.

Table 3. 18: The areas obtained for acetic acid and 1µg of $^{13}C_2$ acetate with a fixed volume 400 µl THF:plasma(300:100)of plasma sample ,100 µl 10MmDPD(THE/water(1:1), 50µl 1MEDC(THE/water(1:3) and heating 60 min at 60°C in the method.

Plasma Sample	(Peak area) acetic acid(a) Derivatised	(Peak area) (I.S) Sodium acetate (Sa) derivatised	a/Sa(internal standard)
1 –Plasma1 with50µl of EDC & 100µl 10Mm DPD	55676975	14390827	**3.868921**
2 –Plasma 2 with 50µl of EDC & 100µl 10Mm DPD	58572310	14239725	**4.113303**
3 –Plasma 3 with 50µl of EDC & 100µl 10Mm DPD	57055516	14381002	**3.967423**

Table 3. 19: The areas obtained for propionic acid and 1µg of D2 propionic acid with a fixed volume 400 µl THF:plasma(300:100)of plasma sample ,100 µl 10MmDPD(THE/water(1:1), 50µl 1MEDC(THE/water(1:3) and heating 60 min at 60°C in the method.

Plasma Sample	(Peak area) Propionic acid(P) derivatised	(Peak area) (I.S) propionic aid-2,2-d2 (PD) derivatised	P/PD(internal standard)
1 –Plasma 1with 50µl of EDC & 100µl 10Mm DPD	219409	6401182	**0.034276**
2 – Plasma 2with50µl of EDC & 100µl 10Mm DPD	265432	6332351	**0.041917**
3 – Plasma 3 with50µl of EDC & 100µl 10Mm DPD	238833	6579915	**0.036297**

3.3.3.2 Method quantification

The method was calibrated as follows. Stock solutions of acetic, propionic and lactic acids (1mg/ml) were prepared in water. Then a mixture with a concentration of 10µg/ml was prepared and the mixture was spiked as follows: 20 µl +80 µl water , 40 µl + 60 µl water , 60 µl + 40 µl water, 80 µl + 20 µl water, 100 µl at the end all volumes were made to 400 ul by adding 300 µl of THF. Furthermore a second series starting with a 50 µg/ml mixture was made up to cover the higher range followed by adding water as follows: 40 µl + 60 µl water , 60 µl + 40 µl water, 80 µl + 20 µl water, 100 ul same as

the previous mixture the volumes were made it up to 400 ul with THF at the end.The two internal standards were included at 1µg/ml in all the samples as usual deuterium 2,2D propionic acid and $^{13}C_2$ sodium acetate. Then the nine samples were used in the derivatisation method in the usual way as nine point calibration curve was created. The calibration curves are shown in figures 3.12-3.17.

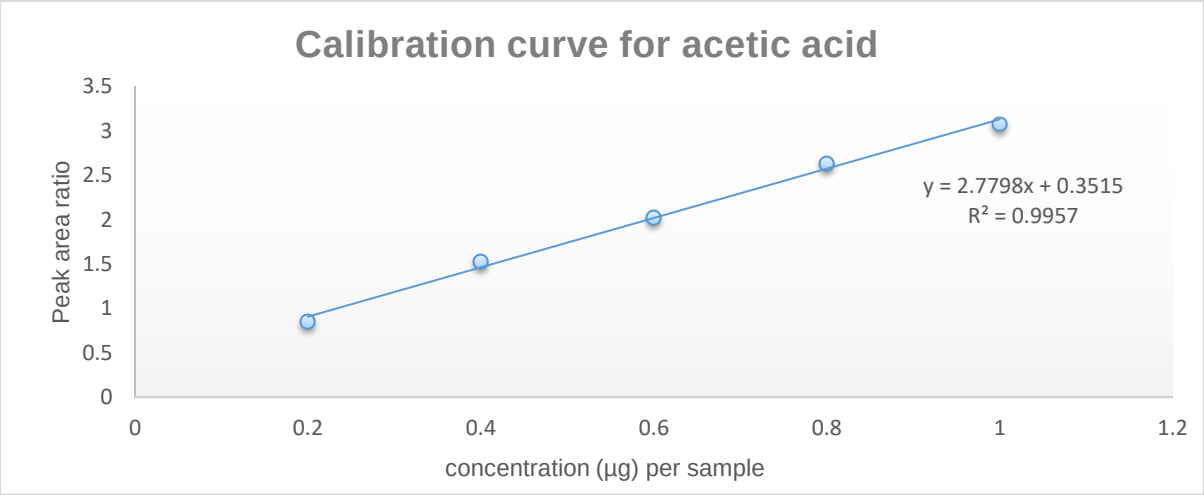

Figure 3. 12: Calibration curve were constructed by plotting the peak area ratio of acetic/$^{13}C_2$ acetate (a/Sa (internal standard)) versus the concentrations points (0.2,0.4,0.6,0.8,1) µg/ml by using mixture of (SCFA).

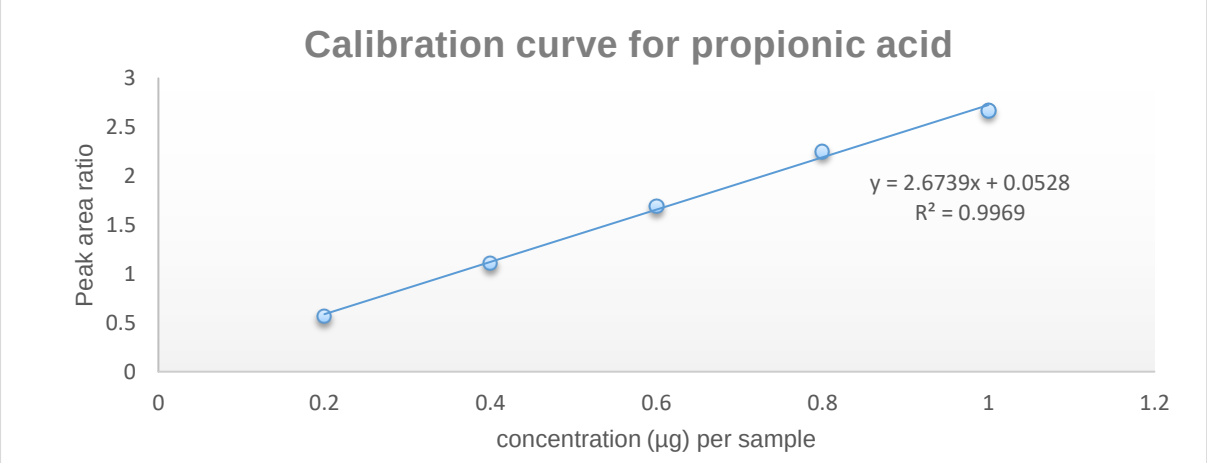

Figure 3. 13: Calibration curve were constructed by plotting the peak area ratio of propionic/ D_2 propionic acid (P/PD (internal standard)) versus the concentrations points (0.2,0.4,0.6,0.8,1) µg/ml by using mixture of (SCFA).

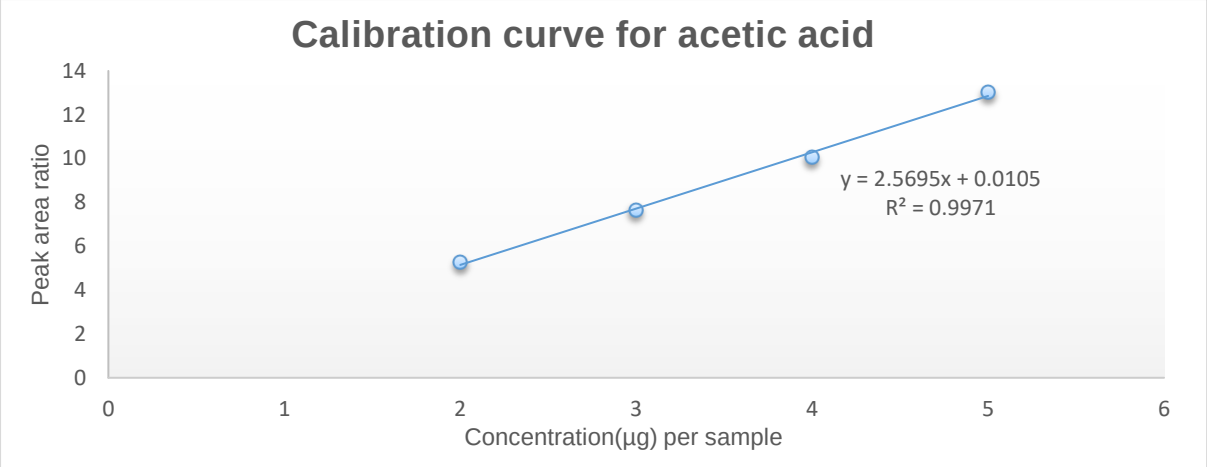

Figure 3. 14: Calibration curve were constructed by plotting the peak area ratio of acetic/$^{13}C_2$ acetate (a/Sa $_{(internal\ standard)}$) versus the concentrations points (2,3,4,5) µg/ml by using mixture of (SCFA).

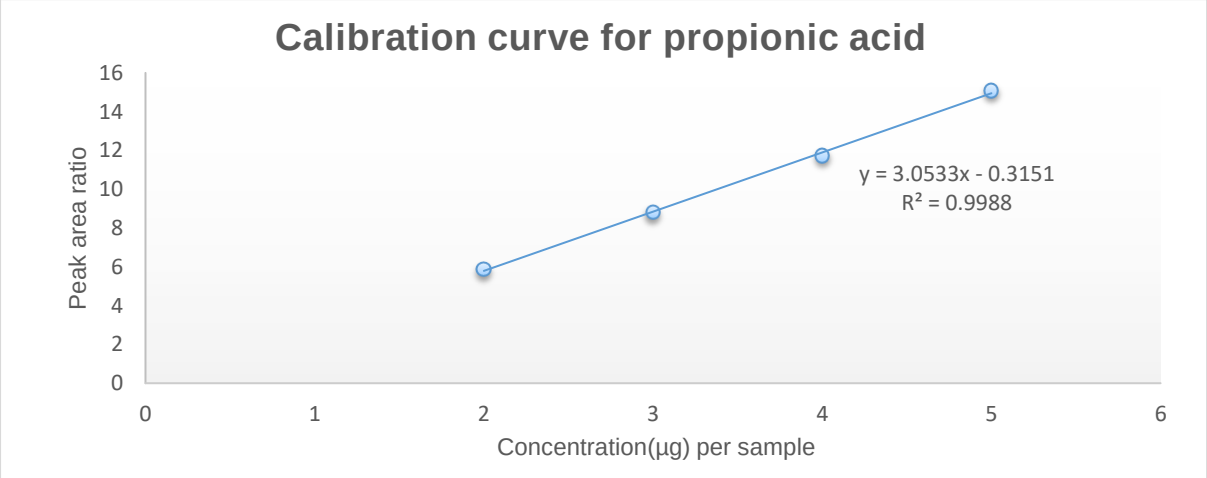

Figure 3. 15: Calibration curve were constructed by plotting the peak area ratio of propionic/ D_2 propionic acid (P/PD $_{(internal\ standard)}$) versus the concentrations points (2,3,4,5) µg/ml by using mixture of (SCFA).

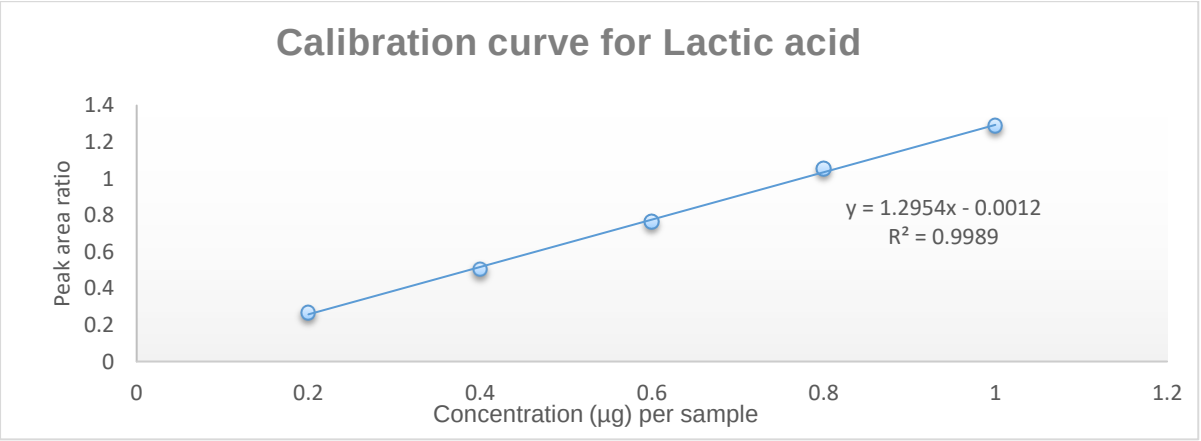

Figure 3. 16: Calibration curve were constructed by plotting the peak area ratio of Lactic acid/$^{13}C_3$ Sodium lactate (L/Sa $_{(internal\ standard)}$) versus the concentrations points (0.2,0.4,0.6,0.8,1) µg/ml by using mixture of (SCFA).

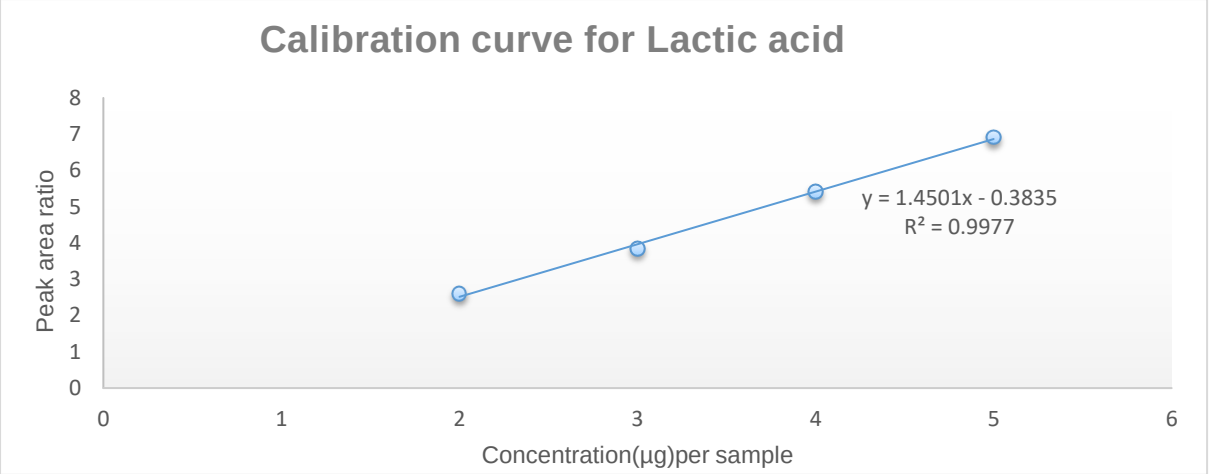

Figure 3. 17: Calibration curve were constructed by plotting the peak area ratio of Lactic acid/$^{13}C_3$ Sodium lactate (L/Sa $_{(internal\ standard)}$) versus the concentrations points (2,3,4,5) µg/ml by using mixture of (SCFA).

At this stage this method was almost complete. However, the matrix effect was assessed using a standard additions method the levels approximately should be as follow those values of acids: acetic acid: 1.29 µg /100µl in urine, 1.25 µg /100 µl in plasma. Propionic acid 0.406 µg/100 µl in urine, 0.0135 µg/100ul in plasma. Lactic is similar to acetic acid. The standard addition method has been conducted by diluting acetic acid, lactic acid stock solutions to 10 µg /ml in THF (in the same solution), also including propionic acid in the mixture at 0.5 µg/ml in THF. Urine/THF (100:300 µl) were spiked as follows 0 µl, 50 µl, 100 µl, 150 µl of the standard mixture(acetic acid and lactic acid) from stock solutions 10 µg /ml and propionic acid from stock solution 0.5 ug/ml , in addition the deuterium D2 - propionic acid and $^{2}C_{13}$ sodium acetate at 1 µg /ml were included. Therefore the spike was 0, 0.5, 1 and 1.5 µg/ml for acetic and lactic. Whereas the spike was 0, 0.0 25, 0.05 and 0.075 µg /ml for propionic acid. The same method was carried out for the plasma supernatant. From the results the level of acetic acid in urine was 0.91 µg /100µl and the level in the plasma was 0.45 µg /100µl. whereas in propionic the level was 0.079 µg /100µl in urine and 0.036 µg /100µl in the plasma. Moreover the level of lactic acid in urine was 31.55 µg /100µl and 2.71 µg /100µl level of lactic in plasma. The calibration curves were satisfactory for all the analytes apart from lactic acid. There was no evidence for marked ion suppression effects since the concentrations obtained for the analytes were close to those obtained from making direct measurements based on the ratio of the analytes to their internal standards.

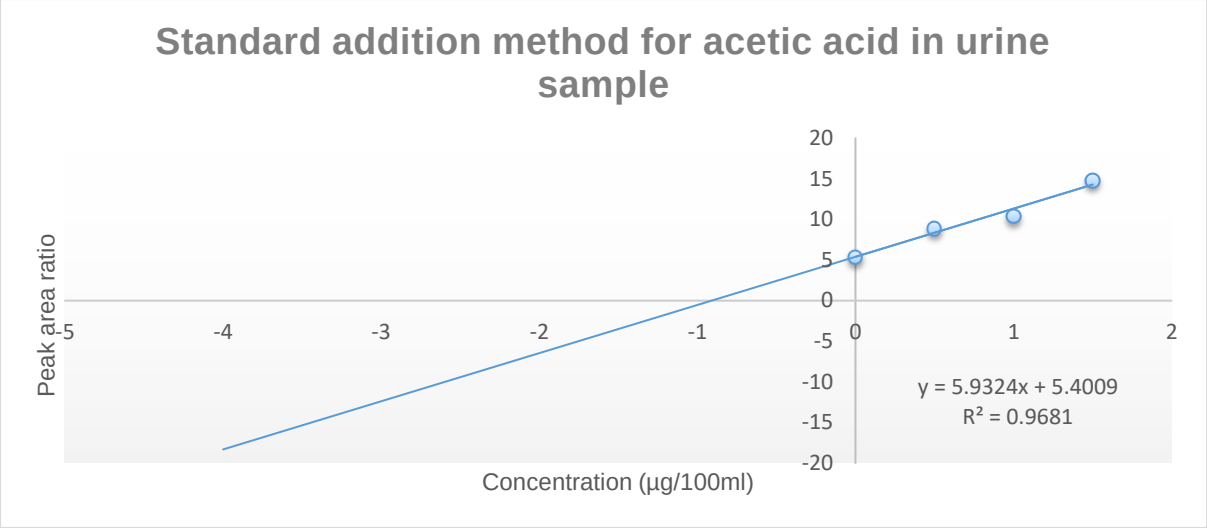

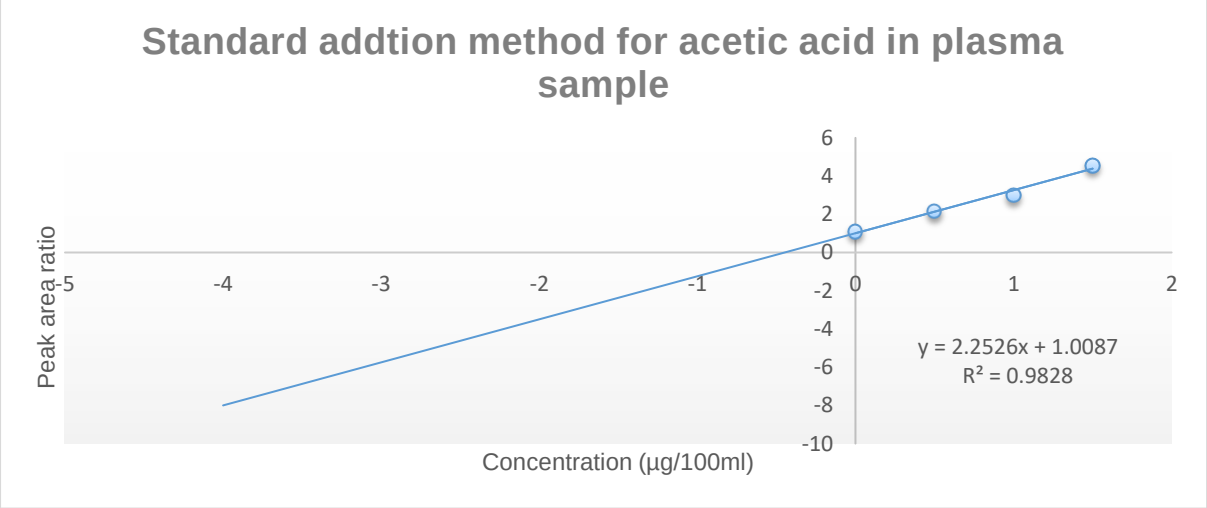

Figure 3. 18: Standard addition method for acetic acid in urine and plasma for testing the matrix effect.

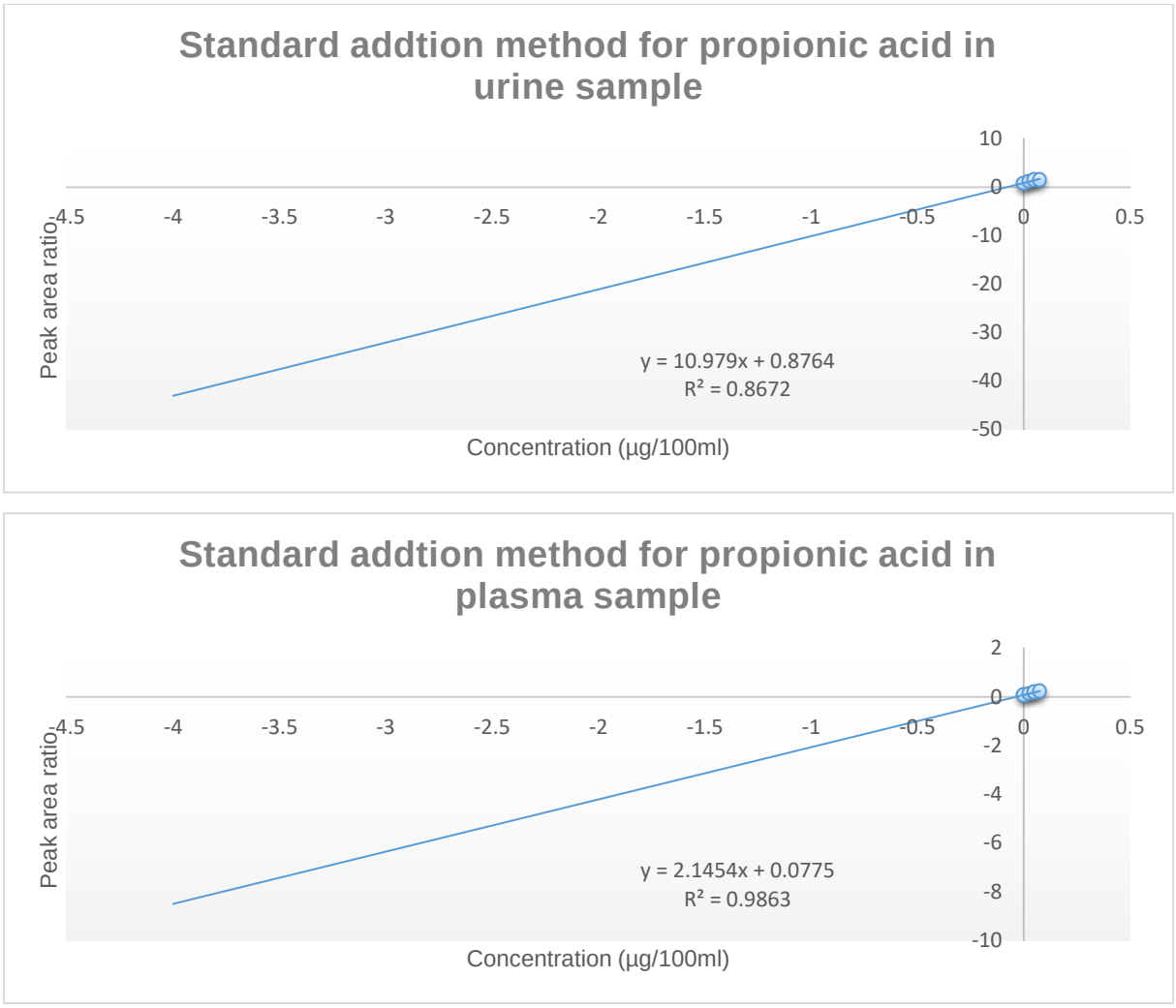

Figure 3. 19: Standard addition method for propionic acid in urine and plasma for testing the matrix effect.

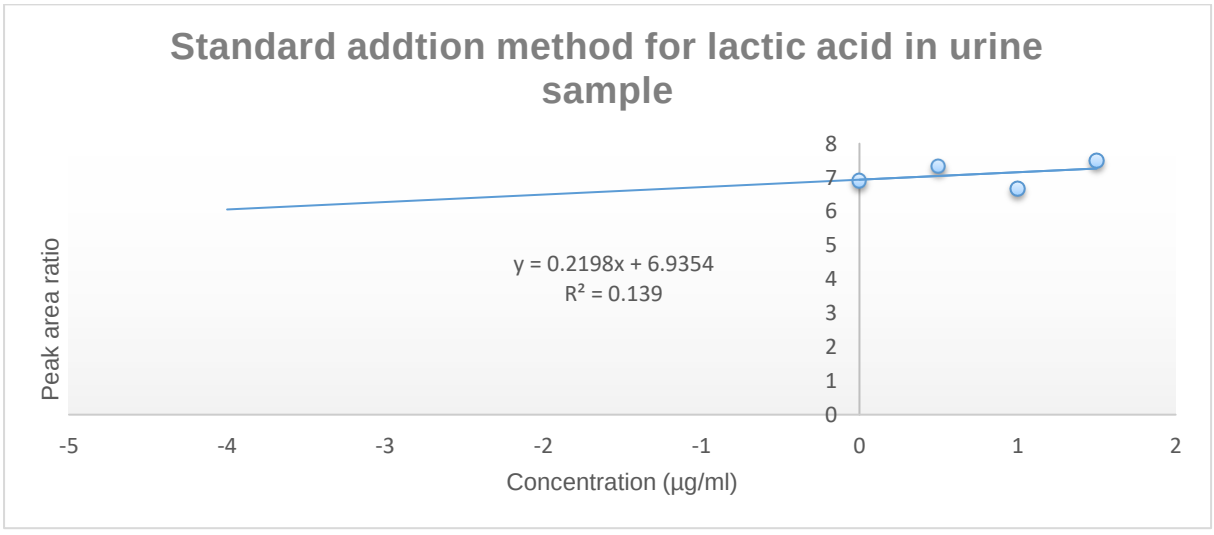

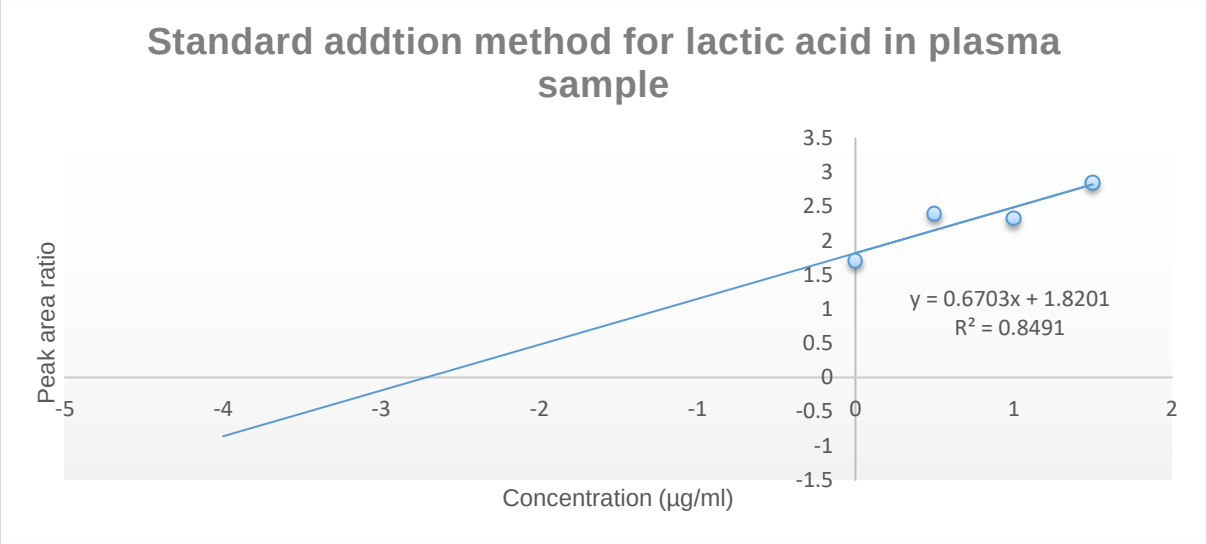

Figure 3. 20: Standard addition method for Lactic acid in urine and plasma for testing the matrix effect.

Finally a calibration curve was constructed for butyric acid using D5 sodium butyrate as an internal standard (table 3.21, figure 3.21).

Table 3. 20: The calibration points of butyric acid and D_5 Sod. Butyrate from the area under the peak of each reading and each concentration points have fixed volume 100µl of acid and keeping the remaining as usual method.

concentration	AUP of butyric	I.S D_5 Sod. Butyrate	Ratio butyric/ Sodium butyrate
0	1352140	60623991	0.022304
0.05	5404207	64361715	0.083966
0.1	7651638	65195472	0.117365
0.2	9204560	67607664	0.136147
0.4	10572887	63152307	0.167419
0.8	22332420	67277937	0.331943
1.6	42123269	68974732	0.610706
3.2	61784827	67562123	0.914489

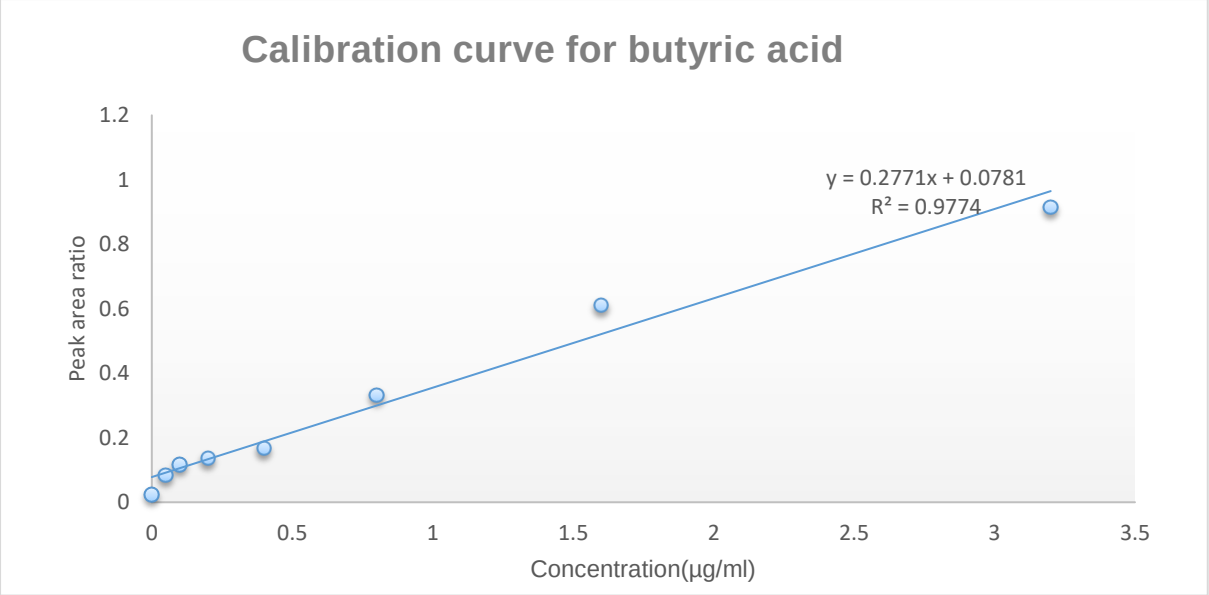

Figure 3. 21: Calibration curve were constructed by plotting the peak area ratio of butyric acid and (sodium butyrate D5) (B/SB $_{(internal\ standard)}$) versus the concentrations points in µg/ml.

3.4 Conclusion

The background of acetate in the environment was quite abundant and was estimated to be around 0.5 µM.The level of propionate was much lower at around 0.054µM and butyrate was around 0.28 µM. Thus these levels reflect the limit of detection rather than instrument response. Working in area completely free from chemicals is the optimum solution to remove these contamination. In the HPLC mobile phase acetic acid is the common additive which is fairly volatile and thus highly likely contaminant in a chemical laboratory. The level of acetate in the environment <10% of the levels detected in biological samples and the same was the case for butyrate. Propionate has more impact because of the very low levels in the samples, despite the low levels of propionate contamination. The precision value obtained in urine were satisfactory for trace analysis method of acetate and butyrate according to FDA guidelines. The method sensitivity was comparable to the GC methods utilising vacuum distillation. However the level of this method sensitivity did not achieve the sensitivity of the previously developed hollow fibre extraction method [104-107]. The use of an HILIC method enabled injection of samples and the derivatisation method was simple to perform with a high content of organic solvent while preserving peak shape.

Chapter-4

Application of derivatisation method in the urine samples of UC patients and control people for quantification of SCFA in those three cohorts (active UC, quiescent UC and control individuals not suffering from IBD).

4.1- Introduction

Gut microbiota play a major role in the prolongation and onset of the chronic intestinal inflammation as witnessed in IBD[96].One of the main functions of the gut microbiota is to break down complex and degradation of polysaccharides, carbohydrates and proteins into SCFAs mostly acetate, propionate and butyrate which are the major energy source for colonocytes an epithelial cells of the colon, also SCFA considered of importance for mucosal metabolism and affect sodium absorption and mucosal cell proliferation. It has been hypothesized that the mucosal atrophy happen because of the lack of luminal SCFAs in the long-term to "nutritional colitis" [108].This fermentation process is specific to the anaerobic bacteria mostly of the phyla Clostridium and Bacteroidetes, and occurs in colon and cecum [109]. Moreover certain has shown that alteration of intestinal bacteria has been observed from the composition of fecal microbiota of the UC patients which differed from that of healthy controls and it was reported that there was a reduction in *Roseburia hominis* and *Faecalibacterium prausnitzii* , the major bacterium of the *Clostridium leptum*, both well-known butyrate-producing bacteria of the Firmicutes phylum which an indication for the dysbiosis in IBD and suggesting that different bacterial species contribute to the pathogenesis of the UC and it was hypothesised that the dysbacteriosis is important in UC pathophysiology because *F prausnitzii* produces high concentrations of butyrate as an important energy source for coloncytes and thus prevents mucosal atrophy. Consequently, the mucosal barrier function of the colon is improved by butyrate, hence deficiency of this species stimulate or enhances inflammation and the most reported observation is the reduction on the phylum of Bacteroidetes and Firmicutes members after mucosal and fecal analysis [96]. Familial polyposis (FAP) and (UC) are diseases associated with a high risk of colon cancer and characterised by high rate of colonic mucosal proliferation and varying severity of colonic inflammation is associated with the changes that occur in the ileal mucosa of the pelvic pouch (atrophy of the villi and crypt hyperplasia). It has recently been demonstrated that the trophic factors for the colonic mucosa in the clinical and endoscopic condition of distal UC and diversion colitis was improved after application of SCFAs. Moreover, a study mentioned that applying enemas containing SCFAs does have some beneficial effects in UC patients but do not control inflammation [110]. Several intestinal function were affected by SCFAs. Mucus is an important physiological component of the intestinal mucosal barrier. Mucus gel layer covering the mucosa of the distal colon and rectum and plays an important role in the

protection of the underlying epithelium against chemical and mechanical damage. A major products of intestinal microbial metabolism are SCFAs for instance acetate, n-butyrate and propionate are considered the most prevalent anions in the intestinal lumen. The effect of organic acids and SCFA on intestinal mucus release is not fully understood. An investigation was carried out into whether or not mucus release was stimulated by lumen SCFAs into the rat colon and it was found that a mixture of SCFAs (20mMbutyrate, 35mM propionate and 75mM acetate) increased the colonic mucus secretion. The individual SCFAs stimulate mucus release into colon in similar concentration-dependent manners but not lactate or succinate. However, lactate and succinate can accumulate in patients with the UC or bowel resection in the colonic lumen. Previous research observed that the stimulatory effect of SCFAs on mucus release from the hindgut mucosa in rats but neither succinate nor lactate stimulated mucus secretion from the rat colon via a cholinergic nerve mechanism and at 20mM butyrate can stimulate the colonic mucus secretion but no other SCFA was active at this concentration. In addition the stimulatory effects of SCFAs on mucus secretion can be diminished if the pre-treatment with anti-cholinergic was carried out [111]. The etiology of UC and IBD is still unclear and several mechanisms have been suggested including inappropriate inflammatory response or abnormal immune response to microbiota. SCFAs are the output of bacterial fermentation of unabsorbed carbohydrates which can play a major role in the maintaining osmolality and colon pH. Impaired oxidation and low SCFA concentration was observed in patients with severe UC, which led to metabolic alteration of colonic mucosa. Butyrate is one of the four-carbon SCFAs and has anti-carcinogenic and anti-inflammatory effects, *in vivo* and *in vitro* that was mentioned in various previous studies, beside that butyrate is the main fuel for colonocytes and therefore is very important for colon integrity [112]. Thus it was of interest to be able to quantify acetate, propionate and butyrate in urine from IBD patients and controls so see if they offered and diagnostic or prognostic benefits.

4.2- Experimental (Derivatisation of (SCFA) in urine samples of the three groups):

4.2.1- Material, Chemical and reagents.

Materials,chemical and reagents have been reported in section 3.2.1(Chapter-3). Creatinine determination kit including creatinine standard, 100mg/dl, catalog No. 80-2395, creatinine detection reagent, 20ml catalog No. 80-2396 (Promega Ltd., Southampton UK) .

4.2.2 Urine samples.

These samples have been reported in detail in sections *2.2.3.4* & *2.2.3.5* (Chapter-2).

4.2.3 Equipment.

All the equipment were utilised is described in section 3.2.2(Chapter-3) in addition to

4.2.3.1 Clear Microtiter Plates, Catalog No. 80-2394:

Two plates of 96 wells, clear uncoated microtiter plates.

4.2.3.2 Plate Sealers, 2each, Catalog No. 30-0012:

4.2.3.3 Colorimetric 96 well microplate reader:

Wallac Victor 2, PerkinElmer, UK

4.2.3.4 LC-MS instrumentation

All the details are reported in section *3.2.2.1*(Chapter-3).

4.2.4 Solutions .

4.2.4.1 Preparation of 100mM DPD in 50% H2O, 50% THF (v/v).

As described in section 3.2.3.

4.2.4.2 Preparation of 1 M EDC in 75% H_2O, 25% THF (v/v)

As described in section 3.2.3.

4.2.4.3 Preparation of solution as mixture of four internal standards (solution D).

By preparing a solution in THF:water (1:1) containing 0.05 mg/ml 13C acetic, 0.05 mg/ml D2 propionic, 0.05 mg/ml 13C lactate and 0.05 mg/ml of sodium butyrate D_5 to the total volume 1ml (water/THF).

4.2.4.4 Purification of THF.

As described in section 3.2.3.

4.2.4.5 Preparation of urine for Derivatisation .

Urine (100 µl) was mixed with 20µl of a solution in THF:water (1:1) containing 0.05 mg/ml $^{13}C_2$ sodium acetate, 0.05 mg/ml $^{2}H_2$- propionic, 0.05 mg/ml $^{2}H_5$ butyric acid and $^{13}C_3$-lactic acid 0.05mg/ml. Then 300µl of THF was added to the sample and it was centrifuged.

4.2.5 Method procedure and protocol:

4.2.5.1 Mobile phase

As described in section 3.2.3.

4.2.5.2 Gradient programme:

As described in section 3.2.4.

4.2.5.3 Derivatisation of urine sample by using EDC and DPD.

To the supernatant was added 50µl of 1M EDC in THF:water (1:1) and 50µl of 10mM DPD in THF:water(1:1).After that the vial was placed in a heating block at 60°C for 60 min. The resulting mixture was diluted with water to 1 ml and was then transferred to a HPLC vial and then analysed by LC–MS .

4.2.5.4-Determination of creatinine in urine.

4.2.5.4.1- creatinine standard curve

Seven glass test tube#1 through#7 were used. Tube#1 was filled with 800 µl water for ion chromatography and the remaining tubes #2-#7 were filled with 500 µl water for ion chromatography. Then 200 of µl of the creatinine standard stock solution 100mg/dl was carefully added to tube#1 and it was vortexed completely. Then 500 µl of creatinine solution in tube#1 was taken then added to the tube #2 and vortexed completely. This method was repeated for tubes#3 through#7 respectively. Diluted standards should be used within 2 hours of preparation.

4.2.5.4.2- preparation of sample

The test samples were diluted with a minimum 1:20 dilution of urine sample into water for ion chromatography, which was recommended to removing matrix interference. Diluted samples should be used within 2 hours of preparation.

4.2.5.4.3- Assay procedure

50 µl of the diluted urine samples, standards and blank (water for ion chromatography) were pipetted to the bottom of appropriate wells. Then 100 µl of creatinine detection reagent was added to each well. After that the sides of the plate was tapped gently to ensure adequate mixing of the reagents. All the samples and standards were pipetted in duplicate, hence the previous procedure was repeated with second plate. Finally, the two plates were incubated at room temperature 30 minutes before putting the plate into the plate reader and zeroing the plate reader against the water blank.

4.3 Results and Discussion:

4.3-1 Quantification of acetate, propionate, butyrate and lactate:

Acetate was quite abundant in the environment and its levels were estimated to be around 0.5 µM. The background for propionate was much lower at around 0.054 µM and butyrate was around 0.28 µM. Thus, these set the limits of detection for the acids rather than instrument response. It would be difficult to remove these contaminants unless working in an area completely free from chemicals. Acetic acid is a common additive in the HPLC mobile phases, which is fairly volatile and thus, a highly likely contaminant in a chemical laboratory. The levels of acetate in the environment were well below (<10%) of the levels detected in biological samples and the same was the case for butyrate. Despite the low levels of propionate contamination, this has more impact because of the very low levels in the samples. However, the derivatisation method was simple to perform and the use of an HILIC method enabled injection of samples with a high content of organic solvent while preserving peak shape. The precision values obtained for acetate and butyrate in urine were satisfactory for a trace analysis method according to FDA guidelines. The sensitivity of the method was comparable to the GC methods utilising vacuum distillation[98, 99, 113-115], although, it did not achieve the level of sensitivity of the previously developed hollow fibre extraction method [116], apart from the case of propionate, as a result of persistent background contamination rather absolute limit of detection. The current method does not require specialised, lengthy or complex sample preparation and has been demonstrated to be capable of the analysis of SCFAs in the ranges required for their determination in small volumes of both plasma and urine The best and optimised method has been successfully used for derivatisation of carboxylic acid containing compounds or metabolites in chapter 3, with the respect to the heating time and amount of EDC reagent using MODDE 10.1 (Umetrics, Umea˚, Sweden) which proposed the experimental design shown in the Table 3. 11 in chapter 3 , therefore the optimised method was applied for derivatisation of all the urine samples of participants whether they have UC(active and remission) or healthy control that were provided from Gastroenterology Unit, Glasgow Royal Infirmary hospital. The calibration data obtained for the SCFAs along with levels determined are shown in Table 4.1. The data for the calibration curves as shown in tables 4.2-4.5 and the calibration curves are shown in figures 4.2, 4.4., 4.6 and 4.8. The levels of the SCFAs determined graphically are shown in figures 4.1, 4.3, 4.5. and 4.7. The raw data for the peak areas of the SCFAs in urine are given in Appendix 2 tables- The calibration curves gave satisfactory linearity apart from lactic acid where the correlation coefficient was low.

Table 4. 1: Calibration data obtained for SCFAs and the results from the analysis of patients with active IBD, in remission from IBD and a control group.

Acid	Calibration curve	Control Concentration µM ±SD	Active Concentration µM ±SD	Remission Concentration µM ±SD	P Value Control active	P value Control remission	P value Active remission
acetic	Y=0.737x+0.038 R^2=0.994	333±101	240±111	270±66	0.016	0.053	0.302
propionic	Y=1.1087x +0.0056 R^2= 0.993	5.04±0.196	5.45±3.15	6.89±3.14	0.45	0.31	0.79
butyric	Y=0.354x + 0.0312 R^2= 0.992	50±18.5	68.4±52.2	71.4±31.6	0.069	0.015	0.431
Lactic	Y=1.7691x R^2= 0.93	28.2±2.84	78±3.2	51±2.9	0.36	0.21	0.63

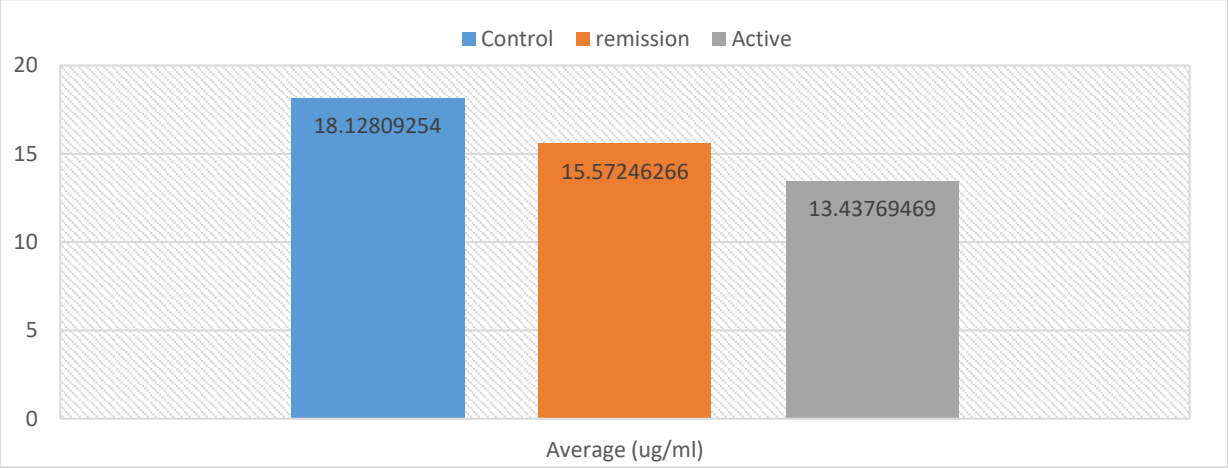

Figure 4. 1: Column chart to demonstrate the Comparison of average concentration in µg/ml of acetic acid in three groups of urine samples.

Table 4. 2: The calibration points of acetic acid and $^{13}C_2$ acetate from the area under the peak of each reading and each concentration points have fixed volume 100µl of acid and keeping the remaining as usual method.

Concentration	Area under the peak of Acetic	Area under the peak of I.S ($^{13}C_2$Sodium Acetate)	Ratio acetic/ $^{13}C_2$ Sodium acetate
0	3030066	78402041	0.038647795
0.05	6270498	70259042	0.089248271
0.1	9070820	67179400	0.135023832
0.2	11907288	70402788	0.169130916
0.4	24065115	75582204	0.318396577

0.8	50621884	83406152	0.606932256
1.6	80610293	75808428	1.0633421
3.2	199669799	81399957	2.452947229

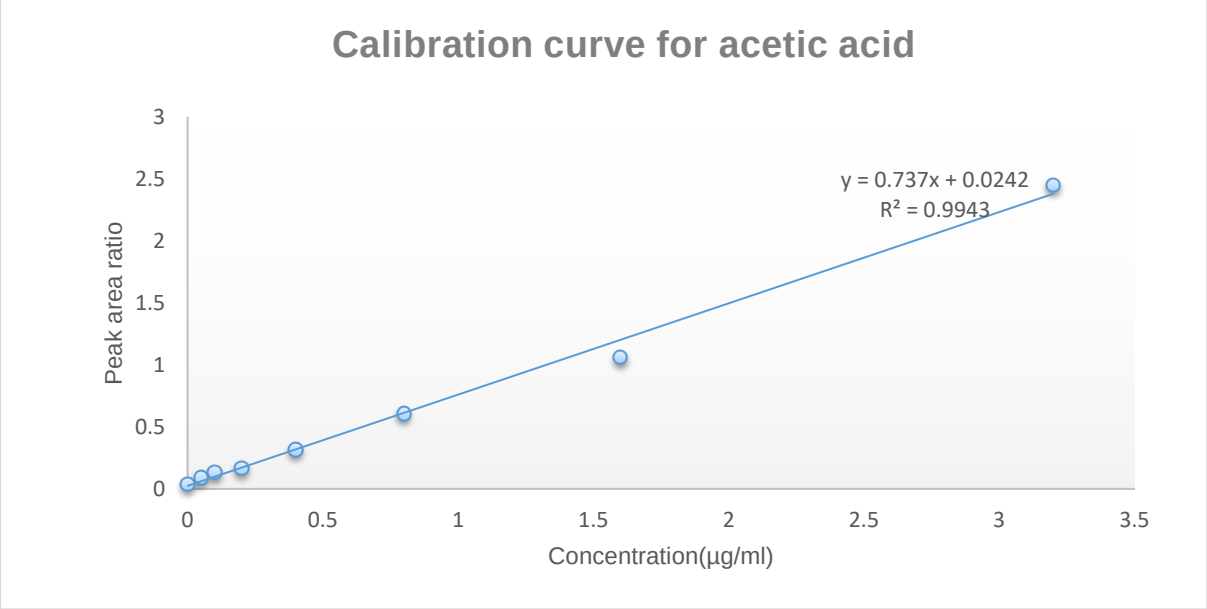

Figure 4. 2: Show Calibration data were constructed by plotting the peak area ratio of acetic acid / $^{13}C_2$ acetate (a/Sa) versus the concentrations points in the range 0.05-3.2 in µg/ml.

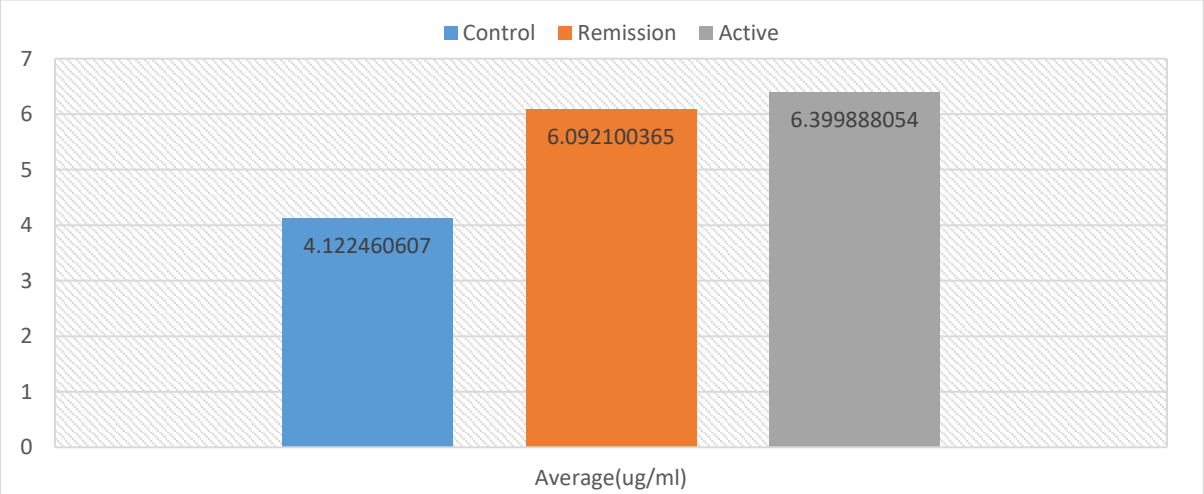

Figure 4. 3: Column chart to demonstrate the Comparison of average concentration in µg/ml of butyric acid in three groups of urine samples.

Table 4. 3: The calibration points of butyric acid and its internal standard (sodium butyrate D5) from the area under the peak of each reading and each concentration points have fixed volume 100µl of acid and keeping the remaining as usual method.

Concentration	Area under the Peak of butyric	Area under the peak of I.S (sodium butyrate D5)	Ratio butyric/ Sodium acetate
0	4448153	142467085	0.031222321
0.05	8965958	122611638	0.073124853
0.1	11214660	121008460	0.092676661
0.2	14855317	131005252	0.11339482
0.4	22872816	126815474	0.180362974
0.8	49999979	157867362	0.316721445
1.6	64004271	108464802	0.590092544
3.2	82926551	102812024	0.80658417

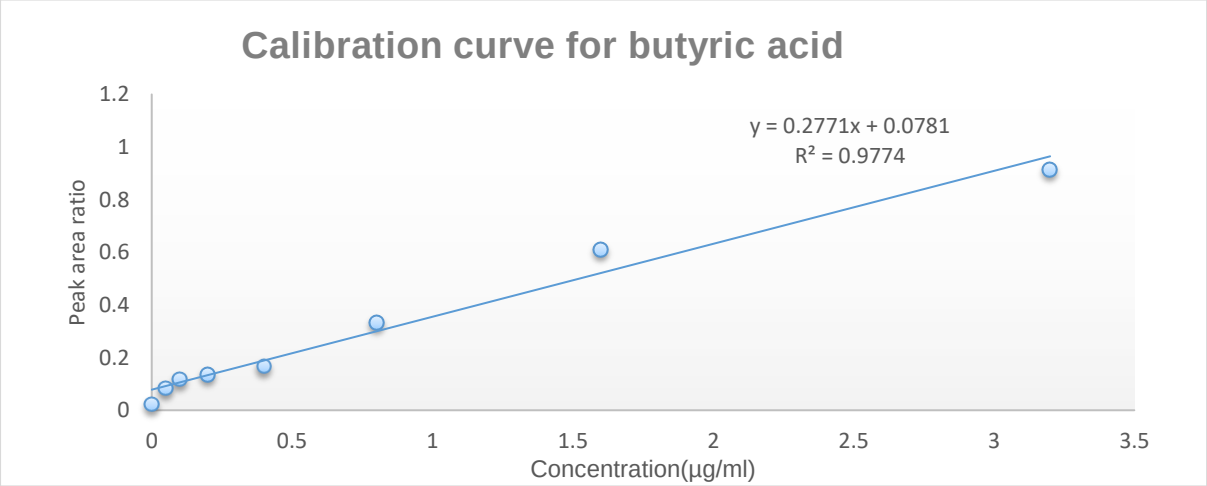

Figure 4. 4: Calibration curve were constructed by plotting the peak area ratio of butyric acid / (sodium butyrate D5) (B/SB (internal standard)) versus the concentrations points in µg/ml.

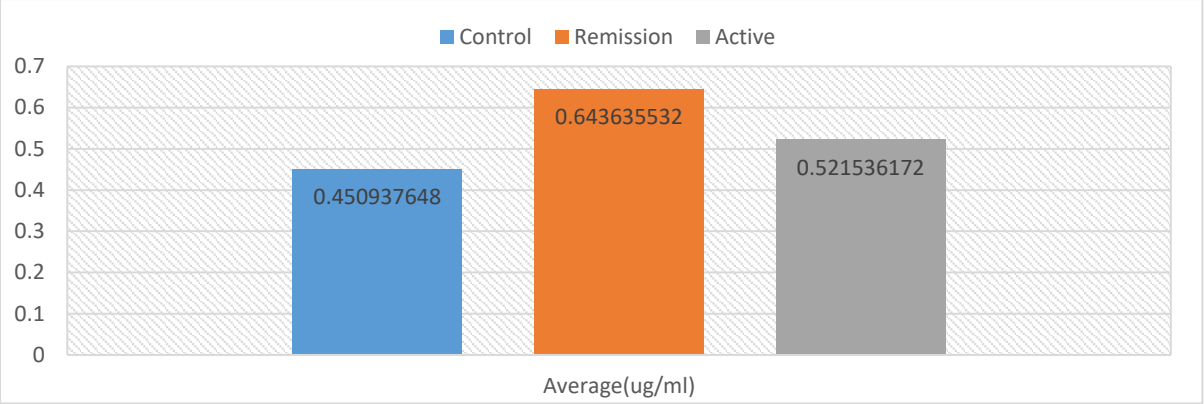

Figure 4. 5: Column chart to demonstrate the Comparison of average concentration in µg/ml of propionic acid in three groups of urine samples.

Table 4. 4: The calibration points of propionic acid and D2 propionic acid from the area under the peak of each reading and each concentration points have fixed volume 100µl of acid and keeping the remaining as usual method.

concentration	Area under the Peak of propionic acid	Area under the D_2 propionic acid	Ratio propionic/ D_2 propionic acid
0	199856	35498510	0.005629983
0.05	2447610	32015509	0.07645076
0.1	4944346	31696786	0.155988875
0.2	10762686	31907890	0.337304848
0.4	12342378	31559060	0.391088264
0.8	29468118	31776601	0.92735274
1.6	52354855	29268512	1.788777475
3.2	105061226	31987068	3.284490657

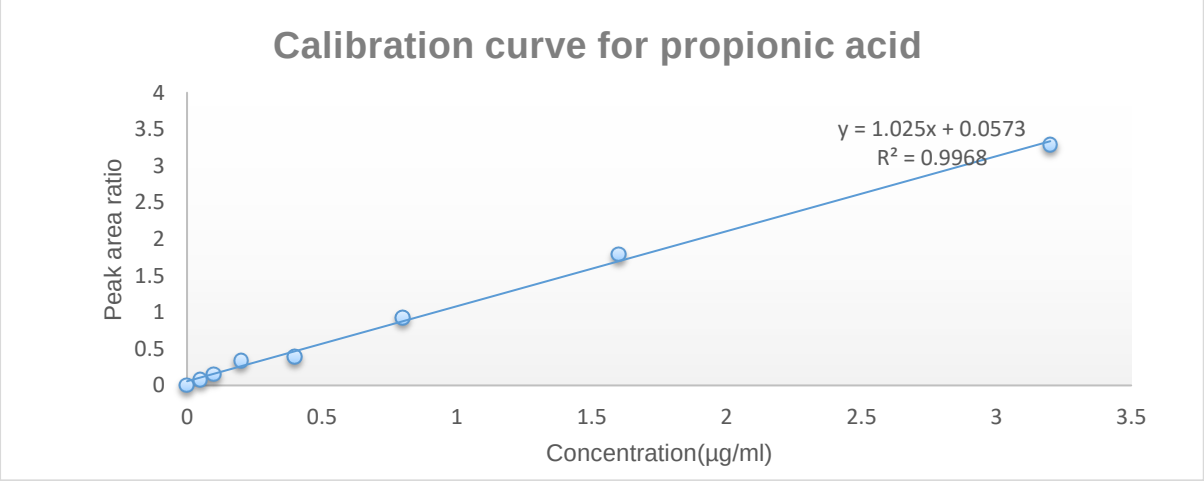

Figure 4. 6: Calibration curve were constructed by plotting the peak area ratio of propionic acid / D_2 propionic acid (P/PD (internal standard)) versus the concentrations points in µg/ml.

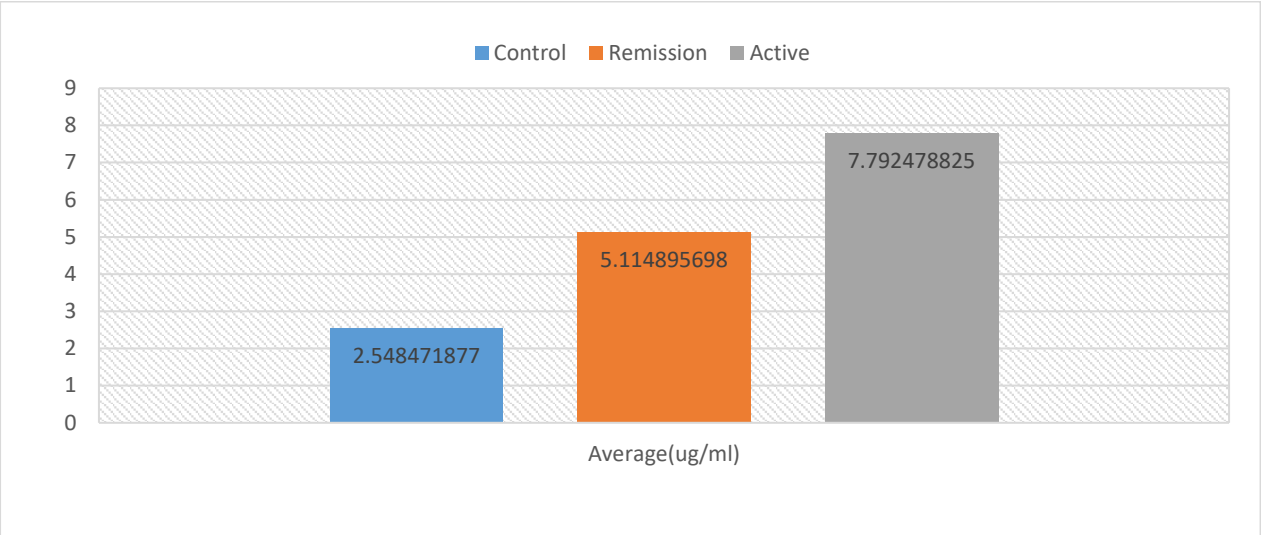

Figure 4. 7: Column chart to demonstrate the Comparison of average concentration in µg/ml of Lactic acid in three groups of urine samples.

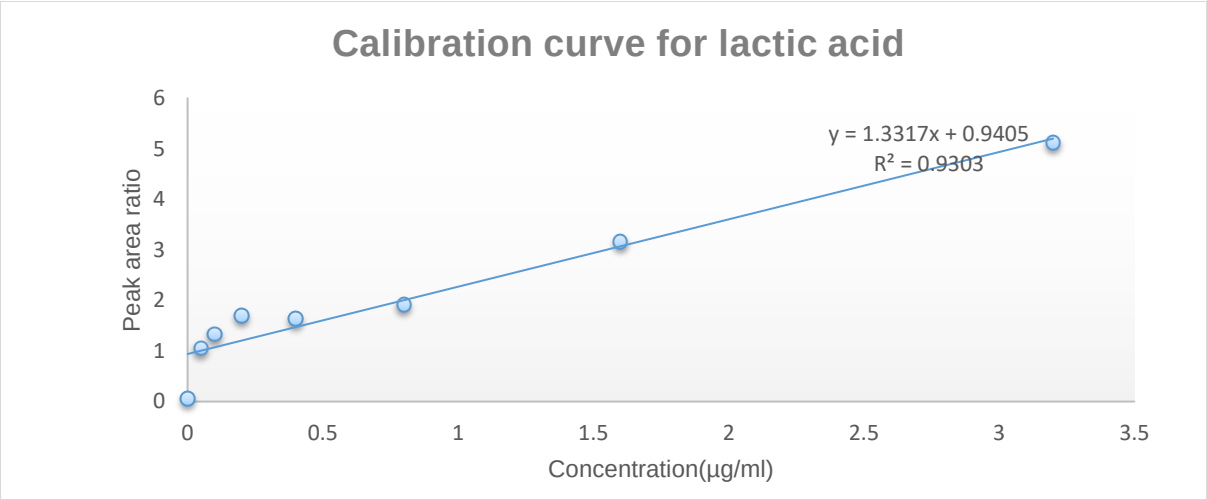

Figure 4. 8: Calibration curve were constructed by plotting the peak area ratio of Lactic acid/$^{13}C_3$ Sodium lactate (L/SL(internal standard)) versus the concentrations points in µg/ml.

Table 4. 5: The calibration points of lactic acid and its internal standard ($^{13}C_3$ Sodium lactate) from the area under the peak of each reading and each concentration points have fixed volume 100µl of acid and keeping the remaining as usual method.

µg	Area under P of Lactic acid	Ara under the peak I.S $^{13}C_3$ Sodium lactate	Ratio lactic/ $^{13}C_3$ Sodium lactate
0	2289756	41254199	0.055503586
0.05	40915586	38759573	1.055625303
0.1	49251825	36779362	1.339115806
0.2	66440330	39122299	1.69827264
0.4	65292593	40002778	1.632201469
0.8	81554969	42454294	1.921006365
1.6	117773561	37285905	3.158661725
3.2	215790978	42148331	5.119798884

4.3.2- Quantitative determination of creatinine in urine :

Creatinine is the useful marker or method for normalizing the level of other molecules found in biological sample, such as urine. Alteration of the level of creatinine possibly associated with cases that result in downregulation of renal blood flow, just as cardiovascular and diabetes diseases [117]. The value of SCFA in urine samples are often recorded in term of µg/mmole of creatinine. However it has been mentioned creatinine is not necessarily useful tool for standardizing the strength of urine [98]. Moreover published research was reported that there was little association between abundant of many urinary metabolites and creatinine [99]. In order to see if there was an association between SCFA levels and creatinine it was determined spectrophotometrically. Table 4.6 shows the layout or the plate used for creatinine determination. Figure 4.9 shows the calibration curve obtained and table 4.7 shows the values for the calibration data. Appendix 2 gives the values obtained for the raw measurement data ((tables A2.13-A2.17)).

From our results there appeared to be very little connection between concentration of creatinine and the concentration of SCFAs and this is shown in the figures 4. 10. - 4. 12, where in the creatinine level in mmoles/L is plotted against the SCFA levels in in µg/ ml of urine. Thus it was concluded that normalisation of these type of metabolites not appropriate against creatinine was not appropriate that the data were reported in µM (table 4.1).

Table 4. 6: Display the position of each urine sample, standard and blank on each plate.

	1	2	3	4	5	6	7	8	9	10	11
A	Urine (2)	Urine (3)	Urine (4)	Urine (5)	Urine (8)	Urine (9)	Urine (10)	Urine (11)	Urine (12)	Standard(1) 20mg/dl	Blank
B	Urine (13)	Urine (15)	Urine (16)	Urine (17)	Urine (18)	Urine (19)	Urine (20)	Urine (21)	Urine (22)	Standard(2) 10mg/dl	Blank
C	Urine (23)	Urine (24)	Urine (25)	Urine (26)	Urine (27)	Urine (28)	Urine (29)	Urine (30)	Urine (31)	Standard(3) 5mg/dl	Blank
D	Urine (32)	Urine (33)	Urine (34)	Urine (35)	Urine (36)	Urine (37)	Urine (38)	Urine (39)	Urine (40)	Standard(4) 2.5mg/dl	Blank
E	Urine (41)	Urine (42)	Urine (43)	Urine (45)	Urine (46)	Urine (47)	Urine (48)	Urine (49)	Urine (50)	Standard(5) 1.25mg/dl	Blank
F	Urine (51)	Urine (52)	Urine (53)	Urine (54)	Urine (55)	Urine (56)	Urine (57)	Urine (58)	Urine (59)	Standard(6) 0.625mg/dl	Blank
G	Urine (60)	Urine (61)	Urine (62)	Urine (63)	----	----	----	----	-----	Standard(1) 0.3125mg/dl	Blank

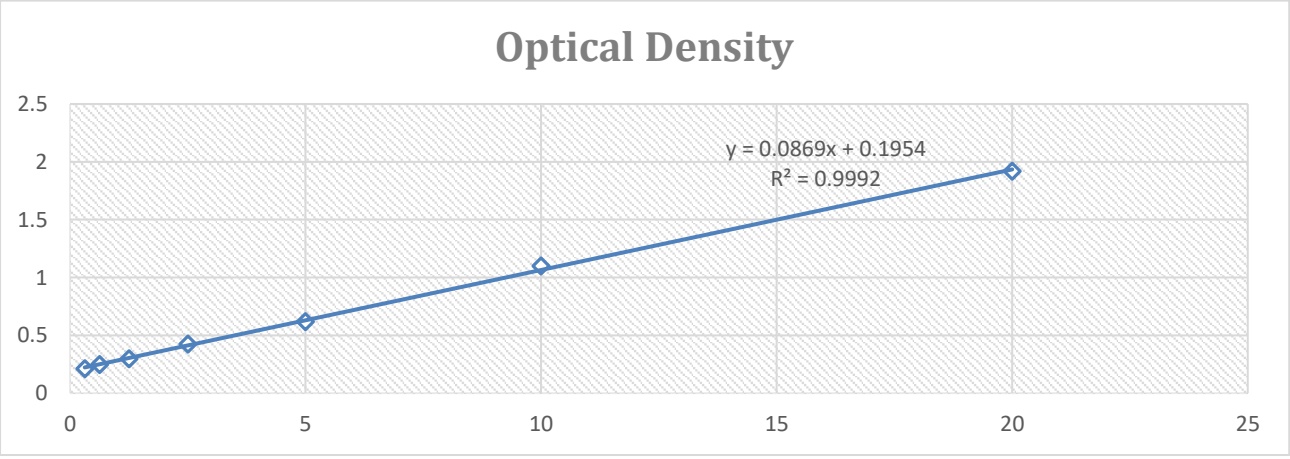

Figure 4. 9: Calibration curve were constructed by plotting the creatinine concentration (mg/dl) versus read optical density.

Table 4. 7: Show the net Optical Density and mean Optical Density at various standard concentration in mg/dl.

Concentration of creatinine in mg/dl	Net Optical Density	Mean Optical Density
20	3.8374	1.9187
10	2.1991	1.0996
5	1.2381	0.6191
2.5	0.8512	0.4256
1.25	0.5962	0.2981
0.625	0.4933	0.2467
0.3125	0.4208	0.2104

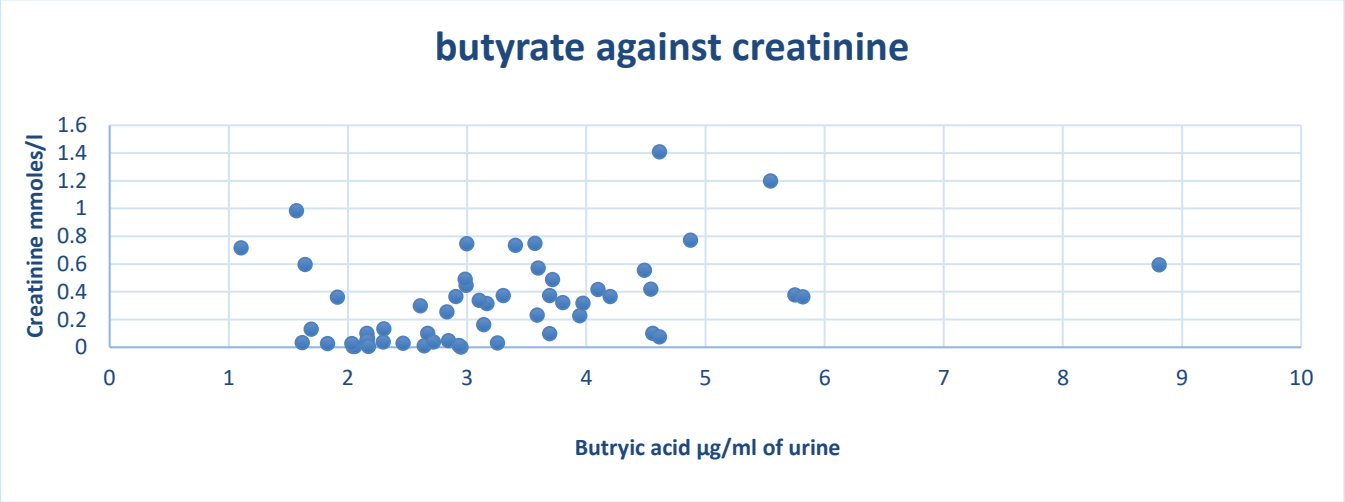

Figure 4. 10: Butyrate concentration plotted against creatinine concentration for 57 urine samples.

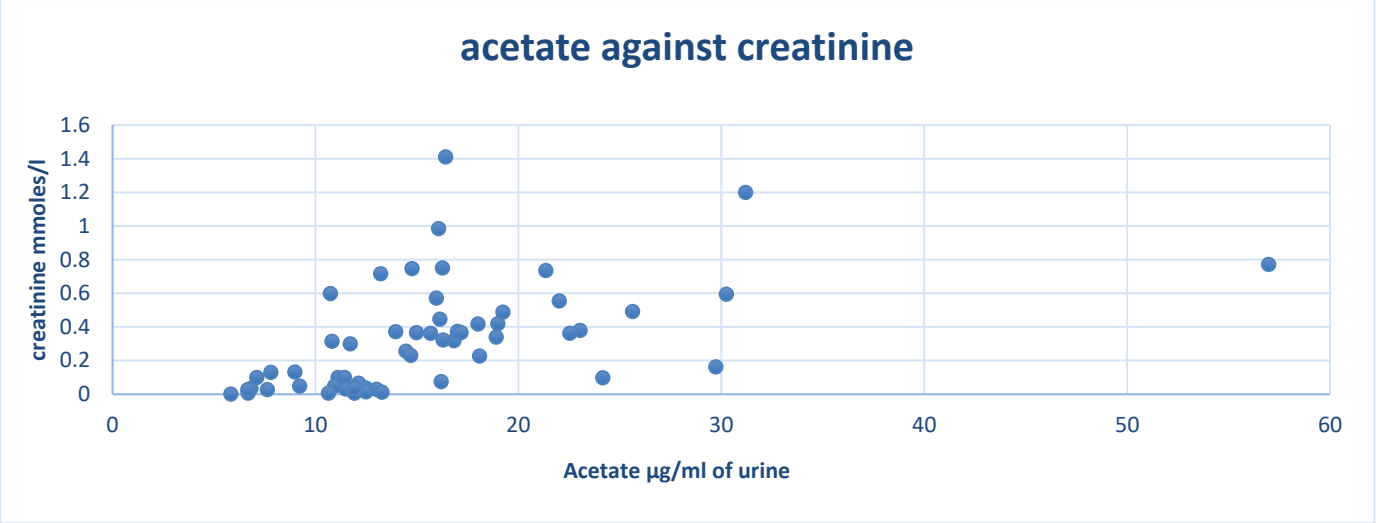

Figure 4. 11: Acetate concentration plotted against creatinine concentration for 57 urine samples.

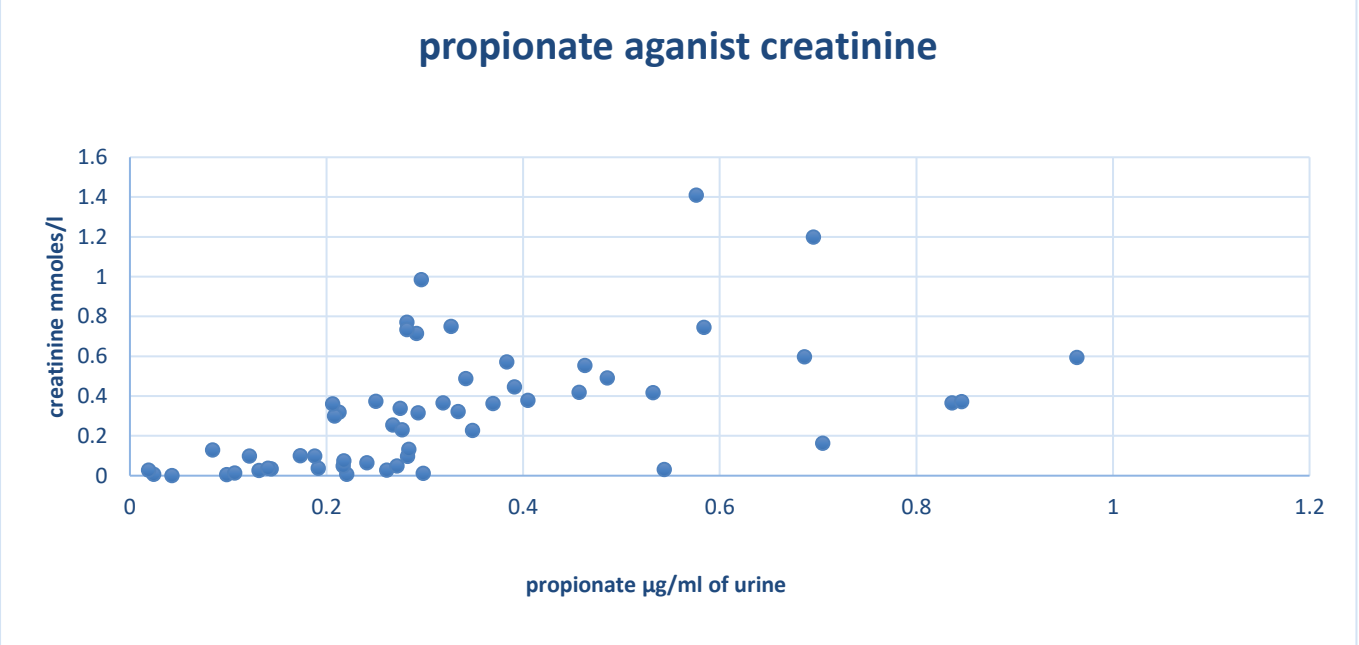

Figure 4. 12: Propionate concentration plotted against creatinine concentration for 57 urine samples.

4.3.3-Discussion

Quantification SCFAs such as acetic acid, butyric acid, propionic acid and lactic acid in the urine samples that were provided from Gastroenterology Unit, Glasgow Royal Infirmary hospital was achieved, these urine samples were taken from three cohorts. The first group patients with active ulcerative colitis and the second group patients with quiescent ulcerative colitis and the third group healthy individuals. The results show that the SCFAs were decreased especially in acetate in the urine samples of active UC (n=14) and remission UC (n=26) cohorts, whereas propionate, butyrate and lactate were elevated in the urine samples of active UC and remission UC cohorts compared to the average concentration of acetate, propionate and butyrate in urine samples of individuals cohort not suffering from UC (n=17).

The average concentration of acetate in healthy control samples is 333 µM which equal to 19.98 µg/ml, the average concentration of acetate in quiescent UC samples is 270 µM which equal 16.2µg/ml in acetate in active UC samples is 240 µM which equal to 14.4µg/ml. Thus the level of acetate was increased in the urine samples of healthy individuals in comparison to the urine samples of active and quiescent UC groups. The difference was significant for the control samples in comparison with remission (p- value= 0.05), also the difference between control samples and active samples was significant (p- value= 0.016). However there is no any significant difference between remission samples and active samples.

On the other hand the results show the average concentration of butyrate in healthy control samples is 50 µM which is equal to 4.39 µg/ml, the average concentration of butyrate in quiescent UC samples is 68.4 µM which is equal to 6.01 µg/ml and the average concentration of butyrate in active UC samples is 71.4 µM which is equal to 6.27 µg/ml. Thus the level of butyrate was upregulated in the urine samples of active (n=14) and quiescent (n=26). UC groups compared to the urine samples healthy controls (n=17). The variation between control group and remission group was significantly different (p- value= 0.015), whereas there is not any significant difference between control samples and active samples as well as between remission samples and active samples. But on closer inspection of the data, there was one sample appearing in the active set of samples with a much higher level of butyrate (238.6 µM) than any other samples. By removing this sample from the set of active samples, the P value will be 0.02 comparing the remission and active samples with the active samples containing a mean level of 55.8 µM butyrate compared to 71.4 µM for the remission samples.

The results show the average concentration of propionate in healthy individuals samples is 5.04 µM which is equal to 0.37 µg/ml, the average concentration of propionate in quiescent UC samples is 6.89 µM which is equal to 0.51 µg/ml in table and the average concentration of propionate in active UC samples is 5.45 µM which is equal to 0.4 µg/ml. Thus the level of propionate was downregulated in the urine samples of healthy individuals in comparison to urine samples of active and quiescent UC groups of the samples provided for this study. However, the difference was not significant between any two groups.

The results show the average concentration of lactate in healthy individuals' samples is 28.2 µM which is equal to 2.54 µg/ml, the average concentration of lactate in quiescent UC samples is 51 µM which is equal to 4.59 µg/ml and the average concentration of lactate in active UC samples is 78 µM which is equal to 7.02 µg/ml. Thus level of lactate was downregulated in the urine samples of healthy controls in comparison to urine samples of active and remission UC groups as shown in the figure 4.7. The

highest level for average concentration of lactate appeared in the quiescent UC cohort. The difference was not significant between any two groups.

Therefore this method was applied successfully for quantification and determination the level of SFCAs in patients suffering from active UC (14), patients with quiescent UC (26) and control cohort not suffering from UC (17) and the level of each SCA in each urine sample with different group in this study was determined against plotted calibration curves the acid against its internal standards and were considered without applying any normalisation. The values of SCAs after repeat analysis of a selected sample (n=5) was as follows: acetate 134.7µM (RSD ± 11.2%), propionate 1.68 µM (RSD ± 23.9%) and butyrate 16.1 µM (RSD ± 8.0%), the acetate and butyrate RSDs values located within the limits of American FDA specification for the bioanalysis methods (https://www.fda.gov/downloads/Drugs/Guidanc/ucm070107.pdf), the poor precision for propionate reflects very low levels of propionate present in urine. The results obtained for SFCAs from the three groups is very consistent with the output of previous researches. Studies demonstrated that patients with IBD show decreased levels of acetate [118, 119]. Furthermore a study was reported that butyrate was increased in quiescent/mild but not moderate/severe disease after investigation of paediatric patients compared with healthy individuals which is compatible with the results for butyrate of the current study [120]. Also another report showed that in colonic mucosal cells of patients with UC butyrate oxidation was reduced and subsequently lead to the elevation of the concentrations of SCFA in the faeces of patients which is similar to the output of the current study where the level of propionate, butyrate and lactate were increased in UC samples with the two phases active and remission compared to the control samples [121]. Lactate is an intermediate organic acid in the bacterial fermentation of carbohydrates and is further converted to SCFA. Lactate was elevated in its level in the urine samples of active UC and remission UC cohorts and the average concentration increased in comparison to the level of lactate and average concentrations in the control urine samples. This finding are very compatible a study where they found the lactate was significantly increased in patients with active colitis and the accumulation of lactate is also known to occur in extra-intestinal inflammation. This research reported the lactic acid concentration was significantly elevated in UC and CD which are barely measurable in healthy individuals. Whereas the SCFAs especially butyrate, were reduced compared to those from CD and control. SCFAs were not reduced and they are almost identical to those of healthy individuals [108, 122]. It was reported that lactate may accumulate as a consequence of inflammation and it has been considered to cause inflammation [123]. Furthermore both D-lactic acid and L- lactic acid are metabolic products of bacteria. Accumulation of L-lactic acid in the faeces of UC patients was increased versus healthy controls but the D-lactic acid was not increased. L- lactic acid correlated with disease severity [96]. Previous studies reported that faecal water from controls was markedly different from the faecal

samples of patients with CD and UC. Colonic mucosa can be directly damaged by the presence of two conditions firstly at low pH and secondly at high lactate amounts due to reduction of electrolyte and water absorption. However, CD patients had an elevated mean fecal water osmotic gap and osmolality that were not observed in either healthy individuals or UC. This phenomena remains unexplained but there are hypothesis suggesting that is due to a failure of absorption of carbohydrate in small bowel which is not converted into acetate and this could contribute to higher osmolality and then diarrhea and an increase in lactic acid. Therefore, a deficiency of acetate may modulate the diarrhea of UC [122]. An old study demonstrated that due to Enterococci breakdown of mucopolysaccharides there was an increase in the concentration of lactic acid in the faeces of UC patients suggested that this might be from the large increase of Enterococci in UC [124]. Finally a therapeutic goal in UC could be considered to aim at restoration of normal levels of SCFAs as an indication of treatment success [125]. In contrast, certain studies found decreased concentrations of SCFAs in the faecal samples of patients with ulcerative colitis and low concentrations of butyrate correlated with increasing severity of inflammation [122, 126]. A study reported that the total SCFAs were decreased in the fecal extracts of in from paediatric patients with moderate to severe UC[120]. In addition, a previous report indicated that SCFAs have anti-inflammatory and immunomodulatory properties and it was observed in this research the concentration of butyrate as well as the acetate and propionate in the faecal samples from UC patients were reduced compared to controls as well there being high lactic acid levels in UC patients. Some studies administered butyrate enemas to patients suffering from distal UC and favourable outcomes were obtained and after local irrigation with butyrate about 50% of UC patients had reduced colon inflammation as well as 50% of patients had improved clinical and histological symptoms [96]. All the previous studies that are reported opposite results the current study were analysed faecal samples whereas in this present study we used urine samples therefore it is difficult to compare the result between two different biological samples. The beneficial effects of butyrate and other SCFAs were provided by certain studies in UC patients which used the route of administration via an enema or indirectly produced by SCFA-producing bacteria supplementation or high fermentable fibre. The other hand the oral route of administration of SCFA and butyrate are difficult to design since SCFA will be rapidly absorbed by the duodenal and gastric routes and therefore would not reach the colon[112]. Several factors can affect the concentration of SCFAs like diet type amount of carbohydrates and fibre in the diet, amount of carbohydrates escaping digestion in the small intestine, the intracellular colonocyte metabolism of butyrate, efficacy of SCFA transport by colonocytes and the transport of propionate and acetate into the portal venous circulation for export to the liver. Impairment of any of these processes can lead to alteration on the SCFA concentration as well as changing in pH and fluids including electrolytes may deactivate bacterial metabolism and alter the

bacterial types which in turn would alter the SCFA concentration. Acetate, butyrate and propionate are all transported by the same pathway and compete with each other for absorption with almost identical rates and any changing uptake or alteration in the colonocyte transporter can account for the alteration of the concentrations of SCFAs in urine. When the inflammation is initiated this alters the mucosal transport based on the size of individual SCFA molecule. This probably decreases acetate absorption and increases butyrate absorption in UC patients, leading to a profile similar to the one found in this current study. To the best of our knowledge no direct measurement of SCFA uptake in colonocytes from patients suffering from UC have been done [120].There is increasing interest in the role of butyrate as an anti-inflammatory agent to enhance the defensive mechanism by preventing harmful bacteria with it in addition acting the major energy source for colonocytes. It was mentioned that butyrate metabolism is impaired in colonocytes isolated from patients suffering from UC which led to accumulation of butyrate and other SCFA in the gut due to decreased uptake by colonocytes or impaired intracellular metabolism and it has been displayed in the pig that the concentration of butyrate in the portal vein reflects the production in the gut of the pig thus its follows that urinary output could reflect the level of butyrate produced in the gut or its level of absorption[127].

4.4- Conclusion

The average concentration of butyrate, propionate and lactate were increased in urine samples which were obtained from UC patients of two phases (active UC and remission UC) and acetate was reduced, compared to the average concentrations the urine samples taken from healthy individuals. The method developed for measurement of SCFAs does not require complex preparation of the sample and is capable for the analysis of SCFAs in small volumes of both plasma and urine in the range required for their determination. As indicated earlier, analysis of SCFAs in urine was applied in very few studies, these studies used NMR for analysis of urine samples are all normalised to creatinine which might be more suitable if the urine samples were collected within 24h. In this current case using creatinine to normalise samples just added greater uncertainty to the measurement because the level of creatinine in these spot samples greatly varied as shown in the Figures (4.10 -4.12) and did not correlated with the levels of SCFAs determined in the samples.

Chapter-5

Application of a derivatisation method for analysis of hexoses and pentose's in urine and saliva samples from patients suffering from UC, in active, remission and controls

5.1-Introduction

Neutral sugars in metabolomics analysis by LC-MS are some of the most difficult metabolites to characterise since they lack ionisable groups and therefore do not ionise strongly in negative ion or positive ion mode and are then difficult to detect by LC-MS. Other reason for the difficulty of analysis is because they are exist in four different ring forms and they tend to give jagged peaks which are broad and in equilibrium with each other. These problems can be treated by raising the pH of the mobile phase which in turn speeds up the equilibration rate between the four forms of the sugars which become more rapid than the chromatographic mass transfer process[128, 129]. On the other hand additives can be used to enhance mutarotation such as ammonia or trimethylamine with a high pH value required increase the rate of mutarotation but these additives are not recommended when mass spectrometry is used because of the background ions produced, also many chromatography columns are not stable to high pH values. For this reason the applications of liquid chromatography are rare for complete chromatographic separation of common monosaccharides. A previous study was applied a calcium ligand exchange column and was able to separate fructose and glucose but was not compatible with mass spectrometery because the sugars tended to form a complex mixture of calcium adducts in the mass spectrometer which made their spectra difficult to interpret [130]. Other research used gas chromatography for the separation of the sugar isomers and although by this method the sugar isomers are close in their elution times especially when the oximation is used which produces two peaks for each sugar [131]. In GC-MS analysis the fragment ions do not confirm sugar structures and only produce results with uninformative spectra where there is no molecular ion. Whereas in LC-MS analysis under electrospray condition all the ion current is carried by the molecular ion with high resolution mass spectrometry giving high sensitivity and precise identification. This permits the extraction of unexpected and unknown sugars from the biological samples from the data obtained[132]. Derivatisation is the optimum method to overcome the ionisation deficiency in mass spectrometry of sugars and application of a derivatising agent can be used to add the ionisable functional groups into the sugars, hence treat the poor ionisation for the metabolites enhancing detection and improving separation of poorly ionising sugars [133, 134].Therefore, in this chapter a strategy for sugar derivatisation has been carried out. Amine react with aldehyde group of a sugar to form Schiff's base, which is not particularly stable and also the Schiff's base can exist in syn- and anti-forms thus potentially producing two chromatographic peaks. Reducing the Schiff's base produces a

single amine product which is stable against hydrolysis. There are several reviews describing methods for derivatising sugars and three basic rules have been determined. Firstly the acyclic form of the sugar is preferred over the cyclic form as it is the aldehyde form that reacts with the base to form the Schiff's base and thus this reaction should be conducted at fairly low pH (e.g. dilute acetic acid). Working at low pH determines the second rule. At low pH bases are protonated and only the unprotonated form of the base reacts with the aldehyde form of the sugars it is essential to use weak base to get a successful reaction, since the weak base is not fully protonated at low pH. A good example for the weak base is aniline which has been used for many years in the detection of sugars following their separation by thin layer chromatography. The required pH for the reaction of a weak base with sugar is about 4.5 even working at pH 3.5 is enough for the unprotonated form of the base to be available and then to react with the sugar, since the pKa value of aniline is about 4.5. Other bases have an even lower pKa value (ca 2) such as aminobenzamide and may be better than aniline for the derivatisation of sugars. Because the para-position of the amide group to the amino group increases the electron withdrawing effect away from the nitrogen of the basic group, which weakens the latter. The third rule where the Schiff's base is reduced by using the reducing agent and this agent should be stable under acidic conditions. For instance sodium borohydride is not used in this present method since it is not stable under acidic conditions, whereas it is often used in reductive amination reactions. Therefore it is important to use a reducing agent which is acid-stable to be appropriate in this case such as 2-methylpyridine-borane complex, that is stable at low pH [135, 136], was used.

5.1.1- Aim of this study

This study will focus on the separation of common hexoses: mannose, glucose, fructose and galactose, pentoses: arabinose, ribose and xylose and the deoxy hexoses: rhamnose and fucose by using a reductive amination method in combination with HILIC chromatography and mass spectrometry to quantify these sugars in urine and saliva samples from patients in UC in comparison with patients in remission and a control group.

5.2- Experimental (Derivatisation of sugars in urine and saliva samples of the three groups) :

5.2.1- Material, Chemical and reagents.

Glucose, galactose, fructose, mannose, arabinose, xylose, ribose, fucose, rhamnose, Aniline-2,3,4,5,6-d_5, formic acid, acetic acid, HPLC grade methanol, HPLC grade acetonitrile and picoline borane complex were obtained from Sigma Aldrich, Dorset UK. $^{13}C_6$-D-glucose was obtained from CK gases, Leicestershire UK.

5.2.2 Urine samples.

These samples have been reported in detail in sections *2.2.3.4* & *2.2.3.5* (Chapter-2).

5.2.3 Saliva samples

These samples have been reported in detail in section *2.2.3.6* (Chapter-2).

5.2.4 Equipment.

5.2.4.1 Guard column.

ZIC®-HILIC Guard, 20x 2.1mm, PEEK coated guard column. 1.50435.0001

In combination with a SeQuant® ZIC®-HILIC - 150x4.6 mm, 3.5µm, 200 A°. PEEK coated HPLC Column – serial No. 634794. Sorbent lot No. TA2022676, Lot No HX60180949 (HiChrom Reading UK). The rest of the equipment was described in section 2.2.2.

5.2.4.2 LC-MS instrumentation

All the details are reported in section *2.2.3* (Chapter-2).

5.2.5 Preparation of Solutions.

5.2.5.1 Preparation of sugars standards (solution A_1) 10mg/ml.

10mg of each sugars was weighed into separate and dissolved in 1ml methanol/water (1:1) and $^{13}C_6$ D-glucose as (internal standard). The sugars were then diluted to 10 µg/ml to establish their individual retention times following derivatisation. The sugar mixtures were prepared at various concentrations to establish calibration curves each time spiking with 1µg of $^{13}C_6$ D-glucose.

5.2.5.2 Preparation of deuterated aniline.

Liquid inside the (5g Ampule of deuterated aniline) was transferred to 10ml vial and the vial was filled with 5ml methanol (solution B).Then 100 µl from (solution B) was transferred to new vial and this vial was filled with 900 µl methanol (solution B_1).

5.2.5.3 Preparation of tagging agent solution 10mg/ml.

100 µl was taken from (solution B_1) and transferred to new vial and then filled with 100 µl of acetic acid, 400 µl methanol and 400 µl H_2O (solution B_2)10mg/ml.

5.2.5.4 Preparation of picoline-borane solution 10mg/ml.

10mg of picoline-borane powder was taken from the bottle and transferred to the vial, then the vial was filled with 1ml (methanol/water) 500 µl methanol and 500 µl H_2O (solution F).

5.2.5.5 Preparation of urine for derivatisation.

Each sample was prepared first by adding 100 µl of urine and 300 µl of methanol into the Eppendorf and was then the centrifuged for 15 min then the supernatant was removed for derivatisation.

5.2.5.6 Preparation of saliva for derivatisation.

Each sample was prepared first by adding 100 µl of saliva and 300 µl of methanol into the Eppendorf and was then the centrifuged for 15 min and then the supernatant was removed for derivatisation.

5.2.6. Method procedure and protocol:

5.2.6.1 Mobile phase

The mobile phase was acetonitrile:water (90:10) containing 0.1% formic acid. The HPLC was run in isocratic mode with a run time of 40 minutes at a flow rate of 0.6 ml/min.

5.2.6.2 Procedure for derivatisation of sugars.

1. 40 µl from Solution B_2 was mixed with aliquot of any sugar in µl.
2. The mixture was then heated at 40^oC for 30 minutes.
3. After that 20 µl of (solution F) was added and then the resulting mixture again heated at 30^oC for 45 minutes, N.B. If there is fructose or biological samples then heating was carried out at 30^oC for two hours instead of 45 minutes, which is the time required for fructose to be derivatised.
4. The next step sample was then blown in stream nitrogen to dryness.
5. After drying the sample was re-dissolved in 200 µl H_2O containing 0.1% formic acid before adding 1000 µl of acetonitrile at the end of this procedure.

5.2.6.3 Calibration curve for glucose, mannose, fructose and Galactose with the 1 µg ***$^{13}C_6$ D-glucose*** *as (Internal standard) and methanol as solvent then Appling the procedure.*

Derivatisation method was applied to carry out a calibration points for glucose, mannose, fructose and galactose, the calibration series was prepared at 0µg, 0.2µg, 0.4µg, 0.8µg, 1.6µg and 3.2µg of glucose and $^{13}C_6$ D-glucose at constant amount of 1µg for each calibration point. Also the calibration series was prepared at 0µg, 0.05µg, 0.1µg, 0.2µg, 0.4µg, and 0.8µg of galactose, mannose and fructose in addition to $^{13}C_6$ D-glucose at constant amount of 1µg for each calibration point. Each sample was mixed with 40 µl from Solution B_2 and then treated with remaining steps of the procedure No. 5.2.6.2 then the resulting mixture was vortexed for ten seconds and then was transferred to HPLC vial prior to LC–MS analysis.

5.2.6.4 Calibration curve for Fucose, L-Rhamnose monohydrate, Arabinose, Xylose and Ribose with the 1 µg/ml ***$^{13}C_6$ D-glucose*** *as (Internal standard) and methanol as solvent then Appling the procedure.*

Derivatisation method was applied to carry out a calibration points for fucose, L-rhamnose, xylose, ribose and arabinose, the calibration series was prepared at 0µg/ml, 0.2µg/ml, 0.4µg/ml, 0.8µg/ml, 1.6µg/ml and 3.2µg/ml of mixture of those mentioned sugars and $^{13}C_6$ D-glucose at an amount of 1µg for each calibration point. Six vials were prepared mixture and $^{13}C_6$ D-glucose each vial contain one concentration from the calibration points. Each sample was mixed with 40 µl from Solution B_2 and then treated with remaining steps of the procedure No. 5.2.6.2 then the resulting mixture was vortexed for ten seconds and then was transferred to HPLC vial prior to LC–MS analysis.

5.2.6.5 Derivatisation of urine samples with deuterated aniline.

120µl of the supernatant from every urine sample of the three groups (active UC, quiescent UC and healthy control). 1µg of $^{13}C_6$ D-glucose was added and then the sample was mixed with 40 µl from Solution B_2 and then the remaining steps were applied of the procedure used for derivatisation of sugars No. 5.2.6.2, therefore 58 vials were prepared for LC-MS analysis.

5.2.6.6 Derivatisation of saliva sample with deuterated aniline

120µl of the supernatant from every saliva was mixed with 1µg of $^{13}C_6$ D-glucose and the sample was mixed with 40 µl from Solution B_2 and then the remaining steps were applied of the procedure used for derivatisation of sugars No. 5.2.6.2, therefore 65 vials were prepared for LC-MS analysis.

5.3 Results and Discussion:

5.3.1- Derivatisation of glucose, mannose, fructose and Galactose in Urine samples.

A method for the analysis of the sugars in biological system was validated in previous study [136]where it was found that deuterated aniline gave a better separation between the critical pair of hexose isomers mannose and galactose. In this study the validated method for derivatisation of sugar was applied to the analysis of urine and saliva samples of participants whether they have UC (active and remission) or healthy controls.

Figure 5.1 shows the standards for fructose, glucose, galactose and mannose as their aniline derivatives analysed on a ZICHILIC column. Figures 5.2-5.4 show the chromatograms obtained for hexoses, pentoses and deoxyhexoses in urine samples. The calibration curves obtained for the sugars are shown in figures 5.5, 5.7, 5.9 and 5.11 and the corresponding calibration data is shown in tables 5.1-5.5. The calibration curves all gave good correlation coefficients over the range examined. However, the response for fructose was low relative to the $^{13}C_6$ glucose internal standard and this is because the reductive amination of fructose, a ketose, is slower and less complete than for the aldehydes. Nonetheless the response for fructose was good despite the poor conversion rate and also fairly consistent because the response relative to the internal standard is quite linear with regards to concentration.

Table 5. 1: Calibration data obtained for hexoses and pentoses and the results from the analysis of urine samples for patients with active IBD, in remission from IBD and a control group.

Sugars	Calibration curve	Control Average Concentration in µg/ml ± RSD	Active Average Concentration in µg/ml± RSD	Remission Average Concentration in µg/ml ± RSD	P Value Control active	P value Control remission	P value Active remission
Glucose	Y=0.9341x R2=0.9958	0.766 ± 137	22.76± 116.7	16.01 ± 88.4	0.038	0.0006	0.41
Fructose	Y=0.0766 R2= 0.984	4.11 ± 177.4	423.1 ± 134.8	5.87 ± 133.4	0.02	0.47	0.02
Mannose	Y=1.526x R2= 0.9989	0.98 ± 86.7	0.013 ± 194	1.13 ± 185.3	0.0048	0.772	0.015
Galactose	Y=1.0777x R2= 0.9987	0.75 ± 204	7.56 ± 101	1.59 ± 244	0.019	0.36	0.036
Fucose	Y=1.3212x R2= 0.9891	0.086 ± 256	4.99 ± 246	5.88 ± 206	0.14	0.028	0.82
Rhamnose	Y=1.3286x R2= 0.9881	15.40 ± 151	9.60 ± 288	2.25 ± 154	0.533	0.038	0.322
Xylose	Y=1.3468x R2= 0.985	31.25 ± 111	3.41 ± 111	5.57 ± 163.5	0.033	0.023	0.28
Ribose	Y=2.7697x R2= 0.9881	0.016 ± 118.6	9.37 ± 111.4	6.52 ± 126.3	0.0077	0.001	0.52
Arabinose	Y=2.7788x R2= 0.9955	9.18 ± 77.4	0 ± 0	0.13 ±160.6	9.4	9.9	0.0055

The calibration curves forced to zero because including the intercept would have made the results negative. The raw data obtained for glucose levels in the urine samples is shown in tables A3.1-A3.3 in

appendix 3. The glucose level and concentration is significantly different between Control group and active UC group (P-value= 0.03) as well as between remission UC cohort and control cohort (P-value= 0.00061). Whereas the difference was not significant between the active UC group and quiescent UC group (P-value= 0.41). Figure 5.6 shows the ratios between control, remission and active in graphical form.

Table 5. 2: The calibration points of glucose and its internal standard ($^{13}C_6$ D-glucose) from the area under the peak of each reading and then calculating the ratio glucose/$^{13}C_6$ D-glucose.

Concentration	Arear under the curve for Glucose	Arear under the curve for $^{13}C_6$ D-glucose	Ratio= glucose/$^{13}C_6$ D-glucose
0	0	67336204	0
0.2	12065910	64152914	0.188080467
0.4	29444158	69189942	0.425555466
0.8	52592821	64468818	0.815786959
1.2	78711463	63832283	1.233098039
3.2	195345470	66818137	2.923539607

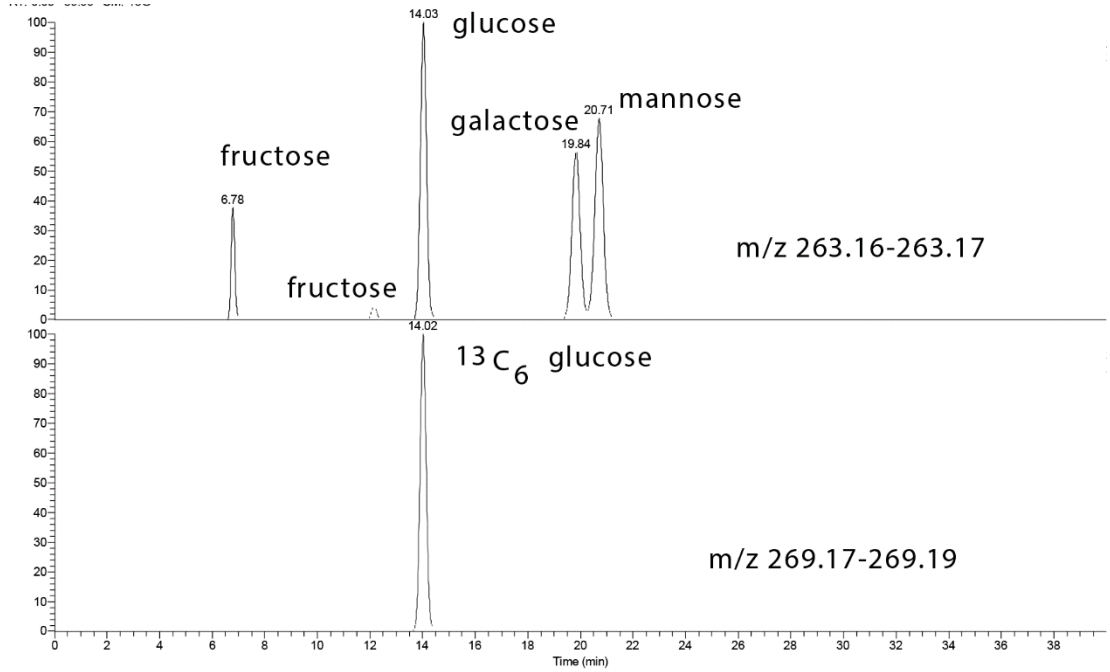

Figure 5. 1: Extracted ion traces for hexose standards and $^{13}C_6$ glucose IS.

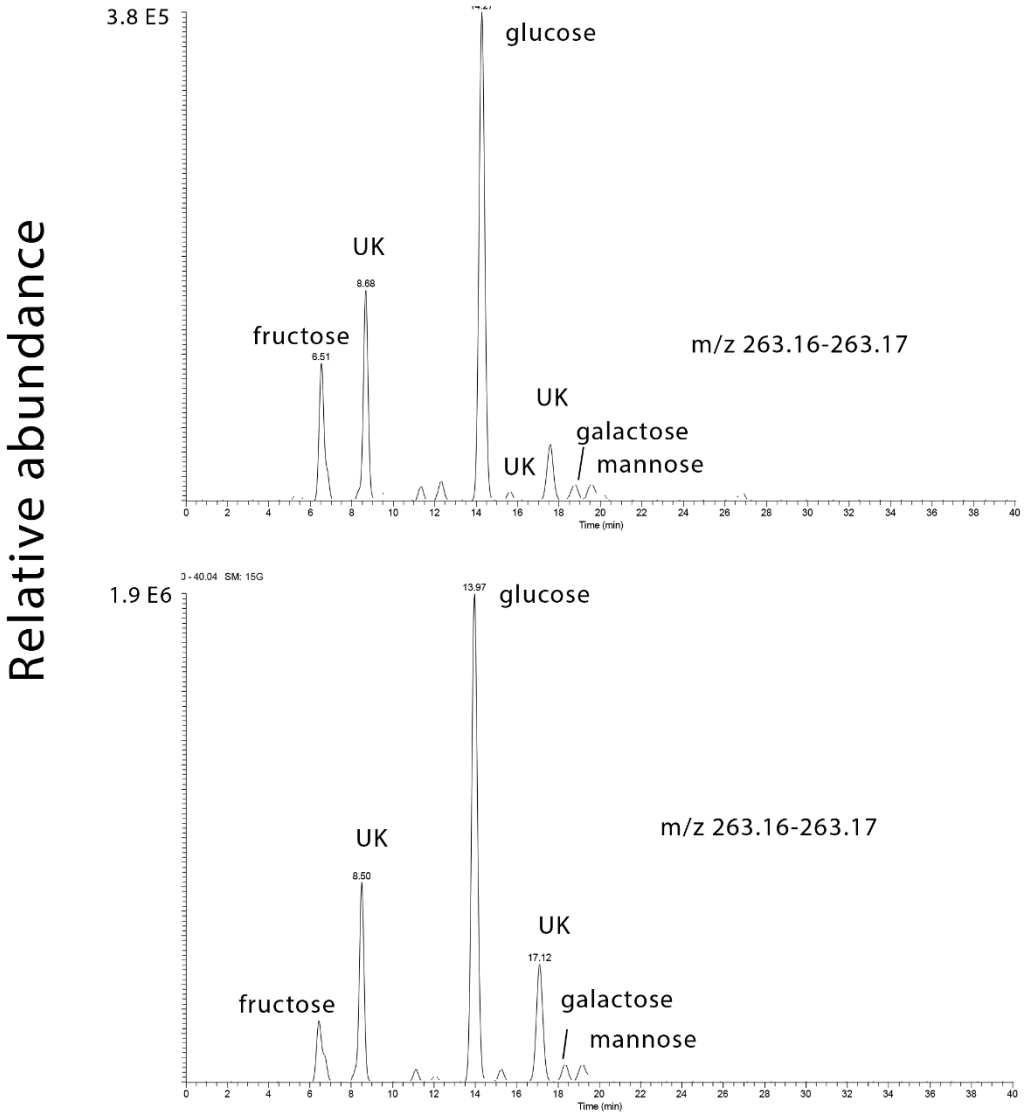

Figure 5. 2: Extracted ion chromatograms showing hexoses in a control and a remission sample.

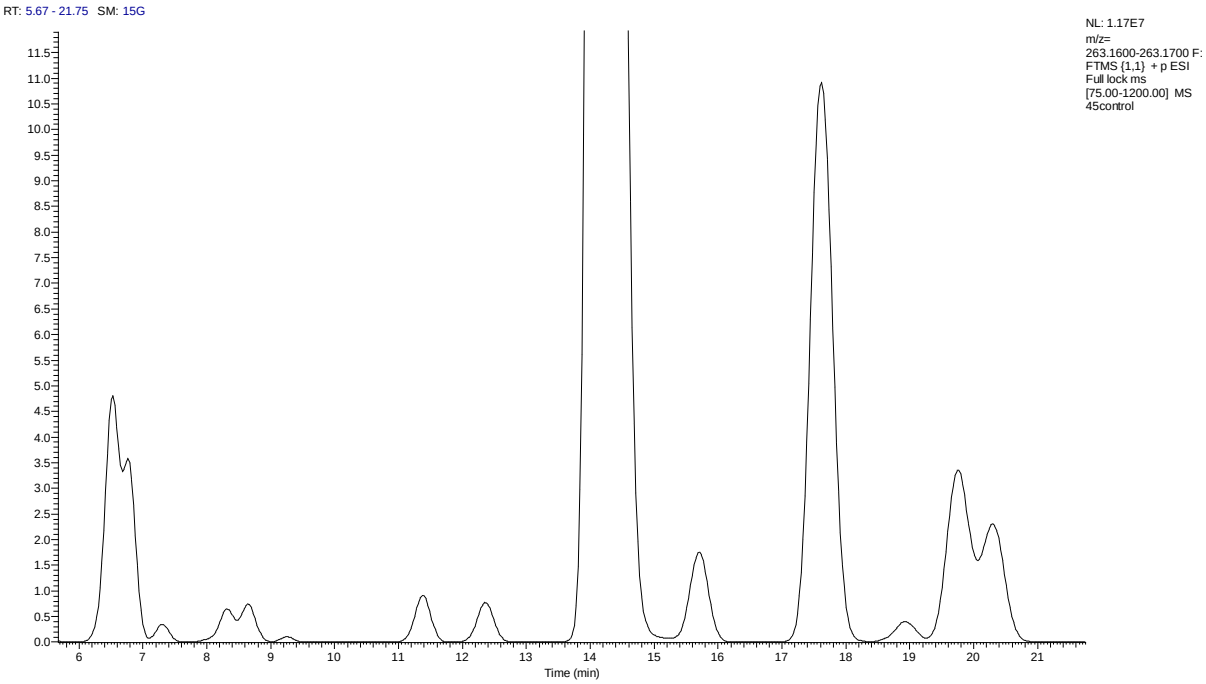

Figure 5. 3: Expansion showing complex pattern of largely unidentified hexose isomers in urine.

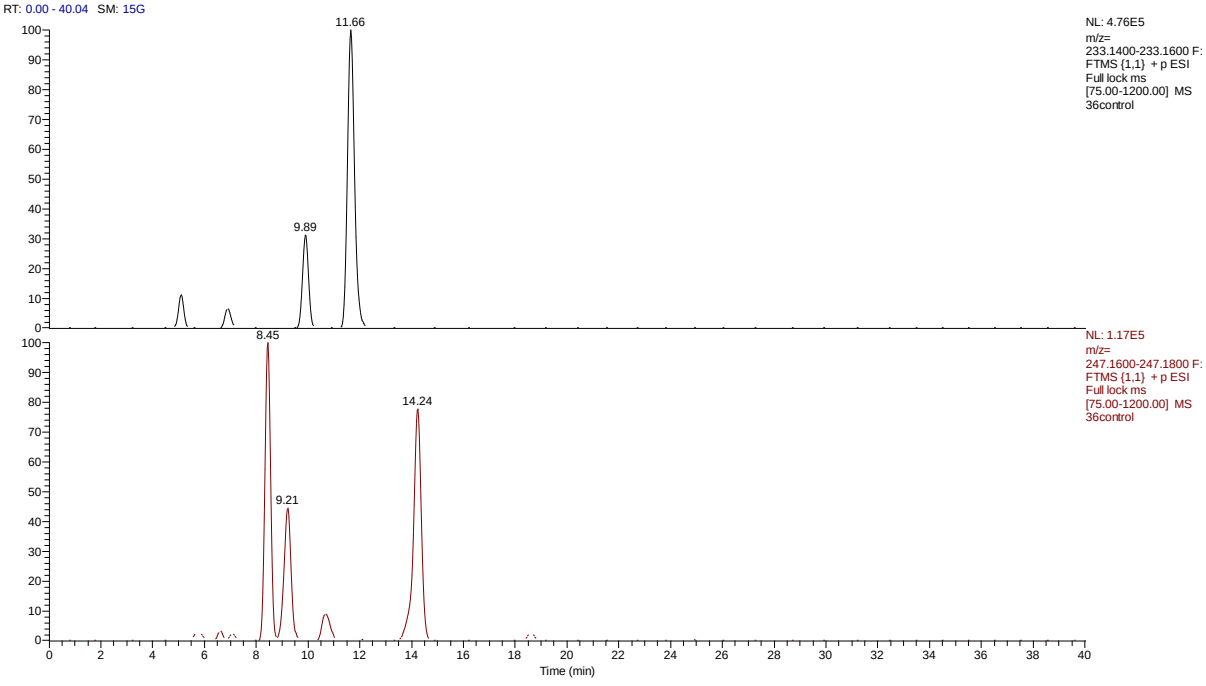

Figure 5. 4: Extracted ion chromatograms showing pentoses and deoxyhexoses in urine.

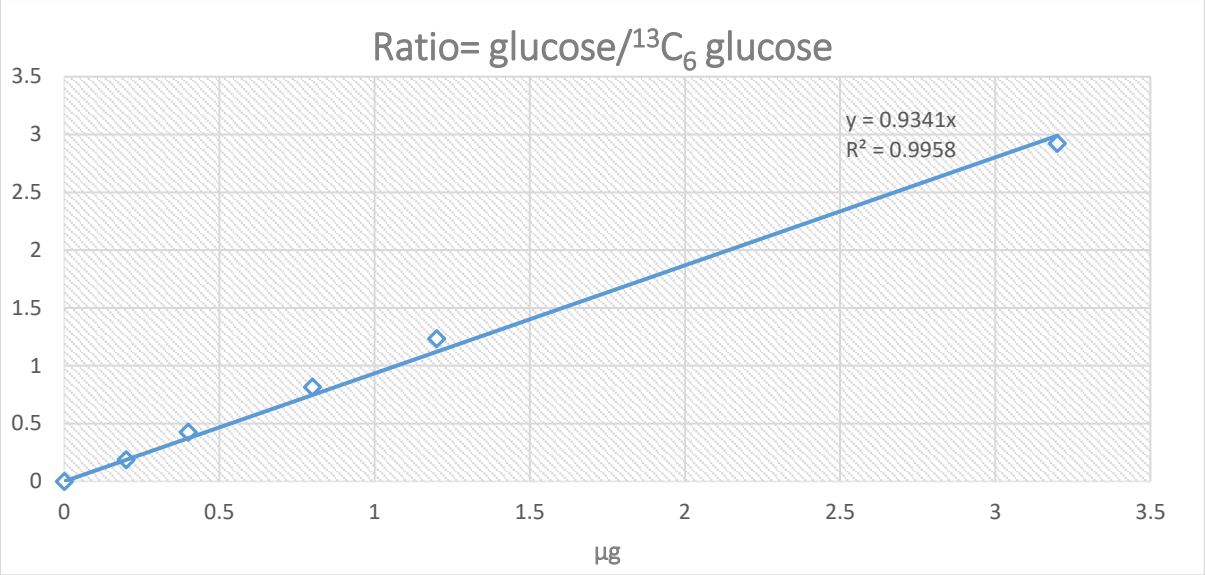

Figure 5. 5: Calibration curve were constructed by plotting the peak area ratio of glucose and its internal standard $^{13}C_6$ glucose versus the concentrations points in µg.

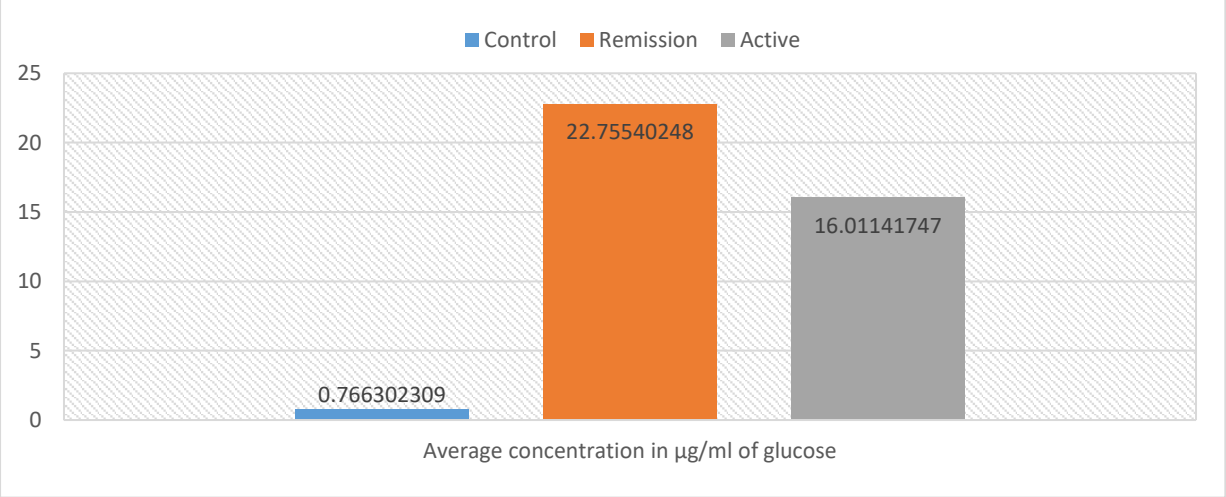

Figure 5. 6: Column chart to demonstrate the Comparison of average concentration in µg of glucose in three groups of urine samples.

Fructose was increased in the urine samples of active UC and quiescent UC cohorts compared to the level and average concentration of fructose in urine samples of controls (figure 5.8). The raw data obtained for fructose levels in the urine samples is shown in tables A3.4-A3.6 in appendix 3. Also the fructose level was significantly different between the control group and active UC group (P-value= 0.02) as well as between the active UC group and remission UC group (P-value= 0.02). Whereas unlike glucose there was no significant difference between quiescent UC cohort and control cohort (P-value= 0.47).

Table 5. 3: The calibration points of Fructose and its internal standard ($^{13}C_6$ glucose) from the area under the peak of each reading and then calculating the ratio Fructose/$^{13}C_6$ glucose.

Concentration	Arear under the curve for Fructose	Arear under the curve for $^{13}C_6$ D-glucose	Ratio= Fructose/$^{13}C_6$ D-glucose
0	0	67336204	0
0.05	233731	64152914	0.003643342
0.1	317942	69189942	0.004595205
0.2	744560	64468818	0.011549149
0.4	2247357	63832283	0.035207216
0.8	4032179	66818137	0.060345577

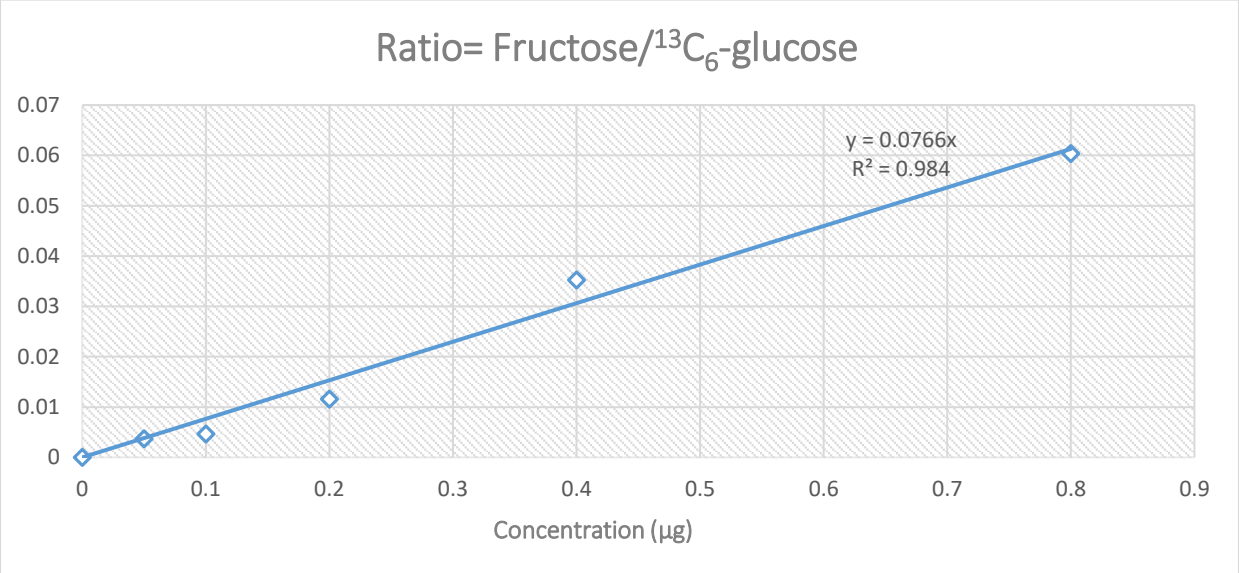

Figure 5. 7: Calibration curve were constructed by plotting the peak area ratio of Fructose and its internal standard ($^{13}C_6$ glucose) (Fructose/$^{13}C_6$ glucose) versus the concentrations points in µg.

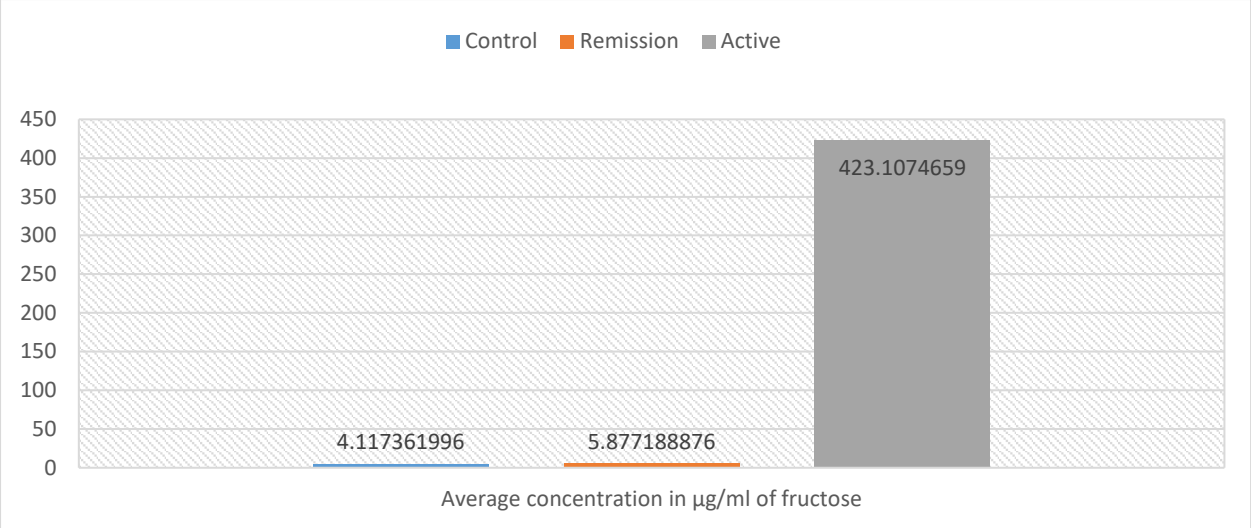

Figure 5. 8: Comparison of average concentration in µg of fructose in three groups of urine samples.

The raw data obtained for Mannose levels in the urine samples is shown in tables A3.7-A3.9 in appendix 3.Mannose concentration was significantly different between control group and active UC group (P-value= 0.0048) as well as between the active UC group and remission UC group (P-value= 0.015).Whereas there was no significant difference between quiescent UC cohort and control cohort (P-value= 0.77). The average levels of mannose in the active group were very low figure 5.10.

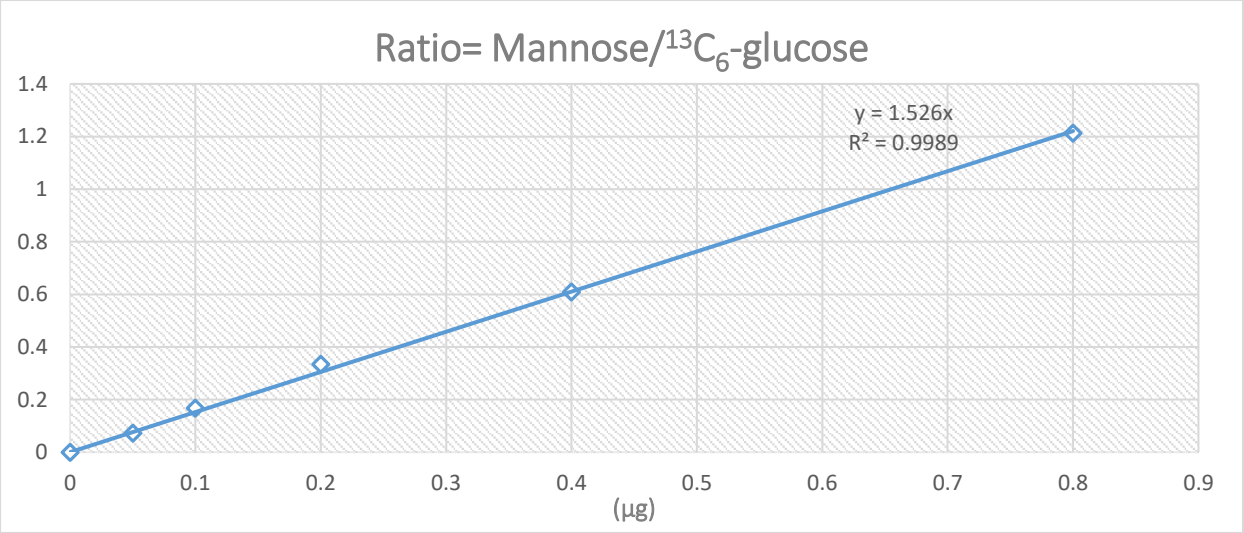

Figure 5. 9: Calibration curve were constructed by plotting the peak area ratio of Mannose and its internal standard ($^{13}C_6$ glucose) (Mannose/$^{13}C_6$ glucose) versus the concentrations points in µg.

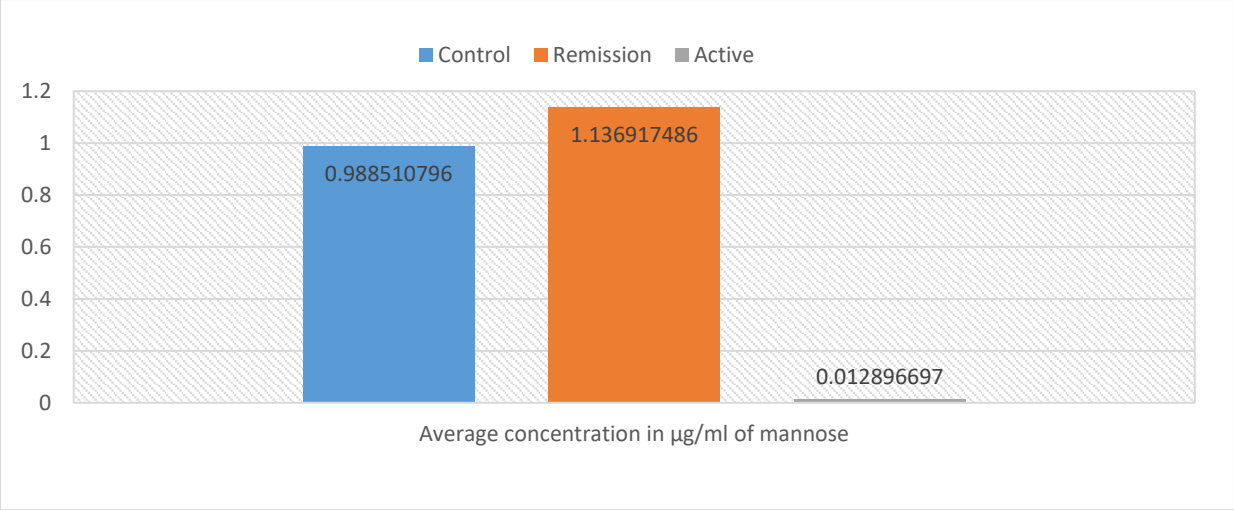

Figure 5. 10: Comparison of average concentration in µg of mannose in three groups of urine samples.

Table 5. 4: The calibration points of Mannose and its internal standard ($^{13}C_6$ glucose) from the area under the peak of each reading and then calculating the ratio Mannose/$^{13}C_6$ glucose.

Concentration	Arear under the curve for Mannose	Arear under the curve for$^{13}C_6$ D-glucose	Ratio= Mannose/$^{13}C_6$ D-glucose
0	0	67336204	0
0.05	4663384	64152914	0.072691694
0.1	11596883	69189942	0.167609376
0.2	21513279	64468818	0.333700534
0.4	38900026	63832283	0.609409913
0.8	81021260	66818137	1.212563888

The raw data obtained for galactose levels in the urine samples is shown in tables A3.10-A3.12 in appendix 3. Galactose concentration was significantly different between the control group and the active UC group (P-value= 0.018) as well as between the active UC group and remission UC group (P-value= 0.036). Whereas like fructose there was no significant difference between remission UC cohort and control cohort (P-value= 0.37). The levels of galactose were much higher in the active group (figure 5.12).

Table 5. 5: The calibration points of Galactose and its internal standard ($^{13}C_6$ glucose) from the area under the peak of each reading and then calculating the ratio Galactose/$^{13}C_6$ glucose.

Concentration	Area under the curve for Galactose	Area under the curve for $^{13}C_6$ D-glucose	Ratio= Galactose /$^{13}C_6$ D-glucose
0	424986	67336204	0.006311404
0.05	3499307	64152914	0.054546345
0.1	8104879	69189942	0.117139555
0.2	12390723	64468818	0.192197149
0.4	27870864	63832283	0.436626464
0.8	57729383	66818137	0.86397774

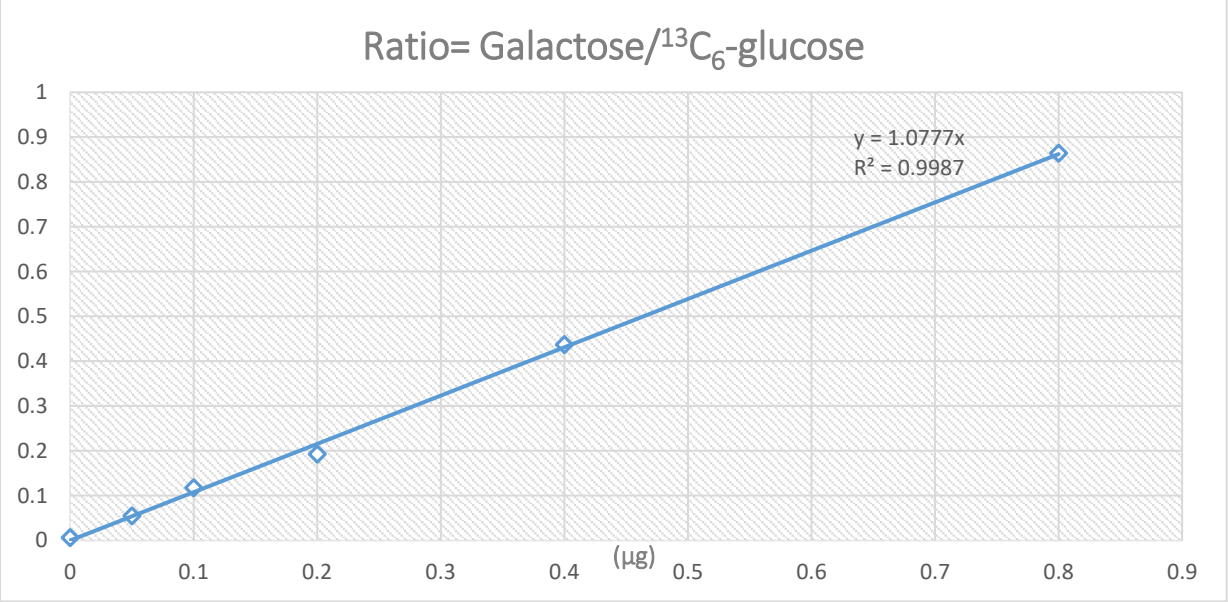

Figure 5. 11: Calibration curve were constructed by plotting the peak area ratio of Galactose and its internal standard ($^{13}C_6$ D-glucose) (Galactose/$^{13}C_6$ D-glucose) versus the concentrations points in µg.

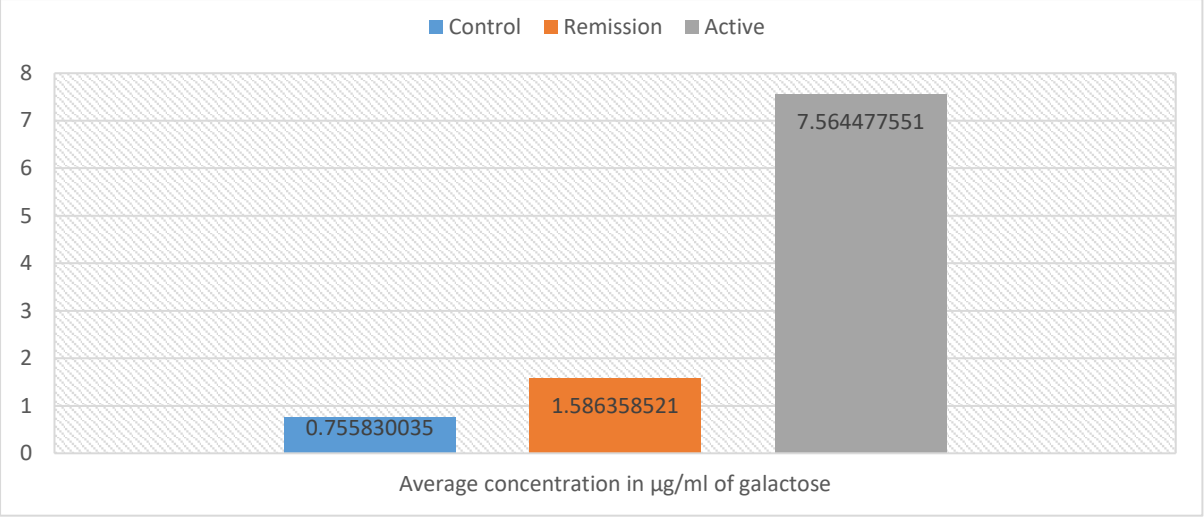

Figure 5. 12: Comparison of average concentration in µg of Galactose in three groups of urine samples.

5.3.2-Derivatisation of Fucose,L-Rhamnose, Arabinose, Xylose and Ribose in Urine samples.

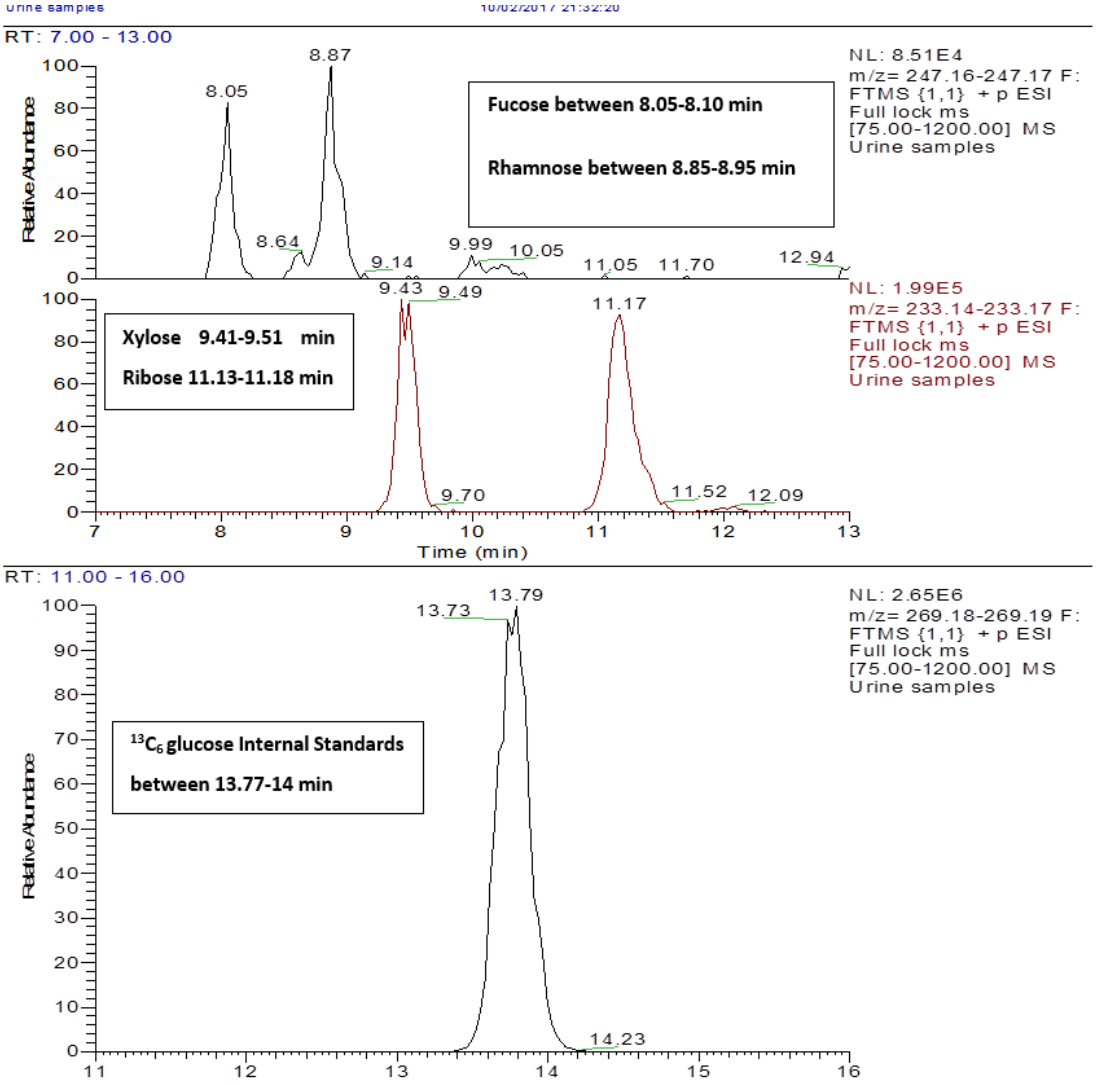

Figure 5. 13: Extacted ion traces for derivatised Fucose between 8.05- 8.10 min, Rhamnose between 8.85-8.95 min, Mass :247.17, Xylose 9.41-9.51 min, Ribose 11.13-11.18 in a urine sample.

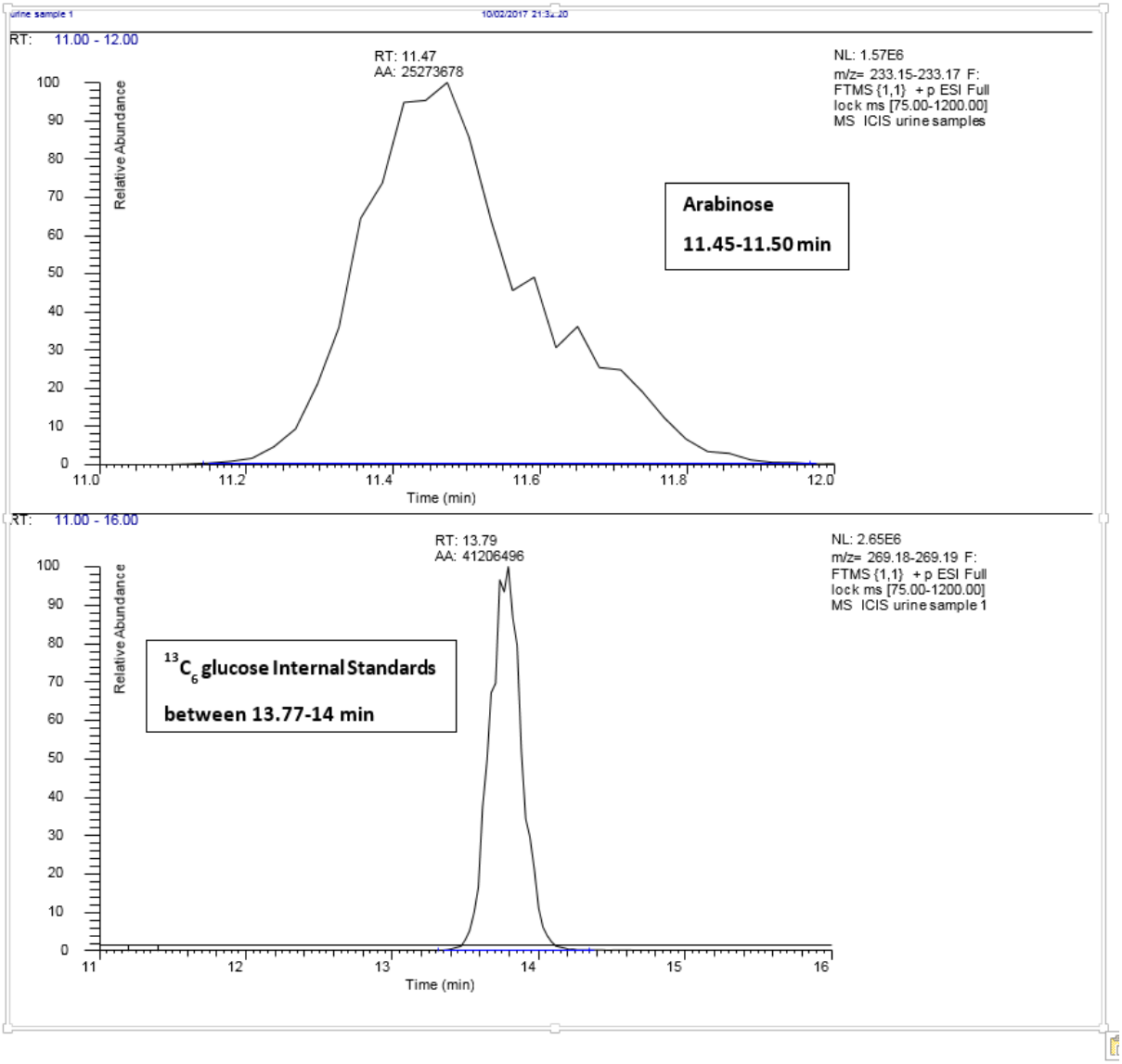

Figure 5. 14: Extacted ion traces for derivatised Arabinose between 11.45- 11.50 min.

The calibration curves for the pentoses and deoxyhexoses are shown in figures 5.14, 5.15, 5.17, 5.19 and 5.21. The calibration curves all displayed good linearity and most of the sugars had greater response factors than the $^{13}C_6$-glucose internal standard and obviously very efficient conversion to the derivatised form, ribose gave a particularly high response factor. The raw data for the level of pentoses and deoxyhexoses in urine samples associated with the calibration curves is shown in tables A3.22-A3.36 in Appendex-3.

The fucose level and concentration was significantly different between the control group and remission UC group (P-value= 0.028), whereas the difference was not significant between Control UC cohort and active UC cohort (P-value= 0.14) and between quiescent UC group and active UC group (P-value= 0.82). The fucose levels were much higher in the active and quiescent groups.

Table 5. 6: The calibration points of Fucose and its internal standard ($^{13}C_6$ D-glucose) from the area under the peak of each reading and then calculating the ratio Fucose/$^{13}C_6$ D-glucose.

Concentration	Fucose	$^{13}C_6$ D-glucose	Ratio= Fucose/$^{13}C_6$ D-glucose
0	0	112803748	0
0.2	29538440	105644954	0.279601049
0.4	66078547	111128109	0.594615958
0.8	141276960	133641358	1.057135023
1.2	198487473	104064611	1.907348436
3.2	508054769	123979321	4.09789927

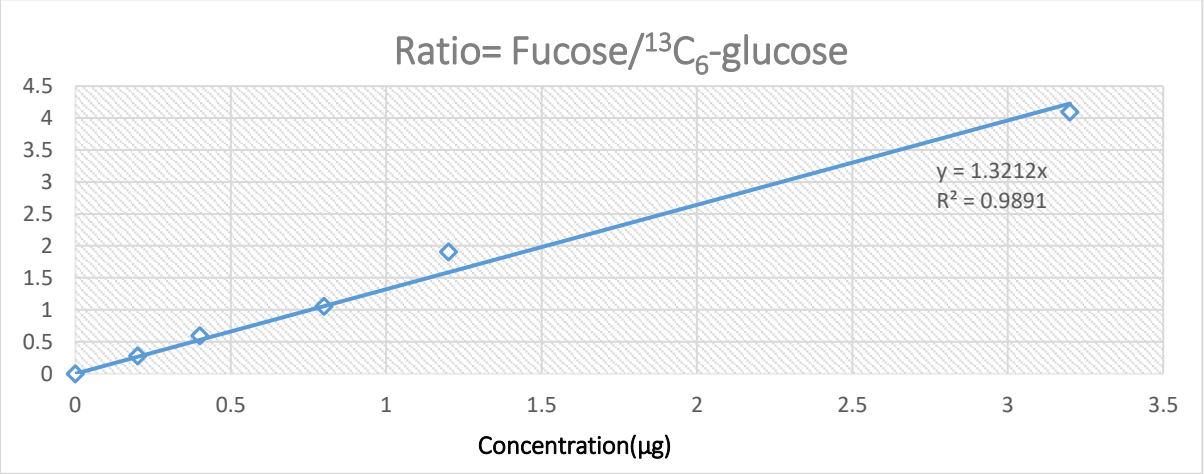

Figure 5. 15: Calibration curve were constructed by plotting the peak area ratio of Fucose and its internal standard ($^{13}C_6$ glucose) (Fucose/$^{13}C_6$ glucose) versus the concentrations points in µg.

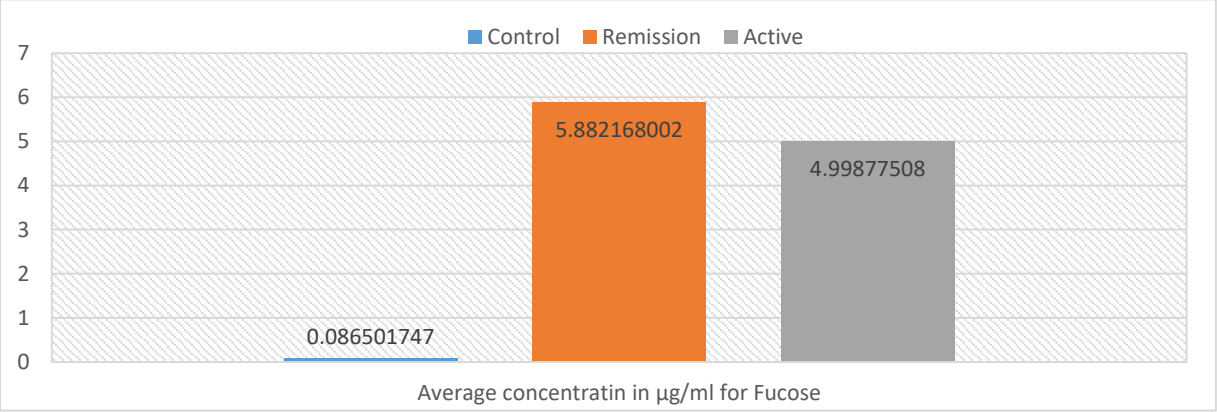

Figure 5. 16: Comparison of average concentration in µg of fucose in three groups of urine samples.

Rhamnose was higher in the control samples than in both the active and remission groups with the lowest levels being in the remission group. The differences were barely statistically significant.

Table 5. 7: The calibration points of Rhamnose and its internal standard ($^{13}C_6$ D-glucose) from the area under the peak of each reading and then calculating the ratio Rhamnose/$^{13}C_6$ D-glucose.

Concentration	Rhamnose	13C6 D-glucose	Ratio= Fucose/13C6D-glucose
0	0	112803748	0
0.2	27253163	105644954	0.257969377
0.4	61652726	111128109	0.554789662
0.8	138111069	133641358	1.033445567
1.2	202399631	104064611	1.944941984
3.2	511386951	123979321	4.124776187

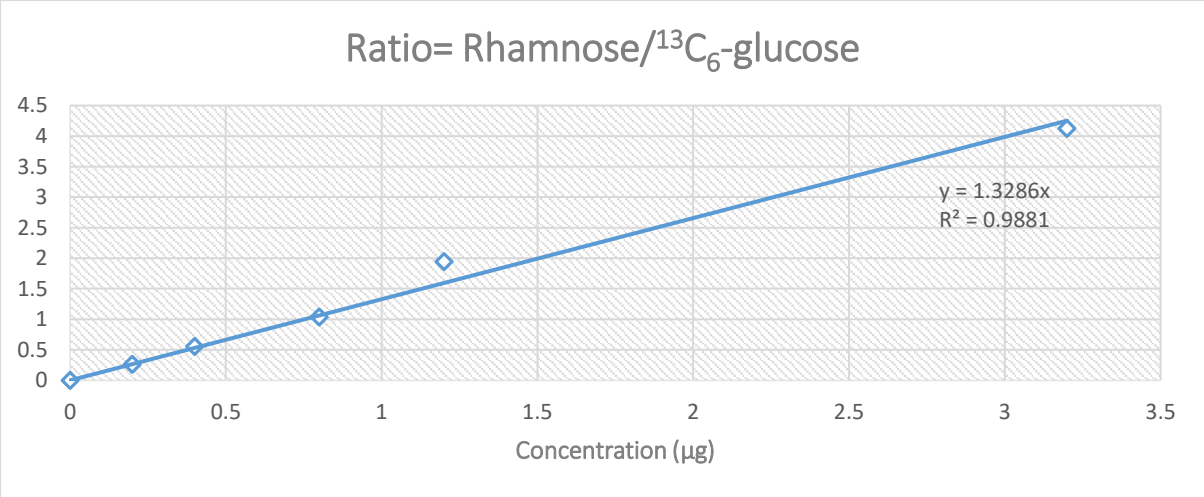

Figure 5. 17: Calibration curve were constructed by plotting the peak area ratio of Rhamnose and its internal standard ($^{13}C_6$ glucose) (Rhamnose/$^{13}C_6$ glucose) versus the concentrations points in µg.

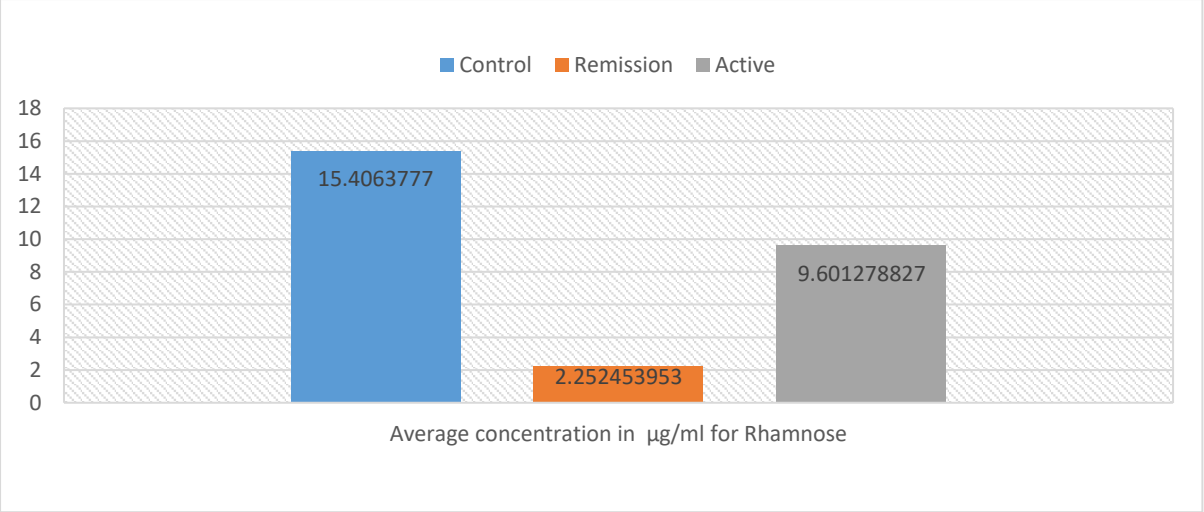

Figure 5. 18: Comparison of average concentration in µg of Rhamnose in three Cohorts of urine samples .

Table 5. 8: The calibration points of Xylose and its internal standard ($^{13}C_6$ glucose) from the area under the peak of each reading and then calculating the ratio Xylose/$^{13}C_6$ glucose.

Concentration	Xylose	$^{13}C_6$ D-glucose	Ratio= Xylose/$^{13}C_6$ D-glucose
0	0	112803748	0
0.2	30847143	105644954	0.291988797
0.4	67272443	111128109	0.605359379
0.8	135007395	133641358	1.010221664
1.2	208681310	104064611	2.005305243
3.2	517092195	123979321	4.170793894

Xylose concentration was significantly different between the control group and remission UC group (P-value= 0.023) and the active group (P-value= 0.033), whereas xylose concentration was not significantly different between the remission UC group and active UC group (P-value= 0.28). The levels were much higher in the control group (figure 5.20).

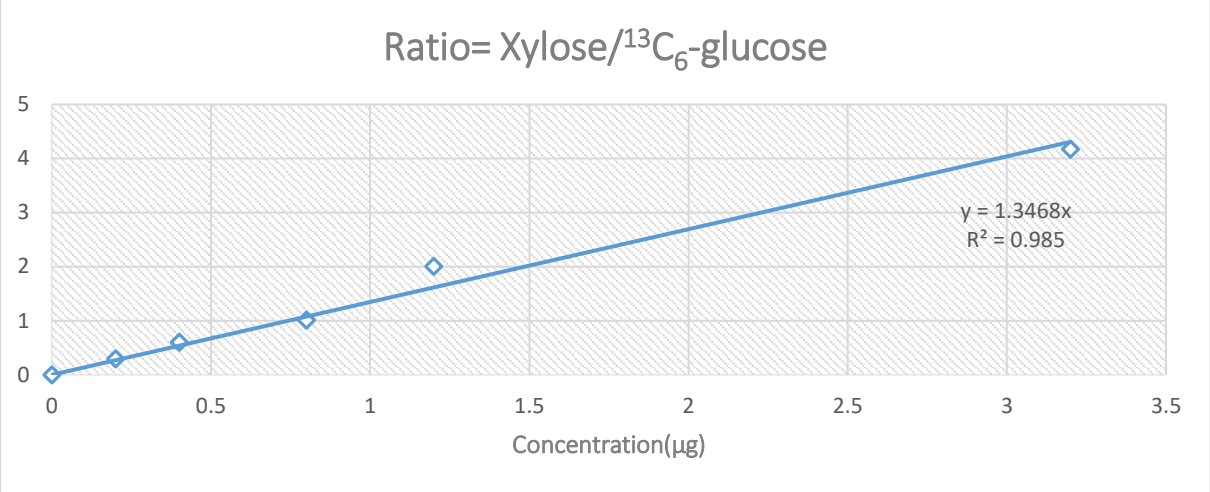

Figure 5. 19:Calibration curve were constructed by plotting the peak area ratio of Xylose and its internal standard ($^{13}C_6$ glucose) (Xylose/$^{13}C_6$ glucose) versus the concentrations points in µg.

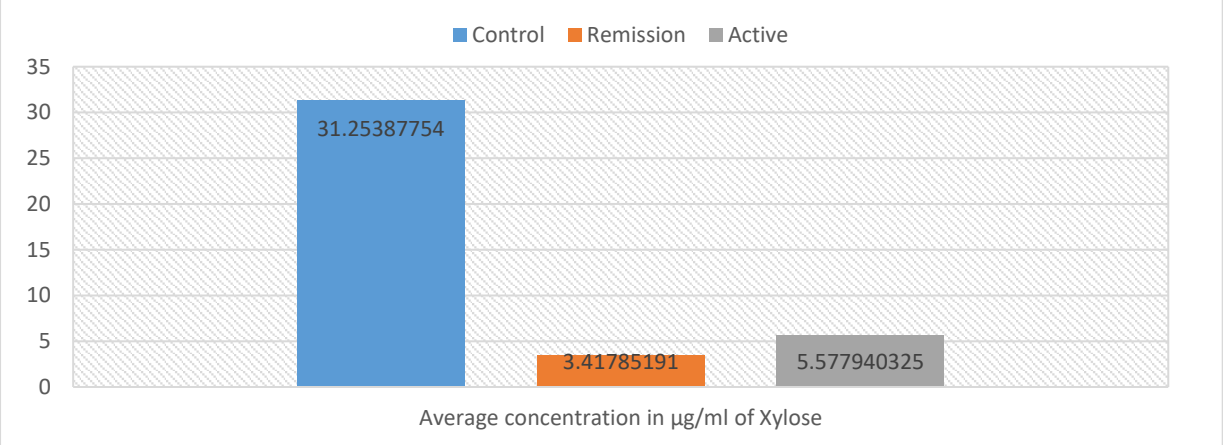

Figure 5. 20: Comparison of average concentration in µg of Xylose in three Cohorts of urine samples.

Table 5. 9: The calibration points of Ribose and its internal standard ($^{13}C_6$ glucose) from the area under the peak of each reading and then calculating the ratio Ribose/$^{13}C_6$ glucose.

Concentration	Ribose	$^{13}C_6$ D-glucose	Ratio= Ribose/$^{13}C_6$ D-glucose
0	0	112803748	0
0.2	64618265	105644954	0.611655006
0.4	137385277	111128109	1.236278366
0.8	297354194	133641358	2.225016256
1.2	419321552	104064611	4.029434675
3.2	1063317673	123979321	8.576572806

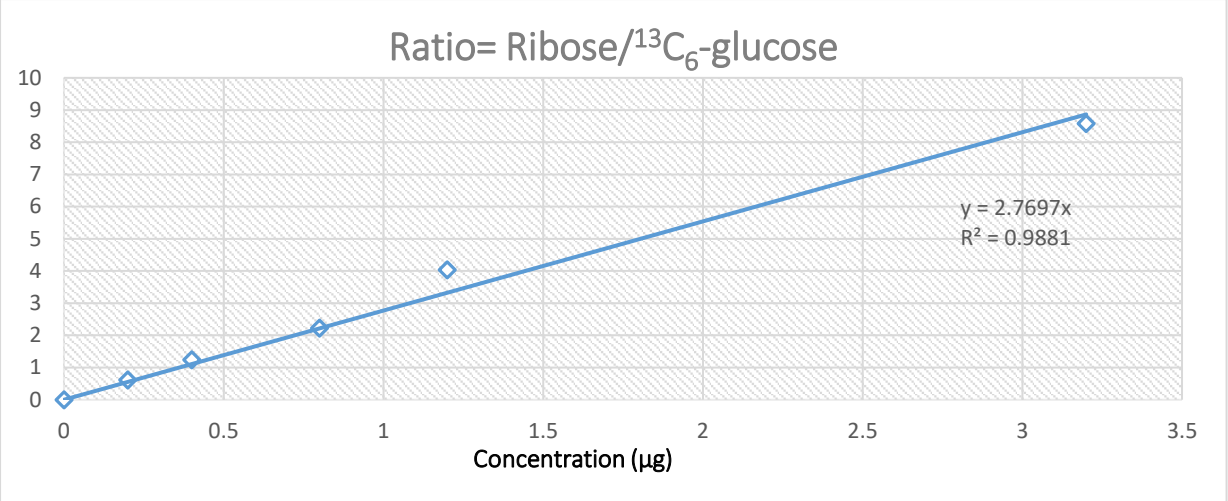

Figure 5. 21: Calibration curve were constructed by plotting the peak area ratio of Ribose and its internal standard ($^{13}C_6$ glucose) (Ribose/$^{13}C_6$ glucose) versus the concentrations points in µg.

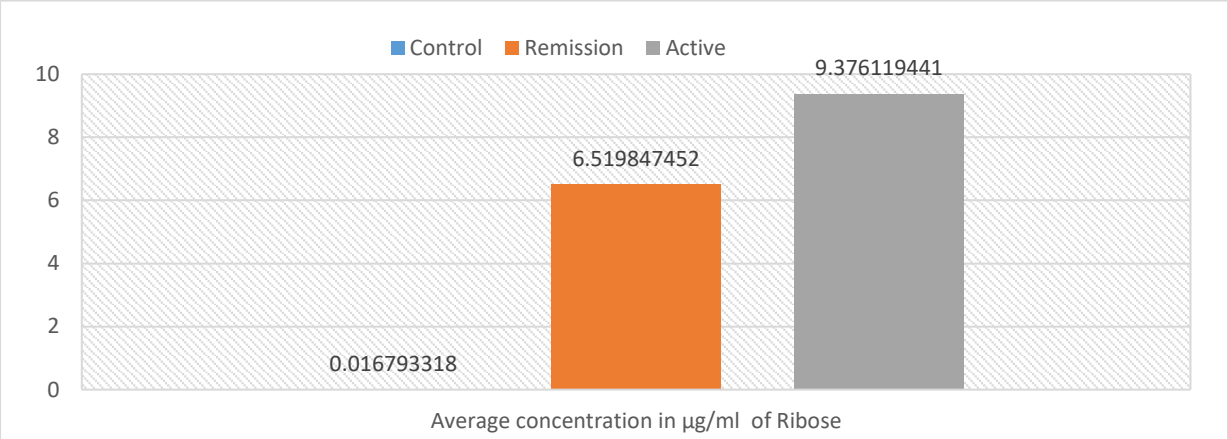

Figure 5. 22: Comparison of average concentration in µg of Ribose in urine samples from three groups.

Ribose is significantly higher (P value 0.0014) in the remission and active groups (P value 0.00050) than the control group and the there is no significant difference between remission and active (figure 5.22). Arabinose is significantly much higher in the control group in comparison with the active and remission groups (figure 5.24)

Table 5. 10: The calibration points of Arabinose and its internal standard ($^{13}C_6$ glucose) from the area under the peak of each reading and then calculating the ratio Arabinose /$^{13}C_6$ glucose.

Concentration	Arabinose	$^{13}C_6$ glucose	Ratio= Arabinose/$^{13}C_6$ D-glucose
0	0	112803748	0
0.2	60000055	105644954	0.567940566
0.4	136504142	111128109	1.228349364
0.8	295403010	133641358	2.210416105
1.2	392053846	104064611	3.767407981
3.2	1080795705	123979321	8.717548187

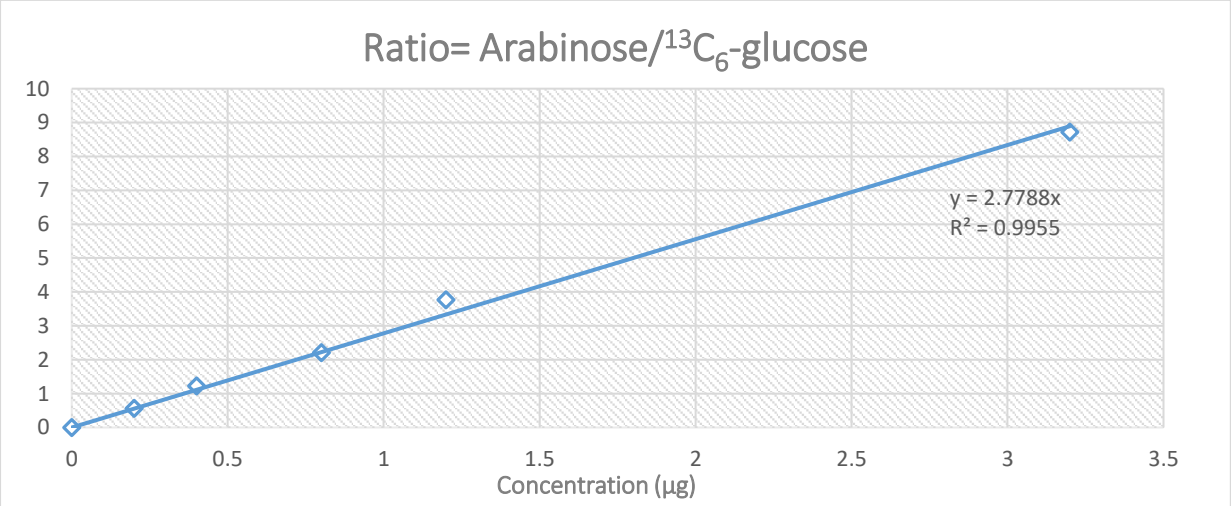

Figure 5. 23: Calibration curve were constructed by plotting the peak area ratio of Arabinose and its internal standard ($^{13}C_6$ glucose) (Arabinose /$^{13}C_6$ glucose) versus the concentrations points in µg.

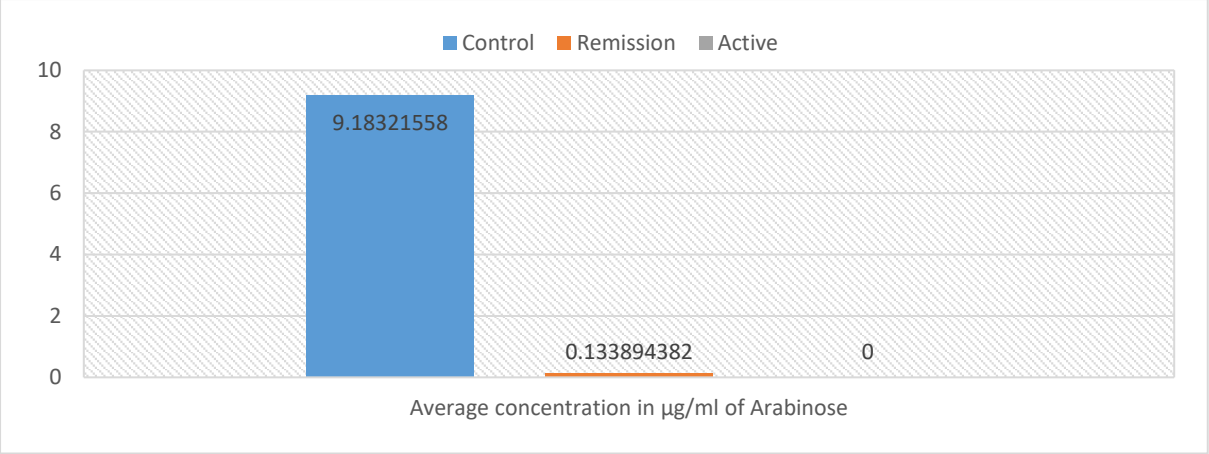

Figure 5. 24: Comparison of average concentration in µg of Arabinose in three samples from three groups

5.3.3 Discussion of the results obtained for sugars in urine samples

Previous research on sugars in urine was focused on quantitative metabolomics profiling by using ^{1}HNMR to discriminate between patients with IBD and healthy individuals, and found higher levels of glucose in IBD patients as compared to healthy individuals. Moreover, another study also found that the level of glucose was elevated in the colonic mucosa of IBD patients [37, 43, 137]. The outcomes appearing in these previous studies are very consistent with the results in the present study where the level of glucose was higher in the quiescent and active UC urine samples as compared to control urine and the changes in glucose indicate a possible shift in energy metabolism. A recently published report mentioned that acetate is very important to lower the pH of the intestine and thereby inhibit enteropathogenic bacteria and high levels of acetate lower the pH in the colon. The pH plays a major role for the relative density and growth of *Desulfovibrio spp,* as the predominant sulfate-reducing bacteria in the human colon, and their main product is hydrogen sulfide. These type of bacteria prefer to grow in the environment that is slightly alkaline or neutral, hence low pH could cause a relative decrease of *Desulfovibrio spp* . Sulfate-reducing bacteria have been earlier correlated to the development of UC because the metabolism of butyrate in colonocytes can be inhibited with high concentrations of sulfide and this induces proliferation and metabolic abnormalities in the epithelial cells similar to those observed with UC. Also it was observed in the colonic mucus of patients with active UC that there were higher levels of *Desulfovibrio spp* than in healthy controls as an indication to the role of this bacterium in the pathogenesis of UC [138]. The previous information indicates that that levels of acetate and *Desulfovibrio spp* are inversely proportional. In the current study the level of acetate was reduced in the urine samples of active UC and remission UC cohorts compared to the levels in controls. Furthermore, in this present study the glucose level was elevated in the urine samples of active UC and remission UC cohorts compared to controls. from this outcome it may be

that the pH level is higher in active and quiescent UC than control urine samples due to low acetate level and high glucose level, thus probably indicates that the level of *Desulfovibrio spp* higher due to pH close to neutral or alkaline as preferred growth environment for this type of bacteria, mean pH range at the in presence of high glucose is between 6.97 and 7.84 [139]. A previous study investigated the oxidative metabolism of glucose and butyrate in colonocytes of an animal model of DSS colitis and compared this with control mice. This study found a decrease in butyrate oxidation by 83.99% in DSS II and by 56.40% (after seven days of DSS feeding) in comparison with controls. Also in DSS treated mice glucose oxidation was significantly increased. The ratio of glucose to butyrate was 1:15 in the control whereas in DSS II was 1:1 and 1:4.6 in DSS I in colonocytes. Therefore the concentration of butyrate increased from 10 to 80 mM. The order of utilization of various substrates by healthy colonocytes is butyrate> glucose > ketone bodies > glutamine. Moreover, this study mentioned that specific metabolic impairment is hypothesised to occur in UC cases in butyrate and glucose oxidation since colonocyte metabolism in mice is similar to that in man [140]. These findings in the previous study are consistent with the present study were the level of butyrate was increased in the urine samples of active and remission UC more than controls and glucose was observed in this present study at higher level and significantly different in urine samples of active and quiescent UC compared to controls. Another study reported that especially in the UC patients there are significant reductions of several serum antioxidants such as zinc, selenium and β-carotene and it was suggested this may depress taste acuity according due to the deficiency of zinc which may cause an increased in the sugar intake and then the level of glucose in the blood which leads to presence of glucose and fructose with high levels in the urine as in diabetes patients[141, 142]. This hypothesis is consistent with the present study where glucose, fructose, galactose levels are higher in the active and remission UC urine samples than in the control[143]. Certain research has noted that diet may alter the composition of the intestinal microbiota leading to dysbiosis of intestinal microbes, for example a high-sugar diet intake leads to alteration of certain types of bacteria like *Clostridium innocuum* and *Enterococcus* spp [143]. It was mentioned from previous studies that those types of bacteria were down regulated in IBD patients especially UC were the *Enterococcus* spp from phylum of *Firmicutes* was depleted in active CD and UC patients compared to controls without any sign of inflammation. Beside that *Clostridium innocuum*, had a higher activity index ratio (AIR) in healthy individuals than in IBD patients, therefore these specific bacterial populations are in an inactive or dormant state in IBD patient[144, 145]. From the previous information it was observed intake of a diet with a high sugar level correlated to dysbiosis of this specific bacterial species and an alteration of this bacterial population was noted in the IBD patients compared to controls. Thus these observations are supported by the present study which

found that higher levels of sugars (glucose, fructose and galactose) are present in the urine samples of active and quiescent UC in comparison to controls.

Several studies have discussed fructose and its correlation to IBD disease. For example fructose enhances the growth of *Lactobacillus species* and *Bifidobacterium* and is a substrate for the production of SCFAs particularly butyrate. On the other hand other studies used a breath hydrogen test for measuring the fructose absorption where the hydrogen produced during fermentation is absorbed into the bloodstream and excreted through the lung, those studies measure the concentration of hydrogen in the breath after consumption of a known amount of fructose to determine the malabsorption of fructose. One of these studies reported that fructose absorption can be impaired in the presence of small intestinal disease and the fructose malabsorption is more common in patients with Crohn's disease which is contradicted with the current study. Another study using the hydrogen breath test (HBT) for determining the malabsorption of fructose in IBS and found that fructose was not considered problematic and was not malabsorbed when foods containing glucose or sucrose in equal amounts to fructose and especially in the presence of glucose this permitted efficient fructose absorption. It is uncommon to find fructose in the foods without glucose and other types of sugars. These two studies have divergent results as they use a similar test [39, 146]. HBT is widely utilised for testing the functional and abnormal pathophysiology of gastrointestinal disorders such as small intestinal bacteria overgrowth (SIBO) and malabsorption of sugars. However, this test has drawbacks with its low sensitivity and variable results. Therefore, it should be used with other techniques and today the regular use of breath test in clinical practice cannot be recommended for the evaluation of patient's symptoms with suspected functional gastrointestinal disorders[144]. Another report noticed that *Bifidobacterium* and *Lactobacillus species* were increased significantly in faecal and biopsy specimens of active UC patients and active CD patients consecutively in comparison to healthy controls. Therefore *Bifidobacterium* and *Lactobacillus* were increased number in active IBD in comparison to healthy controls [147, 148]. This outcome from the previous two studies is very compatible with the results of the present research were the level of fructose was increased in active UC urine samples compared to the level and in healthy controls and quiescent UC.

A study was designed when mice developed IBD and then to detect metabolites by using NMR in urine samples after different periods beginning at 8 weeks of age until 20 weeks of age. Mice developed an intestinal inflammation when the anti-inflammatory cytokine IL-10 was deleted in genetically-engineered mice. This study found that mannose was detected in very low quantity at 20 weeks of age in the urine of IL-10 gene-deficient mice[149]. Another study was designed by providing mice with water containing 3% dextran sulfate sodium (DSS) for 7 days to induce acute ulcerative

colitis and then investigated the metabolic changes in the range of biological tissues by employing NMR. This research found mannose was higher in control mouse in comparison with the DSS-treated mouse[55]. The two previous reports are very consistent with the result obtained from the current research were the level of mannose was increased in the urine samples of the control group not suffering from UC compared to the level of mannose in the urine samples of the active UC group. In contrast a study reported that mannose was prominently increased in the plasma and serum of IBD patients UC and CD. Also this study was measured the alteration in metabolites in urine samples of IBD patients versus healthy individuals, but didn't mention if mannose was detected in the urine. The present study was measured mannose in the urine samples of different cohorts UC versus control therefore this present study has an advantage over the previous study which can detect the mannose in the urine samples by using a derivatisation method. The downregulation in absorption of mannose is probably due to low energy and insufficient absorption through the inflamed intestine.

A study was carried out the metabolic profiling from faecal extracts from male mice with colonic disease using ^{1}HNMR spectroscopy as the analytical tool coupled with multivariate data analysis to compare between control group and lactic acid bacteria (LAB) + DSS treated groups. The study observed higher levels of glucose and galactose in the LAB+DSS induced colitis compared to the control group. UC restricted to the colon and affected only the mucosa of the colon. DSS induced colitis often produces symptoms similar to those found in human ulcerative colitis [54].This result is compatible with the outcome of the current study where the levels galactose were more increased in the urine samples of active UC than in remission and control UC. However, on the other side previous research contradicting the results of this present study worked on the quantitative metabolomics profiling by using ^{1}HNMR to discriminate between patients with IBD and healthy controls and reported that as part of the urine metabolite different saccharides such as galactose, lactose and xylose were typically raised in CD were not increased in UC patients compared to the control subjects [37]. This study relied upon ^{1}HNMR but ^{1}HNMR has limited sensitivity in comparison to LC-MS.

Previous studies demonstrated that fucose was dramatically changed between an IBD group and a control group. In interleukin-10 gene-deficient mice raised in a specific pathogen free (SPF) environment were allowed to spontaneously develop colitis to mimic the colonic inflammation in humans. It was found that the histologic disease started to develop after 8 weeks of age and it was observed by using NMR that there were major differences in metabolites that appeared after 8 weeks of age and that fucose concentration was increased gradually by age in weeks 12 to 20 compared to the week 4 in the IL-10 gene deficient mice. Whereas in the wild-type mice the fucose concentration was low and constant between week 4 and week 20 [45]. Another study was used a similar animal

design with IL-10 gene deficient mice and analysis was performed by GCMS. The outcome of this study showed that fucose was elevated in the urine of IL-10 gene deficient mice[150]. These two studies are very compatible with our finding in this present study.

Rhamnose concentration is significantly different between the control group and remission UC group (P-value= 0.038) whereas the difference was not significant between control UC cohort and active UC cohort (P-value= 0.53) and between quiescent UC group and active UC group (P-value= 0.32).

One of the previously reported studies was mentioned that oxidative stress is one of the factors that plays a role in the initiation and progression of IBD, therefore the effect of probiotic bacteria containing exopolysaccharides (EPS) may attenuate the disease progress in humans and this was evaluated in an experimental colitis rat model. EPS are long-chain polysaccharides containing rhamnose. The study showed that a higher level of malondialdehyde (MDA) activity was associated with significant oxidative damage and reduced antioxidant enzyme activities in the colitis model group. Whereas the antioxidant enzyme activities were higher in both the control group and probiotic –treated group compared with those of in the colitis model group. Inflammation of mucosa and excessive generation of reactive oxygen metabolites (ROM) cause impairment of the antioxidant defence mechanism resulting in oxidative damage to extracellular and cellular components. Besides that inflammatory cytokines in IBD are over produced and are potent inducers of ROM. The results were showed that amelioration of oxidative stress was significantly more in the high-EPS group than in the low-EPS group and hence they conclude that EPS significantly attenuated oxidative stress in experimental colitis. They suggested that EPS containing rhamnose improve the antioxidant state of colonic tissue and are able to scavenge ROM and degrade the superoxide anion and hydrogen peroxide[145]. Their result are very compatible with this present study result where the level of rhamnose is higher in control group suggesting more antioxidant enzyme activities protecting mucosa from the damage as in the EPS group in the previous study where the level of rhamnose was high. Another study demonstrated an intestinal permeability test which was evaluated by measuring the urinary excretion ratio of lactulose/L-rhamnose with HPLC in patients with IBD, and they found that the ratio (L/Rh) was elevated in active UC in comparison with inactive UC (remission). Therefore the intestinal permeability was significantly greater in active UC than remission UC [100].This outcome is consistent with our study where the levels of rhamnose are higher in active UC group compared to the remission UC cohort Two studies evaluated the intestinal permeability similar to the previous study design but with different tools and they showed that the intestinal permeability was altered for several molecules such as rhamnose and the absorption of rhamnose was increased in patients with CD. Thus the intestinal permeability in patients with Crohn's disease was greater than that of normal control [151]. This result contradicts this present study but it

was carried out for Crohn's disease compared to normal control not for ulcerative colitis and in UC it is not clear whether intestinal permeability is increased or not [151, 152].

In the current study the average concentration of xylose was upregulated in the urine samples in the control group in comparison with the level of xylose in the IBD urine samples at the active phase and remission phase. To the best of our knowledge no any study was compatible with our result and the previous studies demonstrated that the level of xylose was increased in the IBD samples compared to the healthy control samples. Xylose was increased in the urine samples of CD patients versus healthy control urine samples. However, although xylose levels were typically higher in CD they were not higher in UC patients. Xylose can be obtained by break down of dietary fiber in the colon by cellulolytic microflora (e.g., hemicellulose and cellulose) including *Enterococcus sp*. Since *Enterococcus sp* are found in CD patients in great abundance, this could contribute to the high production of xylose and an increase of the level of xylose in the urine samples of CD patients[37]. Other research found that xylose was upregulated in the urine of IBD patients in the remission phase compared to healthy control subjects in contradiction to the current study. However, this research didn't mention the subtype of IBD neither CD nor UC, also they used ^{1}H NMR as the equipment for the analysis which has limited sensitivity as major drawback [62]. Although previous studies are inconsistent with the outcome of the current study where xylose was increased in the urine samples of UC patients the phenotype was determined by using NMR which is not sensitive enough for this type of analysis and overlapping of the peaks may affect the results [153].

In the current study ribose was elevated in its level and the average concentration was increased in the urine samples of active UC and remission UC cohorts compared to the level of ribose in urine samples of the control group. Therefore Ribose concentration is significantly different between the control group and remission UC cohort (P-value= 0.00122) in addition the difference was significant between control UC group and active UC group (P-value= 0.0077) whereas ribose concentration was not significantly different between the remission UC cohort and active UC group (P-value= 0.52). To our knowledge only very few studies have mentioned ribose in their reports, no study mentioned ribose as metabolite with significant differences in its levels between IBD patients and controls. Ribose was mentioned in an animal model study where the serum of dogs with IBD and healthy dogs was analysed by GC-TOF/MS. Their finding was that ribose was significantly more abundant in dogs with IBD, their result are very consistent with our finding in this present study where the level of ribose was higher in the UC urine samples in active and remission phases in comparison with control urine samples. Ribose is an important source for further metabolism and is vital for biological systems. The pentose phosphate pathway was found to be more active in IBD which was indicated by enrichment

analysis, mainly due to increased abundance of ribose and gluconic acid lactone. The pentose phosphate pathway is an alternative to critical pathway to glycolysis and is involved in cell proliferation and in cell redox balance. This pathway has an important role in the synthesis of DNA/RNA and in protection from the oxidative stress because this pathway produces ribose and energy sources for further metabolism and is required for glutathione reduction[154]. A study analysed faeces in order to demonstrate how the mono and disaccharides influence the production of SCFA in the colon. They found that in their result incubation of faeces with monosaccharides including hexoses and pentoses such as arabinose, xylose and ribose increased the percentage of production of SCFA more than control incubation of faeces without monosaccharides and thus the composition of dietary fibre ingested probably influences the SCFA production in colon and all the monosaccharide converted to SCFA in vitro with different degrees. All saccharides increased the formation of acetate and ribose entered in the formation of butyrate with a lesser degree [155]. This finding is compatible with our finding in this present study where the level of acetate as discussed in the previous chapter was lower in the UC active and quiescent phases whereas the level of ribose is higher in UC active and remission phases.

Arabinose was lower in the urine samples of quiescent UC and active UC cohorts. Therefore arabinose concentration was not significantly different between the control group and the remission UC group whereas arabinose concentration was significantly different between the remission UC group and active UC group (P-value= 0.0055). To the best of our knowledge no study was applied in metabolomics analysis of IBD biological samples to compare the result with control biological samples where arabinose was mentioned as metabolite with significant differences. Some studies mentioned arabinose in different diseases. For example one study used GC-MS analysis on the oesophageal tissue of patients with oesophageal cancer and they mentioned that the level of arabinose was downregulated in patients with cancer [156]. Other two studies designed animal models using guinea pigs and mice where they applied metabolome analysis to urine and bronchoalveolar lavage (BAL) fluids (BALF) on two cohorts one with asthma as type of inflammation and the other healthy control. They have a similar finding where the level of arabinose was significantly reduced in the asthma group [157, 158]. Thus a correlation has been observed suggesting that the inflammatory cells may be associated with downregulation of arabinose. Arabinogalactan a downstream product formed from arabinose and galactose has been displayed to have protective effects against inflammation [159].

5.3.4- Derivatisation of glucose, mannose, fructose and Galactose in Saliva samples.

Table 5. 11: Calibration data obtained for hexoses and pentoses and the results from the analysis of saliva samples for patients with active IBD, in remission from IBD and a control group.

Sugars	Calibration curve	Control Average Concentration in µg/ml ± RSD	Active Average Concentration in µg/ml± RSD	Remission Average Concentration µg/ml± RSD	P Value Control active	P value Control remission	P value Active remission
Glucose	Y=0.9341x R^2=0.9958	187.13 ± 188.9	14 ± 130.9	12.02 ± 140.8	0.047	0.044	0.73
Fructose	Y=0.0766 R^2= 0.984	48.61 ± 167.45	2.62 ± 204.8	0.32 ± 183	0.045	0.036	0.1
Mannose	Y=1.526x R^2= 0.9989	18.18 ±165	3.62 ±189	5.83 ±177	0.01	0.032	0.38
Galactose	Y=1.0777x R^2= 0.9987	0	0	0	0	0	0
Fucose	Y=1.3212x R^2= 0.9891	11.94± 204.3	7.98± 125.4	35.64 ± 307.7	0.49	0.31	0.23
Rhamnose	Y=1.3286x R^2= 0.9881	89.49 ± 218.5	0.0078 ± 207.2	31.20 ± 338	0.043	0.24	0.16
Xylose	Y=1.3468x R^2= 0.985	0.037 ± 269.7	0.0055 ± 400	0.028 ± 229	0.14	0.71	0.09
Ribose	Y=2.7697x R^2= 0.9881	0.73 ± 202.18	0.71 ± 148.2	0.54 ± 162.9	0.97	0.61	0.59
Arabinose	Y=2.7788x R^2= 0.9955	0.0067 ± 128	0	0	0.095	0.095	No difference

Glucose levels were elevated and the average concentration was increased in the saliva samples of control compared to the level and average concentrations of glucose in saliva samples of quiescent UC and the active UC cohort (figure 5.25 and table 5.11). The raw data obtained for glucose levels in the saliva samples is shown in tables A3.13-A3.15 in appendix 3.Glucose concentrations are significantly different between the control group and active UC group (P-value= 0.048) as well as between the control cohort and remission UC cohort (P-value= 0.044). Whereas there was no significant difference between remission UC cohort and active UC cohort (P-value= 0.73).

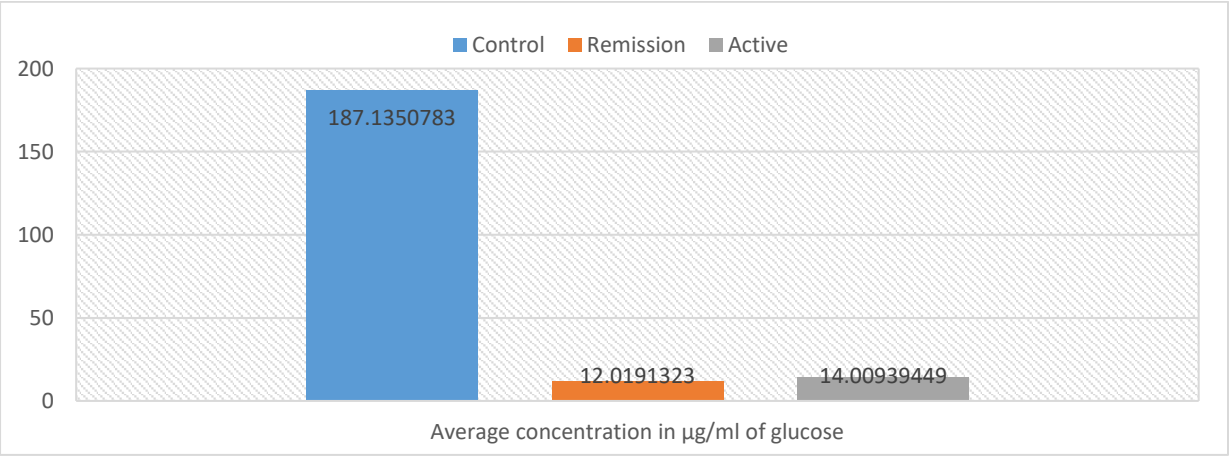

Figure 5. 25: Comparison of average concentration in µg of glucose in three groups of Saliva samples.

To the best of our knowledge no study has applied metabolomic profiling to the saliva samples of IBD patients one study applied metabolome study on celiac disease. Most the previous studies that applied metabolomic profiling IBD samples reported that the level of glucose was elevated in the samples of IBD patients on the both CD and UC subtypes compared to the control [37, 62]. This observation contradicts the results obtained from the saliva samples of UC patients in the present study, whereas upregulation of glucose is are consistent with the result obtained from urine samples of UC patients in the current study.

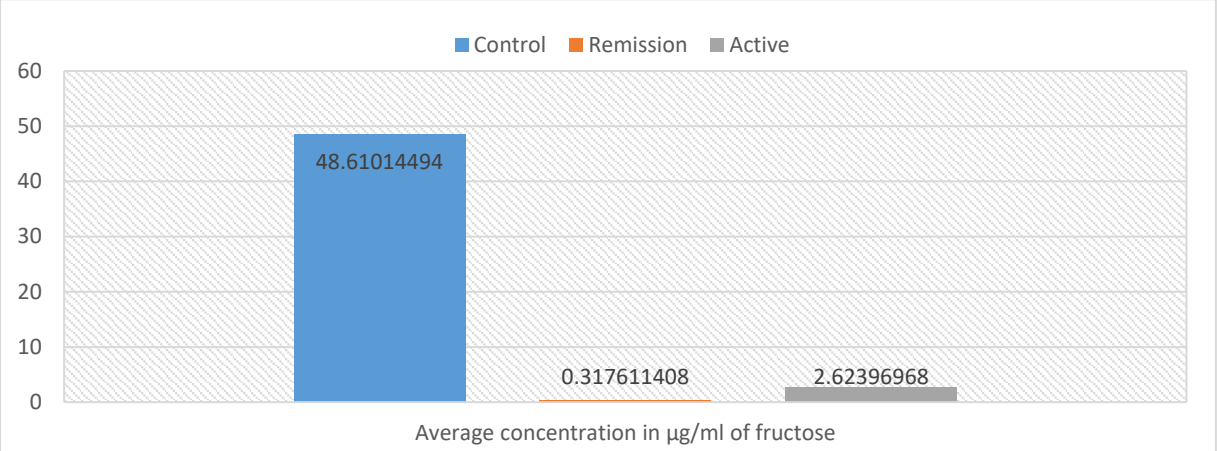

Figure 5. 26: Comparison of average concentration in µg of fructose in three groups of saliva samples.

The raw data obtained for fructose levels in the saliva samples is shown in tables A3.16-A3.18 in appendix 3.Fructose level and concentration was significantly different between the control group and active UC group (P-value= 0.045) as well as between the control group and the remission group (P-value= 0.036) (figure 5.26, table 5.11).Whereas there was no significant difference between remission UC cohort and active UC cohort (P-value= 0.106). The breath hydrogen test has been used for measuring fructose absorption where the hydrogen produced during fermentation is absorbed into the bloodstream and excreted through the lung. These studies measured the concentration of hydrogen in the breath after consumption of known amount of fructose to determine the malabsorption of fructose. One of these studies reported that fructose absorption can be impaired in the presence of small intestinal disease and that fructose malabsorption is more common in patients with Crohn's disease [39, 146].

The raw data obtained for mannose levels in the saliva samples is shown in tables A3.19-A3.21 in appendix 3.Mannose concentration was significantly different between the control group and active

UC group (P-value= 0.01) as well as between the control cohort and remission UC cohort (P-value= 0.032) (figure 5.27, table 5.11). Whereas there was no significant difference between remission UC cohort and active UC cohort (P-value= 0.38).

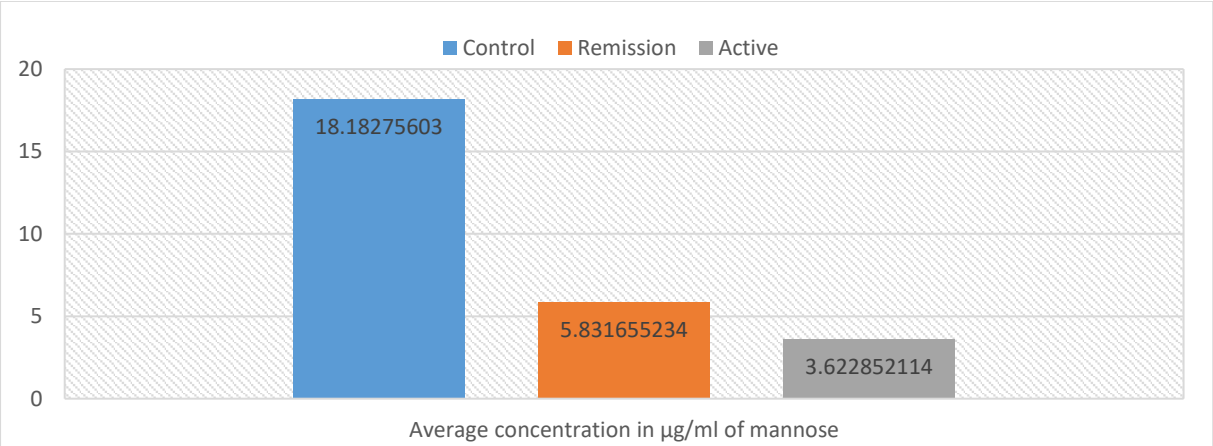

Figure 5. 27: Comparison of average concentration in µg of mannose in three groups of saliva samples.

Two previous studies found that mannose was present in very low quantities at 20 weeks of age in the urine of IL-10 gene-deficient mice compared to the control mice[149]. Another study that was designed to induce acute ulcerative colitis found the level of mannose in the control mouse was upregulated compared to DSS-treated mice[55]. The two previous reports are consistent with the results obtained from this current study where the level of mannose was elevated in the saliva samples of the control group compared to the level of mannose in the saliva samples of active UC cohort. On the other hand two studies found the level of mannose was increased in the serum and plasma of IBD patients compared to control and thus contradicts the current study. However the current study was analysed and detected mannose after it was derivatised in order to enhance sensitivity whereas NMR which was applied in the previous studies has limited sensitivity [37, 43].

5.3.5-Derivatisation of Fucose, L-Rhamnose, Xylose, Ribose and Arabinose in Saliva samples.

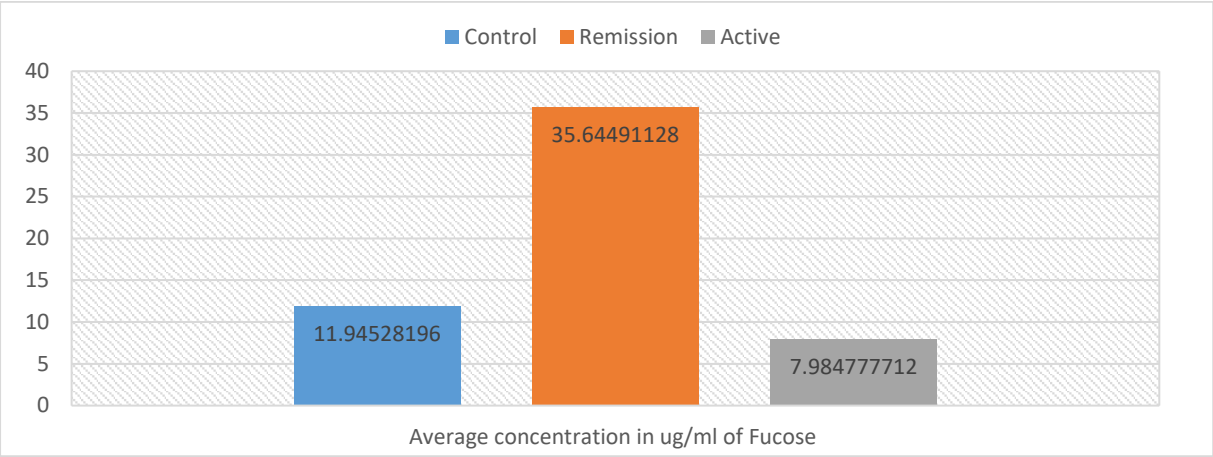

Figure 5. 28: Comparison of average concentration in µg of fucose in in three groups of saliva samples.

Fucose was increased in the saliva samples of quiescent UC groups compared to the level and average concentration of fucose in saliva samples from control and of active UC samples. The raw data obtained for pentoses and deoxyhexoses levels in the saliva samples is shown in tables A3.37-A3.51 in appendix 3. There were not any significant differences concentrations of fucose between any two cohorts; between the control group and remission UC group P-value= 0.311 and the control UC cohort and active UC cohort P-value= 0.49 and between quiescent UC group and active UC group P-value= 0. 23(figure 5.28, table 5.11). Thus fucose levels were very variable within the groups.

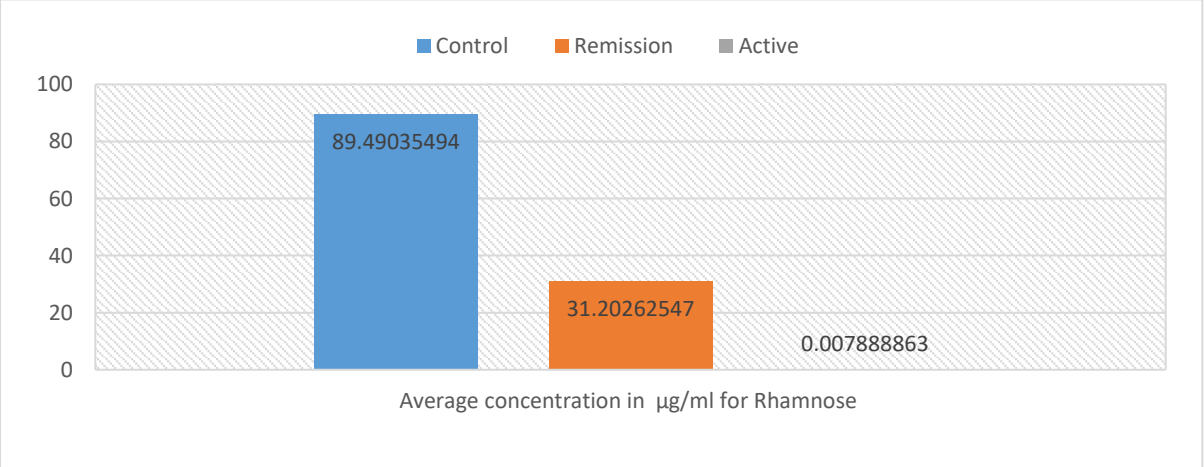

Figure 5. 29: Comparison of average concentration in µg of Rhamnose in three groups of saliva samples.

There are significant differences in the concentration of rhamnose between the control group and the active cohort (P-value= 0.043) and the difference was not significantly different between the control cohort and quiescent UC cohort (P-value= 0.24) and between quiescent UC group and active UC group (P-value= 0. 16) (figure 5.29, table 5.11). The outcome was obtained from the saliva samples are to some extent similar to the results that were obtained from the samples with the levels of rhamnose

being elevated in the control group of saliva and urine samples in comparison to the UC saliva and urine samples of the both phases active and remission. Therefore the results of the present study are consistent with previous studies [39, 145, 146, 148,160]. The result of the current study is not compatible with a study previously discussed[151] where Crohn's disease was compared to normal control but not in ulcerative colitis, which is our concern, and it was suggested that the increased intestinal permeability may be an etiologic factor in patients with CD. However, in UC it is not clear whether intestinal permeability is increased or not[151].

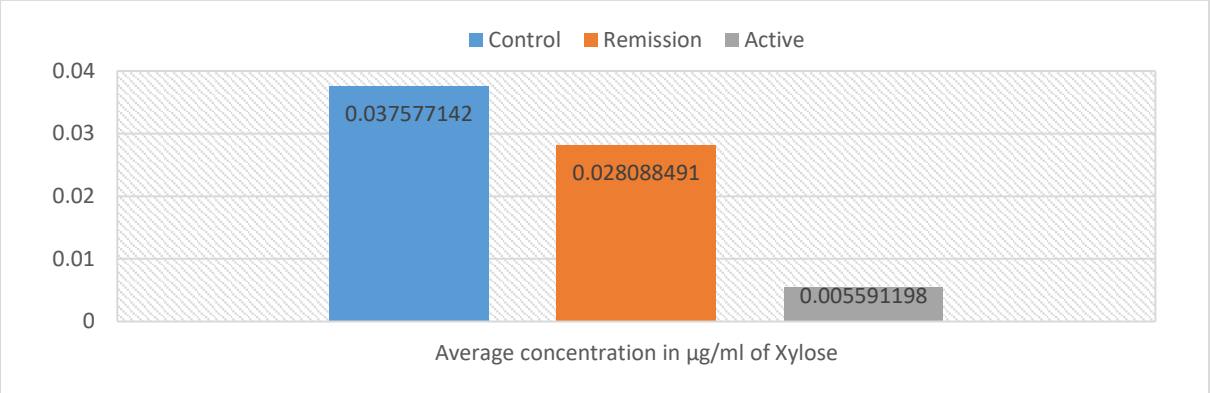

Figure 5. 30: Comparison of average concentration in µg of xylose in three groups of saliva samples.

There were no any significant differences in the concentration of xylose between any two cohorts Therefore difference was not significant between: the control group and remission UC group (P-value= 0.70), the difference was not significant between Control UC cohort and active UC cohort (P-value= 0.14) and between quiescent UC group and active UC group (P-value= 0. 09) (figure 5.30, table 5.11).

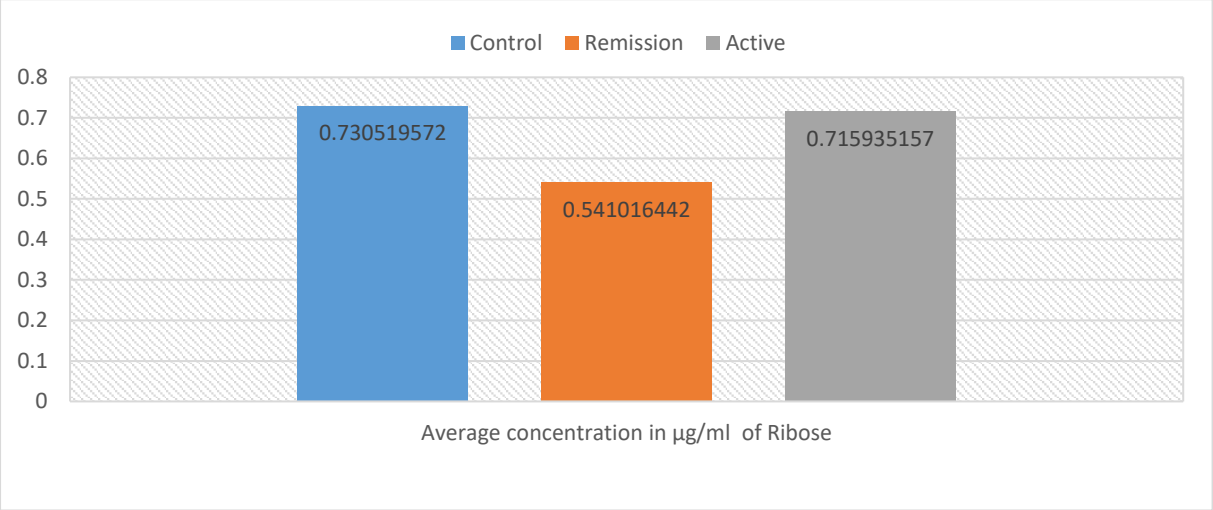

Figure 5. 31: Comparison of average concentration in µg of ribose in three groups of saliva samples.

There were no significant differences in the concentrations of ribose. Therefore difference was not significant between the control group and remission UC group (P-value= 0.6), the control and the

active UC cohort (P-value= 0.97) and between the quiescent UC group and the active UC group (P-value= 0. 58) (figure 5.31, table 5.11).

There are no any significant differences in the concentration of arabinose between any two cohorts. Arabinose was not detected at any saliva sample among 42 saliva samples from quiescent UC group and active UC group and was only detected in three control saliva samples among 23 control saliva samples (figure 5.32, table 5.11).

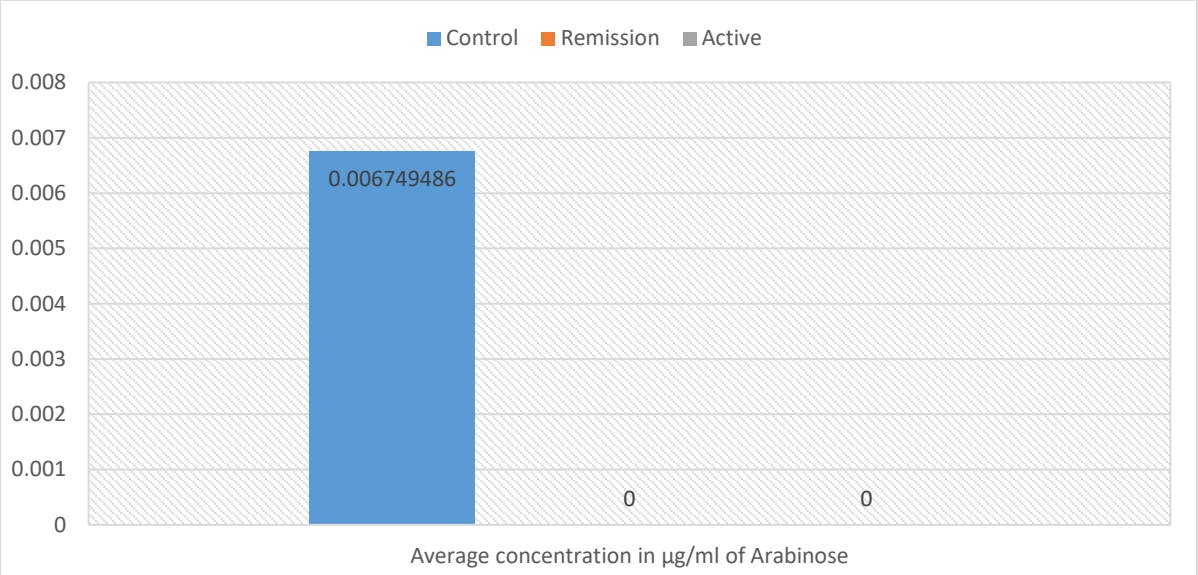

Figure 5. 32: Comparison of average concentration in µg of Arabinose in three groups of saliva samples.

5.4-Conclusion

Monosaccharides, hexoses and pentoses have been successfully derivatised by using reductive amination in urine and saliva samples in combination with hydrophilic interaction chromatography and detection by high resolution mass spectrometry. The levels of some pentoses and hexoses and deoxyhexoses were quantified in a control group and patients suffering from UC and in remission from UC. There were some significant differences between the levels of sugars observed particularly in urine samples. This might be indicative of differences in the microbiome between the different groups.

Chapter-6

Summary and Future work

6.1 Summary

The summary or conclusion of the thesis is that it covers five projects, the details of which are described here briefly as:

The first chapter is the general introduction of metabolomics, instruments used in the metabolomics profiling and fingerprints, type of analysis used for profiling of metabolomes, definition of gut microbiome and alteration in the community of microbiome can affect metabolome then may participate to cause certain diseases such as inflammatory bowel disease.

The second chapter of the thesis describes Quantitative metabolomics profiling of urine and saliva samples by LCMS instrument in order to discriminate between patients with IBD and healthy individuals and can help for understanding of disease perturbation. The samples were collected from 63 patients attending the GI clinic with a confirmed diagnosis of either active UC (12), quiescent UC (26) controls without IBD (25) at the same time saliva samples were collected from 65 patients.

The third chapter in the thesis describes the development of a method to measure Short Chain Fatty Acids (SCFA) in human plasma and urine samples using HILIC chromatography coupled with a high resolution mass spectrometry. In this chapter a highly sensitive method for the determination of the SCFA in urine and plasma samples. The method was validated according to FDA guidelines. The method is already published in current metabolomics journal.

The fourth chapter covers the application of the derivatisation method urine samples, collected from 63 patients attending the GI clinic, for quantification of SCFA in those three cohorts (active UC, quiescent UC and control individuals not suffering from IBD). The results found there are significant difference in the level and amount of SCFA between three groups and also published in current metabolomics journal.

The last chapter of the thesis is about the application of the developed method for the derivatisation of hexoses, deoxyhexoses and pentose's in urine and saliva samples from patients suffering from UC, in active, remission and controls collected from patients attending the GI clinic. The results found there are significant difference in the level and amount of hexoses, deoxyhexoses and pentose's between three groups particularly in urine samples.

6.2 Conclusions and Future work

LCMS-based metabolomics is becoming a useful tool in the study of body fluids and has a strong potential to contribute to IBD disease diagnosis. Untargeted metabolomics profiling as was applied to urine and saliva samples from three groups (active UC, quiescent UC and control individuals not suffering from IBD). Metabolomic differences were observed between the three groups particularly for the saliva samples where there were some clear metabolic markers. Thus the most promising fluid for further metabolomic profiling is saliva.

The validation and a highly sensitive method for the determination of the SCFA in urine and plasma was carried out and this method was used to determine the SCFAs in three patient groups. In future this method could be applied to other body fluids that are readily available and could potentially be used for metabolomics-based disease diagnosis. One such body fluids is stool or fecal extract due to Gut microbiota play a major role in the prolongation and onset of the chronic intestinal inflammation [96] and changes in gut flora are considered to be an element of IBD pathophysiology . Enteric bacterial species such as Clostridia and Bacteroides preferentially produce acetate, butyrate, and other Short Chain Fatty Acids (SCFAs) that are the preferred energy substrates of colonic epithelial cells and are thought to enhance epithelial barrier integrity and modulate the gastrointestinal (GI) immune response. Therefore due to the pathophysiology of IBD is not fully understood, application of derivatisation method for the determination of SCFA on fecal extract give its contact with and transient stay in colon and rectum, stool carry a lot of useful information regarding health/disease status of both the colon and the rectum, it is an obvious target for analysis and given the complex nature of the gut microbiota [47, 161]. In addition to the application of quantitative metabolomics profiling, non-targeted analysis of metabolites provides a window for elucidating the complex metabolic interplay between mammals and their intestinal ecosystems [37, 162].

Application of a method for profiling sugars based on reductive amination revealed many differences between IBD patients, remission patients and controls. This method could be developed further by running a greater number of sugar standards.

References:

1. Ryan, D., et al., *Recent and potential developments in the analysis of urine: A review.* Analytica Chimica Acta, 2011. **684**(1-2): p. 17-29.
2. Lu, H.M., et al., *Comparative evaluation of software for deconvolution of metabolomics data based on GC-TOF-MS.* Trac-Trends in Analytical Chemistry, 2008. **27**(3): p. 215-227.
3. Callahan, D.L., et al., *Profiling of polar metabolites in biological extracts using diamond hydride-based aqueous normal phase chromatography.* J Sep Sci, 2009. **32**(13): p. 2273-80.
4. Cubbon, S., et al., *Hydrophilic interaction chromatography for mass spectrometric metabonomic studies of urine.* Anal Chem, 2007. **79**(23): p. 8911-8.
5. Zhang, T., et al., *Evaluation of Coupling Reversed Phase, Aqueous Normal Phase, and Hydrophilic Interaction Liquid Chromatography with Orbitrap Mass Spectrometry for Metabolomic Studies of Human Urine.* Analytical Chemistry, 2012. **84**(4): p. 1994-2001.
6. Santa, T., O.Y. Al-Dirbashi, and T. Fukushima, *Derivatization reagents in liquid chromatography/electrospray ionization tandem mass spectrometry for biomedical analysis.* Drug Discov Ther, 2007. **1**(2): p. 108-18.
7. Yu, Y.Y., et al., *Determination of pharmaceuticals, steroid hormones, and endocrine-disrupting personal care products in sewage sludge by ultra-high-performance liquid chromatography-tandem mass spectrometry.* Analytical and Bioanalytical Chemistry, 2011. **399**(2): p. 891-902.
8. Wong, C.H.F., et al., *Rapid screening of anabolic steroids in horse urine with ultra-high-performance liquid chromatography/tandem mass spectrometry after chemical derivatisation.* Journal of Chromatography A, 2012. **1232**: p. 257-265.
9. Hernandez, F., et al., *Target and nontarget screening of organic micropollutants in water by solid-phase microextraction combined with gas chromatography/high-resolution time-of-flight mass spectrometry.* Analytical Chemistry, 2007. **79**(24): p. 9494-9504.
10. Soga, T., et al., *Simultaneous determination of anionic intermediates for Bacillus subtilis metabolic pathways by capillary electrophoresis electrospray ionization mass spectrometry.* Analytical Chemistry, 2002. **74**(10): p. 2233-2239.
11. Kaderbhai, N.N., et al., *Functional genomics via metabolic footprinting: monitoring metabolite secretion by Escherichia coli tryptophan metabolism mutants using FT-IR and direct injection electrospray mass spectrometry.* Comparative and Functional Genomics, 2003. **4**(4): p. 376-391.
12. Honda, A., et al., *Highly sensitive analysis of sterol profiles in human serum by LC-ESI-MS/MS.* J Lipid Res, 2008. **49**(9): p. 2063-73.
13. Athanasiadou, I., et al., *Chemical derivatization to enhance ionization of anabolic steroids in LC-MS for doping-control analysis.* Trac-Trends in Analytical Chemistry, 2013. **42**: p. 137-156.
14. Halket, J.M., et al., *Chemical derivatization and mass spectral libraries in metabolic profiling by GC/MS and LC/MS/MS.* Journal of Experimental Botany, 2005. **56**(410): p. 219-243.
15. Quirke, J.M.E., C.L. Adams, and G.J. Vanberkel, *Chemical Derivatization for Electrospray-Ionization Mass-Spectrometry .1. Alkyl-Halides, Alcohols, Phenols, Thiols, and Amines.* Analytical Chemistry, 1994. **66**(8): p. 1302-1315.
16. Holmes, E., et al., *Understanding the role of gut microbiome-host metabolic signal disruption in health and disease.* Trends in Microbiology, 2011. **19**(7): p. 349-359.
17. Brown, K., et al., *Diet-Induced Dysbiosis of the Intestinal Microbiota and the Effects on Immunity and Disease (vol 4, pg 1095, 2012).* Nutrients, 2012. **4**(11): p. 1552-1553.
18. Sekirov, I., et al., *Gut Microbiota in Health and Disease.* Physiological Reviews, 2010. **90**(3): p. 859-904.
19. Weir, T.L., et al., *Stool Microbiome and Metabolome Differences between Colorectal Cancer Patients and Healthy Adults.* Plos One, 2013. **8**(8).

20. Ursell, L.K., et al., *The Intestinal Metabolome: An Intersection Between Microbiota and Host.* Gastroenterology, 2014. **146**(6): p. 1470-1476.
21. Bajaj, J.S., et al., *Randomised clinical trial: Lactobacillus GG modulates gut microbiome, metabolome and endotoxemia in patients with cirrhosis.* Alimentary Pharmacology & Therapeutics, 2014. **39**(10): p. 1113-1125.
22. Lu, K., et al., *Serum Metabolomics in a Helicobacter hepaticus Mouse Model of Inflammatory Bowel Disease Reveal Important Changes in the Microbiome, Serum Peptides, and Intermediary Metabolism.* Journal of Proteome Research, 2012. **11**(10): p. 4916-4926.
23. Moco, S., F.P.J. Martin, and S. Rezzi, *Metabolomics View on Gut Microbiome Modulation by Polyphenol-rich Foods.* Journal of Proteome Research, 2012. **11**(10): p. 4781-4790.
24. Musso, G., R. Gambino, and M. Cassader, *Obesity, diabetes, and gut microbiota: the hygiene hypothesis expanded?* Diabetes Care, 2010. **33**(10): p. 2277-84.
25. Wikoff, W.R., et al., *Metabolomics analysis reveals large effects of gut microflora on mammalian blood metabolites.* Proc Natl Acad Sci U S A, 2009. **106**(10): p. 3698-703.
26. De Preter, V., *Metabolomics in the Clinical Diagnosis of Inflammatory Bowel Disease.* Digestive Diseases, 2015. **33**: p. 2-10.
27. Barrett, J.S., et al., *Comparison of the prevalence of fructose and lactose malabsorption across chronic intestinal disorders.* Aliment Pharmacol Ther, 2009. **30**(2): p. 165-74.
28. Scheltema, R.A., et al., *PeakML/mzMatch: A File Format, Java Library, R Library, and Tool-Chain for Mass Spectrometry Data Analysis.* Analytical Chemistry, 2011. **83**(7): p. 2786-2793.
29. Smith, C.A., et al., *XCMS: Processing mass spectrometry data for metabolite profiling using Nonlinear peak alignment, matching, and identification.* Analytical Chemistry, 2006. **78**(3): p. 779-787.
30. Creek, D.J., et al., *IDEOM: an Excel interface for analysis of LC-MS-based metabolomics data.* Bioinformatics, 2012. **28**(7): p. 1048-1049.
31. Cubbon, S., et al., *Metabolomic Applications of Hilic-Lc-Ms.* Mass Spectrometry Reviews, 2010. **29**(5): p. 671-684.
32. Wu, Z., *Introduction to SIMCA-P and Its Application.* 2010.
33. Yoshie, T., et al., *Regulation of the metabolite profile by an APC gene mutation in colorectal cancer.* Cancer Science, 2012. **103**(6): p. 1010-1021.
34. Lawson, B.R., et al., *Immunomodulation of murine collagen-induced arthritis by N, N-dimethylglycine and a preparation of Perna canaliculus.* BMC Complement Altern Med, 2007. **7**: p. 20.
35. Tso, V.K., et al., *Metabolomic profiles are gender, disease and time specific in the interleukin-10 gene-deficient mouse model of inflammatory bowel disease.* PLoS One, 2013. **8**(7): p. e67654.
36. Murdoch, T.B., et al., *Urinary metabolic profiles of inflammatory bowel disease in interleukin-10 gene-deficient mice.* Anal Chem, 2008. **80**(14): p. 5524-31.
37. Schicho, R., et al., *Quantitative Metabolomic Profiling of Serum, Plasma, and Urine by H-1 NMR Spectroscopy Discriminates between Patients with Inflammatory Bowel Disease and Healthy Individuals.* Journal of Proteome Research, 2012. **11**(6): p. 3344-3357.
38. Jansson, J., et al., *Metabolomics reveals metabolic biomarkers of Crohn's disease.* PLoS One, 2009. **4**(7): p. e6386.
39. Barrett, J.S., et al., *Comparison of the prevalence of fructose and lactose malabsorption across chronic intestinal disorders.* Alimentary Pharmacology & Therapeutics, 2009. **30**(2): p. 165-174.
40. Verma, M., et al., *Anticonvulsant activity of Schiff bases of isatin derivatives.* Acta Pharm, 2004. **54**(1): p. 49-56.
41. Pandeya, S.N., et al., *Biological activities of isatin and its derivatives.* Acta Pharm, 2005. **55**(1): p. 27-46.

42. Thurmond, R.L., E.W. Gelfand, and P.J. Dunford, *The role of histamine H-1 and H-4 receptors in allergic inflammation: The search for new antihistamines.* Nature Reviews Drug Discovery, 2008. **7**(1): p. 41-53.
43. Dawiskiba, T., et al., *Serum and urine metabolomic fingerprinting in diagnostics of inflammatory bowel diseases.* World Journal of Gastroenterology, 2014. **20**(1): p. 163-174.
44. Marchesi, J.R., et al., *Rapid and noninvasive metabonomic characterization of inflammatory bowel disease.* Journal of Proteome Research, 2007. **6**(2): p. 546-551.
45. Murdoch, T.B., et al., *Urinary metabolic profiles of inflammatory bowel disease in interleukin-10 gene-deficient mice.* Analytical Chemistry, 2008. **80**(14): p. 5524-5531.
46. Bjerrum, J.T., et al., *Metabonomics in Ulcerative Colitis: Diagnostics, Biomarker Identification, And Insight into the Pathophysiology.* Journal of Proteome Research, 2010. **9**(2): p. 954-962.
47. Stephens, N.S., et al., *Urinary NMR metabolomic profiles discriminate inflammatory bowel disease from healthy.* J Crohns Colitis, 2013. **7**(2): p. e42-8.
48. Pacheco, S., K. Hillier, and C. Smith, *Increased arachidonic acid levels in phospholipids of human colonic mucosa in inflammatory bowel disease.* Clin Sci (Lond), 1987. **73**(4): p. 361-4.
49. Kuroki, F., et al., *Serum n3 polyunsaturated fatty acids are depleted in Crohn's disease.* Dig Dis Sci, 1997. **42**(6): p. 1137-41.
50. Hontecillas, R., et al., *Nutritional regulation of porcine bacterial-induced colitis by conjugated linoleic acid.* J Nutr, 2002. **132**(7): p. 2019-27.
51. Esteve-Comas, M., et al., *Abnormal plasma polyunsaturated fatty acid pattern in non-active inflammatory bowel disease.* Gut, 1993. **34**(10): p. 1370-3.
52. Rodriguez, J.W., et al., *Human Acetylator Genotype - Relationship to Colorectal-Cancer Incidence and Arylamine N-Acetyltransferase Expression in Colon Cytosol.* Archives of Toxicology, 1993. **67**(7): p. 445-452.
53. Hickman, D., et al., *Expression of arylamine N-acetyltransferase in human intestine.* Gut, 1998. **42**(3): p. 402-409.
54. Hong, Y.S., et al., *H-1 NMR-based metabonomic assessment of probiotic effects in a colitis mouse model.* Archives of Pharmacal Research, 2010. **33**(7): p. 1091-1101.
55. Dong, F.C., et al., *Systemic Responses of Mice to Dextran Sulfate Sodium-Induced Acute Ulcerative Colitis Using H-1 NMR Spectroscopy.* Journal of Proteome Research, 2013. **12**(6): p. 2958-2966.
56. Lin, H.M., et al., *Metabolomic Analysis Identifies Inflammatory and Noninflammatory Metabolic Effects of Genetic Modification in a Mouse Model of Crohn's Disease.* Journal of Proteome Research, 2010. **9**(4): p. 1965-1975.
57. Lin, H.M., et al., *Nontargeted Urinary Metabolite Profiling of a Mouse Model of Crohn's Disease.* Journal of Proteome Research, 2009. **8**(4): p. 2045-2057.
58. van Kuilenburg, A.B.P., et al., *Quantification of 5,6-dihydrouracil by HPLC-electrospray tandem mass spectrometry.* Clinical Chemistry, 2004. **50**(1): p. 236-238.
59. Jansson, J., et al., *Metabolomics Reveals Metabolic Biomarkers of Crohn's Disease.* Plos One, 2009. **4**(7).
60. Fathi, F., et al., *The Differential Diagnosis of Crohn's Disease and Celiac Disease Using Nuclear Magnetic Resonance Spectroscopy.* Applied Magnetic Resonance, 2014. **45**(5): p. 451-459.
61. Marchesi, J.R., et al., *Rapid and noninvasive metabonomic characterization of inflammatory bowel disease.* J Proteome Res, 2007. **6**(2): p. 546-51.
62. Dawiskiba, T., et al., *Serum and urine metabolomic fingerprinting in diagnostics of inflammatory bowel diseases.* World J Gastroenterol, 2014. **20**(1): p. 163-74.
63. Martin, F.P.J., et al., *Metabolic Assessment of Gradual Development of Moderate Experimental Colitis in IL-10 Deficient Mice.* Journal of Proteome Research, 2009. **8**(5): p. 2376-2387.
64. Zhang, Y., et al., *1H NMR-based spectroscopy detects metabolic alterations in serum of patients with early-stage ulcerative colitis.* Biochem Biophys Res Commun, 2013. **433**(4): p. 547-51.

65. Seneff, S., et al., *Is Endothelial Nitric Oxide Synthase a Moonlighting Protein Whose Day Job is Cholesterol Sulfate Synthesis? Implications for Cholesterol Transport, Diabetes and Cardiovascular Disease.* Entropy, 2012. **14**(12): p. 2492-2530.
66. Ito, N., et al., *Change in the concentration of neutrophil elastase in bronchoalveolar lavage fluid during anesthesia and its inhibition by cholesterol sulfate.* Translational Research, 2006. **148**(2): p. 96-102.
67. Pinheiro, M.M.G., et al., *Anti-Inflammatory Activity of Choisya ternata Kunth Essential Oil, Ternanthranin, and Its Two Synthetic Analogs (Methyl and Propyl N-Methylanthranilates).* Plos One, 2015. **10**(3).
68. Manis, J.P., M. Tian, and F.W. Alt, *Mechanism and control of class-switch recombination.* Trends in Immunology, 2002. **23**(1): p. 31-39.
69. Kumar, R., et al., *Biological function of activation-induced cytidine deaminase (AID).* Biomed J, 2014. **37**(5): p. 269-83.
70. Huang, C., et al., *Metabolic influence of acute cyadox exposure on Kunming mice.* J Proteome Res, 2013. **12**(1): p. 537-45.
71. Blackburn, A.C., W.F. Doe, and G.D. Buffinton, *Salicylate hydroxylation as an indicator of hydroxyl radical generation in dextran sulfate-induced colitis.* Free Radical Biology and Medicine, 1998. **25**(3): p. 305-313.
72. Ingelmansundberg, M., et al., *Hydroxylation of Salicylate by Microsomal Fractions and Cytochrome-P-450 - Lack of Production of 2,3-Dihydroxybenzoate Unless Hydroxyl Radical Formation Is Permitted.* Biochemical Journal, 1991. **276**: p. 753-757.
73. McGorum, B.C., et al., *Systemic concentrations of antioxidants and biomarkers of macromolecular oxidative damage in horses with grass sickness.* Equine Veterinary Journal, 2003. **35**(2): p. 121-126.
74. Thomadaki, H., et al., *Enhanced antileukemic activity of the novel complex 2,5-dihydroxybenzoate molybdenum(VI) against 2,5-dihydroxybenzoate, polyoxometalate of Mo(VI), and tetraphenylphosphonium in the human HL-60 and K562 leukemic cell lines.* Journal of Medicinal Chemistry, 2007. **50**(6): p. 1316-1321.
75. Mutch, D.M., et al., *A distinct adipose tissue gene expression response to caloric restriction predicts 6-mo weight maintenance in obese subjects.* American Journal of Clinical Nutrition, 2011. **94**(6): p. 1399-1409.
76. Pizarro, T.T., et al., *IL-18, a novel immunoregulatory cytokine, is up-regulated in Crohn's disease: Expression and localization in intestinal mucosal cells.* Journal of Immunology, 1999. **162**(11): p. 6829-6835.
77. Sirover, M.A., *Role of the glycolytic protein, glyceraldehyde-3-phosphate dehydrogenase, in normal cell function and in cell pathology.* Journal of Cellular Biochemistry, 1997. **66**(2): p. 133-140.
78. Finnie, I.A., B.A. Taylor, and J.M. Rhodes, *Ileal and Colonic Epithelial Metabolism in Quiescent Ulcerative-Colitis - Increased Glutamine-Metabolism in Distal Colon but No Defect in Butyrate Metabolism.* Gut, 1993. **34**(11): p. 1552-1558.
79. Pero, R.W., et al., *Newly discovered anti-inflammatory properties of the benzamides and nicotinamides.* Molecular and Cellular Biochemistry, 1999. **193**(1-2): p. 119-125.
80. Godin, A.M., et al., *Antinociceptive and anti-inflammatory activities of nicotinamide and its isomers in different experimental models.* Pharmacology Biochemistry and Behavior, 2011. **99**(4): p. 782-788.
81. Liu, H., et al., *Development of 18F-labeled picolinamide probes for PET imaging of malignant melanoma.* J Med Chem, 2013. **56**(3): p. 895-901.
82. Dame, Z.T., et al., *The human saliva metabolome.* Metabolomics, 2015. **11**(6): p. 1864-1883.
83. Rombouts, C., et al., *Untargeted metabolomics of colonic digests reveals kynurenine pathway metabolites, dityrosine and 3-dehydroxycarnitine as red versus white meat discriminating metabolites.* Scientific Reports, 2017. **7**.

84. An, D.D., et al., *Membrane sphingolipids as essential molecular signals for Bacteroides survival in the intestine.* Proceedings of the National Academy of Sciences of the United States of America, 2011. **108**: p. 4666-4671.
85. Duan, R.D. and A. Nilsson, *Metabolism of sphingolipids in the gut and its relation to inflammation and cancer development.* Progress in Lipid Research, 2009. **48**(1): p. 62-72.
86. Wanders, R.J.A. and H.R. Waterham, *Biochemistry of mammalian peroxisomes revisited.* Annual Review of Biochemistry, 2006. **75**: p. 295-332.
87. Sun, M.M., et al., *Microbiota metabolite short chain fatty acids, GPCR, and inflammatory bowel diseases.* Journal of Gastroenterology, 2017. **52**(1): p. 1-8.
88. Cummings, J.H., et al., *Short Chain Fatty-Acids in Human Large-Intestine, Portal, Hepatic and Venous-Blood.* Gut, 1987. **28**(10): p. 1221-1227.
89. Fernandes, J., et al., *Adiposity, gut microbiota and faecal short chain fatty acids are linked in adult humans.* Nutrition & Diabetes, 2014. **4**.
90. Vogt, S.L., J. Pena-Diaz, and B.B. Finlay, *Chemical communication in the gut: Effects of microbiota-generated metabolites on gastrointestinal bacterial pathogens.* Anaerobe, 2015. **34**: p. 106-115.
91. Murase, M., Y. Kimura, and Y. Nagata, *Determination of Portal Short-Chain Fatty-Acids in Rats Fed Various Dietary-Fibers by Capillary Gas-Chromatography.* Journal of Chromatography B-Biomedical Applications, 1995. **664**(2): p. 415-420.
92. Moreau, N.M., et al., *Simultaneous measurement of plasma concentrations and C-13-enrichment of short-chain fatty acids, lactic acid and ketone bodies by gas chromatography coupled to mass spectrometry.* Journal of Chromatography B-Analytical Technologies in the Biomedical and Life Sciences, 2003. **784**(2): p. 395-403.
93. Tedelind, S., et al., *Anti-inflammatory properties of the short-chain fatty acids acetate and propionate: A study with relevance to inflammatory bowel disease.* World Journal of Gastroenterology, 2007. **13**(20): p. 2826-2832.
94. Lewis, K., et al., *Enhanced Translocation of Bacteria Across Metabolically Stressed Epithelia is Reduced by Butyrate.* Inflammatory Bowel Diseases, 2010. **16**(7): p. 1138-1148.
95. Manichanh, C., et al., *Reduced diversity of faecal microbiota in Crohn's disease revealed by a metagenomic approach.* Gut, 2006. **55**(2): p. 205-211.
96. Machiels, K., et al., *A decrease of the butyrate-producing species Roseburia hominis and Faecalibacterium prausnitzii defines dysbiosis in patients with ulcerative colitis.* Gut, 2014. **63**(8): p. 1275-1283.
97. Pouteau, E., et al., *Acetate, propionate and butyrate in plasma: determination of the concentration and isotopic enrichment by gas chromatography/mass spectrometry with positive chemical ionization.* Journal of Mass Spectrometry, 2001. **36**(7): p. 798-805.
98. Tollinger, C.D., H.J. Vreman, and M.W. Weiner, *Measurement of Acetate in Human-Blood by Gas-Chromatography - Effects of Sample Preparation, Feeding, and Various Diseases.* Clinical Chemistry, 1979. **25**(10): p. 1787-1790.
99. Dankert, J., J.B. Zijlstra, and B.G. Wolthers, *Volatile Fatty-Acids in Human Peripheral and Portal Blood - Quantitative-Determination by Vacuum Distillation and Gas-Chromatography.* Clinica Chimica Acta, 1981. **110**(2-3): p. 301-307.
100. Tangerman, A., et al., *Quantitative determination of C2-C8 volatile fatty acids in human serum by vacuum distillation and gas chromatography.* Clin Chim Acta, 1983. **133**(3): p. 341-8.
101. Wolever, T.M., et al., *Time of day and glucose tolerance status affect serum short-chain fatty acid concentrations in humans.* Metabolism, 1997. **46**(7): p. 805-11.
102. Vogt, J.A., P.B. Pencharz, and T.M. Wolever, *L-Rhamnose increases serum propionate in humans.* Am J Clin Nutr, 2004. **80**(1): p. 89-94.
103. Zhao, G., et al., *Determination of short-chain fatty acids in serum by hollow fiber supported liquid membrane extraction coupled with gas chromatography.* J Chromatogr B Analyt Technol Biomed Life Sci, 2007. **846**(1-2): p. 202-8.

104. Stein, J., et al., *Simple and rapid method for determination of short-chain fatty acids in biological materials by high-performance liquid chromatography with ultraviolet detection.* J Chromatogr, 1992. **576**(1): p. 53-61.
105. Meesters, R.J., et al., *Application of liquid chromatography-mass spectrometry to measure the concentrations and study the synthesis of short chain fatty acids following stable isotope infusions.* J Chromatogr B Analyt Technol Biomed Life Sci, 2007. **854**(1-2): p. 57-62.
106. Bouatra, S., et al., *The human urine metabolome.* PLoS One, 2013. **8**(9): p. e73076.
107. Kloos, D., et al., *Derivatization of the tricarboxylic acid cycle intermediates and analysis by online solid-phase extraction-liquid chromatography-mass spectrometry with positive-ion electrospray ionization.* Journal of Chromatography A, 2012. **1232**: p. 19-26.
108. Hove, H. and P.B. Mortensen, *Influence of Intestinal Inflammation (Ibd) and Small and Large-Bowel Length on Fecal Short-Chain Fatty-Acids and Lactate.* Digestive Diseases and Sciences, 1995. **40**(6): p. 1372-1380.
109. Vernia, P., et al., *Organic anions and the diarrhea of inflammatory bowel disease.* Dig Dis Sci, 1988. **33**(11): p. 1353-8.
110. Tonelli, F., et al., *Effects of Short-Chain Fatty-Acids on Mucosal Proliferation and Inflammation of Ileal Pouches in Patients with Ulcerative-Colitis and Familial Polyposis.* Diseases of the Colon & Rectum, 1995. **38**(9): p. 974-978.
111. Shimotoyodome, A., et al., *Short chain fatty acids but not lactate or succinate stimulate mucus release in the rat colon.* Comparative Biochemistry and Physiology a-Molecular and Integrative Physiology, 2000. **125**(4): p. 525-531.
112. Vieira, E.L.M., et al., *Oral administration of sodium butyrate attenuates inflammation and mucosal lesion in experimental acute ulcerative colitis.* Journal of Nutritional Biochemistry, 2012. **23**(5): p. 430-436.
113. Tangerman, A., et al., *Quantitative-Determination of C2-C8 Volatile Fatty-Acids in Human-Serum by Vacuum Distillation and Gas-Chromatography.* Clinica Chimica Acta, 1983. **133**(3): p. 341-348.
114. Wolever, T.M.S., et al., *Time of day and glucose tolerance status affect serum short-chain fatty acid concentrations in humans.* Metabolism-Clinical and Experimental, 1997. **46**(7): p. 805-811.
115. Vogt, J.A., P.B. Pencharz, and T.M.S. Wolever, *L-Rhamnose increases serum propionate in humans.* American Journal of Clinical Nutrition, 2004. **80**(1): p. 89-94.
116. Zhao, G.H., et al., *Determination of short-chain fatty acids in serum by hollow fiber supported liquid membrane extraction coupled with gas chromatography.* Journal of Chromatography B-Analytical Technologies in the Biomedical and Life Sciences, 2007. **846**(1-2): p. 202-208.
117. Reid, C.N., et al., *Standardization of Diagnostic Biomarker Concentrations in Urine: The Hematuria Caveat.* Plos One, 2012. **7**(12).
118. Macia, L., et al., *Microbial influences on epithelial integrity and immune function as a basis for inflammatory diseases.* Immunological Reviews, 2012. **245**: p. 164-176.
119. Huda-Faujan, N., et al., *The impact of the level of the intestinal short chain Fatty acids in inflammatory bowel disease patients versus healthy subjects.* Open Biochem J, 2010. **4**: p. 53-8.
120. Treem, W.R., et al., *Fecal Short-Chain Fatty-Acids in Children with Inflammatory Bowel-Disease.* Journal of Pediatric Gastroenterology and Nutrition, 1994. **18**(2): p. 159-164.
121. Roediger, W.E.W., *The Colonic Epithelium in Ulcerative-Colitis - an Energy-Deficiency Disease.* Lancet, 1980. **2**(8197): p. 712-715.
122. Vernia, P., et al., *Organic-Anions and the Diarrhea of Inflammatory Bowel-Disease.* Digestive Diseases and Sciences, 1988. **33**(11): p. 1353-1358.
123. Saunders, D.R. and J. Sillery, *Effect of Lactate and H+ on Structure and Function of Rat Intestine - Implications for the Pathogenesis of Fermentative Diarrhea.* Digestive Diseases and Sciences, 1982. **27**(1): p. 33-41.

124. van der Wiel-Korstanje, J.A. and K.C. Winkler, *The faecal flora in ulcerative colitis.* J Med Microbiol, 1975. **8**(4): p. 491-501.
125. Harig, J.M. and K.H. Soergel, *Treatment of Diversion Colitis with Short Chain Fatty-Acid (Scfa) Irrigation.* Gastroenterology, 1987. **92**(5): p. 1425-1425.
126. Vernia, P., et al., *Fecal Lactate and Ulcerative-Colitis.* Gastroenterology, 1988. **95**(6): p. 1564-1568.
127. Topping, D.L., et al., *Dietary-Fat and Fiber Alter Large-Bowel and Portal Venous Volatile Fatty-Acids and Plasma-Cholesterol but Not Biliary Steroids in Pigs.* Journal of Nutrition, 1993. **123**(1): p. 133-143.
128. Yan, J., et al., *Neutral monosaccharide composition analysis of plant-derived oligo-and polysaccharides by high performance liquid chromatography.* Carbohydrate Polymers, 2016. **136**: p. 1273-1280.
129. Young, J.E., J.J. Pesek, and M.T. Matyska, *Robust HPLC-Refractive Index Analysis of Simple Sugars in Beverages Using Silica Hydride Columns.* Current Nutrition & Food Science, 2016. **12**(2): p. 125-131.
130. Qian, W.L., et al., *Analysis of sugars in bee pollen and propolis by ligand exchange chromatography in combination with pulsed amperometric detection and mass spectrometry.* Journal of Food Composition and Analysis, 2008. **21**(1): p. 78-83.
131. MolnarPerl, I. and K. Horvath, *Simultaneous quantitation of mono-, di- and trisaccharides as their TMS ether oxime derivatives by GC-MS .1. In model solutions.* Chromatographia, 1997. **45**: p. 321-327.
132. Boldizsar, I., et al., *Simultaneous GC-MS quantitation of acids and sugars in the hydrolyzates of immunostimulant, water-soluble polysaccharides of Basidiomycetes.* Chromatographia, 1998. **47**(7-8): p. 413-419.
133. Medeiros, P.M. and B.R.T. Simoneit, *Analysis of sugars in environmental samples by gas chromatography-mass spectrometry.* Journal of Chromatography A, 2007. **1141**(2): p. 271-278.
134. Fischer, K., M. Wacht, and A. Meyer, *Simultaneous and sensitive HPLC determination of mono- and disaccharides, uronic acids, and amino sugars after derivatization by reductive amination.* Acta Hydrochimica Et Hydrobiologica, 2003. **31**(2): p. 134-144.
135. Saba, J.A., et al., *Investigation of different combinations of derivatization, separation methods and electrospray ionization mass spectrometry for standard oligosaccharides and glycans from ovalbumin.* Journal of Mass Spectrometry, 2001. **36**(5): p. 563-574.
136. Bawazeer, S., et al., *A method for the analysis of sugars in biological systems using reductive amination in combination with hydrophilic interaction chromatography and high resolution mass spectrometry.* Talanta, 2017. **166**: p. 75-80.
137. Sharma, U., et al., *Similarity in the metabolic profile in macroscopically involved and un-involved colonic mucosa in patients with inflammatory bowel disease: an in vitro proton (H-1) MR spectroscopy study.* Magnetic Resonance Imaging, 2010. **28**(7): p. 1022-1029.
138. Vigsnaes, L.K., et al., *In Vitro Fermentation of Sugar Beet Arabino-Oligosaccharides by Fecal Microbiota Obtained from Patients with Ulcerative Colitis To Selectively Stimulate the Growth of Bifidobacterium spp. and Lactobacillus spp.* Applied and Environmental Microbiology, 2011. **77**(23): p. 8336-8344.
139. Gordon, J.L., et al., *Fucosylated glycoconjugate production in the gut epithelium of germ-free, ex-germ free, and transgenic mice: Model for studying host-microbial interactions.* Glycobiology, 1996. **6**(7): p. C2-C2.
140. Ahmad, M.S., et al., *Butyrate and glucose metabolism by colonocytes in experimental colitis in mice.* Gut, 2000. **46**(4): p. 493-499.
141. Ali, B.A., et al., *Environmental Factors and the Risk of Type 1 Diabetes Mellitus-A Case-Control Study.* Journal of Diabetes & Metabolism, 2017. **8**(2).

142. Kawasaki, T., H. Akanuma, and T.Y. Yamanouchi, *Increased fructose concentrations in blood and urine in patients with diabetes.* Diabetes Care, 2002. **25**(2): p. 353-357.
143. Geerling, B.J., et al., *Comprehensive nutritional status in recently diagnosed patients with inflammatory bowel disease compared with population controls.* European Journal of Clinical Nutrition, 2000. **54**(6): p. 514-521.
144. Simren, M. and P.O. Stotzer, *Use and abuse of hydrogen breath tests.* Gut, 2006. **55**(3): p. 297-303.
145. Sengul, N., et al., *The Effect of Exopolysaccharide-Producing Probiotic Strains on Gut Oxidative Damage in Experimental Colitis.* Digestive Diseases and Sciences, 2011. **56**(3): p. 707-714.
146. Shepherd, S.J., M. Nut, and P.R. Gibson, *Fructose malabsorption and symptoms of irritable bowel syndrome: Guidelines for effective dietary management.* Journal of the American Dietetic Association, 2006. **106**(10): p. 1631-1639.
147. Sartor, R.B., *Mechanisms of disease: pathogenesis of Crohn's disease and ulcerative colitis.* Nature Clinical Practice Gastroenterology & Hepatology, 2006. **3**(7): p. 390-407.
148. Wang, W., et al., *Increased Proportions of Bifidobacterium and the Lactobacillus Group and Loss of Butyrate-Producing Bacteria in Inflammatory Bowel Disease.* Journal of Clinical Microbiology, 2014. **52**(2): p. 398-406.
149. Tso, V.K., et al., *Metabolomic Profiles Are Gender, Disease and Time Specific in the Interleukin-10 Gene-Deficient Mouse Model of Inflammatory Bowel Disease.* Plos One, 2013. **8**(7).
150. Lin, H.M., et al., *Using Metabolomic Analysis to Understand Inflammatory Bowel Diseases.* Inflammatory Bowel Diseases, 2011. **17**(4): p. 1021-1029.
151. Hollander, D., *Crohn's disease--a permeability disorder of the tight junction?* Gut, 1988. **29**(12): p. 1621-4.
152. Miki, K., et al., *The sugar permeability test reflects disease activity in children and adolescents with inflammatory bowel disease.* J Pediatr, 1998. **133**(6): p. 750-4.
153. De Preter, V., *Metabolomics in the Clinical Diagnosis of Inflammatory Bowel Disease.* Dig Dis, 2015. **33 Suppl 1**: p. 2-10.
154. Minamoto, Y., et al., *Alteration of the fecal microbiota and serum metabolite profiles in dogs with idiopathic inflammatory bowel disease.* Gut Microbes, 2015. **6**(1): p. 33-47.
155. Mortensen, P.B., K. Holtug, and H.S. Rasmussen, *Short-chain fatty acid production from mono- and disaccharides in a fecal incubation system: implications for colonic fermentation of dietary fiber in humans.* J Nutr, 1988. **118**(3): p. 321-5.
156. Yoshida, M., et al., *Diagnosis of gastroenterological diseases by metabolome analysis using gas chromatography-mass spectrometry.* Journal of Gastroenterology, 2012. **47**(1): p. 9-20.
157. Ho, W.E., et al., *Metabolomics Reveals Altered Metabolic Pathways in Experimental Asthma.* American Journal of Respiratory Cell and Molecular Biology, 2013. **48**(2): p. 204-211.
158. Saude, E.J., et al., *Metabolomic Biomarkers in a Model of Asthma Exacerbation Urine Nuclear Magnetic Resonance.* American Journal of Respiratory and Critical Care Medicine, 2009. **179**(1): p. 25-34.
159. Ho, W.E., et al., *Metabolomics reveals altered metabolic pathways in experimental asthma.* Am J Respir Cell Mol Biol, 2013. **48**(2): p. 204-11.
160. Zhang, A.H., et al., *Recent and potential developments of biofluid analyses in metabolomics.* Journal of Proteomics, 2012. **75**(4): p. 1079-1088.
161. Bezabeh, T., R.L. Somorjai, and I.C.P. Smith, *MR metabolomics of fecal extracts: applications in the study of bowel diseases.* Magnetic Resonance in Chemistry, 2009. **47**: p. S54-S61.
162. Saric, J., et al., *Species variation in the fecal metabolome gives insight into differential gastrointestinal function.* Journal of Proteome Research, 2008. **7**(1): p. 352-360.

Appendix 1

The raw data from the Xcailbur displayed the concentration 0ng to 640ng for the acetic and prpionic and their labelled internal standards.

Figure A1. 1: Traces obtained for calibration series from acetic and propionic acids and their labelled internal standards in the range 0 -640 ng.

0 ng

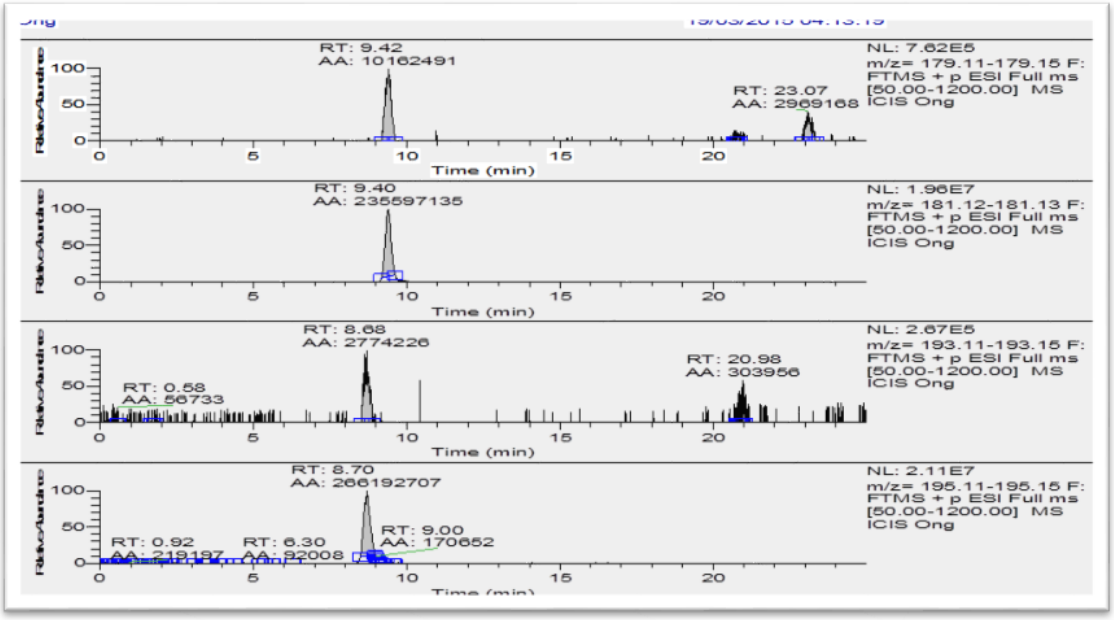

20 ng

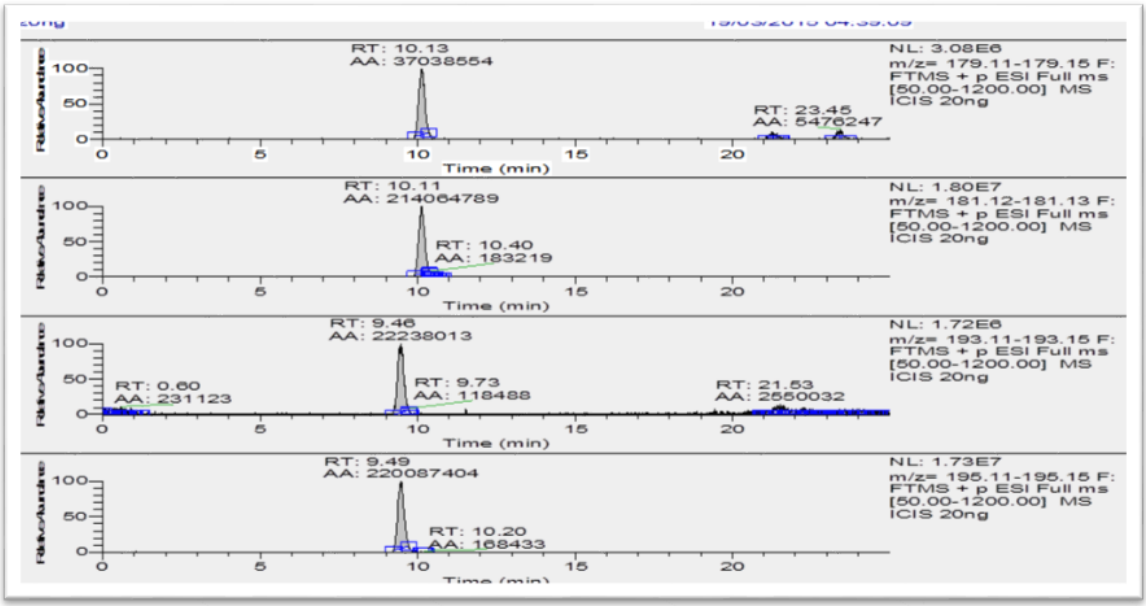

40g n

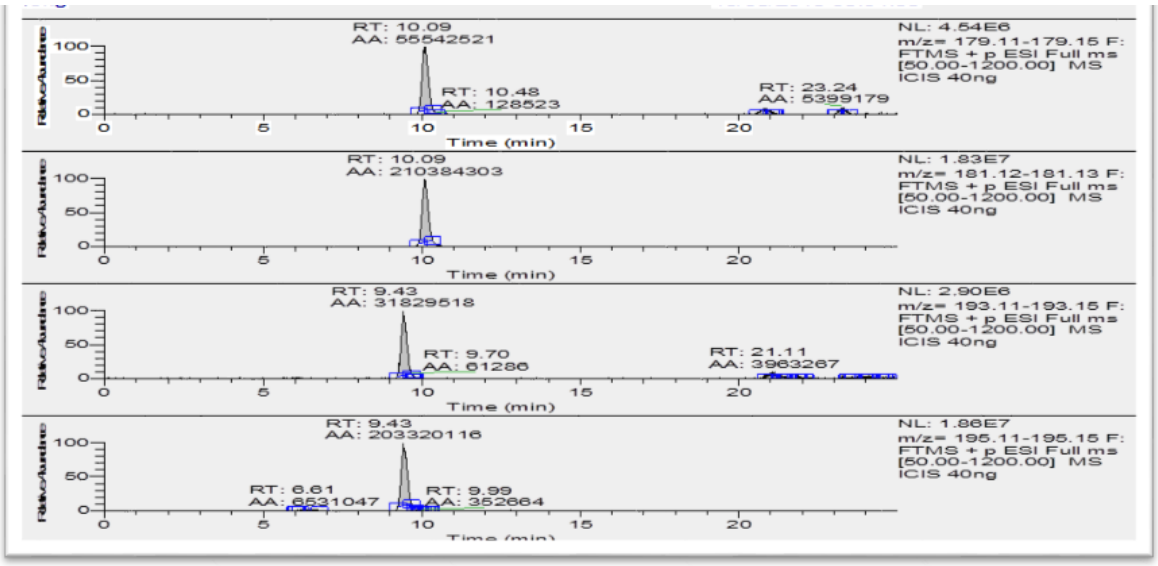
RT: 10.09
AA: 55542521
RT: 10.48
AA: 128523
RT: 23.24
AA: 5399179
NL: 4.54E6
m/z= 179.11-179.15 F:
FTMS + p ESI Full ms
[50.00-1200.00] MS
ICIS 40ng
RT: 10.09
AA: 210384303
NL: 1.83E7
m/z= 181.12-181.13 F:
FTMS + p ESI Full ms
[50.00-1200.00] MS
ICIS 40ng
RT: 9.43
AA: 31829518
RT: 9.70
AA: 61286
RT: 21.11
AA: 3983267
NL: 2.90E6
m/z= 193.11-193.15 F:
FTMS + p ESI Full ms
[50.00-1200.00] MS
ICIS 40ng
RT: 9.43
AA: 203320116
RT: 6.61
AA: 6531047
RT: 9.99
AA: 352664
NL: 1.86E7
m/z= 195.11-195.15 F:
FTMS + p ESI Full ms
[50.00-1200.00] MS
ICIS 40ng
Time (min)

80 ng

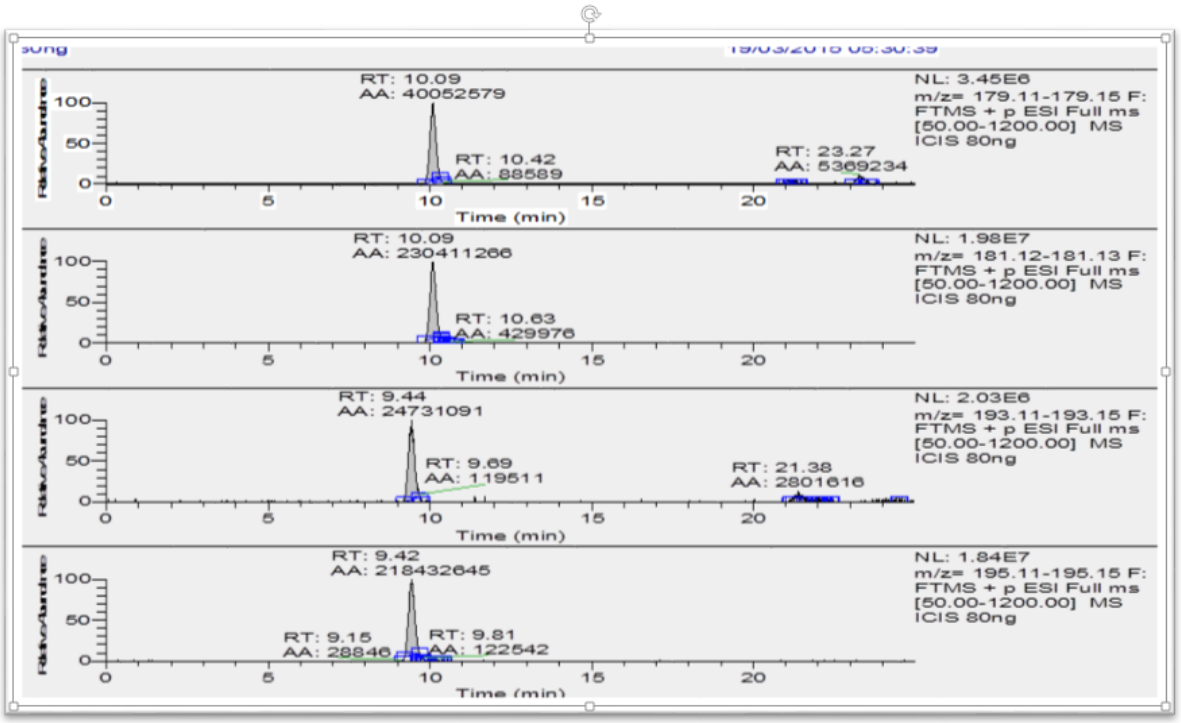
RT: 10.09
AA: 40052579
RT: 10.42
AA: 88589
RT: 23.27
AA: 5369234
NL: 3.45E6
m/z= 179.11-179.15 F:
FTMS + p ESI Full ms
[50.00-1200.00] MS
ICIS 80ng
RT: 10.09
AA: 230411266
RT: 10.63
AA: 429976
NL: 1.98E7
m/z= 181.12-181.13 F:
FTMS + p ESI Full ms
[50.00-1200.00] MS
ICIS 80ng
RT: 9.44
AA: 24731091
RT: 9.69
AA: 119511
RT: 21.38
AA: 2801616
NL: 2.03E6
m/z= 193.11-193.15 F:
FTMS + p ESI Full ms
[50.00-1200.00] MS
ICIS 80ng
RT: 9.42
AA: 218432645
RT: 9.15
AA: 28846
RT: 9.81
AA: 122542
NL: 1.84E7
m/z= 195.11-195.15 F:
FTMS + p ESI Full ms
[50.00-1200.00] MS
ICIS 80ng
Time (min)

160 ng

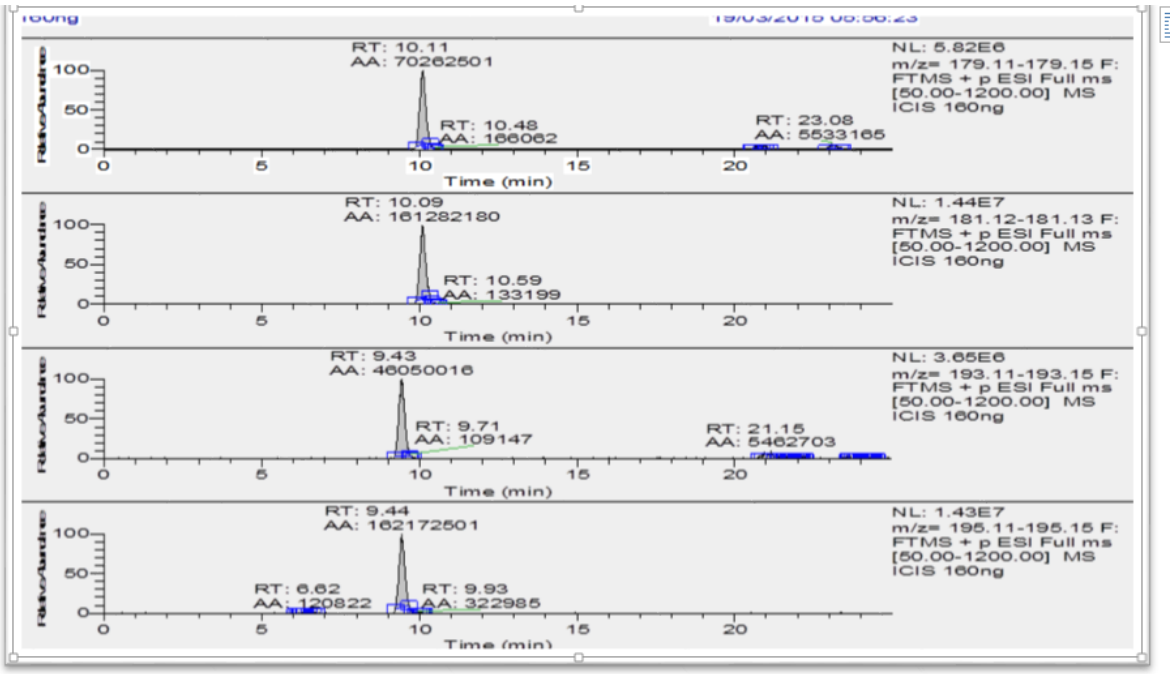
RT: 10.11
AA: 70262501
RT: 10.48
AA: 166062
RT: 23.08
AA: 5533165
NL: 5.82E6
m/z= 179.11-179.15 F:
FTMS + p ESI Full ms
[50.00-1200.00] MS
ICIS 160ng
RT: 10.09
AA: 161282180
RT: 10.59
AA: 133199
NL: 1.44E7
m/z= 181.12-181.13 F:
FTMS + p ESI Full ms
[50.00-1200.00] MS
ICIS 160ng
RT: 9.43
AA: 46050016
RT: 9.71
AA: 109147
RT: 21.15
AA: 5462703
NL: 3.65E6
m/z= 193.11-193.15 F:
FTMS + p ESI Full ms
[50.00-1200.00] MS
ICIS 160ng
RT: 9.44
AA: 162172501
RT: 6.62
AA: 120822
RT: 9.93
AA: 322985
NL: 1.43E7
m/z= 195.11-195.15 F:
FTMS + p ESI Full ms
[50.00-1200.00] MS
ICIS 160ng
Time (min)

320 ng

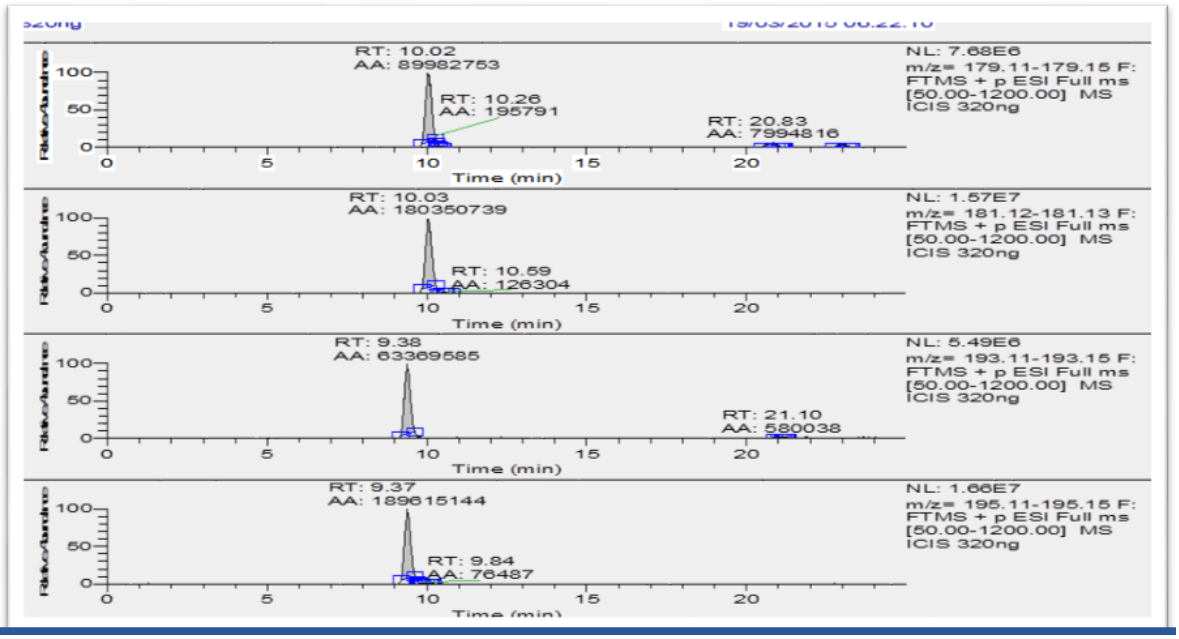
RT: 10.02
AA: 89982753
RT: 10.26
AA: 195791
RT: 20.83
AA: 7994816
NL: 7.68E6
m/z= 179.11-179.15 F:
FTMS + p ESI Full ms
[50.00-1200.00] MS
ICIS 320ng
RT: 10.03
AA: 180350739
RT: 10.59
AA: 126304
NL: 1.57E7
m/z= 181.12-181.13 F:
FTMS + p ESI Full ms
[50.00-1200.00] MS
ICIS 320ng
RT: 9.38
AA: 63369585
RT: 21.10
AA: 580038
NL: 5.49E6
m/z= 193.11-193.15 F:
FTMS + p ESI Full ms
[50.00-1200.00] MS
ICIS 320ng
RT: 9.37
AA: 189615144
RT: 9.84
AA: 76487
NL: 1.66E7
m/z= 195.11-195.15 F:
FTMS + p ESI Full ms
[50.00-1200.00] MS
ICIS 320ng
Time (min)

640 ng

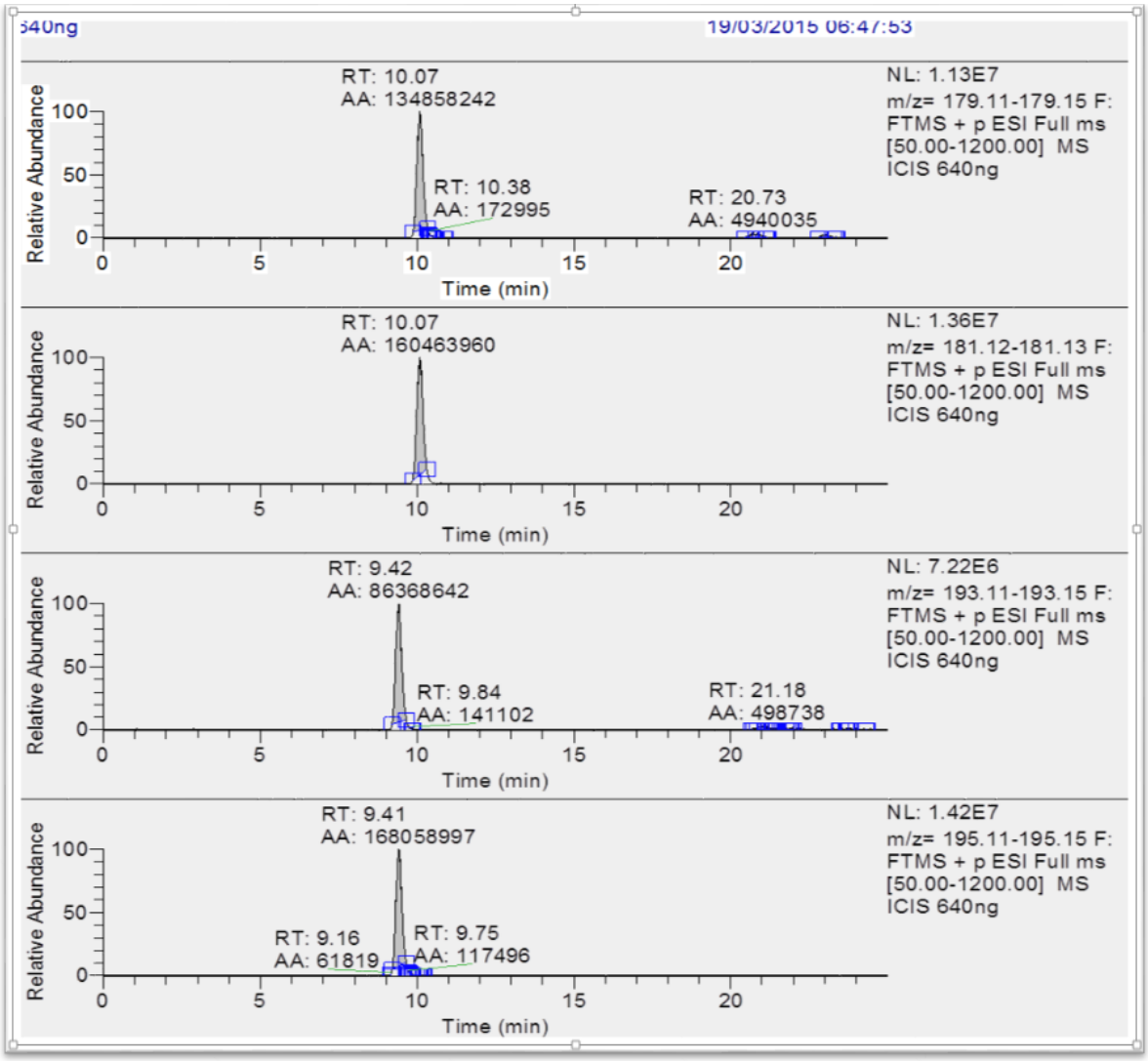
640ng
19/03/2015 06:47:53
RT: 10.07
AA: 134858242
RT: 10.38
AA: 172995
RT: 20.73
AA: 4940035
NL: 1.13E7
m/z= 179.11-179.15 F:
FTMS + p ESI Full ms
[50.00-1200.00] MS
ICIS 640ng
RT: 10.07
AA: 160463960
NL: 1.36E7
m/z= 181.12-181.13 F:
FTMS + p ESI Full ms
[50.00-1200.00] MS
ICIS 640ng
RT: 9.42
AA: 86368642
RT: 9.84
AA: 141102
RT: 21.18
AA: 498738
NL: 7.22E6
m/z= 193.11-193.15 F:
FTMS + p ESI Full ms
[50.00-1200.00] MS
ICIS 640ng
RT: 9.41
AA: 168058997
RT: 9.16
AA: 61819
RT: 9.75
AA: 117496
NL: 1.42E7
m/z= 195.11-195.15 F:
FTMS + p ESI Full ms
[50.00-1200.00] MS
ICIS 640ng
Relative Abundance
Time (min)

Appendix 2

Table A2. 1: The concentration of acetic acid in every control urine sample provided in this research depending on the calibration curve in the figure 4. 2

samples	AUP of acetic acid	AUP of I.S $^{13}C_2$ acetate	Ratio AUP acetic acid / $^{13}C_2$ acetate	Equation (Y=0.737X+0.0242)	conc µg/ml
C5	45368860	53416874	0.849	0.825	11.196
C10	97895162	60864166	1.608	1.584	21.496
C19	66278747	52078967	1.273	1.248	16.940
C25	63902421	63151413	1.012	0.988	13.402
C26	76245710	51912440	1.469	1.445	19.600
C27	47107921	53324912	0.883	0.859	11.658
C28	72969890	56627273	1.289	1.264	17.156
C34	82729308	53856075	1.536	1.512	20.514
C36	33827934	40922403	0.827	0.802	10.888
C37	32350838	42512830	0.761	0.737	9.997
C39	82245832	54735637	1.503	1.478	20.060
C43	46795435	51935701	0.901	0.877	11.897
C45	107016965	51801530	2.066	2.042	27.703
C52	60445374	49799634	1.214	1.190	16.141
C56	103156101	51461445	2.005	1.980	26.870
C57	49434381	45138537	1.095	1.071	14.531
C62	33706764	29792045	1.131	1.107	15.023

Table A2. 2: The concentration of acetic acid in each urine sample in quiescent UC cohort provided in this research depending on the calibration curve in the figure 4. 2.

samples	AUP of acetic acid	AUP of I.S $^{13}C_2$ acetate	Ratio AUP acetic acid / $^{13}C_2$ acetate	Equation (Y=0.737X+0.0242)	conc µg/ml
R2	34341449	38285738	0.89697759	0.873	11.842
R3	12661316	26268269	0.482000394	0.457	6.211
R4	41840739	22786187	1.836232582	1.812	24.586
R8	23762873	38212439	0.621862242	0.597	8.109
R12	16850228	35638741	0.472806489	0.449	6.086
R13	48306454	22252698	2.170813355	2.147	29.126
R15	29555919	36986286	0.799104809	0.775	10.514
R17	33597278	25311764	1.327338466	1.304	17.681
R18	35471247	27372865	1.29585438	1.272	17.254
R23	26137190	33457088	0.781215329	0.757	10.271
R24	41517608	38602963	1.075503142	1.051	14.264
R29	15653795	31329987	0.499642563	0.475	6.451
R31	38220363	35183083	1.086327853	1.062	14.411
R35	66547397	33771046	1.970545923	1.946	26.409
R38	26166863	35881490	0.729257982	0.705	9.566
R40	48592192	22102661	2.198477007	2.174	29.501
R41	18466094	33902071	0.544689261	0.520	7.0622
R42	37561390	27853025	1.348556934	1.324	17.969
R46	42743133	42859213	0.997291597	0.973	13.203
R48	18357129	38980070	0.470936276	0.446	6.0615
R49	39819588	22119446	1.800207293	1.776	24.097
R51	27205151	22670221	1.200039073	1.176	15.954
R53	13042903	31310069	0.416572158	0.392	5.323
R54	20200181	37825645	0.534034013	0.509	6.917

R59	161669267	43215802	3.740975743	3.716	50.431

Table A2. 3:The concentration of acetic acid in each urine sample in active UC group provided in this research depending on the calibration curve in the figure 4. 2.

samples	AUP of acetic acid	AUP of I.S $^{13}C_2$ acetate	Ratio AUP acetic acid / $^{13}C_2$ acetate	Equation (Y=0.737X+0.0242)	conc µg/ml
A9	40126958	54493167	0.736366782	0.712	9.663
A11	70603731	51430600	1.372796176	1.348	18.298
A16	35739741	43956908	0.813063125	0.789	10.703
A20	39764404	48848984	0.814027248	0.789	10.716
A21	59589341	49301939	1.208661205	1.184	16.071
A22	54539874	38238635	1.426302848	1.402	19.024
A30	45724072	43257357	1.057024173	1.032	14.013
A32	48526638	48877889	0.992813704	0.968	13.142
A47	41316806	52614147	0.785279404	0.761	10.326
A50	60660318	54888236	1.10516064	1.080	14.667
A55	60122930	54828112	1.096571226	1.072	14.550
A58	43325495	40029558	1.082337582	1.058	14.357
A60	41556799	48104293	0.863889612	0.839	11.393

Table A2. 4: The concentration of butyric acid in every control urine sample provided in this research depending on the calibration curve in the figure 4. 1.

Samples	AUP butyric acid	AUP I.S (sodium butyrate D5)	Ratio AUP butyric acid / (sodium butyrate D5)	Equation (Y=0.339X+0.0471)	Conc (µg /ml)
C5	3874177	30038149	0.128975224	0.082	2.415
C10	4435793	25259542	0.175608608	0.128	3.790
C19	3236871	15865098	0.204024646	0.157	4.629
C25	3158471	21154100	0.149307746	0.102	3.014
C26	5060048	25020594	0.202235327	0.155	4.576
C27	4158430	30907975	0.134542299	0.087	2.579
C28	3705739	21003523	0.176434163	0.129	3.815
C34	6678460	27323632	0.244420654	0.197	5.820
C36	3014669	24206413	0.124540096	0.077	2.284
C37	3217184	25858988	0.124412603	0.077	2.280
C39	4170378	16905314	0.24669036	0.199	5.887
C43	4515887	32162466	0.140408605	0.0933	2.752
C45	7517525	31639967	0.237595855	0.190	5.619
C52	3950476	21459066	0.184093567	0.136	4.041
C56	5526152	15941132	0.346659949	0.299	8.836
C57	3792975	22111903	0.17153544	0.124	3.670
C62	2420445	13084271	0.184988908	0.137	4.067

Table A2. 5: The concentration of butyric acid in each urine samplein remission UC cohort provided in this research depending on the calibration curve in the figure4. 2.

Samples	AUP butyric acid	AUP I.S (sodium butyrate D5)	Ratio AUP butyric acid / (sodium butyrate D5)	Equation (Y=0.339X+0.0471)	Conc (µg /ml)
R2	2614375	10353264	0.252516984	0.205	6.059
R3	2182773	10550831	0.206881619	0.159	4.713
R4	3509697	13899658	0.2525024	0.205	6.059
R8	3155338	14429664	0.218670234	0.171	5.061
R12	3099668	15721768	0.197157724	0.150	4.426
R13	3425576	11061333	0.309689257	0.262	7.745
R15	3195065	12929324	0.247117715	0.200	5.900
R17	4366861	17635177	0.247622182	0.200	5.915
R18	3941813	16762226	0.235160473	0.188	5.547
R23	3203784	12654554	0.253172415	0.206	6.078
R24	3758899	11805738	0.318395936	0.271	8.002
R29	2912503	14238587	0.204550002	0.157	4.644
R31	3180658	10893692	0.291972455	0.244	7.223
R35	4455022	18352006	0.242753953	0.195	5.771
R38	2201182	8195432	0.268586452	0.221	6.533
R40	4117637	11376285	0.361949178	0.314	9.287
R41	2268936	10860266	0.20892085	0.161	4.773
R42	4681260	19077232	0.245384655	0.198	5.849
R46	3137928	10589684	0.296319324	0.249	7.351
R48	2717930	13986202	0.194329383	0.147	4.343

R49	3701778	11069703	0.334406262	0.287	8.475
R51	3269834	16287579	0.200756294	0.153	4.532
R53	2650543	17582925	0.150745283	0.103	3.057
R54	2990830	14895895	0.200782162	0.153	4.533
R59	4652112	11624123	0.40021187	0.353	10.416

Table A2. 6: The concentration of butyric acid in each urine sample in active UC cohort provided in this research depending on the calibration curve in the figure4. 3.

Samples	AUP butyric acid	AUP I.S (sodium butyrate D5)	Ratio AUP butyric acid / (sodium butyrate D5)	Equation (Y=0.339X+0.0471)	Conc (µg /ml)
A9	7421382	11961360	0.620446337	0.573	16.912
A11	3912646	15743900	0.24851822	0.201	5.942
A16	4203589	33668539	0.124852136	0.077	2.294
A20	4284937	29953126	0.143054752	0.095	2.830
A21	3792206	20038304	0.189247853	0.142	4.193
A22	4410496	16556397	0.266392259	0.219	6.468
A30	2969325	15580002	0.190585662	0.143	4.232
A32	5014875	29133454	0.172134585	0.125	3.688
A47	4062143	16053432	0.253038914	0.205	6.074
A50	5632330	7282921	0.773361403	0.726	21.423
A55	5896037	32874224	0.179351367	0.132	3.901
A58	2513003	14027822	0.179144204	0.132	3.895
A60	4211540	20402054	0.206427255	0.159	4.699
A61	3808137	25348387	0.150231926	0.103	3.042

Table A2. 7: The concentration of propionic acid in every control urine sample provided in this research depending on the calibration curve in the figure 4. 6.

samples	AUP propionic acid	AUP I.S D_2 propionic acid	ratio AUP propionic acid / D_2 propionic acid	Equation (Y=1.0516X)	Conc (µg /ml)
C5	593050	21929710	0.027043221	0.025	0.257
C10	911681	24479070	0.037243286	0.035	0.354
C19	1266477	22302946	0.056785189	0.054	0.539
C25	1069591	25907388	0.041285173	0.039	0.392
C26	1230539	21431129	0.0574183	0.054	0.546
C27	806130	23133588	0.034846735	0.033	0.331
C28	1120011	25541496	0.043850642	0.041	0.416
C34	1148365	22540804	0.050946053	0.048	0.484
C36	545561	16742781	0.03258485	0.030	0.309
C37	387059	15478404	0.02500639	0.023	0.237
C39	1086557	23126939	0.046982309	0.044	0.446
C43	784842	20121430	0.039005279	0.037	0.370
C45	787184	9432225	0.083456873	0.079	0.793
C52	946084	21199697	0.044627242	0.042	0.424
C56	2199406	19382333	0.113474781	0.107	1.079
C57	789002	18706973	0.042176893	0.040	0.401
C62	344040	11695264	0.029417036	0.027	0.279

Table A2. 8: The concentration of propionic acid in each urine sample in quiescent UC cohort provided in this research depending on the calibration curve in the figure4. 6.

samples	AUP propionic acid	AUP I.S D_2 propionic acid	ratio AUP propionic acid / D_2 propionic acid	Equation (Y=1.0516X)	Conc (µg /ml)
R2	939420	11566881	0.081216362	0.077	0.772
R3	418216	9267742	0.045125986	0.042	0.429
R4	972762	9361782	0.103907782	0.098	0.988
R8	893038	11901334	0.075036798	0.071	0.713
R12	190301	10862955	0.017518346	0.016	0.166
R13	863299	11693671	0.073826175	0.070	0.702
R15	732277	11325914	0.064655003	0.061	0.614
R17	1031414	11835326	0.087147071	0.082	0.828
R18	613074	11011023	0.055678205	0.052	0.529
R23	509409	11116116	0.045826168	0.043	0.435
R24	1251212	11785565	0.106164787	0.100	1.009
R29	380277	11804799	0.032213763	0.030	0.306
R31	1200852	10312960	0.116441061	0.110	1.107
R35	1036887	10267050	0.100991716	0.096	0.960
R38	385400	10714662	0.035969403	0.034	0.342
R40	1537968	10491431	0.146592777	0.139	1.393
R41	194374	10927940	0.017786884	0.016	0.169
R42	1268198	11081008	0.114447891	0.108	1.088
R46	1142889	11100129	0.102961776	0.097	0.979
R48	178352	10069953	0.017711304	0.016	0.168

R49	1525540	11198366	0.136228803	0.129	1.295
R51	481720	11115370	0.043338188	0.041	0.412
R53	224066	10547360	0.021243799	0.020	0.202
R54	0	11421872	0	0	0
R59	576258	11504966	0.050087762	0.047	0.476

Table A2. 9: Display the quantification by determining the concentration of propionic acid in each urine sample in active UC cohort provided in this research depending on the calibration curve in the figure4. 6.

samples	AUP propionic acid	AUP I.S D_2 propionic acid	ratio AUP propionic acid / D_2 propionic acid	Equation (Y=1.0516X)	Conc (µg /ml)
A9	1979870	24017637	0.082434005	0.078	0.783
A11	1698928	18318636	0.09274315	0.08	0.881
A16	422201	19387117	0.0217774	0.020	0.207
A20	537322	19212132	0.027967849	0.026	0.265
A21	1327533	19361770	0.068564651	0.065	0.652
A22	1025961	17625694	0.058208261	0.055	0.553
A30	763007	16598859	0.045967437	0.043	0.437
A32	719430	19653257	0.036606146	0.034	0.348
A47	862968	13711097	0.062939384	0.059	0.598
A50	1432517	17426900	0.082201482	0.078	0.781
A55	1078548	25079859	0.043004548	0.040	0.408
A58	990824	15530883	0.063797017	0.060	0.606
A60	696039	13214560	0.052672128	0.050	0.500
A61	443658	15328703	0.028942958	0.027	0.275

Table A2. 10: The concentration of Lactic acid in every control urine sample provided in this research depending on the calibration curve in the figure4. 4.

samples	A UP of Lactic acid	AUP of I.S $^{13}C_3$ Sodium lactate	Ratio AUP Lactic acid/$^{13}C_3$ Sodium lactate	Equation (Y=1.7691x)	Conc (µg /ml)
C5	1999331	17607737	0.113548436	0.064	0.641
C10	8833799	23008435	0.383937413	0.217	2.170
C19	21639617	21669297	0.99863032	0.564	5.644
C25	3272469	15267926	0.214336184	0.121	1.211
C26	7260506	10878039	0.667446219	0.377	3.772
C27	6213452	9615566	0.646186818	0.365	3.652
C28	2608220	14155138	0.184259595	0.104	1.041
C34	2309721	16017792	0.144197215	0.081	0.815
C36	685543	6643809	0.103185236	0.058	0.583
C37	854322	8191185	0.10429773	0.058	0.589
C39	17231315	19154788	0.899582653	0.508	5.084
C43	1500823	16824583	0.089204172	0.050	0.504
C45	15300460	18163997	0.842350943	0.476	4.761
C52	13153092	16041014	0.819966369	0.463	4.634
C56	27593014	21905283	1.259651108	0.7120	7.120
C57	1057411	10745580	0.098404274	0.056	0.556
C62	1025523	10764608	0.09526803	0.054	0.538

Table A2. 11: The concentration of Lactic acid in every remission UC urine sample provided in this research depending on the calibration curve in the figure4. 5.

samples	A UP of Lactic acid	AUP of I.S $^{13}C_3$ Sodium lactate	Ratio AUP Lactic acid/$^{13}C_3$ Sodium lactate	Equation (Y=1.7691x)	Conc (µg /ml)
R2	2610460	32128270	0.081251185	0.045	0.459
R3	3553074	30581461	0.116183919	0.065	0.656
R4	8868767	35522970	0.24966288	0.141	1.411
R8	5786841	31446871	0.184019612	0.104	1.040
R12	6216654	32042165	0.194014793	0.109	1.096
R13	9450229	32938024	0.286909409	0.162	1.621
R15	5030291	31455907	0.159915624	0.090	0.903
R17	6732722	44337692	0.15185098	0.085	0.858
R18	2915505	40520896	0.071950655	0.040	0.406
R23	5092798	34020449	0.149698142	0.084	0.846
R24	1080880	28633052	0.037749381	0.021	0.213
R29	8142332	35793737	0.227479237	0.128	1.285
R31	4206613	30940813	0.13595677	0.076	0.768
R35	373137051	21526582	17.33378067	9.798	97.980
R38	11276602	33201452	0.339641833	0.192	1.919
R40	11220673	33958737	0.330420799	0.186	1.867
R41	18434322	37193206	0.495636811	0.280	2.801
R42	12572453	38973447	0.322590224	0.182	1.823
R46	11254487	30491910	0.369097475	0.208	2.086

R48	11237821	32289598	0.348032236	0.196	1.967
R49	1372680	27007665	0.050825571	0.028	0.287
R51	1366431	40463726	0.033769283	0.019	0.190
R53	0	27937217	0	0	0
R54	0	35979381	0	0	0
R59	32048618	33683357	0.951467456	0.537	5.378

Table A2. 12: The concentration of Lactic acid in every active UC urine sample provided in this research depending on the calibration curve in the figure4. 6.

samples	A UP of Lactic acid	AUP of I.S $^{13}C_3$ Sodium lactate	Ratio AUP Lactic acid/$^{13}C_3$ Sodium lactate	Equation (Y=1.7691x)	Conc (µg /ml)
A9	20094812	10631334	1.890149628	1.068	10.684
A11	11342710	11327916	1.001305977	0.566	5.659
A16	12410186	6103095	2.033425008	1.149	11.494
A20	12559872	9089300	1.381830504	0.781	7.810
A21	15443477	9603015	1.608190449	0.909	9.090
A22	15979329	9747418	1.639339669	0.926	9.266
A30	15129891	7948222	1.90355667	1.076	10.760
A32	55234522	13098713	4.216790001	2.383	23.835
A47	2906123	8127843	0.357551567	0.202	2.021
A50	3345623	9974615	0.335413748	0.189	1.895
A55	8126983	10396504	0.781703446	0.441	4.418
A58	7743863	9566938	0.809440074	0.457	4.575
A60	5236780	7075540	0.740124429	0.418	4.183
A61	5636813	9377140	0.601122837	0.339	3.397

Results obtained for the spectrophotometric determination of creatinine in urine samples.

Table A2. 13: Show the optical density of each urine sample, standard and blank on plate no 1 and read at 490nm.

	1	2	3	4	5	6	7	8	9	10	11
A	0.8929	0.2232	0.4362	0.2204	0.3151	0.916	0.2815	0.6739	0.1972	1.9349	0.1722
B	0.5737	0.497	0.1994	0.4913	0.2429	0.5829	0.2309	0.6266	0.8982	1.0936	0.1794
C	0.2886	0.7503	0.5467	0.7794	0.2205	0.6627	0.1904	0.5405	0.6913	0.6438	0.1822
D	0.4167	0.6914	0.5933	0.4199	0.2578	0.1944	0.2022	0.5515	0.5215	0.4221	0.179
E	0.2892	0.2335	0.206	1.3162	0.917	0.5876	0.221	0.5526	1.591	0.2967	0.1821
F	0.2375	0.4133	0.1913	0.2198	0.513	0.7856	0.9155	1.1798	0.9366	0.247	0.1782
G	0.2712	0.2129	0.5081	0.2158	----------	----------	----------	----------	----------	0.2095	0.18

Table A2. 14: Show the optical density of each urine sample, standard and blank on plate no 2 and read at 490nm.

	1	2	3	4	5	6	7	8	9	10	11
A	0.905	0.2356	0.4583	0.2455	0.337	0.6509	0.3019	0.6851	0.2066	1.9025	0.1933
B	0.5518	0.4834	0.2027	0.5211	0.2452	0.6337	0.2355	0.5868	0.9375	1.1055	0.1852
C	0.2983	0.7655	0.5652	0.7039	0.2276	0.6877	0.197	0.5613	0.5754	0.5943	0.189
D	0.4311	0.7038	0.5783	0.2912	0.2632	0.1959	0.2025	0.5535	0.5911	0.4291	0.1894
E	0.3569	0.2201	0.2093	1.4317	0.9407	0.4689	0.2243	0.5709	1.5717	0.2995	0.1802
F	0.2504	0.425	0.2024	0.2237	0.5131	0.7742	0.9499	1.1478	0.972	0.2463	0.1908
G	0.2693	0.2057	0.5099	0.2104	---------	---------	---------	---------	----------	0.2113	0.1789

Table A2. 15: Show the amount of creatinine in (mg/dl) and in (mmol/L) in the control urine samples.

Sample	Plate(1)	Plate(2)	sum	Average	Equation(Y=0.0869X +0.1954)	Conc mg/dl	Conc in mmol/L
C5	0.2204	0.2455	0.4659	0.23295	0.03755	0.432105869	0.038
C10	0.2815	0.3019	0.5834	0.2917	0.0963	1.108170311	0.098
C19	0.5829	0.6337	1.2166	0.6083	0.4129	4.751438435	0.42
C25	0.5467	0.5652	1.1119	0.55595	0.36055	4.149021864	0.366
C26	0.7794	0.7039	1.4833	0.74165	0.54625	6.285960875	0.555
C27	0.2205	0.2276	0.4481	0.22405	0.02865	0.329689298	0.029
C28	0.6627	0.6877	1.3504	0.6752	0.4798	5.521288838	0.489
C34	0.5933	0.5783	1.1716	0.5858	0.3904	4.492520138	0.379
C36	0.2578	0.2632	0.521	0.2605	0.0651	0.749136939	0.066
C37	0.2944	0.2959	0.5903	0.29515	0.09975	1.147871116	0.101
C39	0.5515	0.5535	1.105	0.5525	0.3571	4.109321059	0.363
C43	0.206	0.2093	0.4153	0.20765	0.01225	0.140966628	0.012
C45	1.3162	1.4317	2.7479	1.37395	1.17855	13.56214039	1.199
C52	0.4133	0.425	0.8383	0.41915	0.22375	2.574798619	0.228
C56	0.7856	0.7742	1.5598	0.7799	0.5845	6.726121979	0.595
C57	0.9155	0.9499	1.8654	0.9327	0.7373	8.484464902	0.75
C62	0.5081	0.5099	1.018	0.509	0.3136	3.608745685	0.319

Table A2. 16: Show the amount of creatinine in (mg/dl) and in (mmol/L) in the quiescent UC urine samples.

Sample	Plate(1)	Plate(2)	sum	Average	Equation(Y=0.0869X +0.1954)	Conc mg/dl	Conc in mmol/L
R3	0.2232	0.2356	0.4588	0.2294	0.034	0.391254315	0.035
R4	0.4362	0.4583	0.8945	0.44725	0.25185	2.898158803	0.256

R8	0.3151	0.337	0.6521	0.32605	0.13065	1.503452244	0.133
R12	0.1972	0.2066	0.4038	0.2019	0.0065	0.074798619	0.007
R13	0.5737	0.5518	1.1255	0.56275	0.36735	4.227272727	0.374
R15	0.497	0.4834	0.9804	0.4902	0.2948	3.392405063	0.3
R17	0.4913	0.5211	1.0124	0.5062	0.3108	3.576524741	0.316
R18	0.2429	0.2452	0.4881	0.24405	0.04865	0.559838895	0.049
R23	0.2886	0.2983	0.5869	0.29345	0.09805	1.1283084	0.1
R24	0.7503	0.7655	1.5158	0.7579	0.5625	6.472957422	0.572
R29	0.2904	0.297	0.5874	0.2937	0.0983	1.13118527	0.1
R31	0.6913	0.5754	1.2667	0.63335	0.43795	5.039700806	0.446
R35	0.4199	0.2912	0.7111	0.35555	0.16015	1.8429229	0.163
R38	0.2022	0.2025	0.4047	0.20235	0.00695	0.079976985	0.007
R40	0.5215	0.5911	1.1126	0.5563	0.3609	4.153049482	0.367
R41	0.2892	0.3569	0.6461	0.32305	0.12765	1.468929804	0.13
R42	0.2335	0.2201	0.4536	0.2268	0.0314	0.361334868	0.032
R46	0.917	0.9407	1.8577	0.92885	0.73345	8.440161105	0.746
R48	0.221	0.2243	0.4453	0.22265	0.02725	0.313578826	0.028
R49	0.5526	0.5709	1.1235	0.56175	0.36635	4.215765247	0.373
R51	0.2375	0.2504	0.4879	0.24395	0.04855	0.558688147	0.049
R53	0.1913	0.2024	0.3937	0.19685	0.00145	0.016685846	0.001
R54	0.2198	0.2237	0.4435	0.22175	0.02635	0.303222094	0.027
R59	0.9366	0.972	1.9086	0.9543	0.7589	8.733026467	0.772

Table A2. 17: Show the concentration of creatinine in (mg/dl) and in (mmol/L) in the active UC urine samples.

Sample	Plate(1)	Plate(2)	sum	Average	Equation(Y=0.0869X +0.1954)	Conc mg/dl	Conc in mmol/L
A9	0.916	0.6509	1.5669	0.78345	0.58805	6.766973533	0.598
A11	0.6739	0.6851	1.359	0.6795	0.4841	5.570771001	0.492
A16	0.1994	0.2027	0.4021	0.20105	0.00565	0.065017261	0.006
A20	0.2309	0.2355	0.4664	0.2332	0.0378	0.434982739	0.038
A21	0.6266	0.5868	1.2134	0.6067	0.4113	4.733026467	0.418
A22	0.8982	0.9375	1.8357	0.91785	0.72245	8.313578826	0.735
A30	0.5405	0.5613	1.1018	0.5509	0.3555	4.090909091	0.362
A32	0.4167	0.4311	0.8478	0.4239	0.2285	2.629459148	0.232
A47	0.5876	0.4689	1.0565	0.52825	0.33285	3.830264672	0.339
A50	1.591	1.5717	3.1627	1.58135	1.38595	15.94879171	1.41
A55	0.513	0.5131	1.0261	0.51305	0.31765	3.655350978	0.323
A58	1.1798	1.1478	2.3276	1.1638	0.9684	11.1438435	0.985
A60	0.2712	0.2693	0.5405	0.27025	0.07485	0.861334868	0.076
A61	0.2129	0.2057	0.4186	0.2093	0.0139	0.15995397	0.014

Appendix 3

Glucose, mannose, fructose and Galactose in urine samples

Table A3. 1 : The concentrations of glucose in every control urine sample provided in this research depending on the calibration curve in the figure 5. 5.

Urine samples	AUP of glucose	AUP of I.S $^{13}C_6$ D-glucose	Ratio AUP of glucose / $^{13}C_6$D-glucose	Equation (Y=0.9341x)	Concentration (µg/ml)
C5	4722273	51374318	0.092	0.098	3.280
C10	75052	47254478	0.002	0.002	0.057
C19	4242750	46766582	0.091	0.097	3.237
C25	427499	34117894	0.013	0.013	0.447
C26	1296129	35207294	0.037	0.039	1.314
C27	0	36804748	0.000	0.000	0.000
C28	252781	37189251	0.007	0.007	0.243
C34	951064	39225469	0.024	0.026	0.865
C36	278708	35350054	0.008	0.008	0.281
C37	52965	34320639	0.002	0.002	0.055
C39	185758	34164214	0.005	0.006	0.194
C43	0	39062672	0.000	0.000	0.000
C45	1668326	36094139	0.046	0.049	1.649
C52	0	37070662	0.000	0.000	0.000
C57	613178	37574845	0.016	0.017	0.582
C62	57977	37073121	0.002	0.002	0.056

Table A3. 2: The concentrations of glucose in each urine sample in quiescent UC cohort provided in this research depending on the calibration curve in the figure 5. 5.

Urine samples	AUP of glucose	AUP of I.S $^{13}C_6$ D-glucose	Ratio AUP of glucose /$^{13}C_6$D-glucose	Equation (Y=0.9341x)	Concentration (µg/ml)
R3	11335196	50748819	0.223	0.239	7.971
R4	34216703	40116493	0.853	0.913	30.437
R8	20855279	44642370	0.467	0.500	16.671

R12	2684154	41206496	0.065	0.070	2.324
R13	44904390	43422403	1.034	1.107	36.903
R15	28684560	44372881	0.646	0.692	23.068
R17	38381222	48018756	0.799	0.856	28.523
R18	11985582	34499266	0.347	0.372	12.398
R23	17530622	38155143	0.459	0.492	16.396
R24	49656419	51218100	0.970	1.038	34.597
R29	0	36500447	0.000	0.000	0.000
R31	44061205	47551501	0.927	0.992	33.066
R35	12064	44630115	0.000	0.000	0.010
R38	3201226	52129038	0.061	0.066	2.191
R40	193832746	53494514	3.623	3.879	129.301
R41	22209585	47036051	0.472	0.505	16.850
R42	37155946	51273896	0.725	0.776	25.859
R46	50788953	34103903	1.489	1.594	53.144
R48	5923959	51774961	0.114	0.122	4.083
R49	53391552	45034618	1.186	1.269	42.307
R51	15108842	49657781	0.304	0.326	10.857
R53	893252	44678673	0.020	0.021	0.713
R54	5349281	50777408	0.105	0.113	3.759
R59	23073063	56004110	0.412	0.441	14.702

Table A3. 3: The concentration of glucose in each urine sample in active UC group provided in this research depending on the calibration curve in the figure 5. 5.

Urine samples	AUP of glucose	AUP of I.S $^{13}C_6$ D-glucose	Ratio AUP of glucose /$^{13}C_6$D-glucose	Equation (Y=0.9341x)	Concentration (µg/ml)
A21	6204595	44711420	0.139	0.149	4.952
A22	27276338	38083160	0.716	0.767	25.559
A30	8084641	37535994	0.215	0.231	7.686
A32	17484049	39705803	0.440	0.471	15.714
A47	5228900	40568364	0.129	0.138	4.599
A50	50761059	39156161	1.296	1.388	46.261
A58	11079285	54091341	0.205	0.219	7.309

Table A3. 4: The concentration of Fructose in each urine sample in control group provided in this research depending on the calibration curve in the figure 5. 7.

Urine samples	AUP of Fructose	AUP of I.S $^{13}C_6$ D-glucose	Ratio AUP Fructose/ $^{13}C_6$ D-glucose	Equation (Y=0.0766x)	Concentration (µg/ml)

C5	0	51374318	0	0	0
C10	0	47254478	0	0	0
C19	688745	46766582	0.014	0.192	6.408
C25	364951	34117894	0.010	0.139	4.654
C26	1927295	35207294	0.054	0.715	23.821
C27	0	36804748	0	0	0
C28	108155	37189251	0.003	0.038	1.265
C34	178089	39225469	0.004	0.059	1.975
C36	192335	35350054	0.005	0.071	2.367
C37	0	34320639	0	0	0
C39	0	34164214	0	0	0
C43	0	39062672	0	0	0
C45	1910628	36094139	0.053	0.691	23.035
C52	0	37070662	0	0	0
C56	405333	37145464	0.011	0.142	4.748
C57	88997	37574845	0.002	0.030	1.030
C62	58541	37073121	0.002	0.020	0.687

Table A3. 5: The concentration of Fructose in each urine sample in quiescent UC cohort provided in this research depending on the calibration curve in the figure 5. 7.

Urine samples	AUP of Fructose	AUP of I.S $^{13}C_6$ D-glucose	Ratio AUP Fructose/ $^{13}C_6$D-glucose	Equation (Y=0.0766x)	Concentration (µg/ml)
R2	2200851	40079303	0.054	0.717	23.895
R3	344032	50748819	0.006	0.088	2.950
R4	435819	40116493	0.011	0.141	4.727
R8	788182	44642370	0.017	0.230	7.682
R12	153225	41206496	0.003	0.048	1.618
R13	251470	43422403	0.005	0.075	2.520
R15	2975590	44372881	0.067	0.875	29.181
R17	959498	48018756	0.019	0.260	8.695
R18	1771463	34499266	0.051	0.670	22.345
R23	0	38155143	0	0	0
R24	565786	51218100	0.011	0.144	4.807
R29	0	36500447	0	0	0
R31	35544	47551501	0.001	0.009	0.325
R35	0	44630115	0	0	0
R38	0	52129038	0	0	0
R40	1153466	53494514	0.021	0.281	9.383
R41	263735	47036051	0.005	0.073	2.439
R42	690950	51273896	0.013	0.175	5.864

R46	906197	34103903	0.026	0.346	11.562
R48	247948	51774961	0.004	0.062	2.083
R49	212041	45034618	0.004	0.061	2.048
R51	315094	49657781	0.006	0.082	2.761
R53	0	44678673	0	0	0
R54	130770	50777408	0.002	0.033	1.120
R59	117989	56004110	0.002	0.027	0.916

Table A3. 6: The concentration of Fructose in each urine sample in Active UC cohort provided in this research depending on the calibration curve in the figure 5. 7.

Urine samples	AUP of Fructose	AUP of I.S $^{13}C_6$ D-glucose	Ratio AUP Fructose/ $^{13}C_6$D-glucose	Equation (Y=0.0766x)	Concentration (µg/ml)
A9	358434	53792908	0.006	0.086	2.899
A11	8597041	42765669	0.201	2.624	87.478
A16	1440770	40808920	0.035	0.461	15.363
A20	167696	41556991	0.004	0.052	1.756
A21	56777463	44711420	1.269	16.577	552.595
A22	35039009	38083160	0.920	12.011	400.376
A30	52086883	37535994	1.387	18.115	603.851
A32	18851905	39705803	0.474	6.198	206.609
A47	24130985	40568364	0.594	7.765	258.843
A50	206156456	39156161	5.264	68.73	2291.114
A55	52831519	39155606	1.349	17.614	587.150
A58	86514674	54091341	1.599	20.880	696.005
A60	18769595	42710083	0.439	5.737	191.238
A61	2887246	44520059	0.065	0.846	28.221

Table A3. 7: The concentration of Mannose in each urine samplein control group provided in this research depending on the calibration curve in the figure 5. 9.

Urine samples	A UP of Mannose	AUP of I.S $^{13}C_6$ D-glucose	Ratio AUP Mannose /AUP $^{13}C_6$ D-glucose	Equation (Y=1.526x)	Concentration (µg/ml)
C5	891285	51374318	0.017	0.0113	0.378
C10	1819252	47254478	0.038	0.025	0.840
C27	102936	36804748	0.002	0.001	0.061
C28	313604	37189251	0.008	0.005	0.184
C36	961103	35350054	0.027	0.017	0.593
C39	1943606	34164214	0.056	0.037	1.242
C43	397665	39062672	0.010	0.006	0.222

C52	3135762	37070662	0.085	0.055	1.847
C56	4857748	37145464	0.130	0.085	2.856
C57	1103666	37574845	0.029	0.019	0.641
C62	3400379	37073121	0.091	0.060	2.004

Table A3. 8: The concentration of Mannose in each urine sample in quiescent UC cohort provided in this research depending on the calibration curve in the figure 5. 9.

Urine samples	A UP of Mannose	AUP of I.S $^{13}C_6$ D-glucose	Ratio AUP Mannose /AUP $^{13}C_6$ D-glucose	Equation (Y=1.526x)	Concentration (µg/ml)
R2	4788145	40079303	0.119	0.078	2.609
R3	50182	50748819	0.000	0.001	0.021
R4	9164865	40116493	0.228	0.149	4.990
R8	1843833	44642370	0.041	0.027	0.902
R12	0	41206496	0	0	0
R13	5248756	43422403	0.120	0.079	2.640
R15	730252	44372881	0.016	0.011	0.359
R17	1248143	48018756	0.025	0.017	0.567
R18	209770	34499266	0.006	0.003	0.132
R23	400353	38155143	0.010	0.006	0.229
R24	140754	51218100	0.002	0.002	0.060
R29	24282	36500447	0.001	0.001	0.015
R31	647332	47551501	0.014	0.008	0.297
R35	0	44630115	0	0	0
R38	0	52129038	0	0	0
R40	1556200	53494514	0.029	0.019	0.635
R41	2315791	47036051	0.049	0.032	1.075
R42	426553	51273896	0.008	0.005	0.181
R46	15126225	34103903	0.444	0.290	9.688
R48	862889	51774961	0.0166	0.011	0.364
R49	2021317	45034618	0.044	0.029	0.980
R51	108900	49657781	0.002	0.002	0.047
R53	0	44678673	0	0	0
R54	112231	50777408	0.002	0.002	0.048
R59	6604589	56004110	0.117	0.077	2.576

Table A3. 9: The concentration of Mannose in each urine sample in Active UC cohort provided in this research depending on the calibration curve in the figure 5. 9.

Urine samples	A UP of Mannose	AUP of I.S $^{13}C_6$	Ratio AUP	Equation	Concentration (µg/ml)

		D-glucose	Mannose /AUP $^{13}C_6$ D-glucose	(Y=1.526x)	
A11	72153	42765669	0.002	0.001	0.036
A16	149269	40808920	0.003	0.002	0.079
A20	0	41556991	0	0	0
A21	0	44711420	0	0	0
A22	0	38083160	0	0	0
A30	0	37535994	0	0	0
A32	92531	39705803	0.002	0.001	0.050
A47	0	40568364	0	0	0
A50	0	39156161	0	0	0
A55	0	39155606	0	0	0
A58	0	54091341	0	0	0
A60	0	42710083	0	0	0
A61	0	44520059	0	0	0

Table A3. 10: The concentration of Galactose in each urine sample in control group provided in this research depending on the calibration curve in the figure 5. 11.

Urine samples	A UP of Galactose	AUP of I.S $^{13}C_6$ D-glucose	Ratio AUP Galactose /AUP $^{13}C_6$ D-glucose	Equation (Y=1.0777x)	Concentration (µg/ml)
C5	0	51374318	0	0	0
C10	0	47254478	0	0	0
C19	393987	46766582	0.008	0.007	0.260
C25	787752	34117894	0.023	0.021	0.714
C26	6810403	35207294	0.193	0.179	5.983
C27	299864	36804748	0.008	0.007	0.252
C28	998178	37189251	0.026	0.024	0.830
C34	336230	39225469	0.008	0.007	0.265
C36	139202	35350054	0.004	0.004	0.121
C37	22745	34320639	0.001	0.001	0.020
C39	30297	34164214	0.001	0.001	0.027
C43	0	39062672	0	0	0
C45	4163190	36094139	0.115	0.107	3.567
C52	80592	37070662	0.002	0.002	0.067
C56	275697	37145464	0.007422091	0.006886973	0.229
C57	368663	37574845	0.009811431	0.009104047	0.303
C62	247522	37073121	0.006676589	0.006195221	0.206

Table A3. 11: The concentration of Galactose in each urine sample in quiescent UC cohort provided in this research depending on the calibration curve in the figure 5. 11.

Urine samples	A UP of Galactose	AUP of I.S $^{13}C_6$ D-glucose	Ratio AUP Galactose /AUP $^{13}C_6$ D-glucose	Equation (Y=1.0777x)	Concentration (µg/ml)
R2	531841	40079303	0.013	0.0123	0.410
R3	983830	50748819	0.019	0.017	0.599
R4	1414640	40116493	0.035	0.032	1.090
R8	57217	44642370	0.001	0.001	0.039
R12	693032	41206496	0.016	0.015	0.520
R13	330600	43422403	0.007	0.007	0.235
R15	2803208	44372881	0.063	0.058	1.953
R18	1406850	34499266	0.040	0.037	1.261
R23	1232793	38155143	0.032	0.029	0.999
R24	4584684	51218100	0.089	0.083	2.768
R29	53703	36500447	0.001	0.002	0.045
R31	12026878	47551501	0.252	0.234	7.822
R35	0	44630115	0	0	0
R38	379795	52129038	0.007	0.006	0.225
R40	32002497	53494514	0.598	0.555	18.503
R41	1337273	47036051	0.028	0.026	0.879
R42	207957	51273896	0.004	0.003	0.125
R46	157607	34103903	0.004	0.004	0.142
R48	0	51774961	0	0	0
R49	0	45034618	0	0	0
R51	176015	49657781	0.003	0.003	0.109
R53	0	44678673	0	0	0
R54	28992	50777408	0.001	0.001	0.017
R59	580974	56004110	0.010	0.009	0.320

Table A3. 12: The concentration of Galactose in each urine sample in Active UC cohort provided in this research depending on the calibration curve in the figure 5. 11.

Urine samples	A UP of Galactose	AUP of I.S $^{13}C_6$ D-glucose	Ratio AUP of Galactose /AUP $^{13}C_6$ D-glucose	Equation (Y=1.0777x)	Concentration (µg/ml)
A9	5257020	53792908	0.09	0.090	3.022
A11	39074196	42765669	0.913	0.847	28.260
A20	596147	41556991	0.014	0.013	0.443
A21	1966215	44711420	0.043	0.040	1.360
A22	4751494	38083160	0.124	0.115	3.859
A32	6350492	39705803	0.159	0.148	4.946
A47	14516509	40568364	0.357	0.332	11.067

A50	16508129	39156161	0.421	0.391	13.040
A55	9106135	39155606	0.232	0.215	7.193
A60	12232585	42710083	0.286	0.265	8.858
A61	1665319	44520059	0.037	0.034	1.156

Glucose, mannose, fructose and Galactose in Saliva samples

Table A3. 13: The concentration of glucose in every control Saliva sample provided in this research depending on the calibration curve in the figure 5. 5.

Saliva samples	AUP of glucose	AUP of I.S $^{13}C_6$ D-glucose	Ratio AUP of glucose/$^{13}C_6$ D-glucose	Equation (Y=0.9341x)	Concentration (µg/ml)
C5	74263291	8855106	8.386	8.978	299.271
C10	3453970	8686100	0.397	0.425	14.189
C16	11048070	8195405	1.348	1.443	48.106
C18	5370748	7198752	0.746	0.798	26.623
C20	1999129	8262388	0.241	0.259	8.634
C22	337072197	10375083	32.48	34.780	1159.355
C23	1001949	7029400	0.142	0.152	5.086
C30	498964	6496252	0.076	0.082	2.740
C33	202866	8266320	0.024	0.026	0.875
C34	1940505	8144330	0.238	0.255	8.502
C36	128412	8850357	0.014	0.015	0.517
C42	32194447	6267624	5.136	5.499	183.300
C49	8938969	7757502	1.152	1.233	41.119
C50	14987363	8854045	1.692	1.812	60.404
C55	912430	7578248	0.120	0.128	4.296
C58	138761658	6403183	21.67	23.199	773.319
C60	18907	6426269	0.002	0.003	0.104
C61	5198710	8267357	0.628	0.673	22.439
C62	440356996	14806601	29.740	31.838	1061.292
C64	5157319	8172287	0.631	0.675	22.519

Table A3. 14: The concentration of glucose in each Saliva sample in quiescent UC cohort provided in this research depending on the calibration curve in the figure 5. 5.

Saliva samples	AUP of glucose	AUP of I.S $^{13}C_6$ D-glucose	Ratio AUP of glucose/$^{13}C_6$ D-glucose	Equation (Y=0.9341x)	Concentration (µg/ml)
R1	174747	9336000	0.018	0.020	0.667

R3	21794313	10642582	2.047	2.192	73.077
R9	13445927	12986383	1.035	1.108	36.947
R12	6096346	13936432	0.437	0.468	15.610
R13	7851867	14176754	0.553	0.592	19.764
R15	0	13204254	0	0	0
R17	554326	10931201	0.050	0.054	1.809
R24	513917	11034331	0.046	0.049	1.662
R25	13252716	14194301	0.933	0.999	33.317
R28	7526490	15942776	0.472	0.505	16.846
R29	4939209	13456985	0.367	0.392	13.097
R31	1212132	14429474	0.084	0.089	2.997
R32	12203098	14361046	0.849	0.909	30.322
R35	227337	5802827	0.039	0.042	1.398
R38	287501	11388814	0.025	0.027	0.900
R39	158085	8920029	0.017	0.019	0.632
R40	0	8583380	0	0	0
R44	5847388	7687092	0.760	0.814	27.144
R46	880718	7339912	0.119	0.128	4.281
R48	783426	7123395	0.109	0.117	3.924
R51	2698528	7826591	0.344	0.369	12.303
R52	0	7680091	0	0	0
R56	784773	9100458	0.086	0.092	3.077
R57	58556	8837986	0.006	0.008	0.236
R63	89335	6976589	0.012	0.013	0.456

Table A3. 15: The concentration of glucose in each Saliva sample in Active UC cohort provided in this research depending on the calibration curve in the figure 5. 5.

Saliva samples	AUP of glucose	AUP of I.S $^{13}C_6$ D-glucose	Ratio AUP of glucose/$^{13}C_6$ D-glucose	Equation (Y=0.9341x)	Concentration (µg/ml)
A2	208886	9585965	0.021	0.024	0.777
A4	480352	3357759	0.143	0.153	5.104
A6	19657884	13742351	1.430	1.531	51.045
A7	770143	12067553	0.063	0.068	2.277
A8	107349	10691445	0.010	0.010	0.358
A11	13593428	13499178	1.006	1.078	35.934
A14	0	12815857	0	0	0
A19	13174396	11358702	1.159	1.241	41.389
A26	40021	5045610	0.007	0.008	0.283
A27	442454	12009119	0.036	0.039	1.314
A41	7316660	12947966	0.565	0.605	20.164
A45	8257	8609898	0.001	0.001	0.034

A47	0	11885331	0	0	0
A53	11305841	13558586	0.833	0.892	29.755
A54	18776682	14567735	1.288	1.379	45.995
A59	671171	14085188	0.047	0.051	1.700
A65	292506	5158047	0.056	0.060	2.023

Table A3. 16: the concentration of Fructose in each Saliva sample in control group provided in this research depending on the calibration curve in the figure 5. 7.

Saliva samples	AUP of Fructose	AUP of I.S $^{13}C_6$ D-glucose	Ratio AUP of Fructose/ $^{13}C_6$ D-glucose	Equation (Y=0.0786X0.0011)	Concentration (µg/ml)
C5	8281825	14855106	0.557	7.278	242.605
C10	119598	8686100	0.013	0.179	5.991
C16	117336	8195405	0.014	0.186	6.230
C18	220053	8798752	0.025	0.326	10.883
C20	127983	8262388	0.015	0.202	6.740
C22	4506989	8375083	0.538	7.025	234.178
C23	49648	7029400	0.007	0.092	3.073
C33	88162	8266320	0.010	0.139	4.641
C34	79929	8144330	0.009	0.129	4.270
C42	77644	8867624	0.008	0.114	3.810
C43	56011	7757502	0.007	0.094	3.141
C55	16071	9403183	0.001	0.022	0.743
C58	1966807	6426269	0.306	3.995	133.184
C61	113159	7806601	0.014	0.189	6.307
C62	2060360	8172287	0.252	3.291	109.710
C64	42227	8172287	0.005	0.067	2.248

Table A3. 17: The concentration of Fructose in each Saliva sample in quiescent UC group provided in this research depending on the calibration curve in the figure 5. 7.

Saliva samples	AUP of Fructose	AUP of I.S $^{13}C_6$ D-glucose	Ratio AUP of Fructose/$^{13}C_6$ D-glucose	Equation (Y=0.0786X0.0011)	Concentration (µg/ml)
R1	0	9336000	0	0	0
R9	31676	12986383	0.002	0.031	1.061
R12	0	13936432	0	0	0
R13	49113	14176754	0.003	0.045	1.507
R15	0	13204254	0	0	0
R17	32123	10931201	0.003	0.038	1.278
R24	0	11034331	0	0	0
R28	71075	15942776	0.004	0.058	1.940

R29	0	13456985	0	0	0
R31	34120	14429474	0.002	0.030	1.028
R32	0	14361046	0	0	0
R35	0	5802827	0	0	0
R38	0	11388814	0	0	0
R39	0	8920029	0	0	0
R40	0	8583380	0	0	0
R44	8626	7687092	0.002	0.015	0.488
R46	0	7339912	0	0	0
R48	0	7123395	0	0	0
R51	0	7826591	0	0	0
R52	0	7680091	0	0	0
R56	0	9100458	0	0	0
R57	0	8837986	0	0	0
R63	0	6976589	0	0	0

Table A3. 18: The concentration of Fructose in each Saliva sample in active UC cohort provided in this research depending on the calibration curve in the figure 5. 7.

Saliva samples	AUP of Fructose	AUP of I.S $^{13}C_6$ D-glucose	Ratio AUP of Fructose/ $^{13}C_6$ D-glucose	Equation (Y=0.0786X0.0011)	Concentration (µg/ml)
A2	0	9585965	0	0	0
A4	0	3357759	0	0	0
A6	99416	13742351	0.007	0.094	3.148
A7	0	12067553	0	0	0
A8	0	10691445	0	0	0
A11	436426	13499178	0.032	0.422	14.069
A14	0	12815857	0	0	0
A19	19000	11358702	0.002	0.021	0.727
A26	0	5045610	0	0	0
A27	0	12009119	0	0	0
A41	0	12947966	0	0	0
A45	0	8609898	0	0	0
A47	4994	11885331	0.001	0.005	0.183
A53	171834	13558586	0.012	0.165	5.514
A54	640622	14567735	0.044	0.574	19.136
A59	59188	14085188	0.004	0.054	1.828
A65	0	5158047	0	0	0

Table A3. 19: The concentration of Mannose in each saliva sample in control group provided in this research depending on the calibration curve in the figure 5. 9.

	A UP of		Ratio AUP	Equation	

Saliva samples	Mannose	AUP of I.S $^{13}C_6$ D-glucose	Mannose /AUP $^{13}C_6$ D-glucose	(Y=1.526x)	Concentration (µg/ml)
C5	5672556	8855106	0.640	0.419	13.993
C10	1243521	8686100	0.143	0.093	3.127
C16	2654017	8195405	0.323	0.212	7.073
C18	3156535	7198752	0.438	0.287	9.578
C20	2168220	8262388	0.262	0.171	5.732
C21	1255937	6604430	0.190	0.124	4.153
C22	2312606	10375083	0.222	0.146	4.868
C23	1063872	7029400	0.151	0.099	3.305
C30	10161246	6496252	1.564	1.025	34.168
C33	3244760	8266320	0.392	0.257	8.574
C34	13329750	8144330	1.636	1.072	35.751
C36	13417348	8850357	1.516	0.993	33.115
C37	24418572	4842797	5.043	3.304	110.140
C42	14421087	6267624	2.301	1.507	50.259
C43	1977441	7757502	0.254	0.167	5.568
C49	4570681	8854045	0.516	0.338	11.276
C50	12738471	7578248	1.680	1.101	36.717
C55	2209947	6403183	0.345	0.226	7.538
C58	954058	6426269	0.148	0.097	3.242
C60	0	8267357	0	0	0
C61	3788765	14806601	0.255	0.167	5.589
C62	6382690	8172287	0.781	0.511	17.060
C64	4342304	12872287	0.337	0.221	7.368

Table A3. 20: The concentration of Mannose in each saliva sample in quiescent UC group provided in this research depending on the calibration curve in the figure 5. 9.

Saliva samples	A UP of Mannose	AUP of I.S $^{13}C_6$ D-glucose	Ratio AUP Mannose /AUP $^{13}C_6$ D-glucose	Equation (Y=1.526x)	Concentration (µg/ml)
R1	378178	9336000	0.040	0.026	0.884
R3	856072	10642582	0.080	0.052	1.757
R9	1640343	12986383	0.126	0.082	2.759
R12	1387246	13936432	0.099	0.065	2.174
R13	3206064	14176754	0.226	0.148	4.939
R15	0	13204254	0	0	0
R17	2054540	10931201	0.187	0.123	4.105
R24	240096	11034331	0.021	0.014	0.475
R25	7184667	14194301	0.506	0.331	11.056
R28	5961139	15942776	0.374	0.245	8.167
R29	5788128	13456985	0.430	0.281	9.395

R31	105891	14429474	0.007	0.005	0.160
R32	4408544	14361046	0.306	0.201	6.705
R35	831506	5802827	0.143	0.094	3.130
R38	342450	11388814	0.030	0.019	0.656
R39	205700	8920029	0.023	0.015	0.503
R40	0	8583380	0	0	0
R44	17330076	7687092	2.254	1.477	49.245
R46	9184909	7339912	1.251	0.820	27.334
R48	392536	7123395	0.055	0.036	1.2036
R51	1600386	7826591	0.204	0.139	4.466
R52	0	7680091	0	0	0
R56	125448	9100458	0.013	0.009	0.301
R57	20384	8837986	0.002	0.002	0.050
R63	2018006	6976589	0.289	0.189	6.318

Table A3. 21: The concentration of Mannose in each saliva sample in active UC cohort provided in this research depending on the calibration curve in the figure 5. 9.

Saliva samples	A UP of Mannose	AUP of I.S $^{13}C_6$ D-glucose	Ratio AUP Mannose /AUP $^{13}C_6$ D-glucose	Equation (Y=1.526x)	Concentration (µg/ml)
A2	203435	9585965	0.021	0.013	0.463
A4	1031583	3357759	0.307	0.201	6.710
A6	9699359	13742351	0.705	0.462	15.417
A7	801946	12067553	0.066	0.043	1.451
A8	645843	10691445	0.061	0.039	1.319
A11	205364	13499178	0.015	0.009	0.332
A14	0	12815857	0	0	0
A19	3546338	11358702	0.312	0.204	6.819
A26	94593	5045610	0.018	0.012	0.409
A27	2819126	12009119	0.234	0.153	5.127
A41	10730441	12947966	0.828	0.543	18.102
A45	0	8609898	0	0	0
A47	0	11885331	0	0	0
A53	3092308	13558586	0.228	0.149	4.981
A54	0	14567735	0	0	0
A59	106553	14085188	0.007	0.004	0.165
A65	67668	5158047	0.013	0.008	0.286

Fucose, L-Rhamnose, Xylose, Ribose and Arabinose in urine samples

Table A3. 22: The concentration of Fucose in each urine sample in control UC cohort provided in this research depending on the calibration curve in the figure 5. 15.

Urine samples	AUP of Fucose	AUP of I.S $^{13}C_6$ D-glucose	Ratio of AUP Fucose /$^{13}C_6$ D-glucose	Equation (Y=1.3212x)	Concentration (µg/ml)
C5	74627	51374318	0.002	0.001	0.036
C10	0	47254478	0	0	0
C19	148723	46766582	0.003	0.002	0.081
C25	197122	34117894	0.005	0.004	0.145
C26	1317360	35207294	0.037	0.028	0.944
C27	0	36804748	0	0	0
C28	99423	37189251	0.003	0.002	0.067
C34	0	39225469	0	0	0
C36	0	35350054	0	0	0
C37	0	34320639	0	0	0
C39	0	34164214	0	0	0
C43	0	39062672	0	0	0
C45	280987	36094139	0.007	0.005	0.196
C52	0	37070662	0	0	0
C56	0	37145464	0	0	0
C57	0	37574845	0	0	0
C62	0	37073121	0	0	0

Table A3. 23: The concentration of Fucose in each urine sample in remission UC cohort provided in this research depending on the calibration curve in the figure 5. 15.

Urine samples	AUP of Fucose	AUP of I.S $^{13}C_6$ D-glucose	Ratio of AUP Fucose /$^{13}C_6$ D-glucose	Equation (Y=1.3212x)	Concentration (µg/ml)
R2	9776319	40079303	0.243	0.184	6.154
R3	4188512	50748819	0.082	0.062	2.082
R4	15411067	40116493	0.384	0.290	9.692
R8	3981441	44642370	0.089	0.067	2.250
R12	498887	41206496	0.012	0.009	0.305
R13	5971933	43422403	0.137	0.104	3.469
R15	4492071	44372881	0.101	0.076	2.554
R17	9673232	48018756	0.201	0.152	5.082
R18	1250960	34499266	0.036	0.027	0.914
R23	1668549	38155143	0.043	0.033	1.103
R24	7856686	51218100	0.153	0.116	3.870
R29	0	36500447	0	0	0
R31	5240404	47551501	0.110	0.083	2.780
R35	0	44630115	0	0	0
R38	606686	52129038	0.011	0.008	0.293
R40	129481427	53494514	2.420	1.832	61.067
R41	3184153	47036051	0.067	0.051	1.707
R42	6189207	51273896	0.120	0.091	3.045

R46	29693600	34103903	0.870	0.659	21.966
R48	2094280	51774961	0.041	0.030	1.021
R49	12606755	45034618	0.279	0.211	7.062
R51	4112195	49657781	0.082	0.062	2.089
R53	255384	44678673	0.005	0.004	0.144
R54	973297	50777408	0.019	0.014	0.483
R59	17566369	56004110	0.313	0.237	7.913

Table A3. 24: The concentration of Fucose in each urine sample in active UC cohort provided in this research depending on the calibration curve in the figure 5. 15.

Urine samples	AUP of Fucose	AUP of I.S $^{13}C_6$ D-glucose	Ratio of AUP Fucose /$^{13}C_6$ D-glucose	Equation (Y=1.3212x)	Concentration (µg/ml)
A9	4664363	53792908	0.086	0.065	2.187
A11	721682	57265669	0.012	0.009	0.317
A16	47672379	52808920	0.902	0.683	22.775
A20	461891	41556991	0.012	0.008	0.280
A21	4205041	44711420	0.094	0.071	2.372
A22	2132697	38083160	0.056	0.042	1.412
A30	867025	37535994	0.023	0.017	0.582
A32	540355	39705803	0.013	0.011	0.343
A33	679229	42245642	0.016	0.012	0.405
A47	455651	40568364	0.011	0.008	0.283
A50	74410360	39156161	1.900	1.438	47.945
A55	78115	52955606	0.001	0.002	0.037
A58	1815797	54091341	0.033	0.025	0.846
A60	269963	42710083	0.006	0.004	0.159
A61	51760	44520059	0.001	0.001	0.029
A63	0	51301735	0	0	0

Table A3. 25: The concentration of Rhamnose in each urine sample in control UC group provided in this research depending on the calibration curve in the figure 5. 17.

Urine samples	A UP of Rhamnose	AUP of I.S $^{13}C_6$ D-glucose	Ratio of AUP Rhamnose/$^{13}C_6$ D-glucose	Equation (Y=1.3286)	Concentration (µg/ml)
C5	4505302	51374318	0.087	0.066	2.200
C10	6613605	47254478	0.139	0.105	3.511
C19	23596331	46766582	0.504	0.379	12.658
C25	10567579	34117894	0.309	0.233	7.771
C26	128566016	35207294	3.651	2.748	91.617

C27	5416569	36804748	0.147	0.110	3.692
C28	8042256	37189251	0.216	0.162	5.425
C34	85416265	39225469	2.177	1.638	54.633
C36	1818495	35350054	0.051	0.038	1.290
C37	749163	34320639	0.021	0.016	0.547
C39	8209309	34164214	0.240	0.180	6.028
C43	864222	39062672	0.022	0.016	0.555
C45	41983404	36094139	1.163	0.875	29.182
C52	16908456	37070662	0.456	0.343	11.443
C56	34295099	37145464	0.923	0.694	23.163
C57	4177362	37574845	0.111	0.083	2.789
C62	7975075	37073121	0.215	0.161	5.397

Table A3. 26: The concentration of Rhamnose in each urine sample in quiescent UC group provided in this research depending on the calibration curve in the figure 5. 17.

Urine samples	A UP of Rhamnose	AUP of I.S $^{13}C_6$ D-glucose	Ratio of AUP Rhamnose/$^{13}C_6$ D-glucose	Equation (Y=1.3286)	Concentration (µg/ml)
R2	5400674	40079303	0.134	0.101	3.380
R3	714550	50748819	0.014	0.011	0.353
R4	3908731	40116493	0.097	0.073	2.444
R8	1921301	44642370	0.043	0.032	1.079
R12	703862	41206496	0.017	0.012	0.428
R13	4034645	43422403	0.092	0.069	2.331
R15	2100120	44372881	0.047	0.035	1.187
R17	4486008	48018756	0.093	0.070	2.343
R18	1273934	34499266	0.036	0.027	0.926
R23	1392251	38155143	0.036	0.027	0.915
R24	4310787	51218100	0.084	0.063	2.111
R29	160642	36500447	0.004	0.003	0.110
R31	2831455	47551501	0.059	0.044	1.493
R35	0	44630115	0	0	0
R38	281588	52129038	0.005	0.004	0.135
R40	34778154	53494514	0.650	0.489	16.31
R41	1485657	47036051	0.031	0.023	0.792
R42	2872730	51273896	0.056	0.042	1.405
R46	7622440	34103903	0.223	0.168	5.607
R48	546627	51774961	0.011	0.007	0.264
R49	3603312	45034618	0.080	0.060	2.007
R51	2075763	49657781	0.041	0.031	1.048
R53	332302	44678673	0.007	0.005	0.186
R54	685331	50777408	0.013	0.010	0.338

R59	20325481	56004110	0.362	0.273	9.105

Table A3. 27: the concentration of Rhamnose in each urine sample in Active UC group provided in this research depending on the calibration curve in the figure 5. 17.

Urine samples	A UP of Rhamnose	AUP of I.S $^{13}C_6$ D-glucose	Ratio of AUP Rhamnose/$^{13}C_6$ D-glucose	Equation (Y=1.3286)	Concentration (µg/ml)
A9	952657	53792908	0.017	0.013	0.444
A11	376649	57265669	0.006	0.004	0.165
A16	90777867	52808920	1.718	1.293	43.127
A20	56456	41556991	0.002	0.001	0.034
A21	1193136	44711420	0.026	0.020	0.669
A22	88712	38083160	0.002	0.001	0.058
A30	0	37535994	0	0	0
A32	132559	39705803	0.003	0.002	0.083
A33	0	42245642	0	0	0
A47	0	40568364	0	0	0
A50	170087571	39156161	4.343	3.269	108.982
A55	26907	52955606	0.001	0.001	0.012
A58	91071	54091341	0.001	0.001	0.042
A60	0	42710083	0	0	0
A61	0	44520059	0	0	0
A63	0	51301735	0	0	0

Table A3. 28: The concentration of Xylose in each urine sample in control UC cohort provided in this research depending on the calibration curve in the figure 5. 19.

Urine samples	A UP of Xylose	AUP of I.S $^{13}C_6$ D-glucose	Ratio of AUP Xylose/$^{13}C_6$ D-glucose	Equation (Y=1.3468x)	Concentration (µg/ml)
C5	15624569	51374318	0.304	0.225	7.527
C10	14189572	47254478	0.300	0.222	7.431
C19	10397124	46766582	0.222	0.165	5.502
C25	10623708	34117894	0.311	0.231	7.706
C26	34710359	35207294	0.985	0.732	24.400
C28	18142461	37189251	0.487	0.362	12.074
C34	30878295	39225469	0.787	0.584	19.483
C39	18653741	34164214	0.546	0.405	13.513
C45	15068205	36094139	0.417	0.309	10.332
C52	112230132	37070662	3.027	2.247	74.929

C56	170716738	37145464	4.595	3.412	113.749
C62	117429296	37073121	3.167	2.351	78.395

Table A3. 29: The concentration of Xylose in each urine sample in remission UC cohort provided in this research depending on the calibration curve in the figure 5. 19.

Urine samples	A UP of Xylose	AUP of I.S $^{13}C_6$ D-glucose	Ratio of AUP Xylose/$^{13}C_6$ D-glucose	Equation (Y=1.3468x)	Concentration (µg/ml)
R2	3847081	40079303	0.095	0.071	2.375
R3	1868618	50748819	0.036	0.027	0.911
R4	5028712	40116493	0.125	0.093	3.102
R8	6804956	44642370	0.152	0.113	3.772
R12	2067437	41206496	0.050	0.037	1.241
R13	9823621	43422403	0.226	0.167	5.599
R15	4316096	44372881	0.097	0.072	2.407
R17	5813782	48018756	0.121	0.089	2.996
R18	4974317	34499266	0.144	0.107	3.568
R23	1994083	38155143	0.052	0.038	1.293
R24	602366	51218100	0.012	0.008	0.291
R29	0	36500447	0	0	0
R31	9788718	47551501	0.205	0.152	5.094
R35	50404	44630115	0.001	0.001	0.027
R38	8973729	52129038	0.172	0.127	4.260
R40	64006150	53494514	1.196	0.888	29.613
R41	4595541	47036051	0.097	0.072	2.418
R42	8422622	51273896	0.164	0.121	4.065
R46	559482	34103903	0.0164	0.012	0.406
R48	2327057	51774961	0.044	0.033	1.112
R49	7745427	45034618	0.171	0.127	4.256
R51	4331889	49657781	0.087	0.064	2.159
R53	6533072	44678673	0.146	0.108	3.619
R54	941223	50777408	0.018	0.013	0.458
R59	889873	56004110	0.015	0.011	0.393

Table A3. 30: The concentration of Xylose in each urine sample in active UC cohort provided in this research depending on the calibration curve in the figure 5. 19.

Urine samples	A UP of Xylose	AUP of I.S $^{13}C_6$ D-glucose	Ratio of AUP Xylose/$^{13}C_6$ D-glucose	Equation (Y=1.3468x)	Concentration (µg/ml)
A9	14331951	53792908	0.266	0.197	6.594
A11	36387465	57265669	0.635	0.471	15.72
A16	637572	52808920	0.012	0.008	0.298

A20	1383115	41556991	0.03	0.024	0.823
A21	14263906	44711420	0.319	0.236	7.895
A22	10971385	38083160	0.288	0.213	7.130
A30	20830964	37535994	0.554	0.412	13.735
A32	1966413	39705803	0.049	0.036	1.225
A33	36468515	42245642	0.863	0.640	21.365
A47	0	40568364	0	0	0
A50	0	39156161	0	0	0
A55	7185037	52955606	0.135	0.100	3.358
A58	0	54091341	0	0	0
A60	8207932	42710083	0.192	0.142	4.756
A61	2509312	44520059	0.056	0.041	1.395
A63	10243508	51301735	0.199	0.148	4.941

Table A3. 31: The concentration of Ribose in each urine sample in control UC cohort provided in this research depending on the calibration curve in the figure 5. 21.

Urine samples	A UP of Ribose	AUP of I.S $^{13}C_6$ D-glucose	Ratio of AUP Ribose/$^{13}C_6$ D-glucose	Equation (Y=2.7697x)	Concentration (µg/ml)
C5	105167	51374318	0.002	0.001	0.024
C10	145524	47254478	0.003	0.001	0.037
C19	171756	46766582	0.003	0.001	0.044
C25	195179	34117894	0.005	0.002	0.068
C26	0	35207294	0	0	0
C27	0	36804748	0	0	0
C28	90061	37189251	0.002	0.001	0.029
C34	49071	39225469	0.001	0.001	0.015
C36	0	35350054	0	0	0
C37	0	34320639	0	0	0
C39	0	34164214	0	0	0
C43	35934	39062672	0.001	0.001	0.011
C45	0	36094139	0	0	0
C52	0	37070662	0	0	0
C57	25689	37574845	0.001	0.001	0.008
C62	93784	37073121	0.002	0.001	0.030

Table A3. 32: The concentration of Ribose in each urine sample in remission UC cohort provided in this research depending on the calibration curve in the figure 5. 21.

Urine samples	A UP of Ribose	AUP of I.S $^{13}C_6$ D-glucose	Ratio of AUP Ribose/$^{13}C_6$ D-glucose	Equation (Y=2.7697x)	Concentration (µg/ml)

R2	25273678	40079303	0.630	0.227	7.589
R3	5781980	50748819	0.113	0.041	1.371
R4	37178257	40116493	0.926	0.334	11.153
R8	11540396	44642370	0.258	0.093	3.111
R12	2645179	41206496	0.064	0.023	0.772
R13	31676385	43422403	0.729	0.263	8.779
R15	36495508	44372881	0.822	0.296	9.898
R17	24100987	48018756	0.501	0.181	6.040
R18	10538708	34499266	0.305	0.110	3.676
R23	6124842	38155143	0.160	0.057	1.931
R24	22842170	51218100	0.445	0.161	5.367
R29	191964	36500447	0.005	0.002	0.063
R31	23280668	47551501	0.489	0.176	5.892
R35	0	44630115	0	0	0
R38	1681025	52129038	0.032	0.011	0.388
R40	145922310	53494514	2.727	0.984	32.829
R41	10300142	47036051	0.218	0.079	2.635
R42	17199896	51273896	0.335	0.121	4.037
R46	81830873	34103903	2.399	0.866	28.877
R48	3619100	51774961	0.069	0.025	0.841
R49	20037739	45034618	0.444	0.160	5.354
R51	13661338	49657781	0.275	0.099	3.310
R53	3606967	44678673	0.080	0.029	0.971
R54	3720139	50777408	0.073	0.026	0.881
R59	80138772	56004110	1.430	0.516	17.221

Table A3. 33: The concentration of Ribose in each urine sample in active UC cohort provided in this research depending on the calibration curve in the figure 5. 21.

Urine samples	A UP of Ribose	AUP of I.S $^{13}C_6$ D-glucose	Ratio of AUP Ribose/$^{13}C_6$ D-glucose	Equation (Y=2.7697x)	Concentration (µg/ml)
A9	92806894	53792908	1.725	0.622	20.763
A11	95401028	57265669	1.665	0.601	20.049
A16	2115697	52808920	0.040	0.014	0.482
A20	6732526	41556991	0.162	0.058	1.949
A21	30831819	44711420	0.689	0.248	8.299
A22	16518673	38083160	0.433	0.156	5.220
A30	96723929	37535994	2.576	0.930	31.012
A32	8883912	39705803	0.223	0.081	2.692
A33	31098588	42245642	0.736	0.265	8.859
A47	22987526	40568364	0.566	0.204	6.819
A50	103779921	39156161	2.650	0.956	31.897

A55	7185037	52955606	0.135	0.048	1.632
A58	46357373	54091341	0.857	0.309	10.314
A60	0	42710083	0	0	0
A61	0	44520059	0	0	0
A63	106757	51301735	0.002	0.001	0.025

Table A3. 34: The concentration of Arabinose in each urine sample in control UC group provided in this research according to the calibration curve in the figure 5. 23.

Urine samples	A UP of Arabinose	AUP of I.S $^{13}C_6$ D-glucose	Ratio of AUP Arabinose/$^{13}C_6$ D-glucose	Equation (Y=2.7788x)	Concentration (µg/ml)
C5	12107499	51374318	0.235	0.084	2.827
C10	15105742	47254478	0.319	0.115	3.834
C19	40914711	46766582	0.874	0.314	10.494
C25	30906654	34117894	0.905	0.325	10.86
C26	54357658	35207294	1.543	0.555	18.520
C27	7915021	36804748	0.215	0.077	2.579
C28	20671556	37189251	0.555	0.200	6.667
C34	70469150	39225469	1.796	0.646	21.550
C36	9204843	35350054	0.260	0.093	3.123
C37	1500708	34320639	0.043	0.015	0.524
C39	19372231	34164214	0.567	0.204	6.801
C43	5668984	39062672	0.145	0.052	1.740
C45	68861664	36094139	1.907	0.686	22.885
C52	24239875	37070662	0.653	0.235	7.843
C56	61236300	37145464	1.648	0.593	19.775
C57	34896475	37574845	0.928	0.334	11.140
C62	15260728	37073121	0.411	0.148	4.937

Table A3. 35: The concentration of Arabinose in each urine sample in quiescent UC group provided in this research according to the calibration curve in the figure 5. 23.

Urine samples	A UP of Arabinose	AUP of I.S $^{13}C_6$ D-glucose	Ratio of AUP Arabinose/$^{13}C_6$ D-glucose	Equation (Y=2.7788x)	Concentration (µg/ml)
R2	759144	40079303	0.018	0.006	0.227
R3	75318	50748819	0.001	0.001	0.017
R4	301943	40116493	0.007	0.003	0.090
R8	363471	44642370	0.008	0.003	0.097
R12	0	41206496	0	0	0
R13	410395	43422403	0.009	0.003	0.113
R15	275449	44372881	0.006	0.002	0.074
R17	430023	48018756	0.008	0.003	0.107

R18	187767	34499266	0.005	0.001	0.065
R23	130066	38155143	0.003	0.001	0.040
R24	324438	51218100	0.006	0.002	0.076
R29	1402164	36500447	0.038	0.013	0.460
R31	556498	47551501	0.011	0.004	0.140
R35	0	44630115	0	0	0
R38	0	52129038	0	0	0
R40	4706132	53494514	0.087	0.031	1.055
R41	166412	47036051	0.003	0.001	0.042
R42	242715	51273896	0.004	0.001	0.056
R46	906248	34103903	0.026	0.009	0.318
R48	80271	51774961	0.002	0.001	0.018
R49	290305	45034618	0.006	0.002	0.077
R51	242925	49657781	0.005	0.001	0.058
R53	73706	44678673	0.002	0.001	0.019
R54	54240	50777408	0.001	0.001	0.012
R59	818335	56004110	0.014	0.005	0.175

Table A3. 36: The concentration of Arabinose in each urine sample in active UC group provided in this research according to the calibration curve in the figure 5. 23.

Urine samples	A UP of Arabinose	AUP of I.S $^{13}C_6$ D-glucose	Ratio of AUP Arabinose/$^{13}C_6$ D-glucose	Equation (Y=2.7788x)	Concentration (µg/ml)
A9	0	53792908	0	0	0
A11	0	57265669	0	0	0
A16	0	52808920	0	0	0
A20	0	41556991	0	0	0
A21	0	44711420	0	0	0
A22	0	38083160	0	0	0
A30	0	37535994	0	0	0
A32	0	39705803	0	0	0
A33	0	42245642	0	0	0
A47	0	40568364	0	0	0
A50	0	39156161	0	0	0
A55	0	52955606	0	0	0
A58	0	54091341	0	0	0
A60	0	42710083	0	0	0
A61	0	44520059	0	0	0
A63	0	51301735	0	0	0

Fucose, L-Rhamnose, Xylose, Ribose and Arabinose in saliva samples

Table A3. 37: The concentration of Fucose in each saliva sample in control UC cohort provided in this research according to the calibration curve in the figure 5. 15.

Saliva samples	A UP of Fucose	AUP of I.S $^{13}C_6$ D-glucose	Ratio of AUP Fucose/$^{13}C_6$ D-glucose	Equation (Y=1.3212x)	Concentration (µg/ml)
C5	9332426	8855106	1.053	0.797	26.589
C10	3734506	8686100	0.429	0.325	10.847
C16	36947661	8195405	4.508	3.412	113.743
C18	38129	7198752	0.005	0.004	0.133
C20	3374154	8262388	0.408	0.309	10.303
C21	116978	6604430	0.017	0.013	0.446
C22	1783154	10375083	0.171	0.130	4.336
C23	1571640	7029400	0.223	0.169	5.640
C30	38453	6496252	0.005	0.004	0.149
C33	87310	8266320	0.010	0.007	0.266
C34	1292561	8144330	0.158	0.120	4.004
C36	0	8850357	0	0	0
C37	24824	4842797	0.005	0.003	0.129
C42	0	6267624	0	0	0
C43	1200252	7757502	0.154	0.117	3.903
C49	3273780	7757502	0.422	0.319	10.647
C50	17354604	8854045	1.960	1.483	49.451
C55	146986	7578248	0.019	0.014	0.489
C58	1083176	6403183	0.169	0.128	4.267
C60	100299	6426269	0.015	0.011	0.393
C61	6640098	8267357	0.803	0.607	20.264
C62	1137853	14806601	0.076	0.058	1.938
C64	2201016	8172287	0.269	0.203	6.795

Table A3. 38: The concentration of Fucose in each saliva sample in quiescent UC cohort provided in this research according to the calibration curve in the figure 5. 15.

Saliva samples	A UP of Fucose	AUP of I.S $^{13}C_6$ D-glucose	Ratio of AUP Fucose/$^{13}C_6$ D-glucose	Equation (Y=1.3212x)	Concentration (µg/ml)
R1	1291718	9336000	0.138	0.104	3.490
R3	734154	10642582	0.068	0.052	1.740
R9	18513072	12986383	1.425	1.079	35.966
R12	1845006	13936432	0.132	0.100	3.340
R13	39041124	14176754	2.753	2.084	69.479
R15	0	13204254	0	0	0
R17	0	10931201	0	0	0
R24	690883	11034331	0.062	0.047	1.579
R25	4737685	14194301	0.333	0.252	8.420

R28	7483832	15942776	0.469	0.355	11.843
R29	7189129	13456985	0.534	0.404	13.478
R31	6706727	14429474	0.464	0.351	11.726
R32	10584103	14361046	0.737	0.557	18.594
R35	1876228	5802827	0.323	0.244	8.157
R38	1195624	11388814	0.104	0.079	2.648
R39	438038	8920029	0.049	0.037	1.238
R40	0	8583380	0	0	0
R44	17207455	7687092	2.238	1.694	56.476
R46	6487920	7339912	0.883	0.669	22.301
R48	2343699	7123395	0.329	0.249	8.300
R51	175440115	7826591	22.415	16.966	565.544
R52	0	7680091	0	0	0
R56	1204262	9100458	0.132	0.100	3.338
R57	385345	8837986	0.043	0.033	1.101
R63	11712623	6976589	1.678	1.270	42.356

Table A3. 39: The concentration of Fucose in each saliva sample in active UC cohort provided in this research according to the calibration curve in the figure 5. 15.

Saliva samples	A UP of Fucose	AUP of I.S $^{13}C_6$ D-glucose	Ratio of AUP Fucose/$^{13}C_6$ D-glucose	Equation (Y=1.3212x)	Concentration (µg/ml)
A2	1377557	9585965	0.143	0.108	3.625
A4	3770364	3357759	1.122	0.849	28.329
A6	11357264	13742351	0.826	0.625	20.850
A7	1055241	12067553	0.087	0.066	2.206
A8	2296995	10691445	0.214	0.162	5.420
A11	129419	13499178	0.009	0.007	0.241
A14	0	12815857	0	0	0
A19	4171535	11358702	0.367	0.277	9.265
A26	583086	5045610	0.115	0.087	2.915
A27	5405745	12009119	0.450	0.340	11.356
A41	12927088	12947966	0.998	0.755	25.188
A45	0	8609898	0	0	0
A47	0	11885331	0	0	0
A53	13656945	13558586	1.007	0.762	25.412
A54	27594	14567735	0.001	0.001	0.047
A59	32713	14085188	0.002	0.001	0.058
A65	167745	5158047	0.032	0.024	0.820

Table A3. 40: The concentration of Rhamnose in each saliva sample in control UC cohort provided in this research according to the calibration curve in the figure 5. 17.

Saliva samples	A UP of Rhamnose	AUP of I.S $^{13}C_6$ D-glucose	Ratio of AUP Rhamnose/$^{13}C_6$ D-glucose	Equation (Y=1.3286)	Concentration (µg/ml)
C5	0	8855106	0	0	0
C10	0	8686100	0	0	0
C16	221478991	8195405	27.024	20.340	678.026
C18	0	7198752	0	0	0
C20	0	8262388	0	0	0
C21	0	6604430	0	0	0
C22	113104	10375083	0.011	0.008	0.273
C23	0	7029400	0	0	0
C30	0	6496252	0	0	0
C33	0	8266320	0	0	0
C34	0	8144330	0	0	0
C36	191138975	8850357	21.596	16.255	541.842
C37	0	4842797	0	0	0
C42	0	6267624	0	0	0
C43	0	7757502	0	0	0
C49	0	7757502	0	0	0
C50	2324633	8854045	0.262	0.197	6.587
C55	0	7578248	0	0	0
C58	0	6403183	0	0	0
C60	24553526	6426269	3.820	2.875	95.860
C61	161873967	8267357	19.579	14.737	491.241
C62	144263234	14806601	9.743	7.333	244.447
C64	0	8172287	0	0	0

Table A3. 41: The concentration of Rhamnose in each saliva sample in remission UC cohort provided in this research according to the calibration curve in the figure 5. 17.

Saliva samples	A UP of Rhamnose	AUP of I.S $^{13}C_6$ D-glucose	Ratio of AUP Rhamnose/$^{13}C_6$ D-glucose	Equation (Y=1.3286)	Concentration (µg/ml)
R1	0	9336000	0	0	0
R3	0	10642582	0	0	0
R9	170275941	12986383	13.111	9.868	328.964
R12	0	13936432	0	0	0
R13	0	14176754	0	0	0
R15	0	13204254	0	0	0
R17	0	10931201	0	0	0
R24	0	11034331	0	0	0
R25	0	14194301	0	0	0
R28	0	15942776	0	0	0
R29	0	13456985	0	0	0
R31	254429915	14429474	17.632	13.271	442.386

R32	18598	14361046	0.001	0.001	0.032
R35	0	5802827	0	0	0
R38	0	11388814	0	0	0
R39	0	8920029	0	0	0
R40	2083	8583380	0.001	0.001	0.006
R44	0	7687092	0	0	0
R46	0	7339912	0	0	0
R48	0	7123395	0	0	0
R51	2706290	7826591	0.345	0.260	8.675
R52	0	7680091	0	0	0
R56	0	9100458	0	0	0
R57	0	8837986	0	0	0
R63	0	6976589	0	0	0

Table A3. 42: The concentration of Rhamnose in each saliva sample in active UC cohort provided in this research according to the calibration curve in the figure 5. 17.

Saliva samples	A UP of Rhamnose	AUP of I.S $^{13}C_6$ D-glucose	Ratio of AUP Rhamnose/$^{13}C_6$ D-glucose	Equation (Y=1.3286)	Concentration (µg/ml)
A2	0	19585965	0	0	0
A4	0	3357759	0	0	0
A6	0	13742351	0	0	0
A7	0	12067553	0	0	0
A8	0	10691445	0	0	0
A11	0	13499178	0	0	0
A14	0	12815857	0	0	0
A19	0	11358702	0	0	0
A26	0	5045610	0	0	0
A27	24754	12009119	0.002	0.002	0.051
A41	12031	12947966	0.001	0.002	0.023
A45	0	8609898	0	0	0
A47	0	11885331	0	0	0
A53	25613	13558586	0.001	0.002	0.047
A54	0	14567735	0	0	0
A59	0	14085188	0	0	0
A65	2403	5158047	0.001	0.001	0.011

Table A3. 43: The concentration of Xylose in each saliva sample in control UC cohort provided in this research according to the calibration curve in the figure 5. 19.

	AUP of			Equation	Concentration

Saliva samples	Xylose	AUP of I.S $^{13}C_6$ D-glucose	Ratio of AUP Xylose/$^{13}C_6$ D-glucose	(Y=1.3468x)	(µg/ml)
C5	12580	8855106	0.001	0.001	0.03
C10	0	8686100	0	0	0
C16	0	8195405	0	0	0
C18	0	7198752	0	0	0
C20	0	8262388	0	0	0
C21	0	6604430	0	0	0
C22	179125	10375083	0.017	0.013	0.427
C23	14393	7029400	0.002	0.002	0.051
C30	0	6496252	0	0	0
C33	0	8266320	0	0	0
C34	0	8144330	0	0	0
C36	0	8850357	0	0	0
C37	0	4842797	0	0	0
C42	18636	6267624	0.003	0.002	0.073
C43	0	7757502	0	0	0
C49	0	7757502	0	0	0
C50	0	8854045	0	0	0
C55	0	7578248	0	0	0
C58	0	6403183	0	0	0
C60	0	6426269	0	0	0
C61		8267357	0	0	0
C62	166036	14806601	0.011	0.008	0.277
C64	0	8172287	0	0	0

Table A3. 44: The concentration of Xylose in each saliva sample in quiescent UC cohort provided in this research according to the calibration curve in the figure 5. 19.

Saliva samples	AUP of Xylose	AUP of I.S $^{13}C_6$ D-glucose	Ratio of AUP Xylose/$^{13}C_6$ D-glucose	Equation (Y=1.3468x)	Concentration (µg/ml)
R1	0	9336000	0	0	0
R3	0	10642582	0	0	0
R9	30793	12986383	0.002	0.002	0.058
R12	15260	13936432	0.001	0.001	0.027
R13	0	14176754	0	0	0
R15	0	13204254	0	0	0
R17	0	10931201	0	0	0
R24	0	11034331	0	0	0
R25	166276	14194301	0.011	0.008	0.289
R28	0	15942776	0	0	0
R29	29817	13456985	0.002	0.002	0.054
R31	0	14429474	0	0	0

R32	18614	14361046	0.001	0.001	0.032
R35	36315	5802827	0.006	0.004	0.154
R38	0	11388814	0	0	0
R39	0	8920029	0	0	0
R40	0	8583380	0	0	0
R44	0	7687092	0	0	0
R46	0	7339912	0	0	0
R48	0	7123395	0	0	0
R51	0	7826591	0	0	0
R52	0	7680091	0	0	0
R56	0	9100458	0	0	0
R57	0	8837986	0	0	0
R63	23872	6976589	0.003	0.002	0.084

Table A3. 45: The concentration of Xylose in each saliva sample in active UC cohort provided in this research according to the calibration curve in the figure 5. 19.

Saliva samples	AUP of Xylose	AUP of I.S $^{13}C_6$ D-glucose	Ratio of AUP Xylose/$^{13}C_6$ D-glucose	Equation (Y=1.3468x)	Concentration (µg/ml)
A2	0	9585965	0	0	0
A4	0	3357759	0	0	0
A6	0	13742351	0	0	0
A7	0	12067553	0	0	0
A8	0	10691445	0	0	0
A11	0	13499178	0	0	0
A14	0	12815857	0	0	0
A19	0	11358702	0	0	0
A26	0	5045610	0	0	0
A27	46120	12009119	0.003	0.003	0.095
A41	0	12947966	0	0	0
A45	0	8609898	0	0	0
A47	0	11885331	0	0	0
A53	0	13558586	0	0	0
A54	0	14567735	0	0	0
A59	0	14085188	0	0	0
A65	0	5158047	0	0	0

Table A3. 46: The concentration of Ribose in each saliva sample in control UC cohort provided in this research according to the calibration curve in the figure 5. 21.

Saliva samples	A UP of Ribose	AUP of I.S $^{13}C_6$ D-glucose	Ratio of AUP Ribose/$^{13}C_6$ D-glucose	Equation (Y=2.7697x)	Concentration (µg/ml)

C5	1407354	8855106	0.158	0.057	1.913
C10	214050	8686100	0.024	0.008	0.296
C16	702293	8195405	0.085	0.030	1.032
C18	15713	7198752	0.002	0.001	0.026
C20	4770885	8262388	0.577	0.208	6.949
C21	32565	6604430	0.004	0.002	0.059
C22	494791	10375083	0.047	0.017	0.573
C23	33136	7029400	0.004	0.002	0.056
C30	9620	6496252	0.001	0.001	0.017
C33	0	8266320	0	0	0
C34	29838	8144330	0.003	0.001	0.044
C36	11805	8850357	0.001	0.001	0.016
C37	17712	4842797	0.003	0.001	0.044
C42	11581	6267624	0.002	0.001	0.022
C43	17966	7757502	0.002	0.001	0.027
C49	594854	7757502	0.076	0.027	0.922
C50	1943716	8854045	0.219	0.079	2.642
C55	233047	7578248	0.031	0.011	0.370
C58	424972	6403183	0.066	0.023	0.798
C60	17093	6426269	0.002	0.001	0.032
C61	379535	8267357	0.045	0.016	0.552
C62	340997	14806601	0.023	0.008	0.277
C64	87081	8172287	0.010	0.003	0.128

Table A3. 47: The concentration of Ribose in each saliva sample in remission UC cohort provided in this research according to the calibration curve in the figure 5. 21.

Saliva samples	A UP of Ribose	AUP of I.S $^{13}C_6$ D-glucose	Ratio of AUP Ribose/$^{13}C_6$ D-glucose	Equation (Y=2.7697x)	Concentration (µg/ml)
R1	165393	9336000	0.017	0.006	0.213
R3	153593	10642582	0.014	0.005	0.173
R9	268151	12986383	0.021	0.007	0.248
R12	59831	13936432	0.004	0.001	0.051
R13	369116	14176754	0.026	0.009	0.313
R15	0	13204254	0	0	0
R17	187442	10931201	0.017	0.006	0.206
R24	367106	11034331	0.033	0.012	0.400
R25	208817	14194301	0.014	0.005	0.177
R28	303093	15942776	0.019	0.006	0.228
R29	242608	13456985	0.018	0.006	0.216
R31	44174	14429474	0.003	0.001	0.036
R32	753178	14361046	0.052	0.018	0.631
R35	193914	5802827	0.033	0.012	0.402

R38	70132	11388814	0.006	0.002	0.074
R39	28095	8920029	0.003	0.001	0.037
R40	0	8583380	0	0	0
R44	2251698	7687092	0.292	0.105	3.525
R46	1741022	7339912	0.237	0.085	2.854
R48	373203	7123395	0.052	0.018	0.630
R51	46490	7826591	0.006	0.002	0.071
R52	0	7680091	0	0	0
R56	882242	9100458	0.096	0.035	1.166
R57	43414	8837986	0.004	0.002	0.059
R63	1046538	6976589	0.150	0.054	1.805

Table A3. 48: The concentration of Ribose in each saliva sample in active UC cohort provided in this research according to the calibration curve in the figure 5. 21.

Saliva samples	A UP of Ribose	AUP of I.S $^{13}C_6$ D-glucose	Ratio of AUP Ribose/$^{13}C_6$ D-glucose	Equation (Y=2.7697x)	Concentration (µg/ml)
A2	147474	9585965	0.015	0.005	0.185
A4	846932	3357759	0.252	0.091	3.035
A6	591960	13742351	0.043	0.015	0.518
A7	148808	12067553	0.012	0.004	0.148
A8	728665	10691445	0.068	0.024	0.820
A11	201205	13499178	0.015	0.005	0.179
A14	0	12815857	0	0	0
A19	472878	11358702	0.04	0.015	0.501
A26	229531	5045610	0.04	0.016	0.547
A27	280903	12009119	0.023	0.008	0.2815
A41	3416565	12947966	0.263	0.095	3.175
A45	0	8609898	0	0	0
A47	0	11885331	0	0	0
A53	2957401	13558586	0.218120164	0.078	2.625
A54	0	14567735	0	0	0
A59	40139	14085188	0.003	0.001	0.034
A65	50850	5158047	0.009	0.003	0.118

Table A3. 49: The concentration of Arabinose in each saliva sample in control UC cohort provided in this research according to the calibration curve in the figure 5. 23.

Saliva samples	A UP of Arabinose	AUP of I.S $^{13}C_6$ D-glucose	Ratio of AUP Arabinose/$^{13}C_6$ D-glucose	Equation (Y=2.7788x)	Concentration (µg/ml)
C5	0	8855106	0	0	0
C10	0	8686100	0	0	0

C16	0	8195405	0	0	0
C18	11677	7198752	0.002	0.001	0.025
C20	13923	8262388	0.002	0.001	0.022
C21	0	6604430	0	0	0
C22	0	10375083	0	0	0
C23	0	7029400	0	0	0
C30	0	6496252	0	0	0
C33	0	8266320	0	0	0
C34	0	8144330	0	0	0
C36	0	8850357	0	0	0
C37	0	4842797	0	0	0
C42	18064	6267624	0.002	0.001	0.034
C43	0	7757502	0	0	0
C49	0	7757502	0	0	0
C50	0	8854045	0	0	0
C55	0	7578248	0	0	0
C58	0	6403183	0	0	0
C60	0	6426269	0	0	0
C61	0	8267357	0	0	0
C62	0	14806601	0	0	0
C64	0	8172287	0	0	0

Table A3. 50: The concentration of Arabinose in each saliva sample in quiescent UC cohort provided in this research according to the calibration curve in the figure 5. 23.

Saliva samples	A UP of Arabinose	AUP of I.S $^{13}C_6$ D-glucose	Ratio of AUP Arabinose/$^{13}C_6$ D-glucose	Equation (Y=2.7788x)	Concentration (µg/ml)
R1	0	9336000	0	0	0
R3	0	10642582	0	0	0
R9	0	12986383	0	0	0
R12	0	13936432	0	0	0
R13	0	14176754	0	0	0
R15	0	13204254	0	0	0
R17	0	10931201	0	0	0
R24	0	11034331	0	0	0
R25	0	14194301	0	0	0
R28	0	15942776	0	0	0
R29	0	13456985	0	0	0
R31	0	14429474	0	0	0
R32	0	14361046	0	0	0
R35	0	5802827	0	0	0
R38	0	11388814	0	0	0
R39	0	8920029	0	0	0

R40	0	8583380	0	0	0
R44	0	7687092	0	0	0
R46	0	7339912	0	0	0
R48	0	7123395	0	0	0
R51	0	7826591	0	0	0
R52	0	7680091	0	0	0
R56	0	9100458	0	0	0
R57	0	8837986	0	0	0
R63	0	6976589	0	0	0

Table A3. 51: The concentration of Arabinose in each saliva sample in active UC cohort provided in this research according to the calibration curve in the figure 5. 23.

Saliva samples	A UP of Arabinose	AUP of I.S $^{13}C_6$ D-glucose	Ratio of AUP Arabinose/$^{13}C_6$ D-glucose	Equation (Y=2.7788x)	Concentration (µg/ml)
A2	0	9585965	0	0	0
A4	0	3357759	0	0	0
A6	0	13742351	0	0	0
A7	0	12067553	0	0	0
A8	0	10691445	0	0	0
A11	0	13499178	0	0	0
A14	0	12815857	0	0	0
A19	0	11358702	0	0	0
A26	0	5045610	0	0	0
A27	0	12009119	0	0	0
A41	0	12947966	0	0	0
A45	0	8609898	0	0	0
A47	0	11885331	0	0	0
A53	0	13558586	0	0	0
A54	0	14567735	0	0	0
A59	0	14085188	0	0	0
A65	0	5158047	0	0	0